UNIVERSITEIT VAN PRETORIA
UNIVERSITY OF PRETORIA
YUNIBESITHI YA PRETORIA

# WIND RESOURCE ASSESSMENT AND GIS-BASED SITE SELECTION METHODOLOGY FOR EFFICIENT WIND POWER DEPLOYMENT

by

**Mohammed Abdul Baseer**

*Submitted in partial fulfilment of the requirements for the degree*

**Doctor of Philosophy in Mechanical Engineering**

*in the*

Faculty of Engineering, Built Environment and Information Technology, Department of Mechanical and Aeronautical Engineering

**University of Pretoria**

Supervisor: **Professor Josua P. Meyer**

Co-supervisors: **Dr. Shafiqur Rehman** and **Dr. Md. Mahbub Alam**

February 2017



© University of Pretoria

## ABSTRACT

**Title** : Wind resource assessment and GIS-based site selection methodology for efficient wind power deployment.

**Author** : Mohammed Abdul Baseer

**Supervisor** : Professor Josua P. Meyer

**Co-Supervisors** : Dr. Shafiqur Rehman and Dr. Md. Mahbub Alam

**Department** : Mechanical and Aeronautical Engineering

**University** : University of Pretoria

**Degree** : Doctor of Philosophy (Mechanical Engineering)

*An enormous and urgent energy demand is predicted due to the growing global population, increase in power intensive industries, higher living standards, electrification of remote areas, and globalisation (transportation). Moreover, the global consciousness about the harmful effects of traditional methods of power generation on the environment. That, in turn, has created a need to strategically plan and develop renewable and sustainable energy generation systems. This study presents a wind resource assessment of seven locations proximate to the largest industrial hub in the Middle East, Jubail Industrial City, Kingdom of Saudi Arabia, and a Geographic Information System, GIS based model considering a multi-criteria wind farm site suitability approach for the entire Kingdom of Saudi Arabia and elsewhere.*

*The hourly mean wind speed data at 10, 50 and 90 m above the ground level (AGL) over a period of five years was used for a meteorological station at the Industrial Area (Central) of Jubail. At the remaining six sites, the meteorological data were recorded at 10 m AGL only. Five years of wind data were used for five sites and three years of data were available for the remaining one site. At the Industrial Area (East), the mean wind speeds were found to be 3.34, 4.79 and 5.35 m/s at 10, 50 and 90 m AGL, respectively. At 50 and 90 m AGL, the availability of wind speed above 3.5 m/s was more than 75%. The local wind shear exponent, calculated using measured wind speed values at three heights, was found to be 0.217. The mean wind power density values at measurement heights were 50.92, 116.03 and 168.46 W/m$^2$, respectively. After the assessment and comparison of wind characteristics of all seven*




© University of Pretoria

*sites, the highest annual mean wind speed of 4.52 m/s was observed at Industrial Area (East) and the lowest of 2.52 m/s at the Pearl Beach with standard deviations of 2.52 and 1.1 m/s, respectively.*

*In general, at all sites, the highest monthly mean wind speed was observed in February/June and the lowest in September/October. The period of higher wind availability coincides with a high power demand period in the region attributable to the air conditioning load. The wind rose plots show that the prevailing wind direction for all sites was from the north-west. Weibull parameters for all sites were estimated using maximum likelihood, least-squares regression method (LSRM), and WAsP algorithm. In general, at all sites, the Weibull parameter, c, was the highest in the months of February/June and the lowest in the month of October. The most probable and maximum energy carrying wind speed was determined by all three methods. The highest value of most probable wind speed was found to be in the range of 3.2 m/s to 3.6 m/s at Industrial Area (East) and the highest value of maximum energy carrying wind speed was found to be in the range 8.6 m/s to 9.0 m/s at Industrial Area 2 (South) by three estimation methods. The correlation coefficient ($R^2$), root mean square error (RMSE), mean bias error (MBE), and mean bias absolute error (MAE) showed that all three methods represent wind data at all sites accurately. However, the maximum likelihood method is slightly better than LSRM, followed by WAsP algorithm. The wind power output at all seven sites, from five commercially available wind turbines of rated power ranging from 1.8 to 3.3 MW, showed that Industrial Area (East) is most promising for wind farm development. At all sites, based on percentage plant capacity factor, PCF, the 1.8 MW wind turbine was found to be the most efficient. At Industrial Area (East), this wind turbine was found to have a maximum PCF of 41.8%, producing 6,589 MWh/year energy output. The second best wind turbine was 3 MW at all locations except the Al-Bahar Desalination Plant and Pearl Beach. At both of these locations, 3.3 MW was the next best option. The energy output from the 3 MW wind turbine at Industrial Area (East) was found to be 11,136 MWh/year with a PCF of 41.3%. The maximum duration of rated power output from all selected wind turbines was observed to be between 8 to 16.6% at Industrial Area 2 (South). The minimum duration of rated power output, less than 0.3% for all wind turbines, was observed at Pearl Beach. The maximum duration of zero power output of between 35 to 60% was also observed at Pearl Beach. The minimum duration of zero power output of between 12 to 23% was obtained in Industrial Area (East). Even though the 1.8 MW wind turbine is found to be most efficient, installation of a higher rated power wind turbine such as the 3 MW*



© University of Pretoria

*is a smart option as it would occupy less of the scarce land in the Industrial City. The cost of electricity, COE per kWh was estimated at each of the seven locations in Jubail, based on present value cost, PVC method for five selected wind turbines, and annual power output at these locations. The minimum cost of 0.023 US$ per kWh is obtained for Industrial Area (East) for the wind turbine of capacity 2,000 kW.*

*This study also presents a multi-criteria wind farm site suitability analysis by developing a model based on a geographic information system (GIS). The site suitability analysis considered different parameters, such as climatic, economic, aesthetic and environmental conditions, and formulated a criterion based on wind resource, accessibility by roads/highways, proximity to the electrical grid, and optimum/safe distance from various settlements and airports. The developed model was then applied to the entire Kingdom of Saudi Arabia by using long-term historical wind speed data from 29 meteorological stations across the country. The wind speed used in the criterion was interpolated to 100 m from 10 m AGL by using traditional one-seventh power law. To predict the wind speed in locations for which data are not available, a spatial interpolation technique, inverse distance weighted, was used to convert wind speed point data to raster structure. The data and GIS shape files of other criteria mentioned above were obtained from governmental organisations. The GIS shape files for roads and highways were merged as identical constraints were applied to both criteria. Subsequently, the data of all the criteria were reclassified into suitability scores. Two different modelling approaches were adopted, one in which equal weightage was given to all the components of the criteria, and the other in which different weightage selected based on the literature, were given to the different components of the criteria of site selection. The resulting suitability maps were distributed into six classes, from the most suitable to least suitable. In the suitability map, based on Method 1, 1.03% of the total classed area fell under the most suitable wind farm area, whereas in Method 2, the percentage was 1.86%. The percentages of the next best areas were 29.13% and 14.65% in the maps based on Method 1 and 2, respectively.*

*The wind farm site suitability indexed map reveals that the most suitable sites for wind farms are (i) Ras Tanura and Safwa along the Arabian Gulf coast in the Eastern Province, (ii) Turaif, Kaf and Al-Isawiyah in the Al-Jawf region along the northern borders, and (iii) Al-Wajh and Yanbu along the Red Sea coast in the western region. These three regions are windy, adequately populated, and well connected by roads/highways and the national*



© University of Pretoria

*electricity grid. Some central and south-eastern regions failed to qualify to be considered for wind farm development mainly because of scarce wind resources, low population, and poor connectivity by roads and electrical grid.*

**Keywords:** *Wind speed, Wind rose, Frequency distribution, Weibull parameters, Wind shear exponent, Wind turbine output, Plant capacity factor, PVC (Present value cost), Maximum energy carrying wind speed, Most probable wind speed, GIS (Geographic information systems), Multi-criteria decision analysis, Wind maps, Site suitability analysis.*




© University of Pretoria

Dedicated to my wife,

Sameera

& children,

Aakifah, Leenah, Mariyah & Hamzah.



© University of Pretoria

# ACKNOWLEDGEMENTS

All praise be to Allah Almighty, for his mercy, blessing and guidance. It is only because of his will and compassion that this research work and thesis were possible.

I would like to express my deep gratitude and appreciation to my supervisor, Prof. J.P. Meyer, Head, Department of Mechanical and Aeronautical Engineering, University of Pretoria, my co-supervisors, Dr. Shafiqur Rehman, Research Engineer-II (Associate Professor), King Fahd University of Petroleum & Minerals, Dhahran, Centre of Engineering Research and Dr. Md. Mahbub Alam, Professor, Harbin Institute of Technology, Harbin, Shenzhen Graduate School, China for their encouragement, guidance, patience, and untiring sincere advise throughout this research work. I have developed a profound interest in the subject after working under their guidance.

I wish to thank and acknowledge the management of the Jubail Industrial College, Royal Commission of Jubail for providing the meteorological data of Jubail for this study and for their support and encouragement. Furthermore, I would like to acknowledge Dr. Shafiqur Rehman for providing the long-term historical meteorological data of 29 weather stations through Presidency of Metrology & Environment, in addition to his profound guidance during this research work. Special thanks are due to Mr. Haris Jayah, Mr. Salman Abdul Gaffar, Dr. Adhi Primartomo, Mr. Masoud Suheel, and Dr. Khaled Ahmed for their support and encouragement.

I wish to express sincere thanks to Dr. Faizur Rahman for his persistent encouragement, advice and guidance throughout this study.

Acknowledgement is due to my Father, Mr. Abdur Rab who has been a source of inspiration throughout my life, my mother, for her unwavering support, my sisters and brother for their affection and encouragement. Last but not the least my wife, Sameera, and children, Aakifah, Leenah, Mariyah and Hamzah. They deserve a personal and special gratitude for their co-operation and understanding, without which I could not have devoted this much time, and this research work would not have been possible.



© University of Pretoria

## PUBLICATIONS IN JOURNALS AND CONFERENCE PROCEEDINGS

The following list of articles and conference papers were published while this study was in progress. It provided independent peer review and very valuable feedback from reviewers, which were implemented. Therefore, some parts of this thesis have exactly the same content as many of the articles and conference papers that were published. The copyright agreements of the publishers that were signed ensured the necessary permissions.

1. **M.A. Baseer**, J.P. Meyer, M.M. Alam, and S. Rehman, Wind speed and power characteristics for Jubail Industrial City, *Renewable and Sustainable Energy Reviews*, vol. 52, pp. 1193–1204, 2016.

2. **M.A. Baseer**, J.P. Meyer, S. Rehman, M.M. Alam, L.M. Al-Hadhrami, and A. Lashin, Performance evaluation of cup-anemometers and wind speed characteristics analysis, *Renewable Energy*, vol. 86, pp. 733-744, 2016.

3. S. Rehman, **M.A. Baseer**, J. P. Meyer, M.M. Alam, L. M. Alhems, A. Lashin and N. Alarefe, Suitability of utilising small horizontal axis wind turbines for off grid loads in eastern Region of Saudi Arabia, *Energy exploration & exploitation*, vol. 34, no. 3, pp 449 – 467, 2015.

4. **M.A. Baseer**, J.P. Meyer, S. Rehman, and M.M. Alam, Wind Power Characteristics of Seven Data Collection Sites In Jubail, Saudi Arabia Using Weibull Parameters, *Renewable Energy*, vol. 102, pp 35-49, 2017.

5. **M.A. Baseer**, J.P. Meyer, S. Rehman, and M.M. Alam, GIS-based site suitability analysis for wind farm development in Saudi Arabia, *International Journal of Geographic Information Science*. **Article submitted.**

6. **M.A. Baseer,** J.P. Meyer, S. Rehman, and M.M. Alam, Wind Resource Assessment for an Industrial City in Saudi Arabia, *11th International Conference on Heat Transfer, Fluid Mechanics and Thermodynamics*, 20 to 23 July 2015. **(Presented)**



© University of Pretoria

7. F. Rahman, **M.A. Baseer**, and S. Rehman (2015). Assessment of electrical storage systems, In "Solar Energy Storage", B. Sorenson (Ed.), 1st Edition (394). **Academic Press**. (**Book chapter**).



© University of Pretoria

# CONTENTS






© University of Pretoria

© University of Pretoria

© University of Pretoria

# LIST OF TABLES






© University of Pretoria

© University of Pretoria

# LIST OF FIGURES






© University of Pretoria

© University of Pretoria

© University of Pretoria

© University of Pretoria

© University of Pretoria

© University of Pretoria

# ACRONYM TABLE

| | |
|---|---|
| AGL | Above the Ground Level |
| COE | Cost of Energy |
| CSP | Concentrated Solar Power |
| GCC | Gulf Cooperation Council |
| GHG | Greenhouse Gases |
| GIS | Geographical Information System |
| IDW | Inverse Distance Weighted |
| KSA | Kingdom of Saudi Arabia |
| LSRM | Least-Squares Regression Method |
| MAE | Mean Bias Absolute Error |
| MBE | Mean Bias Error |
| MENA | Middle East and North Africa |
| MPGA | Multi-Population Genetic Algorithm |
| PCF | Plant Capacity Factor |
| PME | Presidency of Meteorology and Environment |
| PV | Photovoltaic |
| RMSE | Root Mean Square Error |
| SEC | Saudi Electrical Company |
| SIDF | Saudi Industrial development Fund |
| TOE | Tons of oil equivalent |
| WECS | Wind Energy Conversion System |
| WPD | Wind Power Density |
| WRA | Wind Resource Assessment |
| WS | Wind Speed |
| WSE | Wind Shear Exponent |
| WT | Wind Turbine |



© University of Pretoria

# CHAPTER 1

# INTRODUCTION

The ever increasing population, rapid industrialisation, materialistic living standards, and usage of energy intensive appliances, to name a few reasons, are causing growing demands on electricity and are resulting in higher global per capita energy consumption. An enormous energy challenge is expected in the next century so as to meet the needs of billions of people who still lack access to basic, modern grid-connected energy services, while also addressing the global transition to clean, low-carbon energy systems by mitigating the use of fossil fuels for energy generation.

It is imperative to make a conscious and infallible global effort to control the emission of greenhouse gases in the years to come. Wind energy offers an immediate and timely means to decarbonise the global energy mix.

## 1.1 BACKGROUND TO THE STUDY

The average temperature on Earth has increased by about 0.8° Celsius (1.4° Fahrenheit) since 1880. Two-thirds of this warming has occurred since 1975, at a rate of roughly 0.15 to 0.20°C per decade [1]. This accelerated warming of Earth, after 1975 is due to increased emissions of carbon dioxide and other greenhouse gases in the atmosphere by the burning of fossil fuels, land clearing, agriculture, and other human activities [2]. This climate change may cause rising sea levels due to the melting of the polar ice caps, increase in the frequency and severity of storms and other dangerous weather events.

According to the estimates of the US Census Bureau, the current world population is 7.3 billion and projections indicate that the 8 billion mark will be reached by 2025 [3]. The global annual energy demand increased from 16,000 terawatt hour (TWh) to 20,000 TWh from 2001 to 2010, an increase of 25% in only 10 years. Experts forecast that the energy consumption will be more than 25,000 TWh by the end of 2020, an annual increase of 1.5% to 2% in energy consumption [4]. According to Saudi Electricity Company, in Saudi Arabia, the total annual energy consumption increased from 126 to 312 TWh, an increase by 2.5 times in the last one and half decades.



© University of Pretoria

Historically, the increase in human population and industrial growth has been linked to this increase in demand for energy. Fossil fuels (oil, gas and coal) are by far the most important contributors to the world's current energy mix. Not only are the global oil and gas reserves diminishing but also their use for power generation adds poisonous gases, commonly known as greenhouse gases (GHG), to the atmosphere.

Moreover, currently, about 1.2 billion people (17% of the global population) does not have access to electricity [5]. This estimate is 84 million fewer than in the previous year. More than 95% of those without access to electricity live in developing and underdeveloped countries, and are predominantly from rural areas. In Saudi Arabia, 2.3% of the population does not have access to electricity. Some percentage of population living in remote rural areas, where diesel generators supply intermittent power. Diesel needs to be supplied by roads on a regular basis. Another problem is substandard electricity quality, which is faced by a large percentage of the population. All of these countries, which have a share of the population with no access to electricity, have policies in place to accelerate the electrification of its entire population.

Considering all the factors mentioned above, such as increasing population, rapid industrialisation, increasing standard of living, complete electrification of remote areas and globalisation (transportation), an enormous and urgent energy demand is predicted. The challenge is not only to meet these energy demands, but also to control the GHG emissions. Energy generation from clean and renewable sources of energy will meet both the challenges mentioned above. A balanced energy mix of sustainable and conventional energy is strategically important and is the need of the hour.

The cleanest sources of energy are those which use the natural resources of the Earth. These free, clean and abundant sources are known as renewable sources of energy and will never die out, unlike fixed reserves of fossil and nuclear fuels. Some of the common sources of renewable energies are wind, solar photovoltaic, solar thermal, hydro, wave, geothermal, and biomass. Of these sources, solar and wind resources have achieved commercial maturity, both in technological and economic terms. These sources can be tapped anywhere and do not require the national grid connectivity. They can be connected to isolated grids, to groups of houses, or to individual houses or installations. These sources are site-dependent, are available everywhere, and have no political and geographical boundaries.



© University of Pretoria

Wind is a very promising energy source and it is receiving global recognition when compared to other renewable energy sources, due to its low production, operation and maintenance costs and its ease of maintenance, besides the availability of efficient multi-megawatt wind turbines.

Saudi Arabia is experiencing rapid population growth as well as phenomenal industrial growth, subsequently resulting in an ever increasing demand on power and water supplies. The total population of Saudi Arabia increased by more than five times within the last four and a half decades, from 5,772,000 in 1970 to 30,770,375 in 2014 [6]. The number of operating industries has increased by more than 30 times within the last four decades, from 198 in 1974 to 6,471 in 2013 [7]. The total Gross Domestic Product (in constant prices) achieved by the manufacturing industries increased from US $4 billion in 1975 to more than US $45 billion at the end of 2013. Also, the growth rate of the manufacturing industries continued to increase throughout this period at an average of 6% per annum, which is considered to be one of the highest among the other economic sectors [7]. The installed wind power capacity in Africa and the Middle East was just 1% of the global installed capacity of 369,596 MW by the end of year 2014 [8]. Therefore, Saudi Arabia is exploring alternate sustainable and reliable sources of energy for generating power and to reduce consumption of the nation's fossil fuel reserves. Consequently, it was determined that a balanced energy mix of alternative and conventional energy is strategically important to Saudi Arabia's long term prosperity, energy security and its leading position in the global energy market [9]. Wind energy utilisation is one of the renewable energy options Saudi Arabia is considering seriously.

The availability of renewable energy resources is a geographical based criterion, and the first step in the siting process is always an assessment of the availability of a resource at a given location. For wind energy, this consists of assessing and measuring wind characteristics, such as speed, power, density, prevailing direction, daily and seasonal variation, long-term consistency, and so forth.

The first challenge for the wind planner in designing and developing a wind farm is to identify suitable sites. The potential sites should not only cater to the wind energy requirements, but also satisfy several environmental and socio-economic factors. The exactitude of this wind farm planning is largely dependent on the availability and accuracy of the wind and geographic data. A geographical information system (GIS) is a popular decision



© University of Pretoria

support system involving the assimilation of spatially referenced data in a problem solving environment. On the other hand, multi-criteria decision analysis provides a thorough collection of techniques and procedures for structuring, designing, evaluating and prioritising alternative decisions.

## 1.2 OBJECTIVES OF THE STUDY

The overall objective of the present work is to assess the viability of wind power generation and to develop a GIS based model to select suitable wind farm sites and apply it to the case of Saudi Arabia.

The specific objectives include:

- Conducting a wind resource assessment (WRA) of the largest industrial hub in Middle East, Jubail Industrial City.
- Determining energy output from a number of commercially available wind turbines with different rated powers.
- Predicting the wind speed over the entire country of Saudi Arabia using spatial interpolation methods using data from 29 locations spread evenly over the country.
- Developing a GIS-based model for optimal site selection to develop wind farm and apply it for the case of Saudi Arabia.

## 1.3 APPROACH TO THE STUDY

### 1.3.1 Wind resource assessment of Industrial Area

To investigate the viability of wind power generation at a given location in Jubail Industrial City, five years' worth of historical wind and other weather parameter data were obtained from the Environment and Control Department (Royal Commission for Jubail). The data were collected over a period of 5 years (2008 – 2012). At this location, the weather data are available at 10, 50 and 90 m AGL. To find the annual, seasonal and diurnal trend of wind speed at this location, the detailed wind speed statistical analysis was carried out at all three heights AGL. To find the duration and direction of wind speed in different direction bins, the rose plots were developed at all the heights. The wind data at all of the heights were fitted to Weibull distribution, and Weibull parameters were determined based on the maximum



© University of Pretoria

likelihood method. The site-specific wind shear coefficient was determined and used for the calculation of annual, seasonal and diurnal wind power density at all heights. Finally, the energy output from five different wind machines, of rated power ranging from 1.8 to 3.3 MW, was determined.

### 1.3.2 Wind resource assessment at seven different locations in Jubail.

The wind resource assessment at seven different locations in Jubail, Saudi Arabia was performed by using wind speed data measured at 10 m in height AGL at six locations and at 10, 50, and 90 m at one location only. The names of seven sites are as follows:

1. Industrial Area (Central)
2. Al-Bahar Desalination Plant
3. Pearl Beach
4. Naval Base
5. Industrial Area 2 (South)
6. Al-Reggah District
7. Industrial Area (East)

The wind data were collected over a period of five years (2008 – 2012) at all the sites, except the Naval Base station, where the data were available for three years (2010 – 2012). Detailed wind speed statistical analysis was done with rose plots at all locations. The wind data at all seven sites were fitted to Weibull distribution, and shape and scale parameters were established based on three different estimations methods, namely, maximum likelihood method, Least-Squares Regression Method (LSRM) and WAsP Algorithm. The most probable and maximum energy carrying wind speeds at all locations were determined. Finally, the energy output from five different wind machines of rated power ranging from 1.8 to 3.3 MW was determined at all sites and the most efficient wind machines, based on specific sites, were determined.



© University of Pretoria

### 1.3.3 GIS-based model for site suitability analysis

A GIS-based model has been developed to conduct site suitability analysis. The long-term historical wind data from 29 meteorological data measurements stations spread over the entire Kingdom was obtained from the Presidency of Meteorology and Environment (PME). All 29 locations are spread throughout the country. The wind speed statistics at all 29 stations at 10 m AGL have been analysed. A spatial interpolation technique, inverse distance weighted (IDW), was used to estimate the wind speed at locations where data were not available and to convert the point data into raster format. The climatic, economic, aesthetic and environmental criteria constraints, such as wind resources, accessibility by roads/highways, proximity to the national electrical grid, and optimum/safe distance from settlements and airports were applied to find suitable locations for wind farm development. Two different approaches were used in this analysis, one in which equal weightage was given to all the criteria, and the other in which different weightage was given to different criteria for site selection. Finally, wind farm suitability maps were developed based on the two aforementioned approaches.

## 1.4 ORGANISATION OF THE THESIS

The overall content of this thesis is covered in a total of eight chapters with sub-sections in each chapter. Chapter 1 contains the introduction, objectives and approaches employed in conducting this research. Chapter 2 describes the background material related to Global, Middle East and Saudi Arabian population and energy demand trends. A comprehensive literature review of global wind power scenario, wind power resource assessment, Weibull shape and scale parameters, wind power technology, energy output analysis and site suitability analysis is presented in Chapter 3. The description of data and sites is provided in Chapter 4, while Chapter 5 is dedicated to detailed wind resource assessment at Jubail. Chapter 6 provides energy yield estimation, plant capacity factor, rated and zero energy output analysis and site specific ranking of wind machines. Chapter 7 presents a GIS-based model and its application in multi-criteria wind farm site suitability analysis for the entire Kingdom of Saudi Arabia. Finally, the summary of findings, conclusions and recommendations for future work is presented in Chapter 8.



© University of Pretoria

# CHAPTER 2

## REGIONAL AND GLOBAL POPULATION AND ENERGY DEMAND PATTERNS

Historically, the increase in human population and industrial growth has been linked to an increase in demand for energy. The operation of present industrial civilisation is wholly dependent on access to a very large amount of energy of various types. If the availability of this energy was to decline significantly, it could have serious repercussions for civilisation and the human population it supports. Over the last 40 years, the per capita energy consumption has averaged about 1.5 tons of oil equivalent (toe) per person per year. As industrialisation has progressed, the amount of per capita energy has also increased, rising from a global average of 1.2 toe per person in 1966 to 1.7 toe per person in 2006. As the global energy supply tripled over that time, the population has doubled [10]. Figure 2.1 shows the close relationship between global energy consumption, world gross domestic product, Gross Domestic Product and global increase in population.

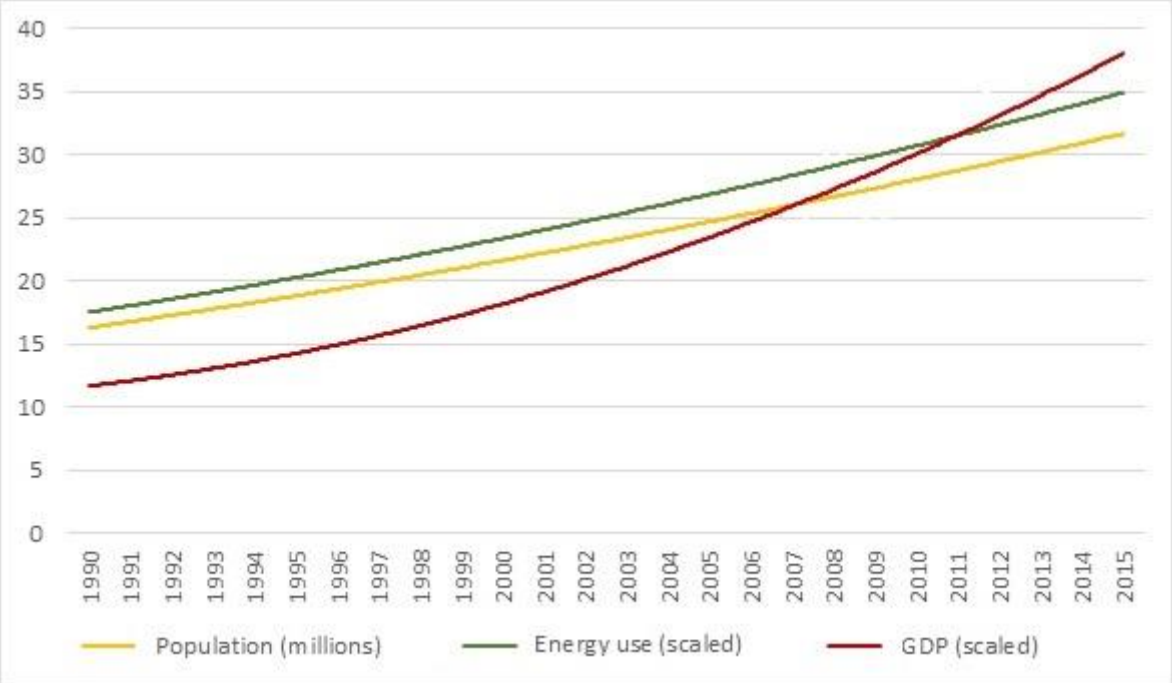


Figure 2.1 Variation in world energy, Gross Domestic Product and population [11]

The factors that relate to population growth and increasing power demands on regional, national and global levels are described in the following sub-sections.



© University of Pretoria

## 2.1 GLOBAL POPULATION AND ENERGY DEMAND PATTERNS

The world population, as of 15 February 2016, was estimated to be 7.305 billion by the United States Census Bureau [3]. The United Nations Population Fund [12] designated 12 October 1999 as the approximate day on which world population reached 6 billion. According to the estimates of United States Census Bureau [3], the world population reached 7 billion in 2012 and the new projections indicate that the 8 billion marker will be reached in 2025. That indicates that the world population has increased from 6 billion to 7 billion in approximately 13 years, as shown in Figure 2.2. A few centuries ago, the world population was less than 1 billion. Since the 18th century, the world population has seen a rapid increase, from between 1900 and 2000 the increase in world population was three times as great as the increase during the entire history of humankind – in just 100 years the world population increased from 1.5 to 6.1 billion [13].

But this development is now coming to an end, and we will not experience a similarly rapid increase in population growth over the course of this century. To see this, it is helpful to not look at the increasing total population but at the rate of growth. We already reached the maximum in 1964 when the growth rate of the world population was 2.1% per year [13]. World history can be divided into three periods of distinct trends in population growth, as shown in Figure 2.2. The first period (pre-modernity) was a very long age of very slow population growth. The second period, beginning with the onset of modernity (with rising standards of living and improving health) and lasting until 1962, had an increasing rate of growth. Now that period is over, and the third period has begun, the population growth rate is now falling.

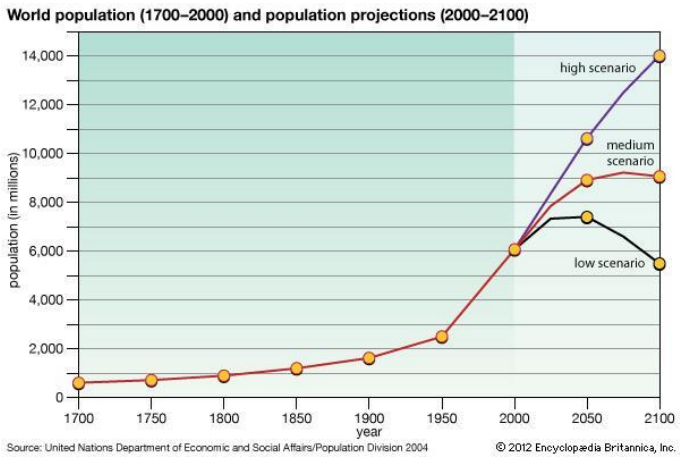


Figure 2.2 World population growth trends and future projections [12].



© University of Pretoria

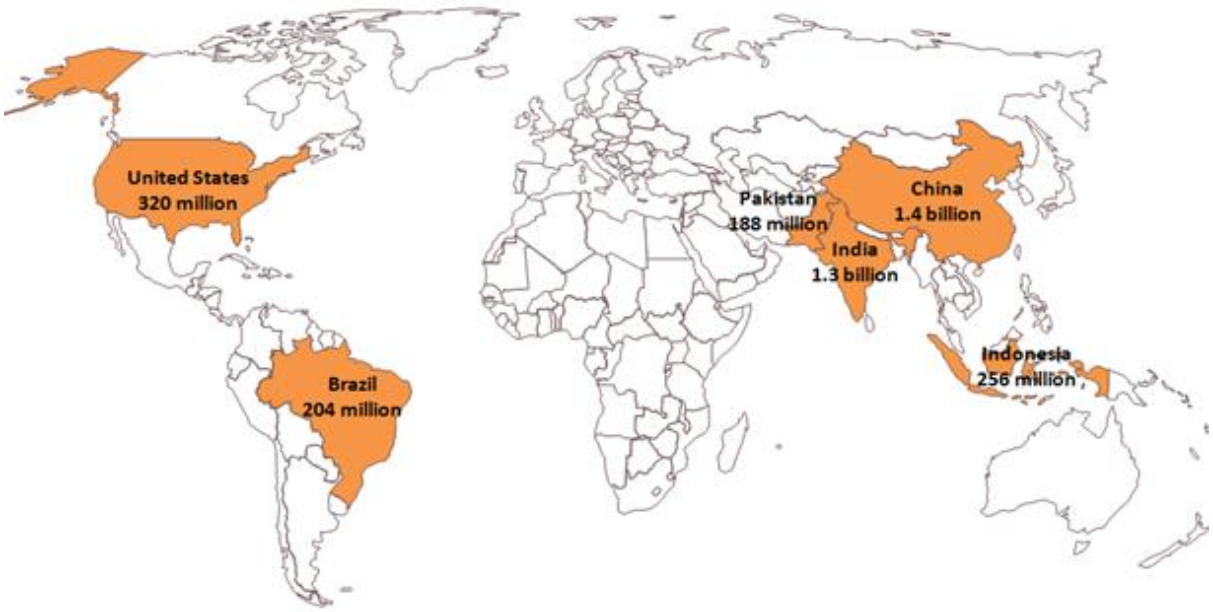


Figure 2.3 The population of six most populated countries. [13].

As shown in Figure 2.3, half of the world's population, currently lives in just six countries: China, India, the United States, Indonesia, Brazil and Pakistan with populations of approximately 1.4, 1.3, 0.32, 0.256, 0.204 and 0.188 billion respectively. However, the population of some countries is not even known to the nearest million, so there is a considerable margin of error in such estimates. The recent historical and predicted trend of the global population is shown in Figure 2.4. The prediction model is mainly based on the long-term aggregate effects of energy decline [10]. The predicted trend of declining population and energy in Figure 2.4 is in-line with the low scenario world population projection, depicted in Figure 2.2. The declining population scenario is based mainly on the long-term aggregate effects of energy decline. The mechanisms of the population decline it projects are not specified. However, it is likely that they will include such things as major regional food shortages, a spread of diseases due to a loss of urban medical and sanitation services and an increase in deaths due to exposure to heat and cold [10]. The recent historical and predicted trend of global energy consumption is shown in Figure 2.5. The current global total energy use is about 1.7 toe per person per year, and in the model that declines evenly to a consumption of 1.0 toe per person per year by 2100 [10].

Figure 2.5 has all the energy curves added together to illustrate the overall shape of the total world energy consumption. As you can see, fossil fuels are by far the most important contributors to the world's current energy mix, but all three are in rapid decline by the second



© University of Pretoria

half of the century. Hydro and renewables are making respectable contributions by mid-century, while nuclear power plays a constant role. By the end of the current century, oil and natural gas will have dropped out of the picture almost entirely, while the dominant players will be hydro, renewable sources, coal and nuclear power, in that order. This graph aggregates all the rises, peaks and declines to give a sense of the complete energy picture out to 2100. The graph shows a strong peak in approximately 2020, with a steepening decline out to 2100. The main reason for the decline is the loss of oil, gas, and (to a lesser extent) coal. The decline is cushioned by an increase in hydro and renewables over the middle of the century, and averages out to a little less than 3% per year [10].

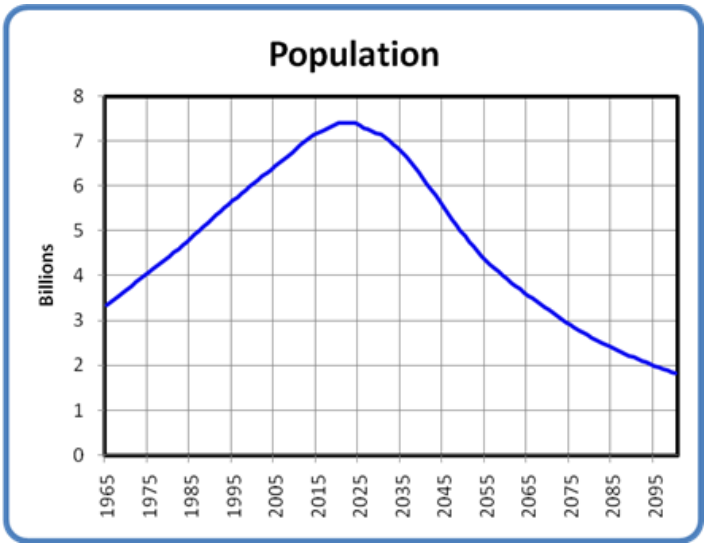


Figure 2.4 World Population with Declining Energy, 1965 to 2100 [10].

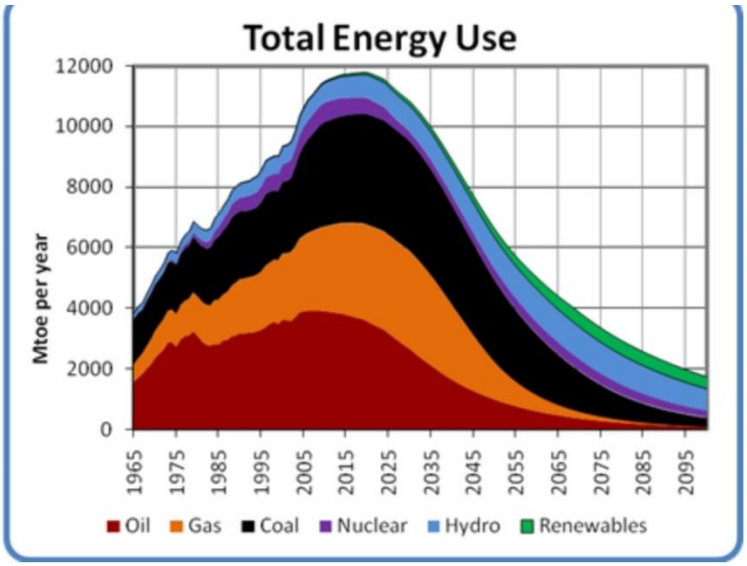


Figure 2.5 Total Energy Use, 1965 to 2100 [10].



© University of Pretoria

Unfortunately, the loss of the enormous contribution of fossil fuels means that the total amount of energy available to humanity by the end of the century may be less than one-fifth of the amount we use now, and less than one-sixth the amount we will use at our energy peak, a decade or so from now.

## 2.2 MIDDLE EAST POPULATION AND ENERGY DEMAND TRENDS

The United States Census Bureau estimates that the Middle East is a region where the population will nearly double between now and 2030. From 1950 to 2000, the Middle East experienced an explosive population growth. The region's population grew from 92 million to 349 million, a 3.8-fold increase, or 2.7% a year [14]. The total population of the Arabian Gulf has grown from 30 million in 1950 to 39 million in 1960, 52 million in 1970, 74 million in 1980, 109 million in 1990, and 139 million in 2000. Conservative projections put it at 211 million in 2020, 249 million in 2030, 287 million in 2040, and 321 million in 2050 [14].

Rapid population growth in the Middle East and North Africa (MENA) carries serious implications for employment, access to services and the cost of subsidies along with energy needs. Population data for MENA is extremely sensitive and needs to be treated cautiously [15]. Nonetheless, it is clear that since the 1970s, MENA has experienced a dramatic rise in population compared to other parts of the developing world. The result has been that the region's population has grown from 127 million in 1970 to 305 million in 2005. For example, in the 10 years between 1976 and 1986, the population of Iran grew by 50%.

The energy consumption in the Middle East was 366 TWh in 1997 (see Figure 2.6), which reached to 614 TWh in 2010, and it is expected to reach more than 900 TWh in 2020, an increase of about 50% within next 10 years. According to a report in 2001 [15], the respective total power installed capacity of Bahrain, Kuwait, Oman, Qatar, Saudi Arabia and the United Arab Emirates was 1.1, 8.5, 2.4, 1.5, 26.6 and 5.6 GW, respectively, and the energy consumption was reported as 6.19, 32.33, 8.05, 9.15, 126.01 and 36.54 TWh, respectively. The energy demands are increasing at 3 to 5% per annum in Gulf Cooperation Council (GCC) countries.



© University of Pretoria

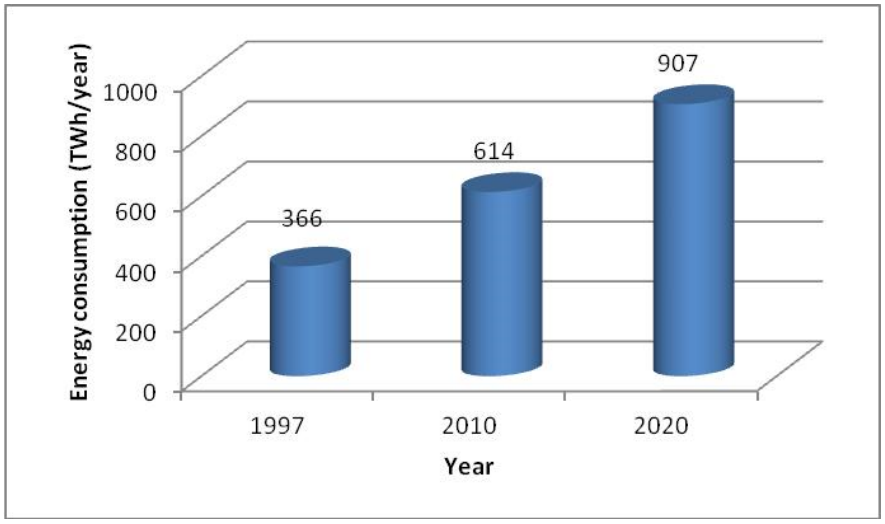


Figure 2.6 Annual consumption of energy in Middle East countries [15].

## 2.3 SAUDI ARABIAN POPULATION AND ENERGY DEMAND TRENDS

Saudi Arabia is a vast country with a total area of 2,149,690 $km^2$ and it has an international boundary of 4,431 km (bordering countries: Iraq 814 km, Jordan 744 km, Kuwait 222 km, Oman 676 km, Qatar 60 km, UAE 457 km, and Yemen 1,458 km). Most of the cities and villages are either connected to the national electrical grid or to the isolated grids. Most of the remotely located villages get power through diesel power generating plants. It is extremely cumbersome to maintain a regular supply of fuel and to ensure the continuous electricity supply during breakdowns and scheduled shutdowns of the diesel units.

Saudi Arabia is experiencing rapid population, industrial and agricultural growth, subsequently resulting in an ever increasing demand on power and water supplies. The total population of Saudi Arabia increased by more than five times within the last four and a half decades, from 5,772,000 in 1970 to 30,770,375 in 2014, as shown in Figure 2.7 [6]. The number of operating industries has increased by more than 30 times within the last four decades, from 198 in 1974 to 6,471 in 2013 [7]. The total Gross Domestic Product (in constant prices) achieved by the manufacturing industries increased from US $4 billion in 1975 to more than US $45 billion at the end of 2013. Also, the growth rate of the manufacturing industries continued to increase throughout this period, at an average of 6% per annum, which is considered to be one of the highest among the other economic sectors [7].



© University of Pretoria

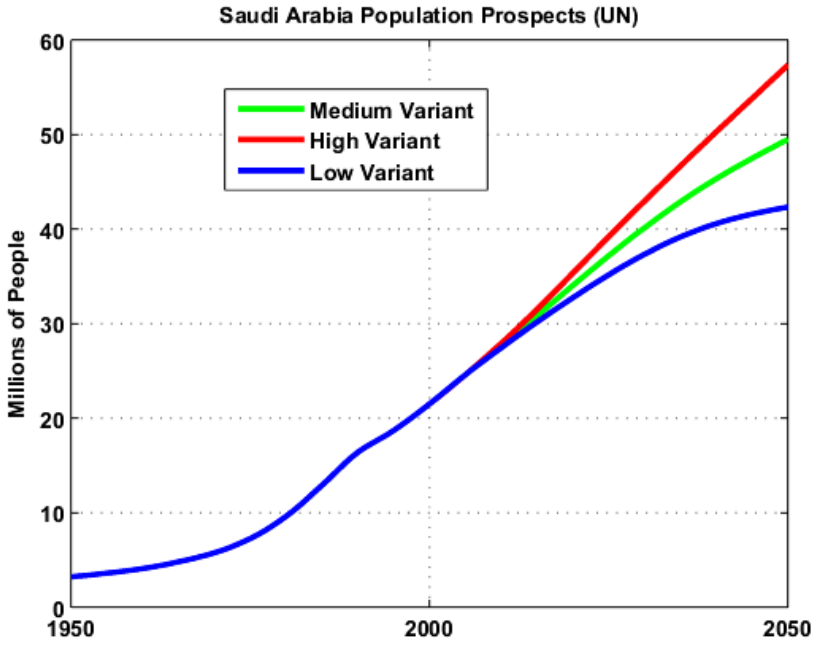


Figure 2.7 Saudi Arabian population, History and forecast [6].

Manufacturing industries in the Kingdom have witnessed a steady progress over the past years. As shown by Figure 2.8 below, the total Gross Domestic Product (in constant prices) achieved by the manufacturing industries increased from the level of SR 15 billion in 1975 to more than SR 171 billion at the end of 2013. Also, the growth rate of the manufacturing industries continued to increase throughout this period at an average of 6% per annum, which is considered one of the highest among the other economic sectors. Owing to the substantial growth achieved by the manufacturing industries during this period, the contribution of the sector in the country's Gross Domestic Product has increased from 4.1% in 1975 to 13.5% at the end of 2013. Also, the contribution of the manufacturing industries sector in the non-oil Gross Domestic Product increased from 7.7% in 1975 to 17% in 2013. These rates show the success of the development plans in pushing forward the industrial progress and the fruitful cooperation these plans have received from the private sector [7].

A more important aspect in the development of the manufacturing industries in the Kingdom is indicated by the change that occurred in the sectoral composition of Saudi manufacturing over the past period, as the share of the manufacturing industries (other than oil refining) in manufacturing Gross Domestic Product increased from (57%) in 1975 (at constant prices) until it reached (87%) by the end of 2013. This trend reflects the dynamism of the Saudi manufacturing industries sector (other than oil refining). In this regard, we refer in particular to the substantial progress and expansion experienced by the petrochemical industries in the



© University of Pretoria

Kingdom over the last two decades under the auspices of SABIC, Saudi Basic Industries Corporation [7].

The statistics and analysis made by SIDF, Saudi Industrial Development Fund show that the Gross Domestic Product's mix for the manufacturing industries sector (excluding oil refining) has been a subject of a substantial growth throughout the past two and half decades. Since the early nineties, the Chemical Products Sector has been occupying the leading position of the Gross Domestic Product's mix of manufacturing industries (excluding oil refining). In the past two and a half decades, the manufacturing sector's Gross Domestic Product increased from 10.5 to 45 thousand USD (40 to 170 thousand Saudi Riyal, SR). Other sectors that have been showing a notable growth include: Machinery and Equipment, Building Material Products, and Food Products. At present, these four sectors contribute to the major part of the Saudi manufacturing industries' Gross Domestic Product [7].

The total energy consumption in Saudi Arabia from 2000 to 2014 is shown in Figure 2.9. It can be observed that from 2000 to 2014, the total energy consumption increased from 126,191 to 311,807 GWh, an increase by 2.5 times in the last one and a half decades [16].

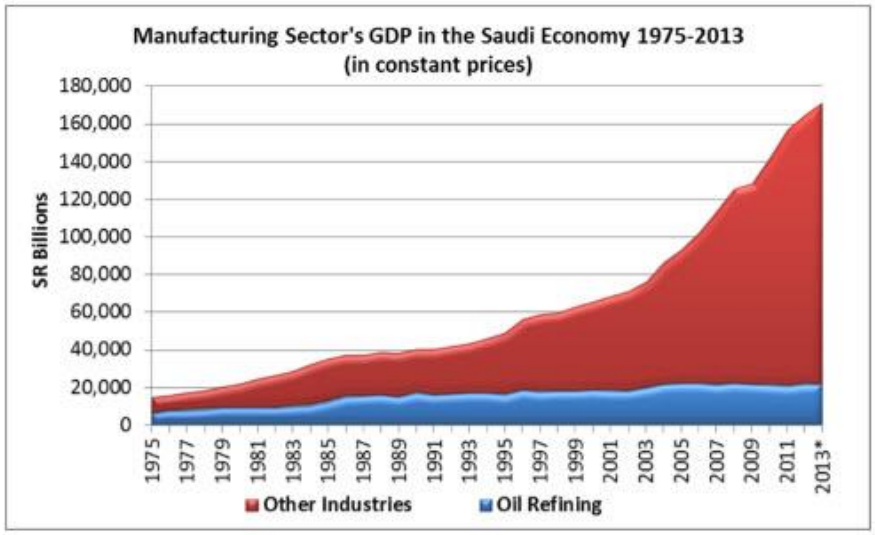


Figure 2.8 Total Gross Domestic Product (in constant prices) achieved by the manufacturing industries [6].



© University of Pretoria

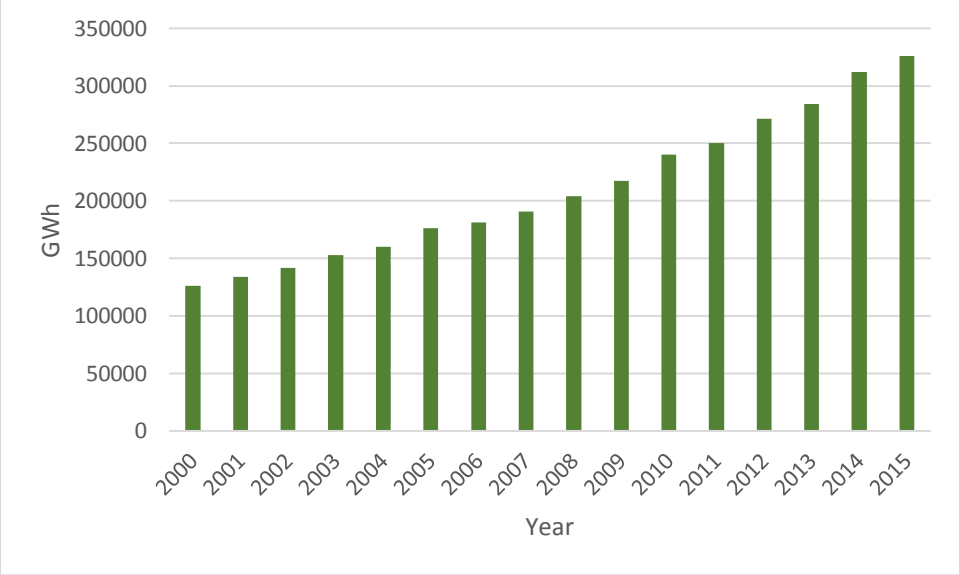


Figure 2.9 Total energy consumption (GWh) in KSA [16].

In Saudi Arabia, the per capita energy consumption has reached 9,000 kWh in 2014, compared to 5,500 kWh in 2000, as shown in Figure 2.10 [16], an increase of around 65% in one and a half decades. The per capita electricity consumption in Saudi Arabia is three times the world average [17]. Saudi Arabia requires investments worth $150 billion to meet growing electricity requirements in the next 10 years. The housing sector consumes about half of the electricity supply, followed by industries that consume 21% the trade sector 15% and government facilities 12%. Currently, the government provides subsidised fuel worth $40 billion to the Saudi Electricity Co. for power generation [17].

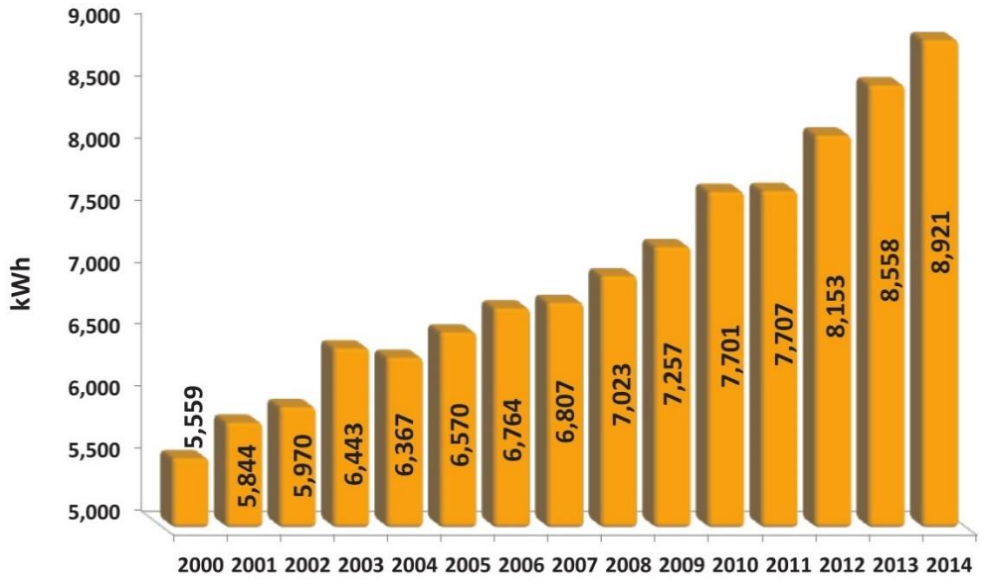


Figure 2.10 Trend of per capita annual energy consumption in Saudi Arabia [16].



© University of Pretoria

The total annual capacity and peak load from 2000 to 2014 is shown in Figure 2.11. The total capacity at the end of the year increased from 25,800 MW in 2000 to 65,500 MW in 2014, an average annual increase of 2,835 MW [16].

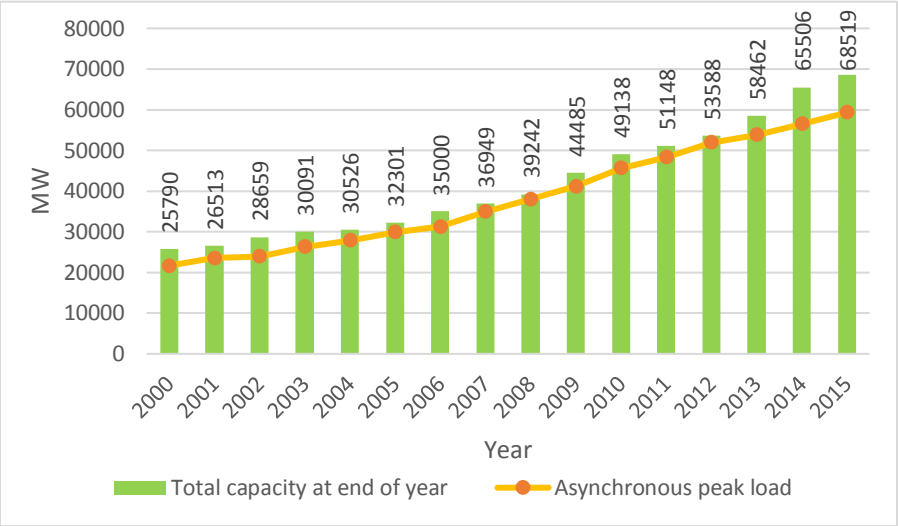


Figure 2.11 Peak load and total available electricity capacity in Saudi Arabia [16].

Crude oil is a fossil fuel that primarily consists of hydrocarbons and lesser amounts of sulphur, nitrogen and oxygen extracted from the oil wells. Diesel oil and heavy fuel oil, HFO are residual fuel acquired during the distillation of crude oil at different temperatures. Heavy fuel oils are mostly used as marine fuel, whereas, diesel is used in road transport, agriculture, shipping, and rail transport. The annual consumption of all the three variants i.e. crude oil, HFO and diesel during the past one and half decade in Saudi Arabia is depicted in Figure 2.12 [16]. Even though, the consumption of diesel has witnessed steady increase during the last one and half decade, the consumption of crude oil increased substantially from 2008 to 2010, this is mainly due to increased refining of crude oil locally, subsequently decreasing HFO consumption. Saudi demand for crude is exacerbated by fast growth in the power generation sector, where low, subsidised electricity prices have encouraged consumption and waste. Saudi Arabia has vast open land and is the largest producer and supplier of fossil fuels in the world but still encourages the utilisation of clean and renewable sources of energy [18].



© University of Pretoria

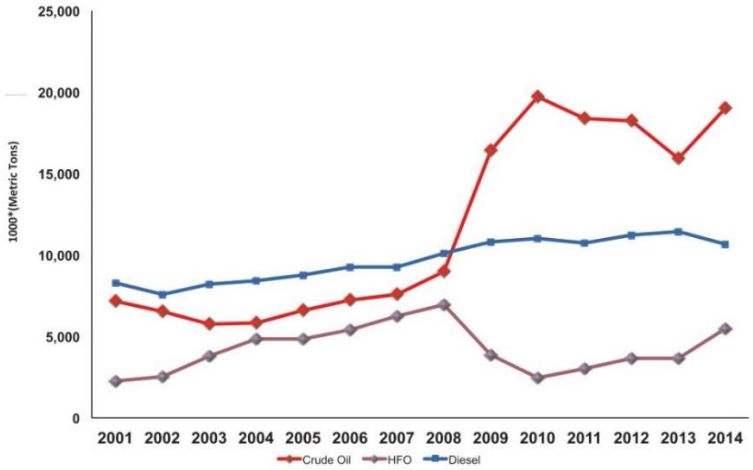


Figure 2.12 Annual resources consumed (thousand toe) in Saudi Arabia [16].

The Kingdom will experience higher demands of energy in the coming future and it has to meet these demands and at the same time keep the atmosphere clean. Therefore, to minimise the addition of pollutant gases into the atmosphere, new and renewable sources of energy are being sought to meet the increasing power demands. The power of the wind can be utilised to partially supplement the existing national grid. For wind power development, an accurate knowledge of the availability of wind and its intensity over the year is a must.

## SUMMARY

This chapter discussed the population and electricity demand growth on global, Middle East and Saudi Arabian level. The percentage of increasing rates of population and energy are alarming on all scales, particularly in the Middle East and Saudi Arabian region. These trends dictate the community to utilise and develop new and renewable sources of energy on all levels. Saudi Arabia is not an exception. This effort has to be extended to the point where we see some real time visible wind power working projects in Saudi Arabia.



© University of Pretoria

# CHAPTER 3

# LITERATURE REVIEW

A comprehensive literature review has been carried out in order to comprehend the advances of the current research topic. In this study, a large number of research papers published in international journals, official reports and articles published by organisations from the energy sector have been reviewed to provide an update on the state-of-the-art of wind energy technology and current global wind energy planning procedures. More specifically, the study sought answers to the following questions. What is the global wind power installed capacity and its growth rate? What has been done in wind resource assessment (WRA) world-wide, and how? What are the world renowned and accurate practices in the estimation of wind energy? What are the wind farm site suitability analysis practices and how is the site-specific model developed? A detailed review of the literature related to the topics aforementioned is provided in the following sections.

## 3.1 GLOBAL WIND POWER SCENARIO

Total investments in the renewable energy sector in 2015 reached a record US $329 billion, up 4% from 2014's investment of US $316 billion and beating the previous record set in 2011 by 3% [19]. In 2015, the annual wind power new installations crossed the 60 GW mark for the first time in history, and more than 63 GW of new wind power capacity was added. The second-highest global annual increase in new wind power installations of 51.7 GW was set in 2014. At the end of 2015, total global installed wind power capacity reached 432.9 GW, from 369.7 GW in the previous year, representing a growth of 17%. The global new and existing annual installed wind power capacity from 2000 to 2015 is shown in Figure 3.1. In 2013, there was a sudden decrease in the capacity addition, due to the global economic crisis, but the growth was recovered again in 2014. There was a 25-fold increase in global cumulative installed wind power capacity in last 15 years as shown in Figure 3.1 [19].



© University of Pretoria

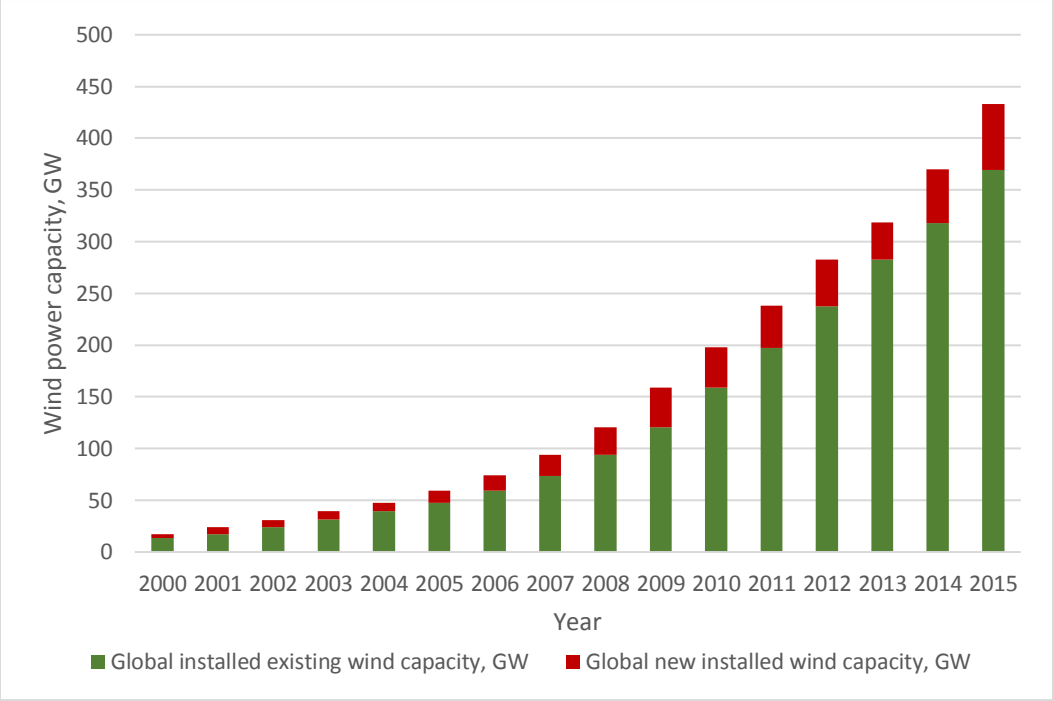


Figure 3.1 Global installed wind power capacity, 2000 – 2015 [19].

The region-wise percentage share of the global installed wind power capacity is presented in Figure 3.2 [8]. Installations in Asia again led global markets, with Europe and North America in second and third place, respectively. The installed wind power capacity in Africa and the Middle East was just 1% of the global installed capacity by the end of 2015. Figure 3.3 shows the annual installed capacity by region during the years 2007 to 2015 [8]. Therefore, Saudi Arabia is exploring alternate sustainable and reliable sources of energy for generating power and reducing consumption of the nation's fossil fuel reserves [9]. Thus, it was determined that a balanced energy mix of alternative and conventional energy is strategically important to Saudi Arabia's long term prosperity, energy security and its leading position in the global energy market [9]. Wind energy utilisation is one of the renewable energy options Saudi Arabia is considering seriously.



© University of Pretoria

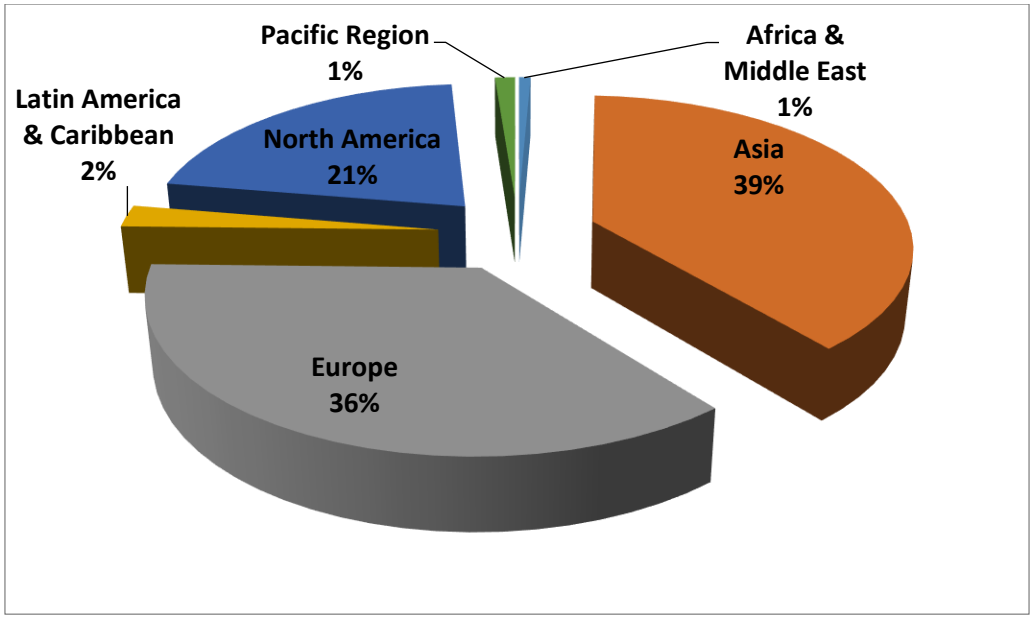


Figure 3.2 Regional distribution of percentage of global installed wind power capacity, 2015 [8].

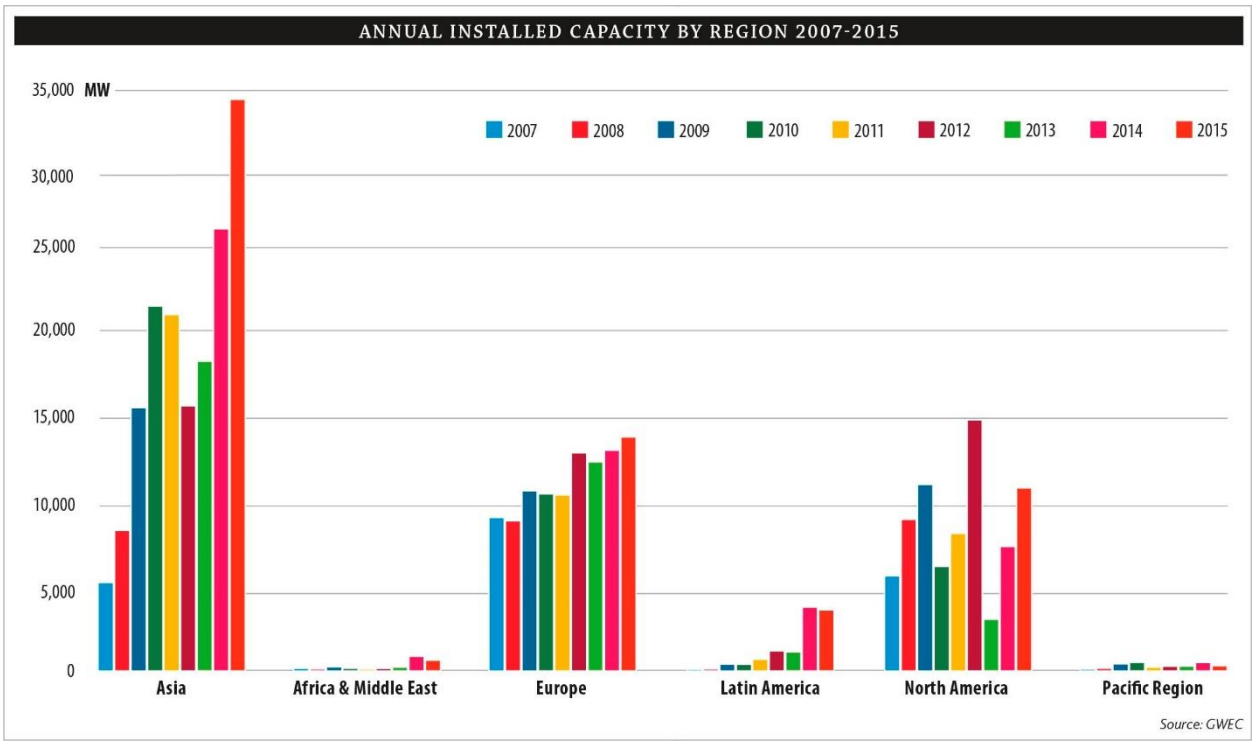


Figure 3.3 Annual installed capacity by region, 2007 to 2015 [8].



© University of Pretoria

## 3.2 WIND RESOURCE ASSESSMENT

Meteorological parameters, such as wind speed, wind direction, temperature, relative humidity, barometric pressure, global solar radiation and so forth, are site and time dependent in general, while wind speed and wind direction are highly fluctuating components among these parameters. Hence, it is necessary and critical to understand the wind speed variability and availability during different hours of the day and different months of the year for successful and profitable development and utilisation of wind power. Thus, it is required to perform a wind resource assessment of the site of interest to determine the feasibility of the wind farm development. Moreover, a small error in wind speed data gives a large error in energy yield calculations. Hence, accuracy in wind speed measurements can minimise the risk of huge investments [21].

The wind speed measurements are typically made at a different and lower height compared to the wind turbine hub height. The wind speed increases with height by a site-dependent power factor known as wind shear exponent (WSE). Wind speed can be extrapolated to the hub height by using the wind power law in conjunction with the local WSE. If the estimated WSE is not accurate, the wind power law will lead to an error in the calculation of the wind speed at hub height and consequently the energy yield estimation [25]. Air density is another critical parameter that depends on local air pressure and temperature at the site and directly affects the wind power density (WPD) and hence the energy yield estimate. Therefore, the actual air density should be calculated using the local pressure and temperature measurements for accurate energy output estimation [21].

To optimise the design of a wind turbine, data on the speed range over which the turbine must operate to maximise energy extraction is required. This in turn requires the knowledge of the frequency distribution of the wind speed. Masseran et al. [22] presented nine frequency distribution functions suitable for fitting wind data: Weibull, Burr, Gamma, Inverse Gamma, Inverse Gaussian, Exponential, Rayleigh, Lognormal and Erlang. Rehman and Halawani [23] fitted the wind speed data of 10 locations in Saudi Arabia to Weibull distribution function and concluded that this distribution accurately describes the wind data of this region. Similar studies elsewhere also claim that among all the frequency distribution functions that have been proposed for wind speed, the two-parameter Weibull distribution is most widely used to accurately describe wind regimes [24, 25, 26].



© University of Pretoria

Various studies on wind resource assessment are reported for Saudi Arabian locations. In 1986, Ansari et al, [27] developed a wind atlas for Saudi Arabia by using measured wind speed at 8 to 12 m in height AGL for 20 different locations. The hourly mean wind speed and direction data during the period 1970–1982 was used to develop the wind atlas. This atlas showed the seasonal average wind speed contours in different months over the entire Kingdom. The long term annual mean wind speed was found to be below 4 m/s in most of the regions. However, the data used were not reliable enough to determine the wind potential because the sensors were mounted at a height of 8 to 12 m, and the weather stations were located at low windy sites, like airports. This wind atlas, which was the first effort towards wind resource assessment, also included the wind speed frequency distribution in different wind speed bins and the wind rose diagrams [27]. To better understand the wind power potential in the Kingdom, in 1996, Alawaji et al. [28] performed wind speed measurements at 20, 30 and 40 m AGL at different locations in the Kingdom. In this study, six anemometers were installed on every wind tower, two each at 20, 30 and 40 m in height to get reliable results. The annual average wind speed at 40 m AGL at Arar, Dhahran, Gassim and Riyadh was reported to be 5.3, 4.5, 4.0 and 4.5 m/s, respectively [28]. Wind shear coefficients of wind speed at 20, 30, and 40 m AGL for Dhahran, Saudi Arabia was determined by Rehman and Al-Abbadi [21]. In this study, the energy yield was found to be around 120,000 MWh/year from a wind farm of 60 MW installed capacity consisting of 40 wind turbines, each of 1500 kW rated power with a plant capacity factor of 24% [21]. In similar studies conducted by Shaahid et al. [29] at Taif, the wind speed was found to be less than 3 m/s for 46% of the time during the year. The annual energy produced from 15 MW wind farm (from 25 commercially available wind turbines of 600 kW rated power capacity each at 50 m hub height) was around 20,000 MWh/year. The cost of energy, COE in this analysis was found to be 0.0576 US$/kWh. [29].

Some of the wind resource assessment studies reported for different countries were reviewed and discussed below. Prasad et al. [30] performed an extensive literature survey on wind resource assessment (WRA) and discussed different WRA techniques. This methodology included a preliminary wind survey to choose the best site for installing wind speed sensors, potential site selection, selecting the optimum wind turbine suitable for a site and the uncertainties involved in estimating the wind resource assessment using the different techniques. It was concluded that each WRA technique has its own advantages and selection of optimum technique is site dependent.



© University of Pretoria

Fazelpour et al. [31] employed the Weibull probability distribution function for WRA using mean wind data at 10 m AGL over a six-year period at Tabriz and Ardabil, Iran. The hourly, diurnal, seasonal, monthly, and annual wind speed variations were analysed. The yearly values of the Weibull shape parameter vary from 1.81 to 2.13 m/s with a mean of 1.99 m/s for Tabriz, and from 2.62 to 2.98 m/s with a mean of 2.86 m/s for Ardabil. Also, yearly values of the Weibull scale parameter vary from 3.35 to 4.45 m/s with a mean of 4.18 m/s for Tabriz, and from 3.68 to 4.55 m/s with a mean of 4.16m/s for Ardabil. The results show that the highest wind power potential occurs during the months of August and July in Tabriz, and October and September in Ardabil.

Komleh et al. [32] analysed the wind speed data of Firouzkooh, Iran. For this purpose, 10-year period (2001-2010) wind data were analysed to estimate the wind power generation potential. Weibull and Rayleigh distribution functions were applied to find out the best fitting tool to the wind speed data. Results showed that Weibull and Rayleigh distribution functions can fit the values of wind speed well with almost the same coefficient of determination value of 0.97. The average values of wind power density based on mean and root mean cube speed approaches were 203 and 248 W/m$^2$/year, respectively.

Chandel et al. [33] assessed wind resource potential of the western Himalayan Indian state of Himachal Pradesh. Weibull parameters and WPD were determined for these locations. The highest daily mean wind speeds were observed in summers and lowest in winters in the region. Wind shear analysis showed that wind speeds at 30 m, 50 m, 80 m and 100 m hub heights were found to increase by 10-17%, 26%, 34% and 39%, respectively, than those measured at 10 m in height. The mean wind speed and WPD for the 12 locations were found to be in the range 3.9-4.7 m/s, 4.7-5.8 m/s, 5.7-7 m/s, 6.2-7.7 m/s and 14.09-22. W/m$^2$, 52.67-82.79 W/m$^2$, 97.23-152.82 W/m$^2$, 170.9-268.62 W/m$^2$, 223.37-351.1 W/m$^2$ at 30 m, 50 m, 80 m and 100 m in heights, respectively, thereby indicating fairly good wind potential for rooftop micro-wind turbines, battery charging, water pumping and wind power generation in the western Himalayan region.

For wind resource assessment of Selcuk University campus in Turkey, one year worth of wind data at three different heights was analysed [34]. Energy output from a 6 MW installed capacity wind farm composed of 1.0, 1.5, and 2.0 MW rated power wind turbines was calculated and reported by Faruk et al. [34]. The minimum basic payback period was found to be 6.44 years. Wind characteristics of six locations in Turkey were analysed using the wind



© University of Pretoria

speed data during the period 2000–2006 by Ucar et al. [35]. The annual mean wind speed of the six stations fell in the range from 5.9 to 8.7 m/s at 10 m in height. The mean annual value of Weibull shape parameter *k* was between 1.71 and 1.96 while the annual value of scale parameter *c* was between 6.81 and 9.71 m/s. A technical assessment of electricity generation from four wind turbines of rated capacities of 600 kW, 1000 kW, 1500 kW and 2000 kW was made by Ucar et al. The annual energy obtained from 2000 kW rated power wind turbine was in the range of 4250 to 6900 MWh with a plant capacity factor between 24 to 39% at these six locations.

Jowder [36] assessed the wind power potential of the Kingdom of Bahrain by analysing hourly wind speed data for two years at 10 m in height. The measured wind speed data at 10 m was extrapolated to 30 m and 60 m in heights using the wind power law with WSE of 0.409. The average annual wind power density was 114.54 W/m$^2$ at 10 m in height, 433.29 W/m$^2$ at 30 m in height and 816.70 W/m$^2$ at 60 m in height. Fyrippis et al. [37] conducted the wind power potential assessment of Koronos village, Greece, using measured wind data at different heights and studied the wind characteristics using the Weibull and Rayleigh distribution functions. The annual mean wind speed was found to be 7.4 m/s and the corresponding wind power density was 420 W/m$^2$ at 10 m AGL. The results revealed that the Weibull model adequately fitted the actual experimental wind speed data.

The wind energy potential was estimated by Gao et al. [38] using five types of mixture probability functions for 11 years of measured wind data in Hong Kong. Based on the WRA, they identified and selected a potential offshore area for the development of the wind farm. The authors used multi-population genetic algorithm (MPGA) for getting minimum COE with maximum power output. The study found annual offshore wind power potential of 112.81×108 kWh which accounted for 25% of the total annual power consumption of Hong Kong in 2011. Onea et al. [39] presented the wind resource assessment of the north-western side of the Black Sea using measured wind speed data over a period of 11 years. The analysis indicated that the Romanian coastal region had more wind energy potential during the winter season, with an average annual wind speed of about 9.7 m/s at 80 m and a power density of 870 W/m$^2$. This study concluded that the north-western side of the Black Sea was a promising site for the wind farm development. Thus, wind resource assessment studies have been conducted in many parts of the world and reported in the literature. Some of the similar studies reported for countries such as Korea [40], China [41], Malaysia [42], India [33],



© University of Pretoria

Kyrgyzstan [43], Pakistan [44], Oman [45], Turkey [46], Algeria [47], Iran [48], Egypt [49], Nigeria [50], Greece [51], Mexico [52], USA [53] and Venezuela [54] were reviewed to assess the methodology and techniques used for WRA.

## 3.3 WEIBULL FREQUENCY DISTRIBUTION AND ESTIMATION OF PARAMETERS

Wind speed frequency distribution is an important statistical tool in predicting the wind energy output at a particular location [23]. In most of the locations worldwide, the Weibull distribution function is found to represent the variable nature of wind speed better than other distributions [24, 25, 26, 55]. The Weibull function is a two-parameter function, namely, shape parameter, $k$ and scale parameter, $c$. The scale parameter, $c$ in m/s, is indicative of mean wind speed and $k$ is the dimensionless shape factor, which describes the shape and width of the distribution. The Weibull distribution is therefore determined by the parameters, $c$ and $k$. There are several methods available in the literature for the determination of these two parameters. Stevens and Smulders [56] found the values of $k$ and $c$ by five different estimation methods, namely, method of moments, method of energy pattern factor, maximum likelihood method, Weibull probability paper method and percentile estimators. Almost same values were obtained by all five methods.

Seguro and Lambert [57] calculated the Weibull parameters using the maximum likelihood method, graphical method and modified maximum likelihood method. It was reported that when wind speed data are available in time-series format, the maximum likelihood method is the recommended method for estimating the parameters. When wind speed data are available in frequency distribution format, the modified maximum likelihood method is the recommended method. The graphical method is reported to be the least accurate. Bagiorgas et al. [58] calculated the Weibull parameters using the wind data from seven different sites in Saudi Arabia. The parameter estimation methods used were least-squares regression method, method of moments, alternative maximum likelihood estimation method, maximum likelihood method, and WAsP Algorithm. The calculated values using the five different methods were found to be in good agreement at all the measurement heights. The correlation between the monthly mean values of Weibull scale parameter and the measured wind speed values was found to be linear at all the sites.



© University of Pretoria

Rocha et al. [59] compared seven numerical methods for determining the Weibull parameters at the northeast region of Brazil. The estimation methods were the graphical method, maximum likelihood method, energy pattern factor method, moment method, empirical method, modified maximum likelihood method, and equivalent energy method. The equivalent energy method was found to be efficient for determining the *k* and *c* parameters to fit Weibull distribution curves for wind speed data. Akdag and Dinler [60] developed a new method called the power density method for the estimation of Weibull parameters. This new method was compared with graphic, maximum likelihood and moment methods and it was concluded that the power density method is suitable and efficient for Weibull parameters estimation for the given location.

Wind speed assessment of six sites in the island of Crete, Greece was reported by Deligiorgi et al. [51]. The effect of topographical features on wind characteristics was studied. The Weibull, Rayleigh, Lognormal, Gamma, and Inverse Gaussian distributions probability distributions were examined for their ability to model the wind speed frequency distributions. The most efficient methods for the estimation of the distribution parameters were found to be moment method, maximum likelihood method, and least-squares method. For the wind resource assessment of Selcuk University campus in Turkey, one year worth of wind data at three different heights was analysed [34]. The energy output from a 6 MW installed capacity wind farm composed of 1.0, 1.5, and 2.0 MW rated power wind turbines was calculated and reported by Ukar et al. [35]. The minimum basic payback period was found to be 6.44 years. Onea et al. [39] presented the wind resource assessment of north-western side of the Black Sea using measured wind speed data over a period of 11 years. The analysis indicated that the Romanian coastal region has more wind energy potential during the winter season, with an average annual wind speed of about 9.7 m/s at 80 m and a power density of 870 W/m$^2$. This study concluded that the north-western side of the Black Sea is a promising site for the wind farm development.

## 3.4 GIS-BASED PRIORITISING OF WIND FARM SITES

The first challenge for the wind planner in designing and developing a wind farm is to identify suitable sites for wind farm development. The potential sites should not only cater to the wind energy requirements, but also satisfy several environmental and socio-economic factors. The exactitude of this wind farm planning is largely dependent on the availability and accuracy of the wind and geographic data. GIS is a popular decision support system



© University of Pretoria

involving the assimilation of spatially referenced data in a problem solving environment. On the other hand, multi-criteria decision analysis provides a thorough collection of techniques and procedures for structuring, designing, evaluating and prioritising alternative decisions.

To assess the eminence of GIS-based multi criteria decision making analysis, Malczewski [61] conducted a comprehensive literature review to find out the number of refereed journal papers published on this topic from 1990 to 2004. A total of 319 articles were published out of which around 60 were published in the initial 10 years, from 1990 to 2000 and the remaining 259 in only four years, from 2000 to 2004. Many of the GIS-based multi-criteria decision making analyses for identifying locations for renewable energy resources are reviewed in this study. Omitaomu et al. [62] presented an approach which takes inputs, such as water bodies, environmental indicators, population and tectonic and geological hazards to provide an in-depth analysis for power generation siting options. Rodrígueza et al. [63] presented a GIS-based methodology to assess solar and wind energy potential of islands and small regions worldwide. This methodology takes into account territorial constraints, as natural protected area, urban areas or even an isolated house, and techno-economic constraints as minimum wind speed or maximum slope. This methodology was applied to a practical case, the Canary Islands, a Spanish archipelago located just off the southern coast of Morocco, and the results provide relevant data that can also be useful for similar regions.

In general, GIS method has been used for biomass assessment and site selection of biomass based power plants (Viana et al. [64], Höhn et al. [65], Comber et al. [66]), hydropower potential assessment (Kusre et al. [67]) in India, coal fired power plant and site selection (Xu et al. [68]), and for photovoltaic based power plant optimisation and site identification (Kucuksari et al. [69]), to name a few applications. In particular, the use of GIS-based multi-criteria decision making analysis for planning of wind farms gained significant interest in early 2000's and hence, being utilised in several countries like Turkey [70], Greece [71], Denmark [72], USA [73], UK [74], Germany [75], Poland [76], Vietnam [77] and Sweden [78].

The layers (restriction criteria) used for the GIS-based multi-criteria decision making for the afore-mentioned studies is detailed in Table 3.1. Aydin et al., and Hansen [70, 72] represented the criteria (economic, planning and ecological) as fuzzy sets by first defining the maximum and minimum restriction ranges and then giving a tolerance limit from 0 to 1 between these ranges. Latinopoulos & Kechagia [71], developed a tool for wind-farm



© University of Pretoria

planning at the regional level. Siting criteria, mentioned in Table 3.1, were used either as restrictions and/or as assessment factors so as to identify the best sites for wind farms and then to evaluate these sites using a combined suitability index. Haaren & Fthenakis [73] estimated the cost of electricity grid construction as a function of distance to the nearest electricity line or substation, whereas all other studies applied a restriction of a critical distance from the grid after which the wind farm siting is unsuitable. Baban & Parry [74] applied criteria restrictions, as shown in Table 3.1, using two different methods. In the first method, all the criteria were considered as equally important and in the second, the criteria were grouped and graded according to perceived importance. The final suitability maps, composed of 11 classes, with zero as the most ideal location and 10 as most unsuitable location for wind farm, were developed.

Table 3.1 Literature review of restriction criteria (unsuitable land) from nine wind farm site selection studies.

| **Study Criteria** | **Economic** | | | **Planning** | | | **Ecological** | |
|---|---|---|---|---|---|---|---|---|
| | Wind potential | Proximity to electricity grid, m | Proximity to roads & highways, m | Buffer distance from forests & parks, m | Buffer distance from airports, m | Buffer distance & proximity from settlements, m | Buffer distance from lakes & rivers, m | |
| **Turkey** | 200–400 W/m$^2$ | × | × | 3,000-6,000 | 3,000-6,000 | 1,000-2,000 | 2,500-5,000 | Aydin et al. [70]* |
| **Greece** | > 5-7.5 m/s | × | 5,000-200 | 1,000 | 3,000 | 1,500 | 1,000 | Latinopoulos & Kechagia [71] |
| **Denmark** | 250–650 W/m$^2$ | × | × | 300–800 | 5,000–7,500 | 500–1,500 | 150–650 | Hansen [72]* |
| **USA** | × | Cost analysis | < 5,000 | × | × | > 2,000 | > 3,000 | Haaren & Fthenakis [73]* |
| **UK** | > 5 m/s | < 10,000 | < 10,000 | > 500 | × | > 2,000 | > 400 | Baban & Parry [74] |
| **Germany** | > 4 m/s (at 10 m AGL) | × | >500 | > 500 | × | >500 | × | Krewitt et al. [75] |
| **Poland** | Turbine output | > 200 | >100 | 200-1,000 | 3,000 | >500 | > 200 | Sliz et al. [76]* |
| **Vietnam** | Turbine output | × | >100 | > 500 | 2,500 | > 2,000 | > 400 | Nguyen [77]* |
| **Sweden** | Turbine output | >200 | >200 | × | 2,500 | >500 | > 100 | Siyal et al [78]* |

*Denoted distances like '500–1,500 m' are fuzzy sets, thus the tolerance goes from 0 to 1 between 500 and 1,500 m from the object.

Haaren & Fthenakis [73], considered restriction criteria of spatially dependent costs (grid connection, road access and land clearing) to be less than 20% of total cost.



© University of Pretoria

Sliz et al. [76] calculated energy output throughout the region from three reference turbines of 0.6, 1.65 and 2.5MW. Various spatial and ecological restrictions were applied on three energy potential maps obtained using three reference turbines.

Nguyen [77], calculated energy output throughout the region from a reference turbine of 1.8 MW rated power and then applied social and technical restraints to eliminate areas.

Siyal et al [78], eliminated areas (grid cells) with Plant capacity factor less than 20% achieved using a reference turbine of 3 MW rated power.

## SUMMARY

Many research papers, reports published on different aspects of wind power development, and government websites were reviewed and recorded. Specifically, the topics considered in the review were wind resource assessment (WRA), Weibull distribution and its shape and scale parameter estimation, annual, seasonal and diurnal wind statistics, local wind shear exponent estimation, energy yield estimation from selected wind turbines, and site suitability analysis. It was observed that no study has been reported in the literature about GIS-based site suitability analysis with respect to Saudi Arabia. Being a major energy supplier of the world, Saudi Arabia should thoroughly explore the future energy outlook to partially cater its domestic and global energy demands through new and renewable sources of energy. Therefore, Saudi Arabia is investigating alternate sustainable and reliable sources of energy for generating power and reducing consumption of the nation’s fossil fuel reserves. Thus, it was determined that a balanced energy mix of alternative and conventional energy is strategically important to Saudi Arabia’s long term prosperity, energy security and maintaining its leading position in the global energy market.



© University of Pretoria

# CHAPTER 4

## STUDY AREA AND DATA DESCRIPTION

Saudi Arabia, one of the driest and hottest countries in the world, and it is located approximately between the north latitudes of 17 and 31 and east longitudes of 37 and 56 [79]. The land elevation varies from 0 to 2600 m above mean sea level. The east and the west coasts of the Kingdom are located on the Arabian Gulf and Red Sea, respectively. Saudi Arabia consists of desert and semi-desert with oases, where half of the total surface is uninhabitable desert. The major part of the western area of Saudi Arabia is a plateau while the east is lowland with a very hot climate. The southwest region has mountains as high as 3000 m. Maximum summer temperatures often exceed 45°C, relative humidity is very low and skies are clear most of the time. Very little precipitation is observed in the central region of Saudi Arabia.

The wind data from 36 meteorological data measurement stations spread over the entire Kingdom were obtained for this study. The wind data from 29 stations out of these 36 stations were obtained from the Presidency of Meteorology and Environment (PME) [80]. This governmental organisation is responsible for the maintenance, calibration and collection of meteorological data in Saudi Arabia. In general, the data collection period varied from 1970 to 2013 for most of the data collection stations. The data were missing for the year 1976 and 1984 for almost all the stations. At all of these stations, the hourly values of all the parameters, such as wind speed (WS), wind direction (WD), dry bulb temperature (T), wet bulb temperature ($T_w$), station pressure (P), sea level pressure ($P_{sl}$), relative humidity (RH), vapour pressure ($V_p$), total rainfall (R), and others are recorded manually and then daily average, maximum and minimum values are saved on the computer. The mean wind speed, data duration, standard deviation, location coordinates and altitude at all the stations at 10 m AGL are given in Table 4.1. The data from the remaining seven stations located in the industrial city of Jubail were obtained from the Environment and Control Department (Royal Commission for Jubail). At the site, Industrial Area (central), the data are available at 10, 50 and 90 m AGL. On the other hand, at all the other sites, in Jubail, the data are available at 10 m AGL only. The weather parameters recorded at these stations are wind direction, wind speed, temperature, relative humidity and precipitation. Table 4.2 shows the details of wind



© University of Pretoria

speed data and location coordinates at these seven locations. All the parameters, including wind speed are ten minutes, hourly averaged recorded values.

The location maps of 29 PME weather stations spread all over the country and seven stations in Jubail Industrial City are shown in Figures 4.1 and 4.2, respectively. The meteorological stations at Al-Wejh, Yanbo, Jeddah, Gizan and Dhahran are situated near the coast. Hence these stations could be considered as representative of coastal locations, associated with higher wind resource, as shown in Table 4.1. Tabouk, Al-Jouf, Arar, Guriat, Turaif, Rafha and Qaisumah are located in the northern region. Most of the time of the year, higher speed winds in Saudi Arabia comes from northern neighbouring countries like Iraq and Jordan. Turaif, Jouf and Tabouk are around 800 metres above mean sea level (AMSL). Guriat is situated at around 500 metres AMSL. Bisha, Gizan, Abha, Khamis-Mushait and Nejran in the southern part of the country near Yemen border. This region is usually associated with mediocre wind speeds. Abha and Khamis-Mushait are situated at around 2 100 m AMSL while Al-Baha, Bisha and Nejran at 1,000 to 1,200 metres AMSL. The central stations Gassim and Riyadh are situated at 600 metres while Hail at around 1,000 metres AMSL. In the western region, most of the meteorological stations are near sea shore and represent a flat area. The eastern region south and north of Dhahran increases in elevation. Taif is a hill station and is located in the western region of the Kingdom. The operating ranges and accuracies of various sensors used for the measurements are given in Table 4.3.

In this study, the emphasis was given to Jubail Industrial City as it is considered to be the largest industrial base in the whole Middle East. In the year 1933, geologists explored oil in Jubail, Saudi Arabia. In 1983, the largest engineering and construction project ever was started in Jubail to establish the biggest industrial base in the region. Presently, Jubail Industrial City is host to more than 160 industrial enterprises and home to almost 70,000 residents. Additionally, Jubail's infrastructure is capable of running continuously without power failure in any of the existing facilities while meeting community requirements within high modern living standards where all the necessities of life, tourism and recreation are available.



© University of Pretoria

Table 4.1 Country wide wind tower locations with hourly average wind speed and data duration.

| Station # | Wind tower location | Av. WS, m/s at 10 m AGL | Standard Deviation | Data duration | Latitude | Longitude | Altitude (m) |
|---|---|---|---|---|---|---|---|
| 1. | Abha | 3.24 | 1.34 | 1978 – 2013 | 18.23 | 42.66 | 2084 |
| 2. | Al-Ahsa | 3.59 | 1.89 | 1985 – 2013 | 25.29 | 49.49 | 172 |
| 3 | Al-Baha | 3.41 | 1.37 | 1985 – 2013 | 20.29 | 41.64 | 1021 |
| 4. | Al-Jouf | 3.85 | 1.81 | 1974 – 2013 | 29.78 | 40.10 | 771 |
| 5. | Arar | 3.61 | 1.72 | 1970 – 2013 | 30.91 | 41.14 | 552 |
| 6. | Bisha | 2.50 | 1.15 | 1970 – 2013 | 19.99 | 42.62 | 1157 |
| 7. | Dammam | 4.34 | 1.60 | 1999 – 2013 | 26.47 | 49.80 | 567 |
| 8. | Dhahran | 4.35 | 1.65 | 1970 – 2013 | 26.27 | 50.15 | 17 |
| 9. | Gassim | 2.96 | 1.39 | 1973 – 2013 | 26.30 | 43.77 | 650 |
| 10. | Gizan | 3.27 | 0.96 | 1970 – 2013 | 16.90 | 42.59 | 3 |
| 11. | Gurait | 4.25 | 2.17 | 1985 – 2013 | 31.41 | 37.28 | 499 |
| 12. | Hafr-Al-Batin | 3.49 | 1.73 | 1990 – 2011 | 28.45 | 45.96 | 355 |
| 13. | Hail | 3.24 | 1.32 | 1970 – 2013 | 27.92 | 41.91 | 1013 |
| 14. | Jeddah | 3.63 | 1.32 | 1970 – 2011 | 21.67 | 39.15 | 12 |
| 15. | Khamis-Mushait | 3.00 | 1.25 | 1970 – 2013 | 18.31 | 42.73 | 2054 |
| 16. | Madinah | 3.18 | 1.14 | 1970 – 2013 | 24.48 | 39.60 | 631 |
| 17. | Makkah | 1.45 | 0.76 | 1985 – 2013 | 21.43 | 39.81 | 310 |
| 18. | Najran | 2.24 | 1.00 | 1974 – 2013 | 17.50 | 44.13 | 1203 |
| 19. | Qaisumah | 3.71 | 1.89 | 1970 – 2013 | 28.31 | 46.13 | 355 |
| 20. | Rafha | 3.82 | 1.76 | 1970 – 2013 | 29.64 | 43.50 | 447 |
| 21. | Riyadh-New | 2.89 | 1.42 | 1984 – 2013 | 24.65 | 46.71 | 612 |
| 22. | Sharorah | 3.32 | 1.31 | 1985 – 2013 | 17.49 | 47.12 | 722 |
| 23. | Sulayel | 3.50 | 1.63 | 1970 – 1989 | 20.47 | 45.57 | 612 |
| 24. | Tabuk | 2.79 | 1.31 | 1970 – 2013 | 28.39 | 36.58 | 770 |
| 25. | Taif | 3.73 | 1.42 | 1970 – 2013 | 21.45 | 40.35 | 1449 |
| 26. | Turaif | 4.13 | 1.87 | 1973 – 2013 | 31.68 | 38.65 | 813 |
| 27. | Wadi-Al-Dawasser | 3.53 | 1.51 | 1978 – 2013 | 20.44 | 44.79 | 627 |
| 28. | Wejh | 4.20 | 1.36 | 1970 – 2011 | 26.23 | 36.46 | 16 |
| 29. | Yanbo | 4.11 | 1.73 | 1970 – 2011 | 24.08 | 38.08 | 14 |

Table 4.2 Wind tower locations at Jubail Industrial City with hourly average wind speed and data duration

| Station | Av. WS, m/s at 10 m AGL | Standard Deviation | Data duration | Latitude | Longitude |
|---|---|---|---|---|---|
| Industrial Area (Central) | 3.27 | 1.98 | 2008 –12 | 27.03 | 49.53 |
| Al-Bahar Desalination Plant | 3.74 | 2.19 | 2008 –12 | 27.07 | 49.6 |
| Pearl Beach | 2.26 | 1.10 | 2008 –12 | 27.01 | 49.65 |
| Naval Base | 3.78 | 2.22 | 2010 –12 | 26.92 | 49.71 |
| Industrial Area 2 (South) | 4.31 | 2.98 | 2008 –12 | 26.92 | 49.48 |
| Al-Reggah District | 2.91 | 1.51 | 2008 –12 | 27.13 | 49.53 |
| Industrial Area (East) | 4.53 | 2.52 | 2008 –12 | 27.03 | 49.61 |



© University of Pretoria

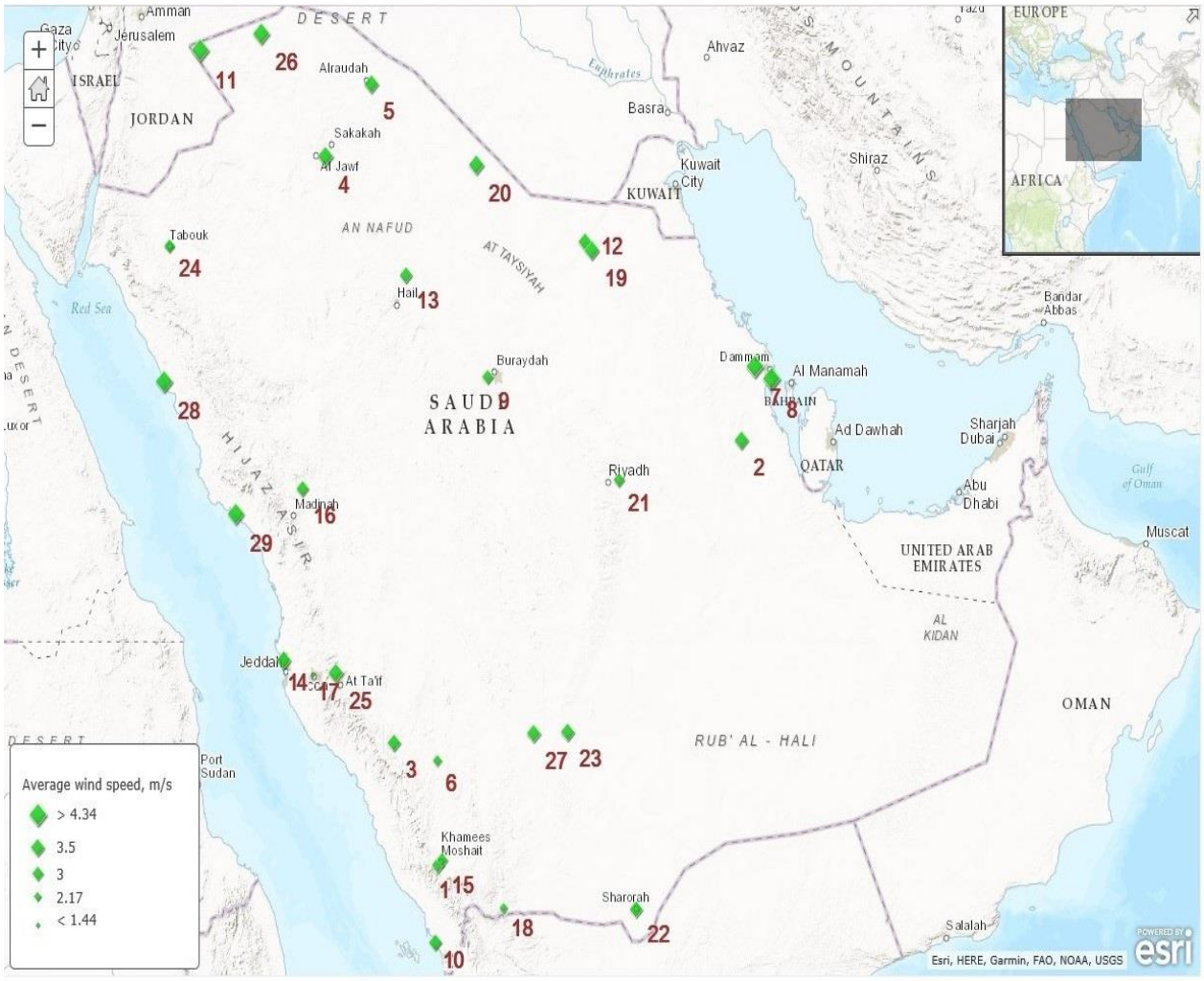


| | | | | | | | | | |
|---|---|---|---|---|---|---|---|---|---|
| 1. | Abha | 7. | Dammam | 13. | Hail | 19. | Qaisumah | 25. | Taif |
| 2. | Al-Ahsa | 8. | Dhahran | 14. | Jeddah | 20. | Rafha | 26. | Turaif |
| 3 | Al-Baha | 9. | Gassim | 15. | Khamis-Mushait | 21. | Riyadh-New | 27. | Wadi-Al-Dawasser |
| 4. | Al-Jouf | 10. | Gizan | 16. | Madinah | 22. | Sharorah | 28. | Wejh |
| 5. | Arar | 11. | Gurait | 17. | Makkah | 23. | Sulayel | 29. | Yanbo |
| 6. | Bisha | 12. | Hafr-Al-Batin | 18. | Najran | 24. | Tabuk | | |

Figure 4.1 Locations of meteorological stations countrywide with station names.



© University of Pretoria


Figure 4.2 Locations of meteorological stations at Jubail Industrial City.

The technical specifications of the meteorological sensors installed on all seven wind towers in Jubail Industrial City are presented in Table 4.4. The list of weather parameters recorded at site 1 i.e. Industrial Area (Central) is tabulated in Table 4.5. The photos of the wind towers at Industrial Area (Central), Al Bahar Desalination Plant, Pearl Beach and Al-Reggah District are shown in Figures 4.3, 4.4, 4.5 and 4.6, respectively. The description of the terrain in the vicinity of all the sites is given in Table 4.6.

Table 4.3 Specifications of the wind speed sensor at 29 stations in Saudi Arabia

| ITEM DESCRIPTION | TECHNICAL INFORMATION |
|---|---|
| Wind speed sensor, NRG#40<br>Three-cup anemometer | AC sine wave, Accuracy: 0.1 m/s, Range: 1-96 m/s<br>Output: 0-125 HZ, Threshold: 0.78 m/s |
| Wind direction vane, NRG#200P<br>Potentiometer | Accuracy: 1%, Range: 360º Mechanical, Output: 0-Exc. Voltage,<br>Threshold: 1 m/s, Dead band: Max - 8º and Typical 4º |
| Temperature sensor #110S<br>Integrated circuit | Accuracy: ±1.1 ºC, Range: -40 ºC to 52.5 ºC, Output: 0 – 2.5 volts DC,<br>Operating temperature range: -40 ºC to 52.5 ºC |
| Barometric pressure sensor BP20 | Accuracy: ±15 mb, Range: 150 – 1150 mb, Output: Linear voltage |
| Relative humidity sensor RH-5<br>Polymer resistor | Accuracy: ±5%, Range: 0 – 95 %<br>Output: 0 – 5 volts, Operating temperature range: -40 ºC to 54 ºC |
| Pyranometer Li-Cor #LI-200SA<br>Global solar radiation | Accuracy: 1%, Range: 0 – 3000 W/m$^2$ , Output: Voltage DC, Operating<br>temperature range: -40 ºC to 65 ºC |



© University of Pretoria

Table 4.4 Specifications of the wind speed sensor at all seven stations in Jubail.

| **PERFORMACE CHARACTERISTICS** | |
|---|---|
| Maximum Operating Range: | 0 - 125 mph (0 - 60 m/s) |
| Starting Speed: | 0.5 mph (0.22 m/s) |
| Calibrated Range: | 0 - 100 mph (0 - 50 m/s) |
| Accuracy: | ±1% or 0.15 mph (0.07 m/s) |
| Resolution | <0.1 mph or m/s |
| Temperature Range: | -50°C to +65°C (-58°F to +149°F) |
| Distance Constant: | less than 5 ft. (1.5m) of flow (meets EPA specifications) |
| **ELECTRICAL CHARACTERISTICS** | |
| Power Requirements: | 12 VDC at 10 mA, 12 VDC at 350 mA for internal heater |
| Output Signal: | 11 volt (pulse frequency equivalent to speed) |
| Output Impedance: | 100 Ω maximum |
| **PHYSICAL CHARACTERISTICS** | |
| Weight: | 1.5 lbs (.68 kg) |
| Finish: | Clear anodised aluminium; Lexan cup assembly. |
| **CABLE & MOUNTING** | |
| PN 1953 Mounting: | Cable Assembly; specify length in feet or meters PN 191 Cross arm Assembly |

Table 4.5 Parameter list of the weather data collection tower at Industrial Area (Central).

| **Parameter Code** | **Description** | **Unit** |
|---|---|---|
| ATM | Ambient Temperature | °C |
| PRE | Precipitation | mm |
| PRS | Pressure | mb |
| RH | Relative Humidity | % |
| GSR | Global Solar Radiation | Langley |
| VWD10 | Wind Direction 10m | deg |
| VWD50 | Wind Direction 50m | deg |
| VWD90 | Wind Direction 90m | deg |
| VWS10 | Wind Speed 10m | m/s |
| VWS50 | Wind Speed 50m | m/s |
| VWS90 | Wind Speed 90m | m/s |



© University of Pretoria

Figure 4.3 Wind tower at Industrial Area (Central)

Figure 4.4 Wind tower at Al-Bahar Desalination Plant



© University of Pretoria

Figure 4.5 Wind tower at Pearl Beach

Figure 4.6 Wind tower at Al-Reggah District



© University of Pretoria

Table 4.6 Description of the terrain in the vicinity of weather stations.

| Site | Description |
|---|---|
| Industrial Area (Central) | Only station where weather data are available at three heights AGL. Tower surrounded mainly by plain terrain with some warehouses of 8 - 10 m in height about 200 m away in the west direction. |
| Al-Bahar Desalination Plant | Located on sea shore near desalination plant. The terrain is mostly plain and surrounded by very small shrubs. |
| Pearl Beach | Located in the Jubail residential area and surrounded by 3-4 story buildings. This station recorded minimum wind speed out of all weather stations. |
| Naval Base | Located near Dhahran-Jubail highway. The terrain is mostly plain and surrounded by very small shrubs and few residential buildings 200 m away towards the east. |
| Industrial Area 2 (South) | Surrounded mainly by plain terrain with some warehouses of 8 - 10 m in height about 1,000 m away in north-west direction. |
| Al-Reggah District | Location mostly surrounded by shrubs. Surrounding clear with a 3 story building around 150 m away in north-eastern direction. |
| Industrial Area (East) | Surrounded mainly by plain terrain with some warehouses of 8 - 10 m in height about 150 m away in north-west direction |



© University of Pretoria

# CHAPTER 5

# WIND RESOURCE ASSESSMENT AT JUBAIL INDUSTRIAL CITY

The cleanest sources of energy are those which use the natural resources of the earth. These are known as renewable sources of energy and will never die out, unlike fixed reserves of fossil and nuclear fuels. Some of the common sources of renewable energy are wind, solar photovoltaic, solar thermal, hydro, wave, geothermal, and biomass. Wind is a very promising energy source and is receiving global recognition compared to other renewable energy sources, due to its low production, operation and maintenance costs and ease of maintenance, in addition to the availability of efficient multi-megawatt wind turbines.

The forecast of energy demand in Saudi Arabia is expected to be more than double in the next one and a half decades, from 58 GW in 2015 to 121 GW in 2030 [9]. It is an urgent requirement to fill this gap of approximately 60 GW of power generation, and at the same time reduce the load on diminishing oil and gas reserves, as well as using the oil and gas to produce higher value products. Wind energy, along with solar energy, Photovoltaic (PV) and Concentrated Solar Power (CSP), are serious considerations to fill this energy gap [9].

This work aims at conducting a systematic, comprehensive and accurate wind resource assessment at the largest industrial enterprise in the Middle East by finding Weibull parameters, maximum energy carrying capacity, most probable wind speed, energy output from a few commercially available wind machines. Finally, comparing different methods for the estimation of Weibull parameters and recommending the best option.

## 5.1 WIND SPEED STATISTICS

### 5.1.1 Meteorological tower at Industrial Area (East)

This study aims at conducting the first comprehensive and accurate wind resource assessment for the largest industrial city of Saudi Arabia, and to calculate energy output based on a few commercially available wind machines. The size of this industrial city is expanding and is expected to more than double in the next decade. The Kingdom has taken initiatives to supplement its existing fossil fuel based energy through renewable sources of energy, particularly wind energy besides solar PV and solar thermal options [9].



© University of Pretoria

This meteorological tower is located in the middle of the Jubail Industrial Area. It is mostly surrounded by plain terrain with industrial sheds, of around 10 to 12 m in height, in the south-west direction located 100 m away. There is a mobile phone network tower, of approximately 30 m in height, located in the south-east direction, 150 m away. An industrial worker's camp with around 8,000 residents is located in west direction from the weather station at a distance of 900 m. Monthly averaged meteorological data (temperature, atmospheric pressure and relative humidity) at Industrial Area (East) is given Table 5.1.

Table 5.1 Metrological data at the weather data collection tower.

| **Monthly Average (2008 – 2012)** | | | |
|---|---|---|---|
| | Temperature (°C) | Atmospheric pressure, (mb) | Relative humidity, (%) |
| Jan | 15.28 | 1,017.9 | 63.12 |
| Feb | 17.42 | 1,015.5 | 58.62 |
| Mar | 21.05 | 1,013.2 | 47.05 |
| Apr | 26.06 | 1,009.2 | 45.03 |
| May | 32.16 | 1,004.9 | 36.88 |
| June | 35.71 | 999.5 | 27.98 |
| July | 36.77 | 996.3 | 32.96 |
| Aug | 36.14 | 998.0 | 43.69 |
| Sep | 33.56 | 1,003.6 | 45.59 |
| Oct | 29.15 | 1,010.3 | 54.04 |
| Nov | 22.68 | 1,014.8 | 58.64 |
| Dec | 17.19 | 1,017.5 | 60.58 |
| Mean | 26.93 | 1,008.4 | 47.85 |

The complete set of 10 minute average wind speed values were first checked for erroneous values and completeness as per the existing standard practices. The annual mean wind speeds at 10, 50 and 90 m in height were found to be 3.34, 4.79 and 5.35 m/s with respective standard deviations of 0.14, 0.17, and 0.22. The other meteorological parameters, such as average ambient temperature, barometric pressure, global solar radiation, and relative humidity values near ground level were found to be 27.35 °C, 1,008.39 mb, 1,550 kWh/$m^2$, and 42%, respectively. The derived parameters, such as a monthly average air density, was found to vary between a minimum of 1.114 kg/$m^3$ and a maximum of 1.238 kg/$m^3$ with an



© University of Pretoria

overall mean of 1.17 kg/m$^3$. The long term average values of wind power density (WPD), calculated using 10 minute mean wind speed values at different heights were 50.92, 116.03, and 168.46 W/m$^2$. The annual energy production from a commercially available wind machine of 3 MW rated power was estimated to be 6,285 MWh/year.

#### 5.1.1.1 Annual, seasonal and diurnal behaviour of mean wind speed

The wind rose diagrams at 10, 50 and 90 m in heights for Industrial Area (Central) are shown in Figures 5.1, 5.2 and 5.3, respectively. The hourly mean values of wind speed and direction were used for the entire period of data collection in these wind rose diagrams. It can be observed from these plots that the most prevailing wind direction at all the heights was from the north-west. The percentage of calm winds (wind speed less than 0.5 m/s) decreased with increasing height, i.e. 1.82, 0.61 and 0.56% at 10, 50 and 90 m, respectively.

The annual, seasonal and diurnal variations of hourly mean wind speed at 10, 50 and 90 m AGL over the entire period of data collection at Industrial Area (Central) are shown in Figures 5.4, 5.5 and 5.6, respectively. Over the period of five years, the annual mean wind speeds at heights of measurements were 3.34, 4.79 and 5.35 m/s with respective values of standard deviation of 0.14, 0.17 and 0.22. The annual mean wind speed over the five years of data collection is reasonably consistent, which indicates that the data is accurate. At 90 m, the annual average wind speed was always above 5.0 m/s during the data collection period with a minimum of around 5.0 m/s occurring in the year 2010, as can be seen in Figure 5.4. At 50 m, the annual mean wind speed always remained above 4.75 m/s with a maximum of more than 5.0 m/s in 2011. This is an indication that a wind turbine with 50 m and more hub heights can be used in the study area for wind farm development. These measured mean speed values are comparable to the values reported in similar studies in Dhahran [21] and Bahrain [31]. The seasonal variation of wind speed shows that wind speed was the highest in the month of June and the lowest in October, as shown in Figure 5.5. Wind speed is relatively higher during the summer season as compared to other three seasons; this may be due to the topography. Moreover, in summer, the wind particles are more agile due to rapid convection process. The summer season starts from early June to end of August. The winter season in Saudi Arabia starts from early December to end of February. This seasonal trend of wind speed coincides with the load pattern of Saudi Arabia and should be helpful in partial replacement of fossil fuel based energy generated by wind. Similar seasonal wind speed trend was also reported for the location of Dhahran south of Jubail [21]. The monthly mean wind speed was more than



© University of Pretoria

5.5 m/s during February, March, May, June, July, November and December months as seen from Figure 5.5 which means that more power can be generated during these months from wind. The monthly mean wind speed values at 10, 50 and 90 m in heights were 3.34, 4.8, and 5.35 m/s with a standard deviation of 0.33, 0.42 and 0.54, respectively.

The diurnal variation showed two peaks at 90 m, one from 04:00 hours to 07:00 hours and another from 13:00 to 16:00 hours with lows between 08:00 and 10:00, and 20:00 and 22:00 hours, as observed from Figure 5.6. A similar type of trend was noticed in the hourly mean values of wind speed at 50 m, while at 10 m the wind speed started increasing from 00:00 hours and continued to increase until it reached a peak between 14:00 to 15:00 hours and then continued to decrease until 23:00 hours. During the afternoon, the boundary layer is convective and the wind shear is less which causes daytime gustiness. These gusty surface winds usually begin in the late morning hours, peak in the afternoon, and end by early evening. The highest values of wind speed were 5.26, 6.28 and 6.33 m/s at 15:00 hours corresponding to 10, 50 and 90 m AGL, while the lowest values were 2.29, 4.19 and 4.77 m/s at around 21:00 to 22:00 hours, as seen from Figure 5.6.

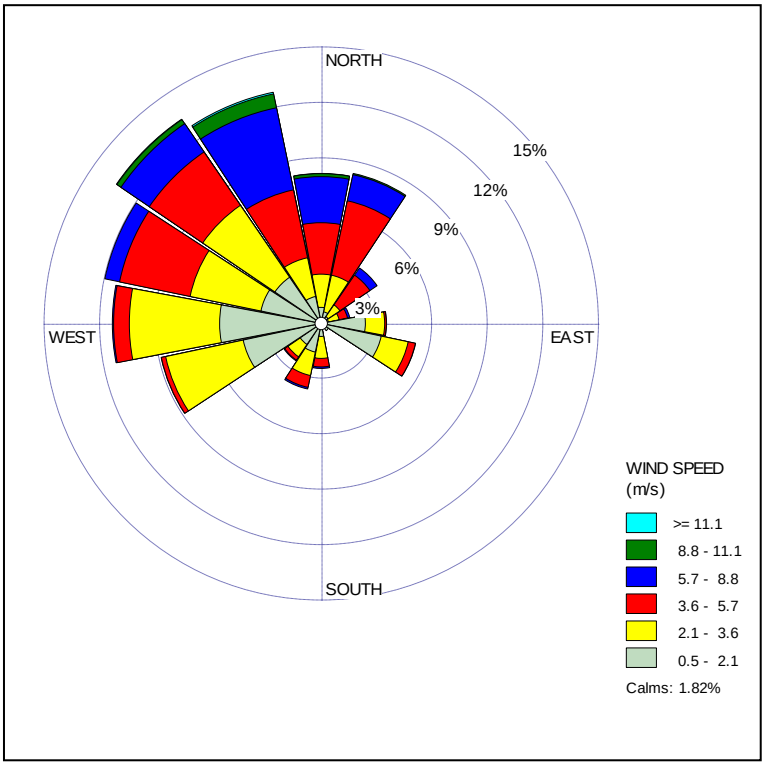


Figure 5.1 Wind rose plot at 10 m in height at Industrial Area (Central).



© University of Pretoria

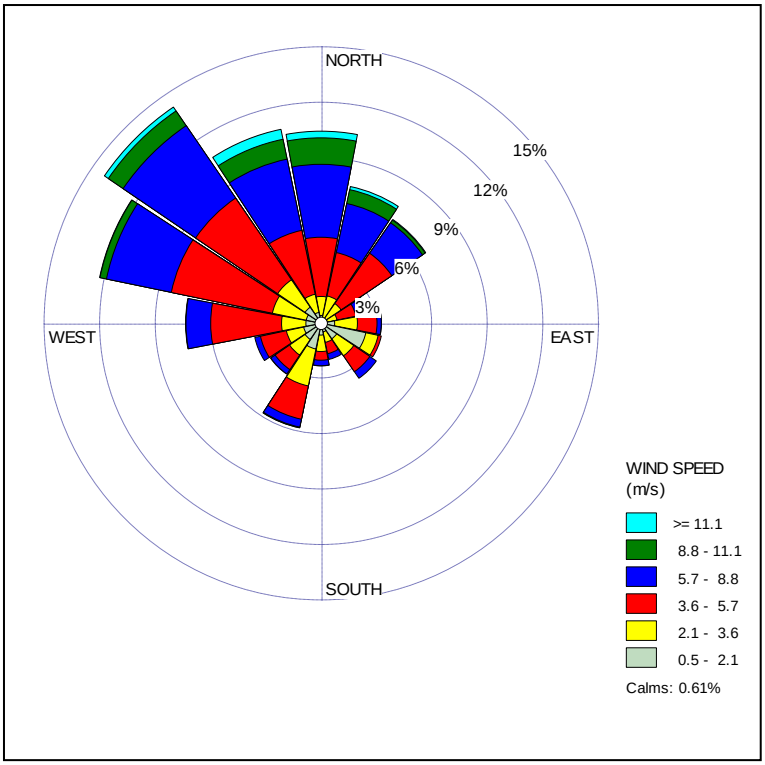


Figure 5.2 Wind rose plot at 50 m in height at Industrial Area (Central).

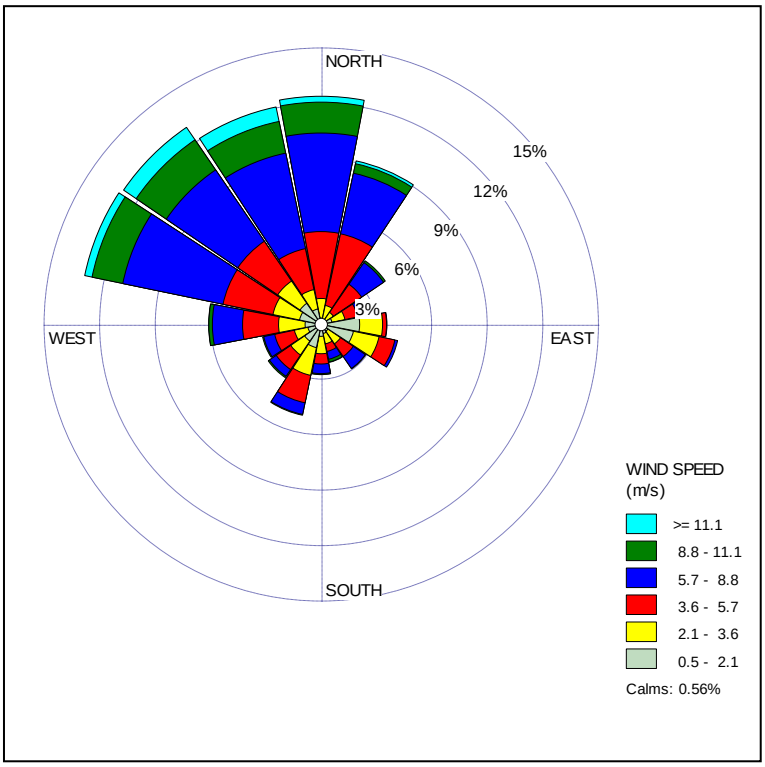


Figure 5.3 Wind rose plot at 90 m in height at Industrial Area (Central).



© University of Pretoria

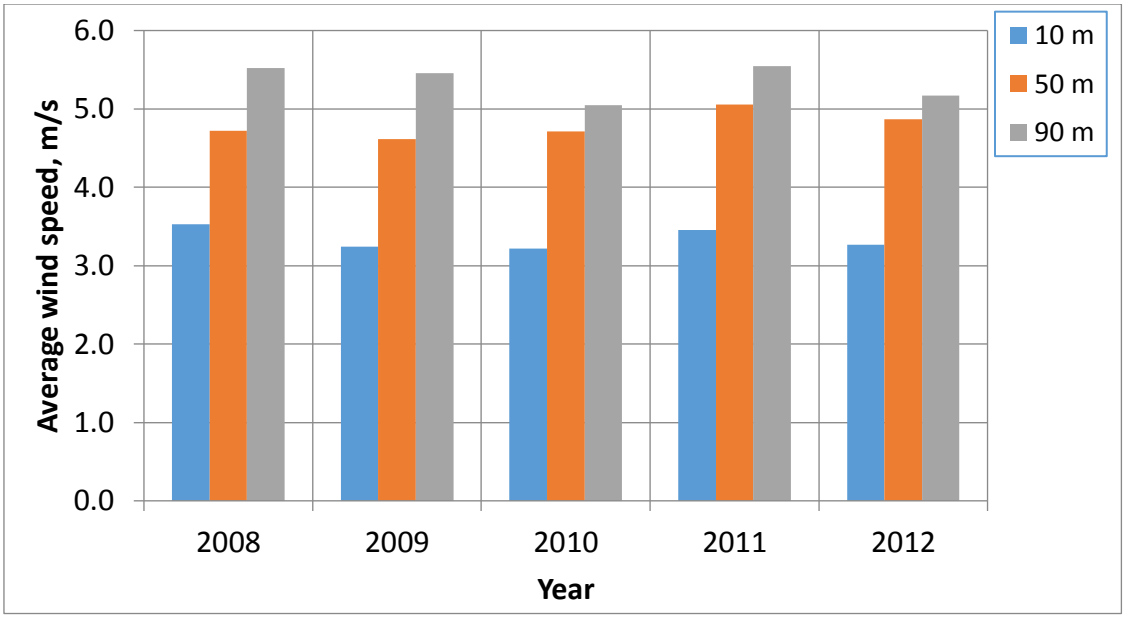


Figure 5.4 Annual variation of hourly mean wind speed at different heights at Industrial Area (Central).

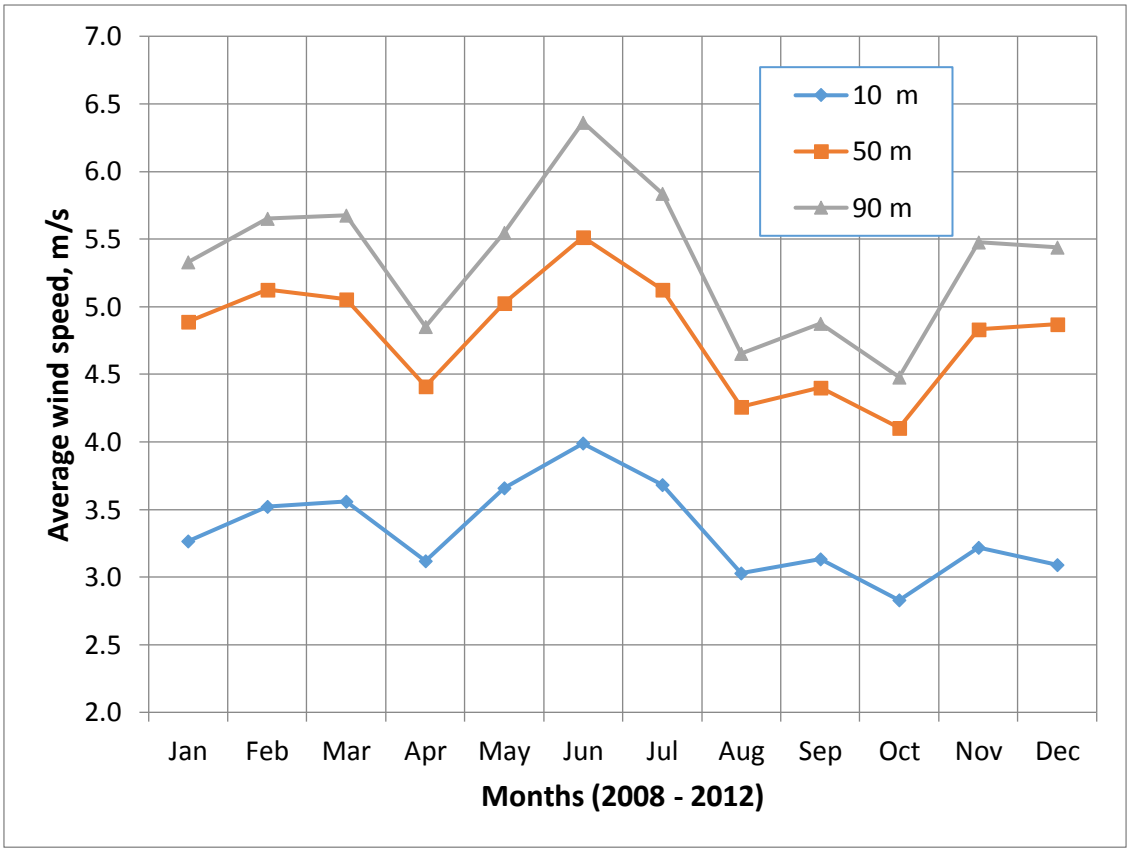


Figure 5.5 Seasonal variation of hourly mean wind speed at different heights at Industrial Area (Central).



© University of Pretoria

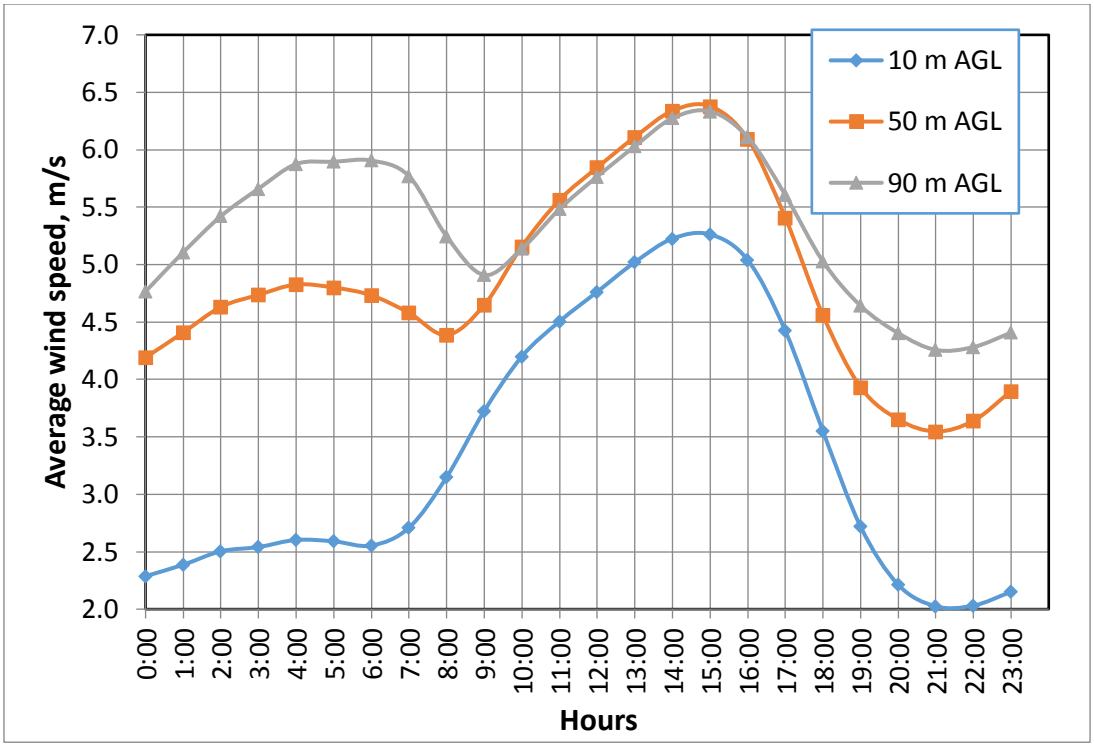


Figure 5.6 Diurnal variation of hourly mean wind speed at different heights at Industrial Area (Central).

### 5.1.1.2 Weibull parameters and wind frequency analysis

The two-parameter Weibull distribution is frequently used to characterise the wind behaviour because it provides a good representation of wind data [24, 25, 53]. This distribution function shows the probability of the wind speed in a 1 m/s bin centred on a particular wind speed. The Weibull distribution function is expressed as [81]:

$$P_{(v)} = \frac{k}{v}\left(\frac{v}{c}\right)^{k-1} exp\left\{-\left(\frac{v}{c}\right)^{k}\right\}, \qquad (5.1)$$

Where $P_{(v)}$ is the frequency of incidence of wind speed, $v$. The scale factor, $c$ in m/s, is indicative of mean wind speed and $k$ is the dimensionless shape factor, which describes the shape and width of the distribution. The Weibull distribution is, therefore, determined by the parameters, $c$ and $k$.

The cumulative Weibull distribution, $P_{(v)}$ which gives the probability of the wind speed greater than the value, v, is expressed as:



© University of Pretoria

$$P_{(v)} = exp\left\{-\left(\frac{v}{c}\right)^{k}\right\}, \qquad (5.2)$$

In this study, the Weibull distribution parameters, *c* and *k* are determined by maximum likelihood method, presented later, Equations (5.5) and (5.6). The seasonal values of both the scale (*c*) and shape (*k*) parameters are summarised in Table 5.2. The maximum values of the shape parameter of 2.11, 2.80, and 2.43 were found in November, October and November at 10, 50, and 90 m while the corresponding minimum values of 1.52, 1.96, and 1.67 were observed in the month of July. The highest values of scale parameter *c* of 4.35, 6.33, and 6.74 m/s were found in the months of February, March and June at 10, 50, and 90 m in height, respectively. The overall mean values of scale and shape parameters at measurement heights were 3.67, 5.49, 5.82 m/s and 1.72, 2.22, 1.91, respectively.

The actual wind speed frequency distribution and Weibull fit at 10, 50 and 90 m AGL are shown in Figures 5.7, 5.8 and 5.9, respectively. It is evident from these figures that actual wind speed data are characterised well by the two-parameter Weibull distribution. The analyses of the Weibull percentage frequency distributions revealed that wind speed remained above 3.5 m/s for 49.28, 75.7 and 77.7% of the time at 10, 50 and 90 m in height, respectively. This implies that at Jubail, a wind turbine with a hub height of 50 m and cut-in wind speed of 3.5 m/s can produce energy for approximately 76% of the time and about 78% of the time with a hub height of 90 m. The values of the scale factor, *c* increases with height, whereas no definite trend could be seen in the values of the shape parameter, *k*. However, highest value of the shape parameter, *k* was found at 50 m in height, followed by 90 m and then 10 m.

Table 5.2 Weibull shape and scale parameters for Jubail.

| **Month** | **10 m AGL** | | **50 m AGL** | | **90 m AGL** | |
|---|---|---|---|---|---|---|
| | ***k*** | ***c*** | ***K*** | ***c*** | ***K*** | ***c*** |
| Jan | 1.92 | 3.58 | 2.64 | 5.76 | 2.00 | 5.81 |
| Feb | 1.85 | 4.26 | 2.02 | 6.33 | 1.91 | 6.51 |
| Mar | 1.69 | 4.35 | 2.10 | 6.23 | 1.91 | 6.74 |
| Apr | 1.78 | 3.07 | 2.43 | 4.59 | 1.99 | 4.58 |
| May | 1.75 | 3.99 | 2.31 | 5.90 | 1.96 | 6.25 |
| Jun | 1.71 | 4.23 | 2.02 | 6.33 | 1.96 | 6.79 |
| Jul | 1.52 | 3.64 | 1.96 | 5.33 | 1.67 | 5.72 |
| Aug | 1.80 | 3.93 | 2.37 | 5.50 | 2.21 | 6.28 |
| Sep | 1.82 | 3.61 | 2.37 | 5.14 | 2.17 | 5.80 |
| Oct | 1.92 | 2.78 | 2.80 | 4.62 | 2.09 | 4.29 |
| Nov | 2.11 | 3.38 | 2.74 | 4.99 | 2.43 | 5.84 |
| Dec | 1.78 | 3.30 | 2.52 | 5.36 | 1.90 | 5.61 |



© University of Pretoria

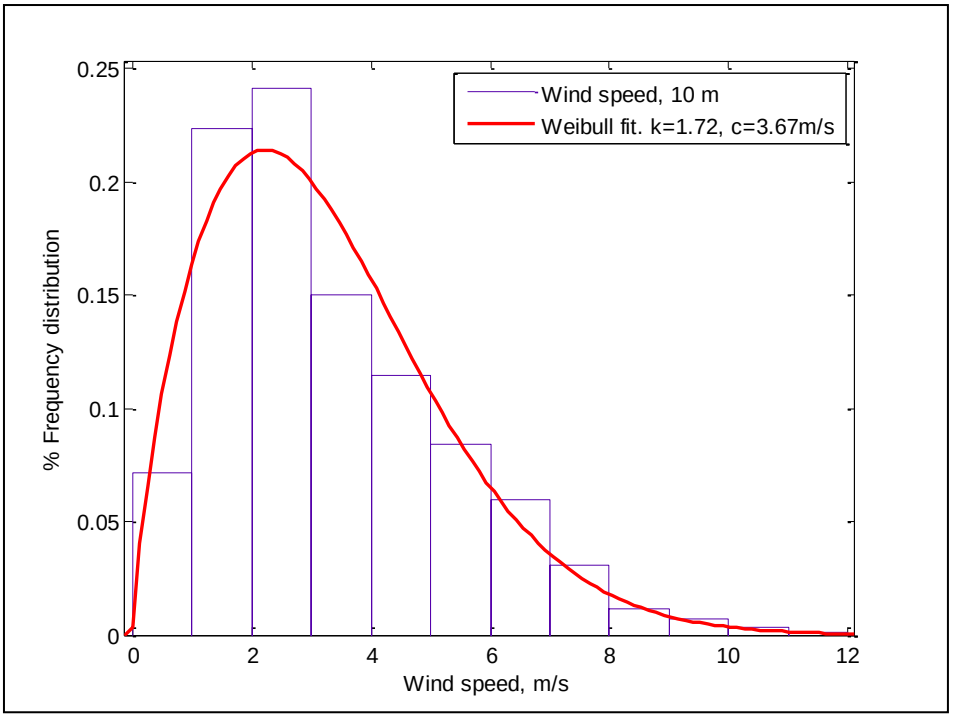


Figure 5.7 Actual wind speed frequency distribution and Weibull fit at 10 m AGL at Industrial Area (Central).

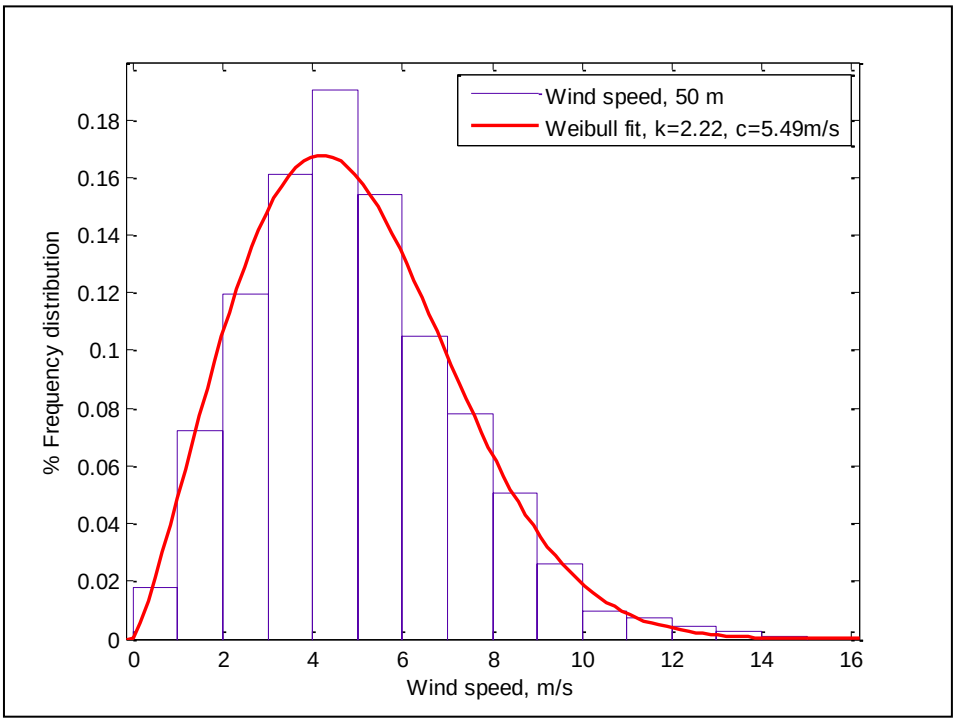


Figure 5.8 Actual wind speed frequency distribution and Weibull fit at 50 m AGL at Industrial Area (Central).



© University of Pretoria

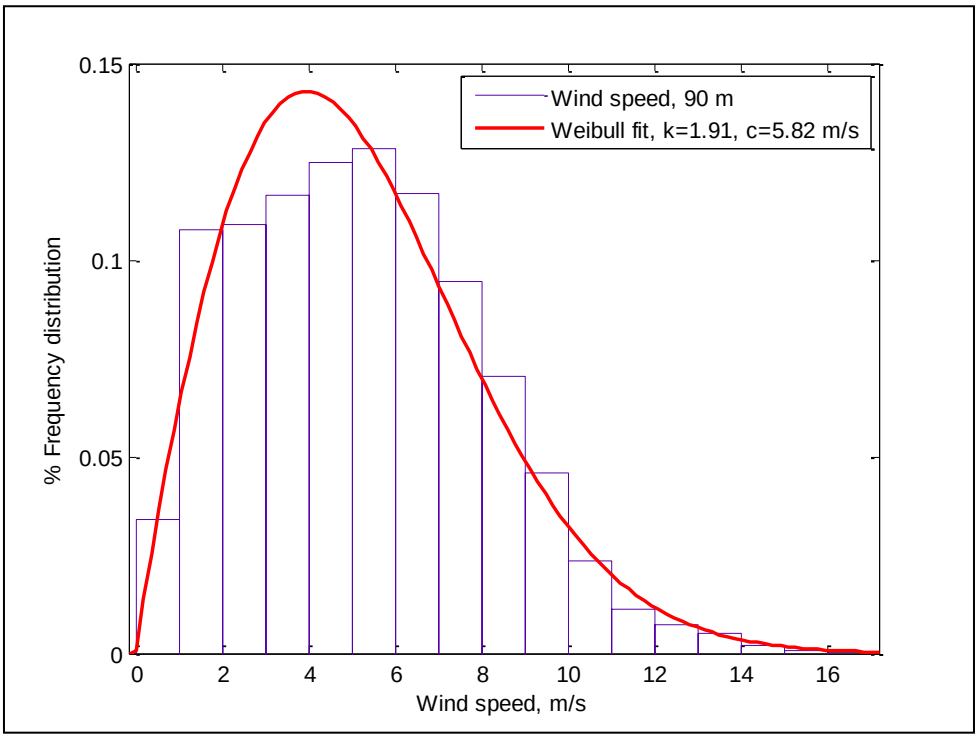


Figure 5.9 Actual wind speed frequency distribution and Weibull fit at 90 m AGL at Industrial Area (Central).

### 5.1.1.3 Air density, wind power density (WPD), wind shear exponent (WSE)

The air density was estimated using the following expression:

$$P = \frac{\rho}{RT} \qquad (\text{kg/m}^3) \qquad (5.3)$$

Where $P$ is the air pressure in Pascals, $R$ is the specific gas constant of air, 287.05 J/kg.K and $T$ is the local air temperature in degrees Kelvin. The WPD is calculated using the well know following equation:

$$\text{WPD} = ½\ \rho\ \text{V}^3 \qquad (\text{W/m}^2) \qquad (5.4)$$

Where $V$ is the 10 minute or hourly mean wind speed. The lowest air density was observed in July and the highest in January, as shown in Figure 5.10. This simply means that air is lighter



© University of Pretoria

in the summer time compared to that in the winter season, and hence less wind power density is expected in summer compared to that in winter. The mean wind power density values during the five year data collection period at 10, 50, and 90 m AGL were found to be 50.92, 116.03, and 168.46 W/m$^2$, respectively. The annual, seasonal and diurnal variations of wind power density are shown in Figures 5.11, 5.12, 5.13, respectively. The annual WPD trend followed almost the same pattern as the annual mean wind speed illustrated in Figure 5.4, with the highest value of 186 W/m$^2$ in 2008 and a minimum of 146.2 W/m$^2$ in the year 2010 at 90 m in height, as seen from Figure 5.11. The seasonal variation of wind power density shows the highest values in June and the lowest in October, as demonstrated in Figure 5.12. Higher values of WPD, (between 170 and 270 W/m$^2$), were observed during January to March, May to July, and November to December, while less than 150 W/m$^2$ during the rest of the months in the year at 90 m. Similar seasonal trends were observed at 50 and 10 m in heights with lesser magnitudes of WPD. The diurnal variation of WPD showed clearly two peaks first between 03:00 and 07:00 hours and the second between 13:00 and 15:00 hours at 90 m in height as shown in Figure 5.13. However, the first peak was not distinctive at 50m, while the second peak was still visible and that too during the same time duration. Finally, at 10 m, the WPD started increasing right from 00:00 hours and after reaching its peak between 13:00 to 15:00 hours started decreasing towards the end of the day as seen from Figure 5.13.

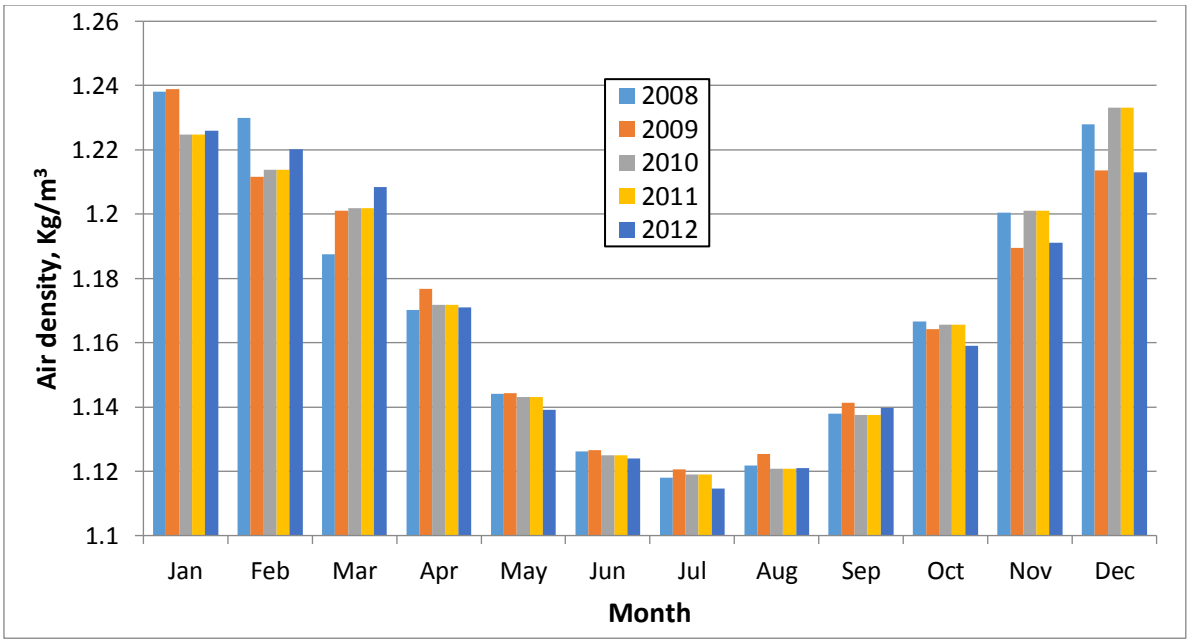


Figure 5.10 Seasonal air density variation at at Industrial Area (Central).



© University of Pretoria

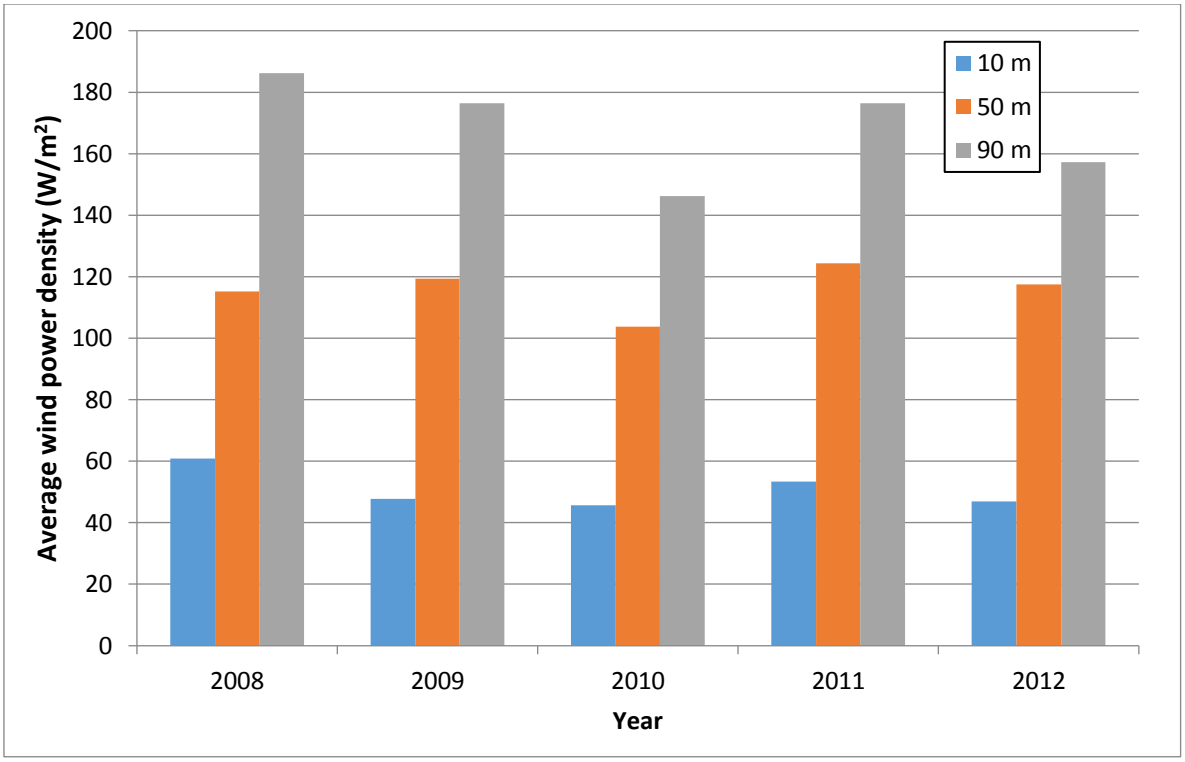


Figure 5.11 Variation of mean annual wind power density at Industrial Area (Central).

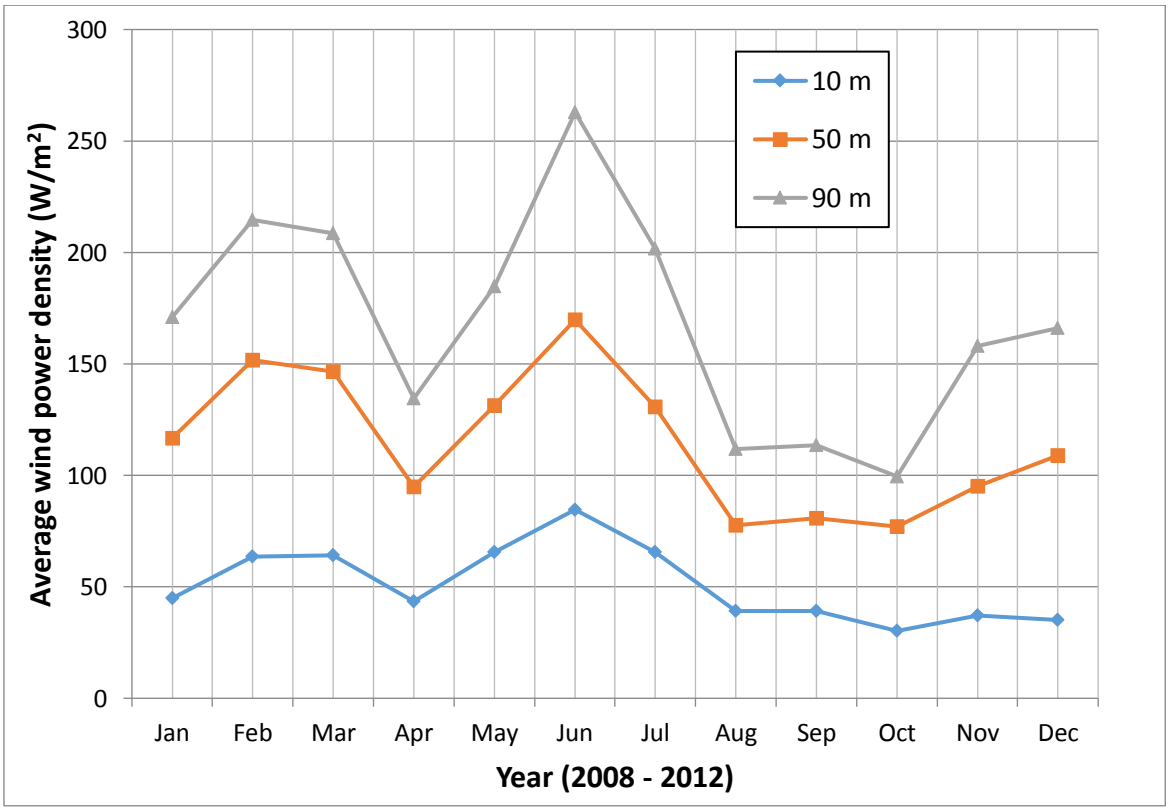


Figure 5.12 Variation of mean seasonal wind power density at Industrial Area (Central).



© University of Pretoria

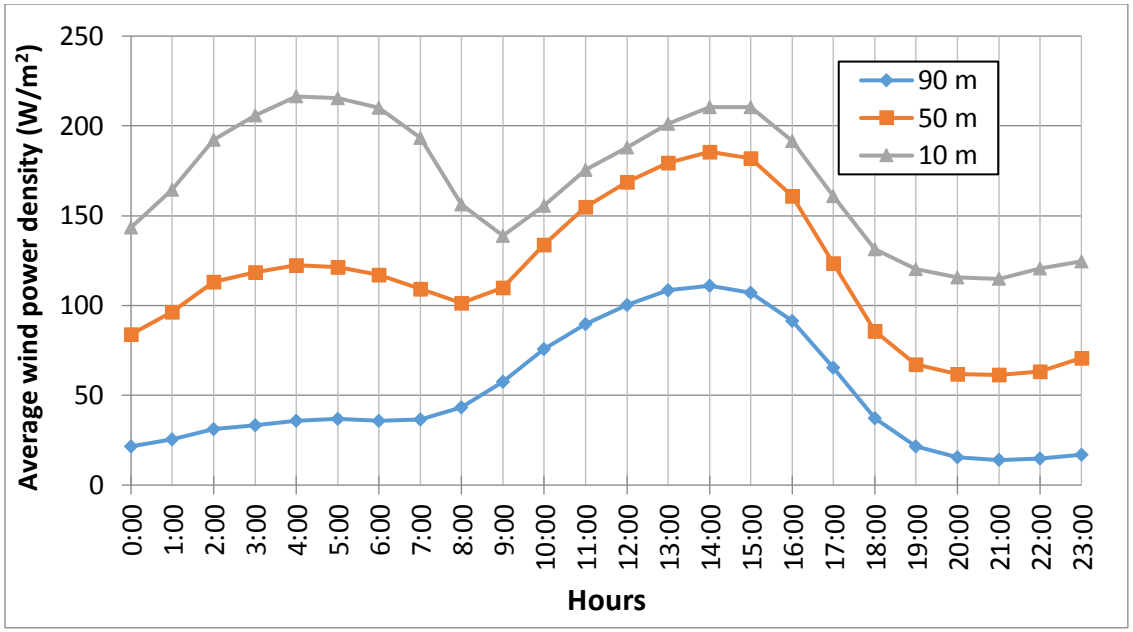


Figure 5.13 Variation of mean diurnal wind power density at Industrial Area (Central).

Wind shear is defined as the exponent α (alpha) in the power law equation that relates wind speeds at two different heights. It is important to perform WSE calculations only where valid upper and lower wind speed measurements are available for a given time interval. In practice, it has been found that α varies with elevation, time of day, season, temperature, terrain, and atmospheric stability. The larger the exponent, the larger the vertical gradient in the wind speed. Although the power law is a useful engineering approximation of the average wind speed profile, actual profiles tend to deviate from this relationship. The wind shear profile obtained using the long term mean value of wind speed at three heights is shown in Figure 5.14.

The following equation was used to estimate the wind shear exponent (WSE), α:

$$\alpha = \frac{\ln(V_2) - \ln(V_1)}{\ln(Z_2) - \ln(Z_1)} \qquad (5.5)$$

Where $V_1$ and $V_2$ are the wind speeds at heights $Z_1$ and $Z_2$, respectively. Equation (5.5) was used to find the annual, seasonal and diurnal variations of the WSE, as shown in Figures 5.15, 5.16 and 5.17. The annual values of WSE varied between 0.18 and 0.25 calculated based on WS at 10 m and 50 m with an increasing trend from 2008 to 2012, as shown in Figure 5.15. However the WSE values calculated using WS values at 10 m and 90 m varied between 0.20 and 0.24 with almost constant values of WSE of a little more than 0.20 for all the years



© University of Pretoria

except 2009. Largest variation in WSE values, calculated using WS values at 50 m and 90 m, was observed with a minimum of 0.10 in 2012 and a maximum of 0.28 in the year 2009, as can be seen from Figure 5.15. The monthly mean values of WSE calculated using WS data between 10 and 50 m, and 10 and 90 m showed a decreasing trend from January to May with persistence until August and then an increasing trend towards the end of the year, as shown in Figure 5.16. However, the WSE values obtained using wind speed between 50 and 90 m did not show a seasonal change. The diurnal variation of the WSE showed the lowest value during daytime, i.e. from 09:00 to 15:00 hours, mainly due to high temperature and turbulence. The hourly mean values of WSE, based on WS between 10 and 50 m, and 10 and 90 m, showed almost the same values during 00:00 to 06:00 hours and a sudden decrease in a short duration of 3 hours from 06:00 to 09:00 hours while the lowest and almost constant values during 09:00 to 17:00 hours, as can be seen from Figure 5.17. These WSE values again started increasing from 18:00 until midnight. The WSE values estimated based on WS values between 50 and 90 m behaved a little differently, with an increasing trend from 00:00 until 07:00 hours and then a decreasing trend from 10:00 hours, and lowest and almost constant values from 11:00 - 16:00 hours. An increasing trend was seen between 17:00 and 20:00 hours and then again decreasing towards the midnight. The wind shear is most distinct near the boundary and the wind speeds are more at higher altitudes because of the drag of the boundary and the viscosity of the air. From Figure 5.17, it is evident that the heating and cooling phase of air adjacent to the earth during the day influences the wind shear. In the early morning, the temperature near the ground is greater than at upper heights due to solar irradiation, higher and nearly constant values of WSE were observed. Whereas, during daytime as the temperature of the earth surface and the air on top of it increases, values of WSE decreases.

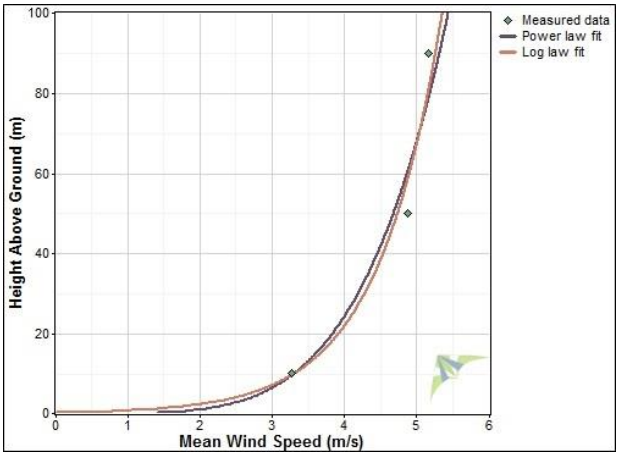


Figure 5.14 Variation of wind speed with height and fitting curve at Industrial Area (Central).



© University of Pretoria

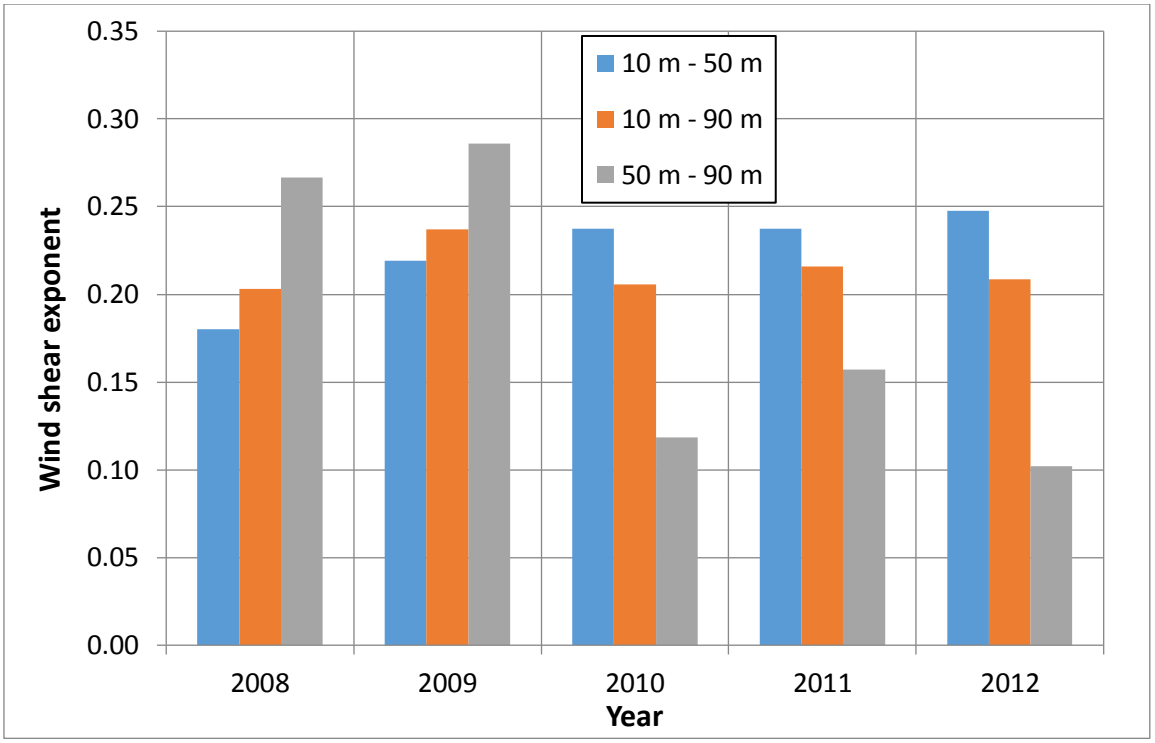


Figure 5.15 Variation of mean annual wind shear at different heights at Industrial Area (Central).

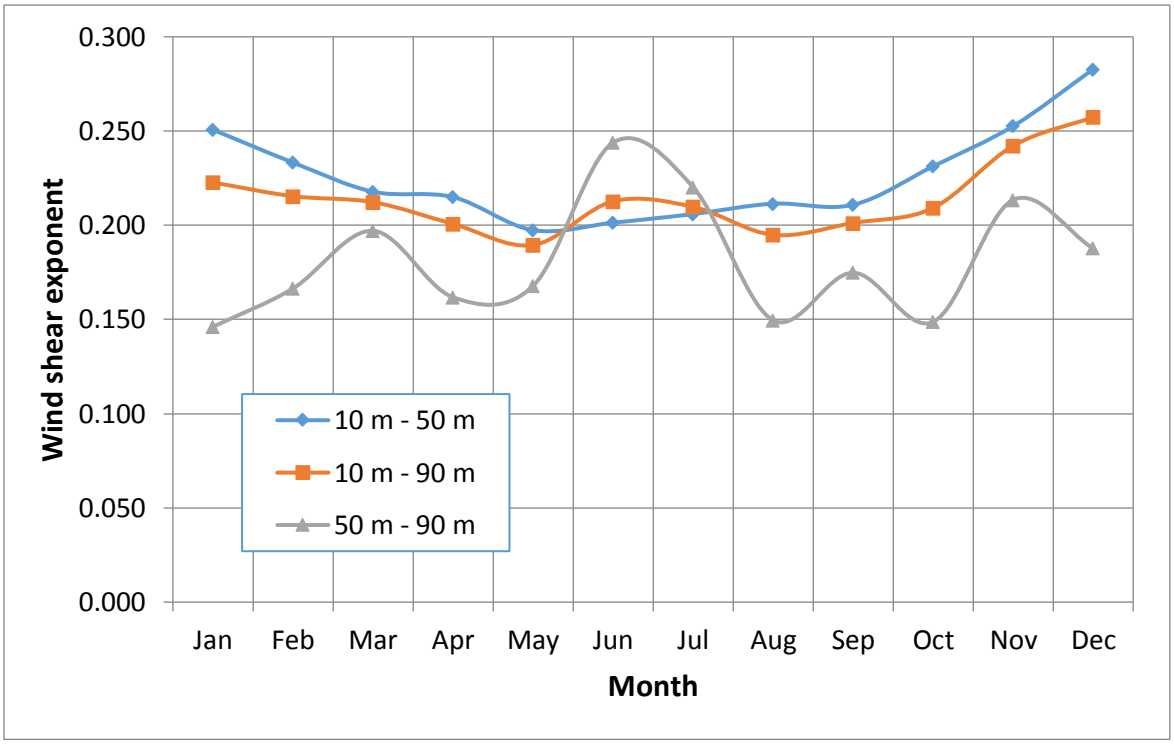


Figure 5.16 Variation of mean monthly wind shear at different heights at Industrial Area (Central).



© University of Pretoria

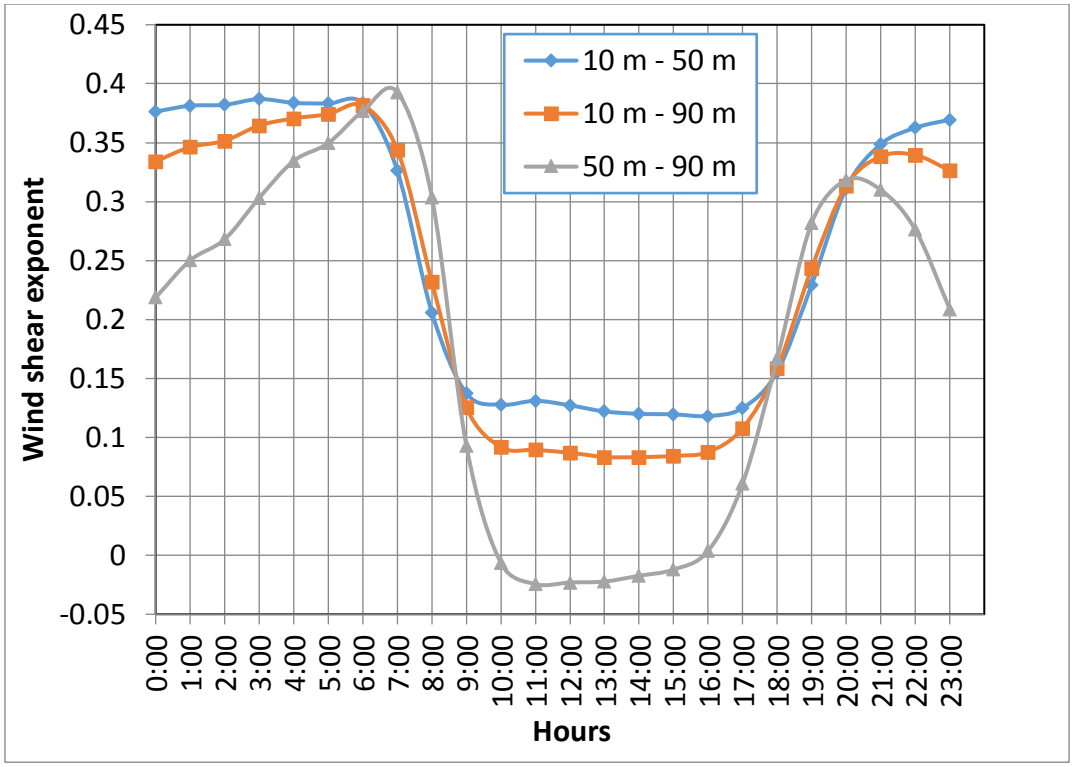


Figure 5.17 Variation of mean diurnal wind shear at different heights at Industrial Area (Central).

### 5.1.2 Analyses of Wind Speed data at seven locations in Jubail Industrial City

The hourly average wind speed values over the entire period of data collection for all seven sites at 10 m in height are presented in Table 5.3. The wind speed statistics (median, maximum, minimum, 75th percentile and 25th percentile) at 10 m in height of all seven weather stations at Jubail are illustrated in Figure 5.18. Since these weather stations lie within the radius of 15 kilometres boundary, it can be observed from Figure 5.18 that there is not much variation in wind speed statistics. Site 4 and 9 seem to have the highest mean wind speed. The highest annual mean wind speed of 4.53 m/s was observed at Industrial Area (East) and the lowest of 2.25 m/s at the Pearl Beach with standard deviations of 2.52 and 1.1 m/s, respectively. To assess the seasonal variation of wind speed over all sites, the data are sorted month-wise and the monthly maximum, daily high/low (in that month), mean, and monthly minimum wind speeds are plotted. These plots are shown in Figures 5.19 to 5.25. It was observed that the highest monthly mean wind speed was witnessed in February/June at all sites. This period coincides with the high energy demand period for the region due to the air conditioning load. The lowest mean wind speed was witnessed in September/October at all sites. To visualise the wind patterns at all the sites, the wind rose charts, showing the



© University of Pretoria

frequency and speed of wind blowing from each of 16 cardinal directions were plotted, as shown in Figures 5.26 to 5.32. These rose plots for a particular site can help in the initial orientation of the wind machine. It can be observed from these plots that the most prevailing wind direction at all sites was from the north-west.

Table 5.3 Wind speed statistics of all sites.

| **Station #** | **Station** | **Annual mean wind speed, m/s** | | |
|---|---|---|---|---|
| | | **Mean** | **Maximum** | **Standard Deviation** |
| 1. | Industrial Area (Central) | 3.27 | 11.90 | 1.985 |
| 2. | Al-Bahar Desalination Plant | 3.74 | 2.40 | 2.193 |
| 3. | Pearl Beach | 2.26 | 8.70 | 1.109 |
| 4. | Naval Base | 3.78 | 13.80 | 2.220 |
| 6. | Industrial Area 2 (South) | 4.31 | 27.00 | 2.983 |
| 8. | Al-Reggah District | 2.91 | 13.60 | 1.511 |
| 9. | Industrial Area (East) | 4.53 | 19.30 | 2.520 |

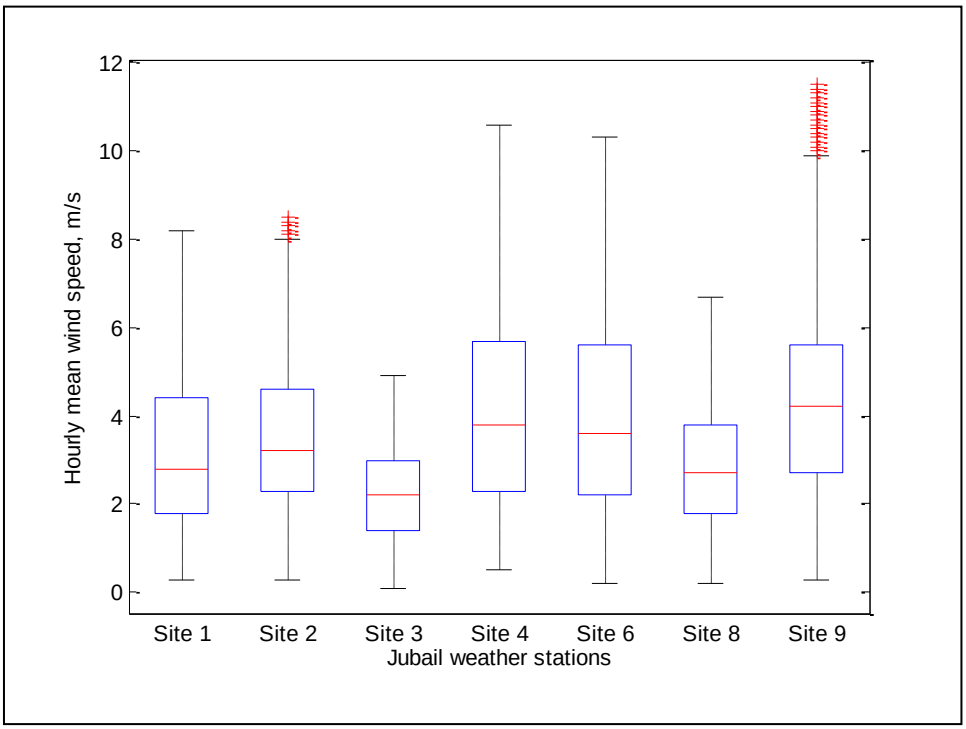


Figure 5.18 Wind speed statistics of all weather stations at Jubail at 10 m AGL.



© University of Pretoria

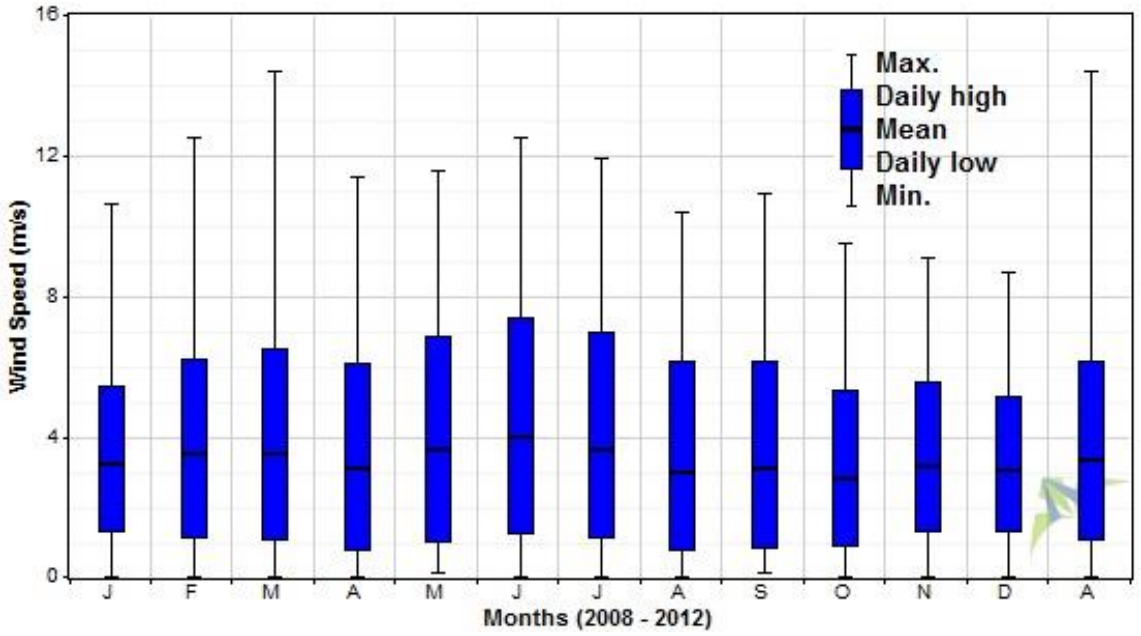


Figure 5.19 Monthly maximum, daily high, daily mean, daily low and minimum wind speed at Industrial Area (Central)

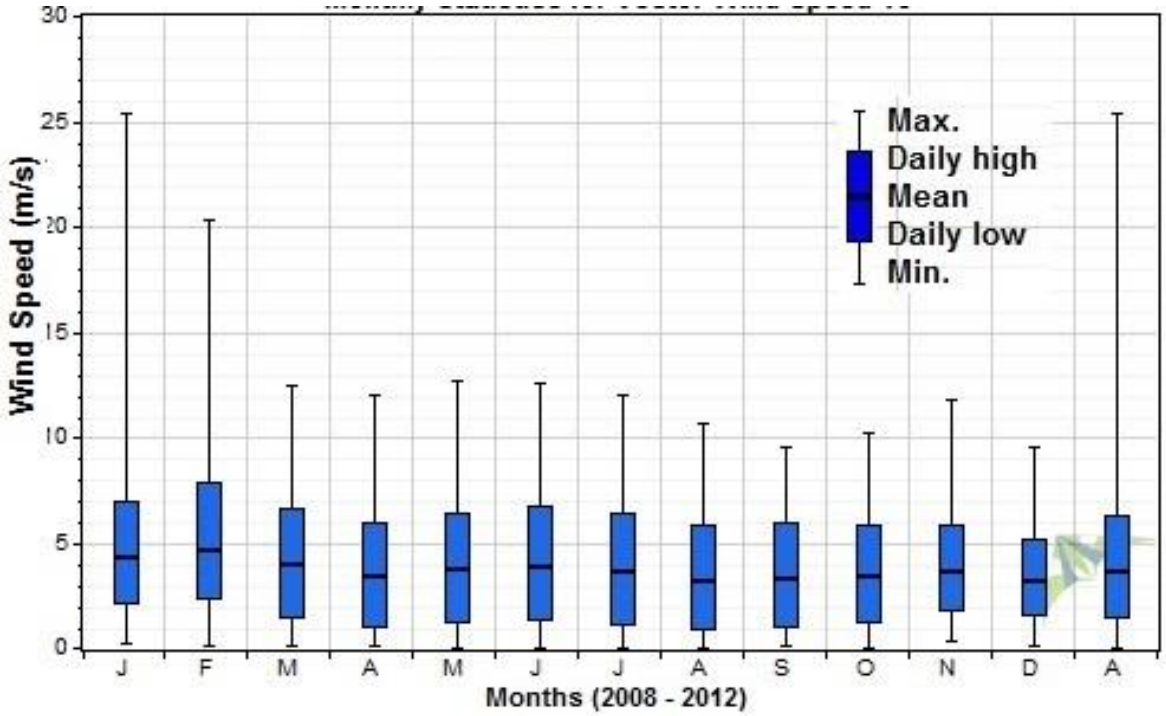


Figure 5.20 Monthly maximum, daily high, daily mean, daily low and minimum wind speed at Al-Bahar Desalination Plant



© University of Pretoria

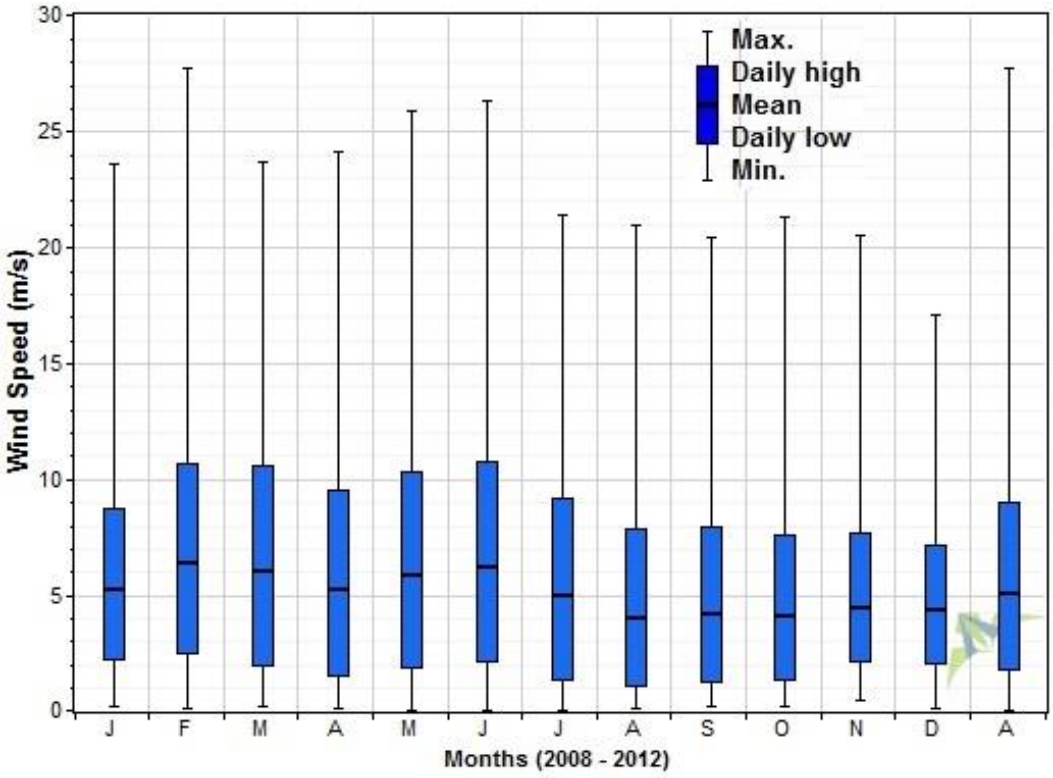


Figure 5.21 Monthly maximum, daily high, daily mean, daily low and minimum wind speed at Pearl Beach

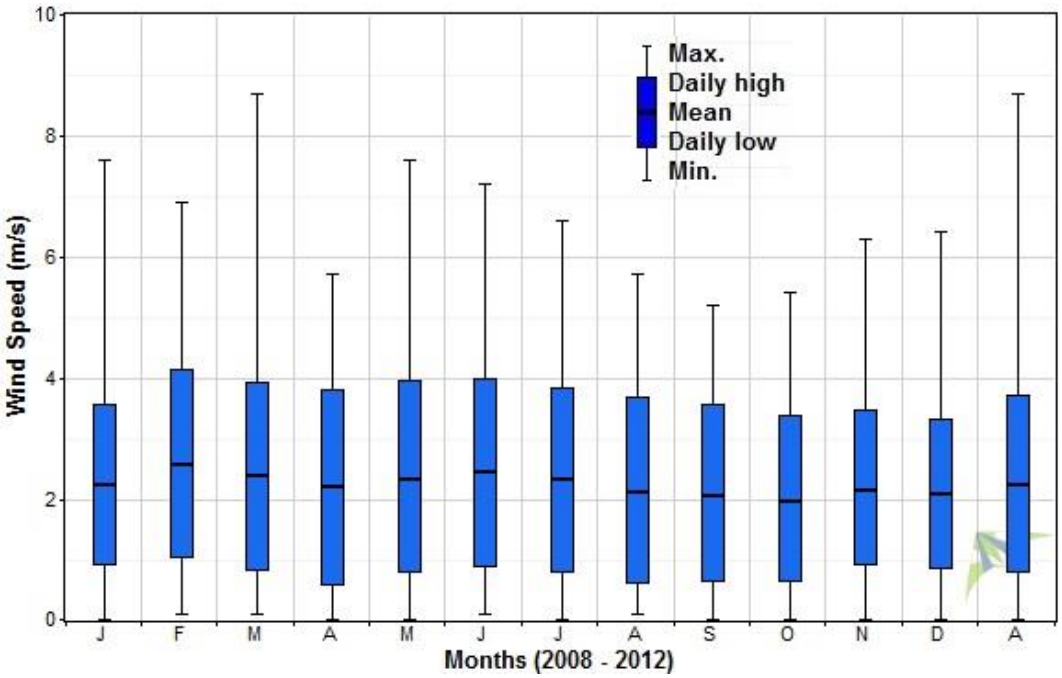


Figure 5.22 Monthly maximum, daily high, daily mean, daily low and minimum wind speed at Naval Base



© University of Pretoria

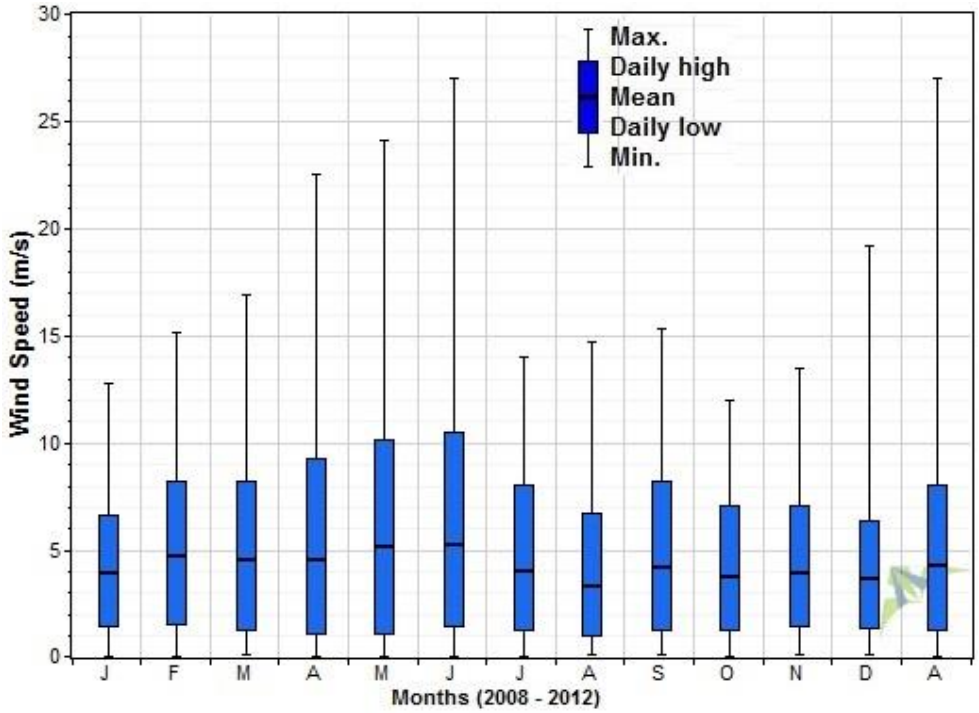


Figure 5.23 Monthly maximum, daily high, daily mean, daily low and minimum wind speed at Industrial Area 2 (South)

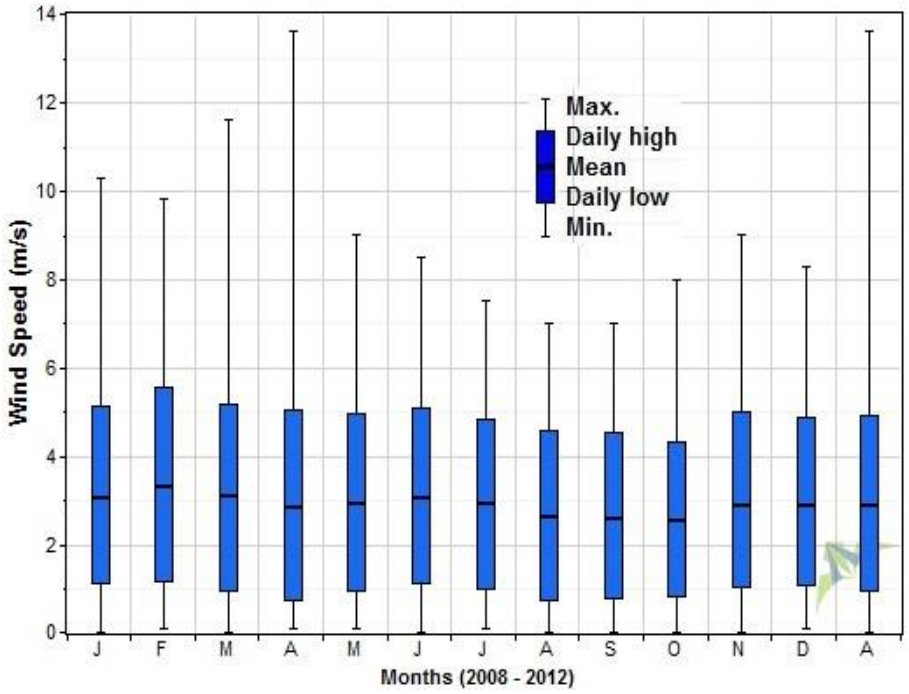


Figure 5.24 Monthly maximum, daily high, daily mean, daily low and minimum wind speed at Al-Reggah District



© University of Pretoria

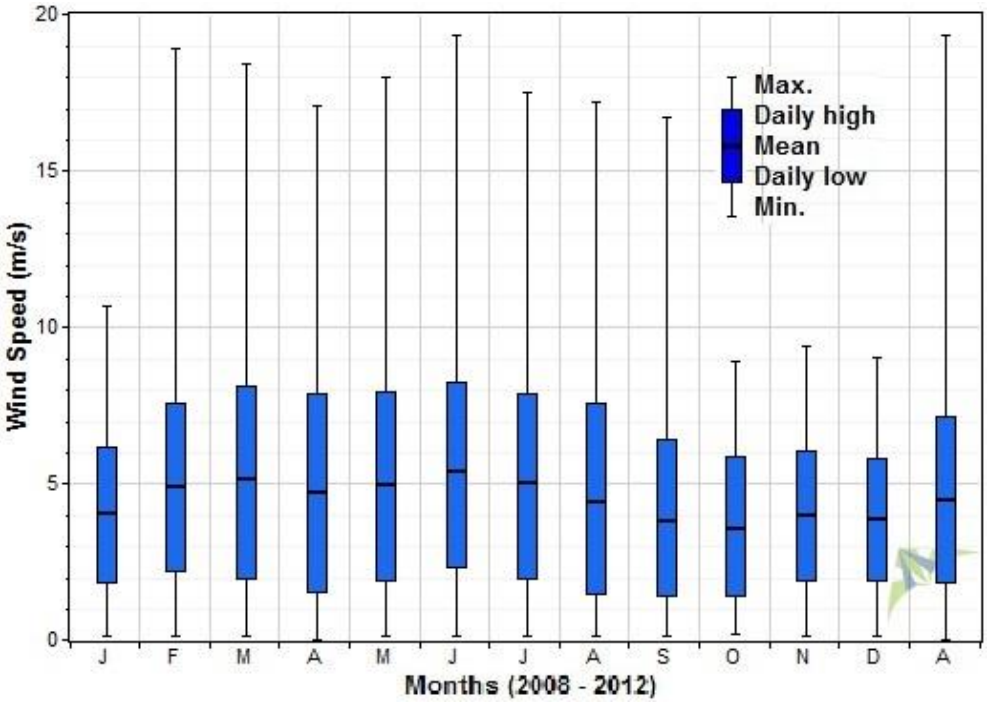


Figure 5.25 Monthly maximum, daily high, daily mean, daily low and minimum wind speed at Industrial Area (East)

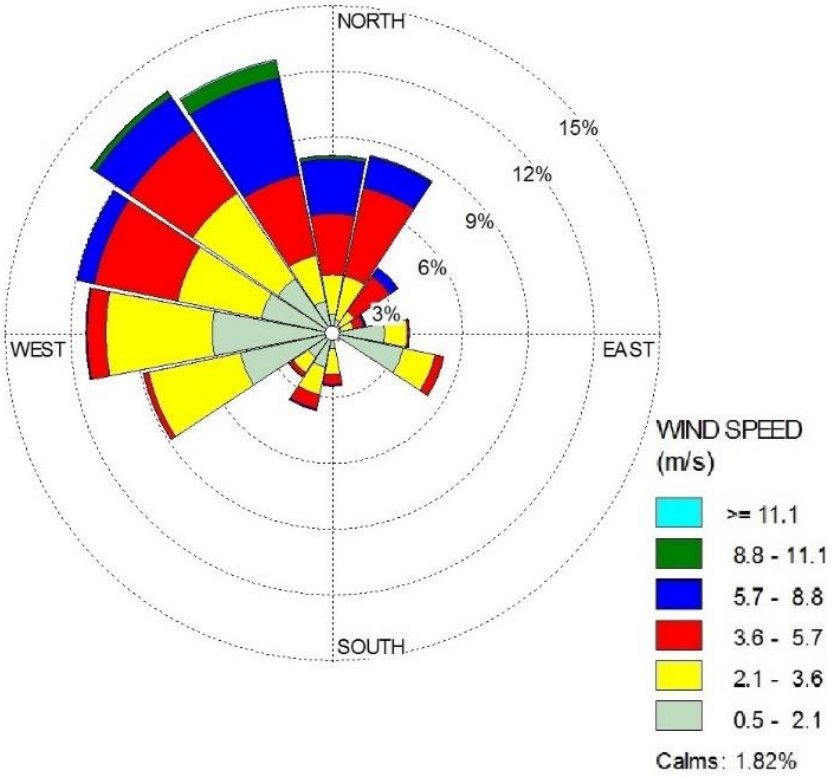


Figure 5.26 Wind rose plots at 10 m AGL at Industrial Area (Central)



© University of Pretoria

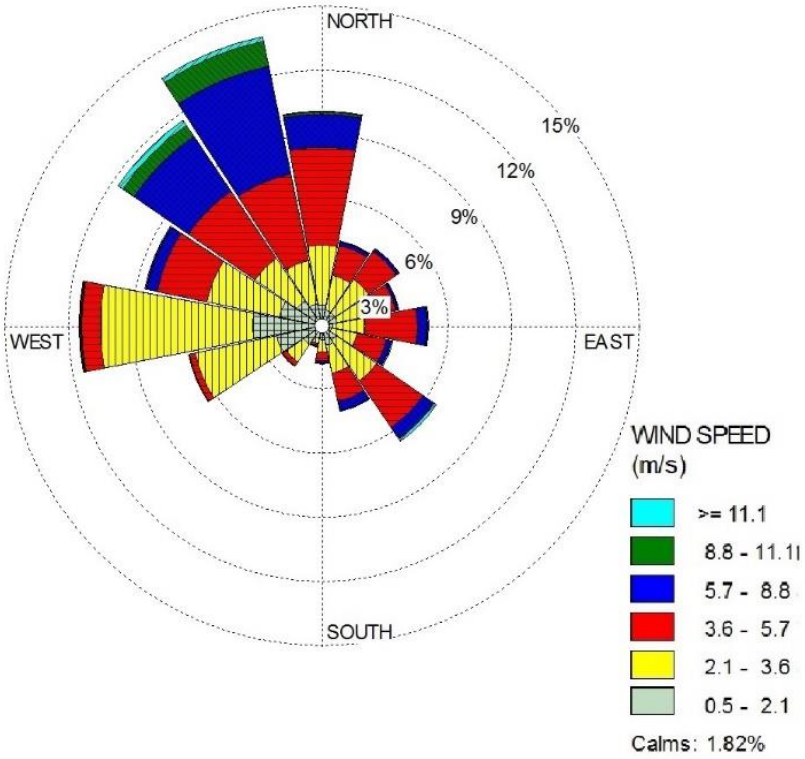


Figure 5.27 Wind rose plots at 10 m AGL at Al-Bahar Desalination Plant

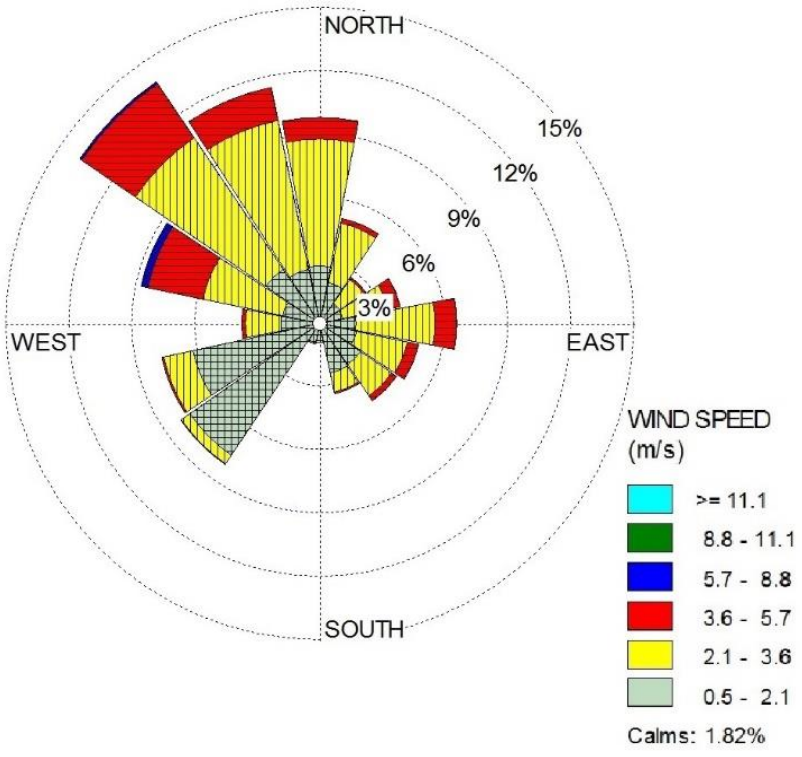


Figure 5.28 Wind rose plots at 10 m AGL at Pearl Beach



© University of Pretoria

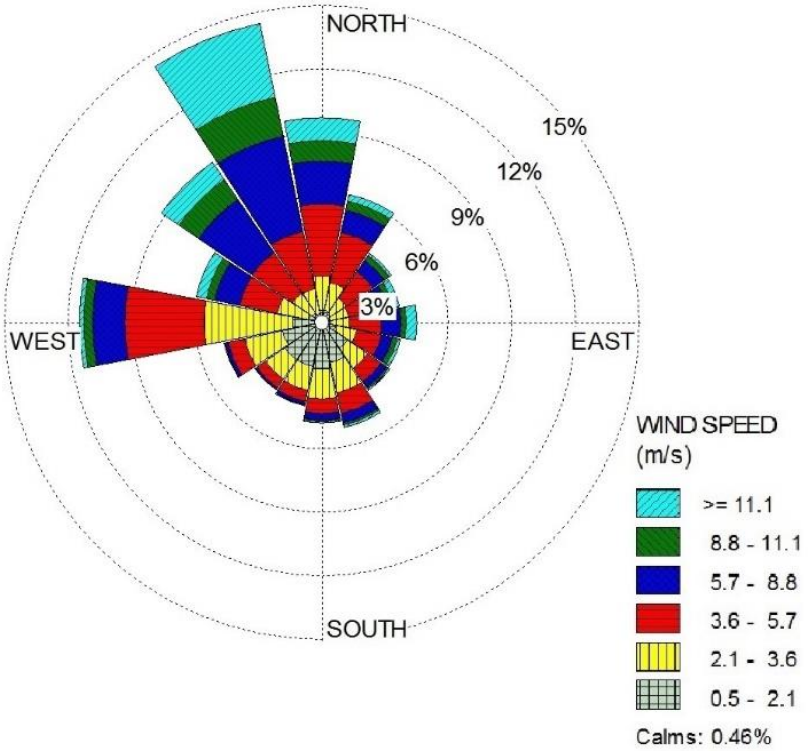


Figure 5.29 Wind rose plots at 10 m AGL at Naval Base

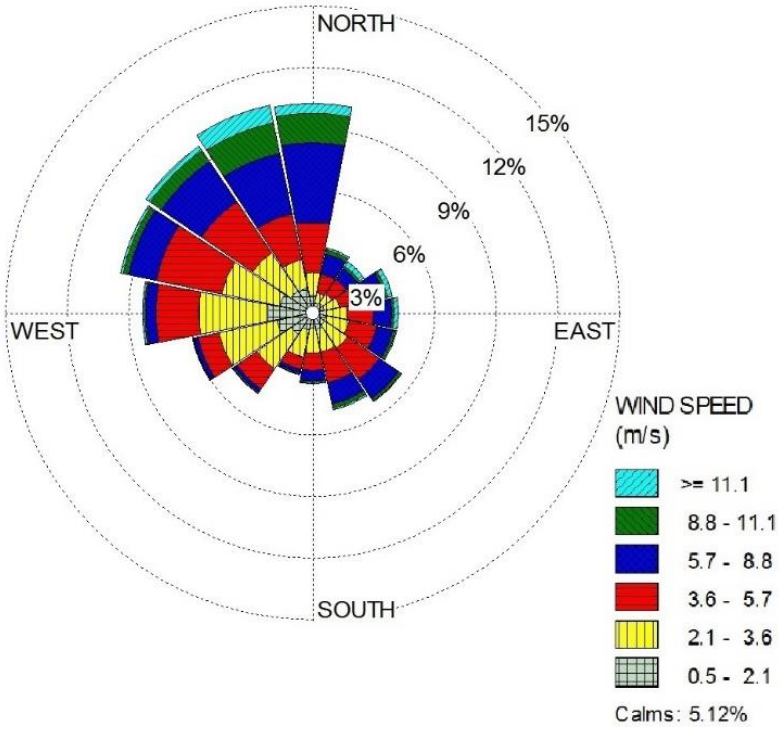


Figure 5.30 Wind rose plots at 10 m AGL at Industrial Area 2 (South)



© University of Pretoria

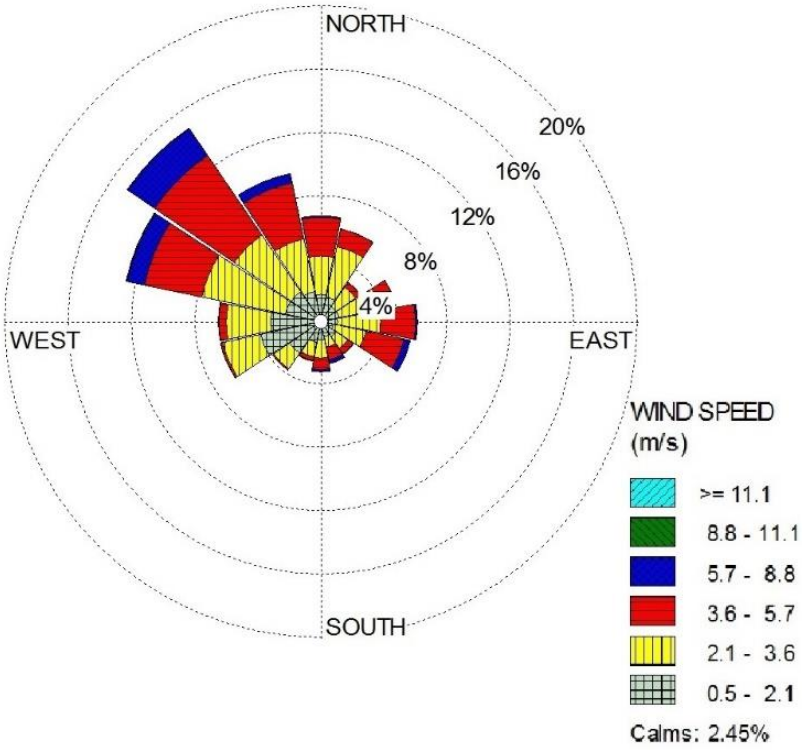


Figure 5.31 Wind rose plots at 10 m AGL at Al-Reggah District

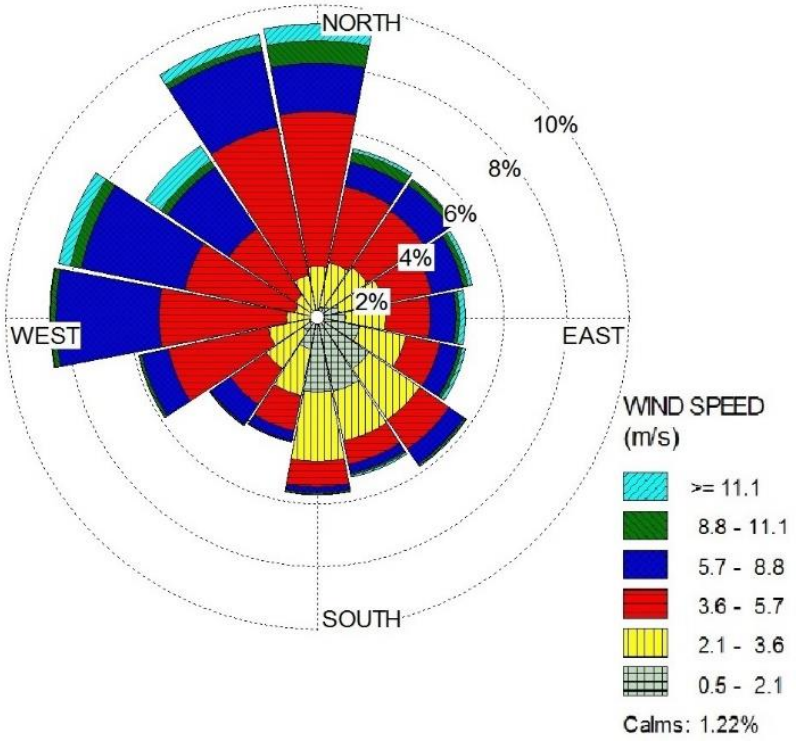


Figure 5.32 Wind rose plots at 10 m AGL at Industrial Area (East)



© University of Pretoria

### 5.1.2.1 Numerical methods for determining the Weibull parameters

There are several methods to estimate the parameters of Weibull distribution function given earlier in equations (5.1) and (5.2). However, three methods commonly used are discussed in this study.

*Maximum Likelihood Method*

Maximum likelihood method was suggested by Stevens and Smulders [57]. This method requires an extensive iterative calculation. Shape and scale parameters of Weibull distribution are estimated by these two equations:

$$k = \left( \frac{\sum_{i=1}^{n} v_i^k \ln(v_i)}{\sum_{i=1}^{n} v_i^k} - \frac{\sum_{i=1}^{n} \ln(v_i)}{n} \right)^{-1} \tag{5.6}$$

$$c = \left( \frac{\sum_{i=1}^{n} (v_i)^k}{n} \right)^{\frac{1}{k}} \tag{5.7}$$

Where $v_i$ is the wind speed and $n$ is the number of nonzero wind speeds. This method is implemented by taking care of zero wind speeds, which make the logarithm indefinite and then calculate shape parameter. The scale parameter is found using a numerical technique in order to find the root of Equation (5.6) around $k = 2$.

*Least-Squares Regression Method (LSRM)*

The equation of the probability density function, after a double logarithmic transformation, can be written as follows:

$$ln[-\ln(1 - F(v))] = k \ln(c) \tag{5.8}$$

The above equation is linear and can be fitted using the least-squares regression method, LSRM [84]. The cumulative distribution function $F(v)$ can be estimated easily, using an estimator, which is the median rank.



© University of Pretoria

The wind power density, WPD, for maximum likelihood method and least-squares regression method is computed using the following equation:

$$WPD = \frac{1}{2}\rho c^3 \tag{5.9}$$

Where:

$\rho$: air density within the time step, kg/m$^3$.

*c*: weibull scale parameter, a measure of average wind speed within the time step, m/s.

*WAsP Algorithm*

There are two requirements of WAsP algorithm:

a. The power density of the fitted Weibull distribution is equal to that of the observed distribution, and
b. The proportion of values above the mean is the same for the fitted Weibull distribution as for the observed distribution.

Let *X* represents the proportion of the observed wind speeds that exceed the mean wind speed. The cumulative distribution function *F(U)* gives the proportion of values that are less than *U*, so *1–F(U)* is the proportion of values that exceed *U*. One can therefore write the second requirement as follows:

$$X = 1 - F(\overline{U}) \tag{5.10}$$

Since the mean wind speed is given by the following equation:

$$\overline{U} = c\Gamma\left(\frac{1}{k} + 1\right) \tag{5.11}$$

Substituting the aforementioned mean value in the expression of the cumulative distribution function will get the second requirement:



© University of Pretoria

$$X = exp\left[-\Gamma\left(\frac{1}{k}+1\right)^{k}\right] \tag{5.12}$$

Taking the natural logarithm of both sides of the equation gives

$$-lnX = \Gamma\left(\frac{1}{k}+1\right)^{k} \tag{5.13}$$

In performing the WAsP algorithm to fit the Weibull distribution, WindoGrapher [85] software (http://www.mistaya.ca/) calculates *X* and then solves the above equation iteratively by using the Brent method, in order to find the *k* parameter. Requirement (1) allows us to calculate the *c* parameter. On the basis of the Weibull distribution, in WAsP algorithm, the mean WPD, assuming a constant air density, is calculated as follows:

$$WPD = \frac{1}{2}\rho c^{3}\Gamma\left(\frac{3}{k}+1\right) \tag{5.14}$$

We can also write an equation for the mean power density of the observed wind speeds as follows:

$$WPD = \frac{1}{2N}\rho\sum_{N} U_i^3 \tag{5.15}$$

As per requirement (1), these must be equal, so one can write,

$$c^{3}\Gamma\left(\frac{3}{k}+1\right) = \frac{1}{N}\sum_{N} U_i^3 \tag{5.16}$$

Solving this for *c* gives us the following:

$$c = \sqrt[3]{\frac{\sum_{N} U_i^3}{N\Gamma\left(\frac{3}{k}+1\right)}} \tag{5.17}$$

The actual wind data and Weibull curves at all seven sites (maximum likelihood method, lease squares regression methods and WAsP method) are also shown in Figures 5.33 to 5.39.



© University of Pretoria

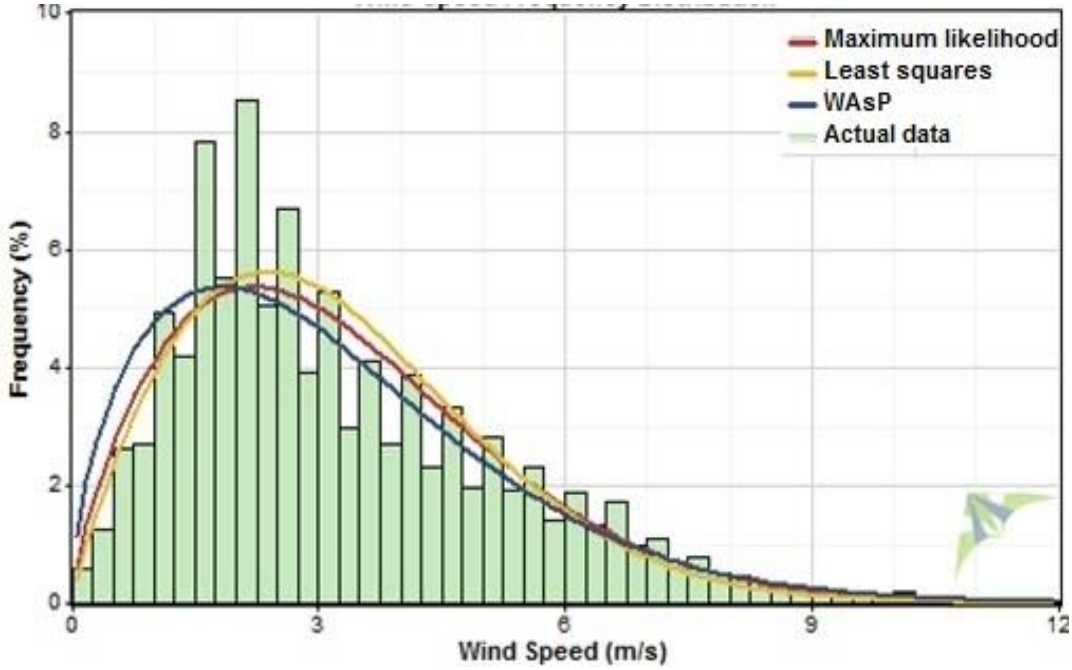


Figure 5.33 Weibull probability distributions (three methods) and actual data at Industrial Area (Central).

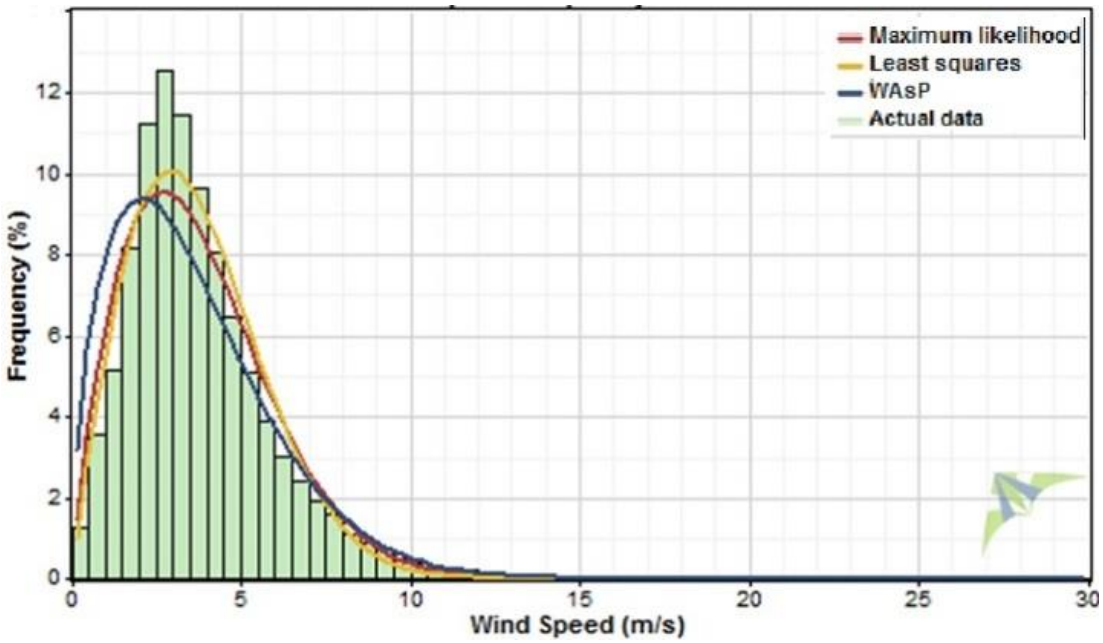


Figure 5.34 Weibull probability distributions (three methods) and actual data at Al-Bahar Desalination Plant.



© University of Pretoria

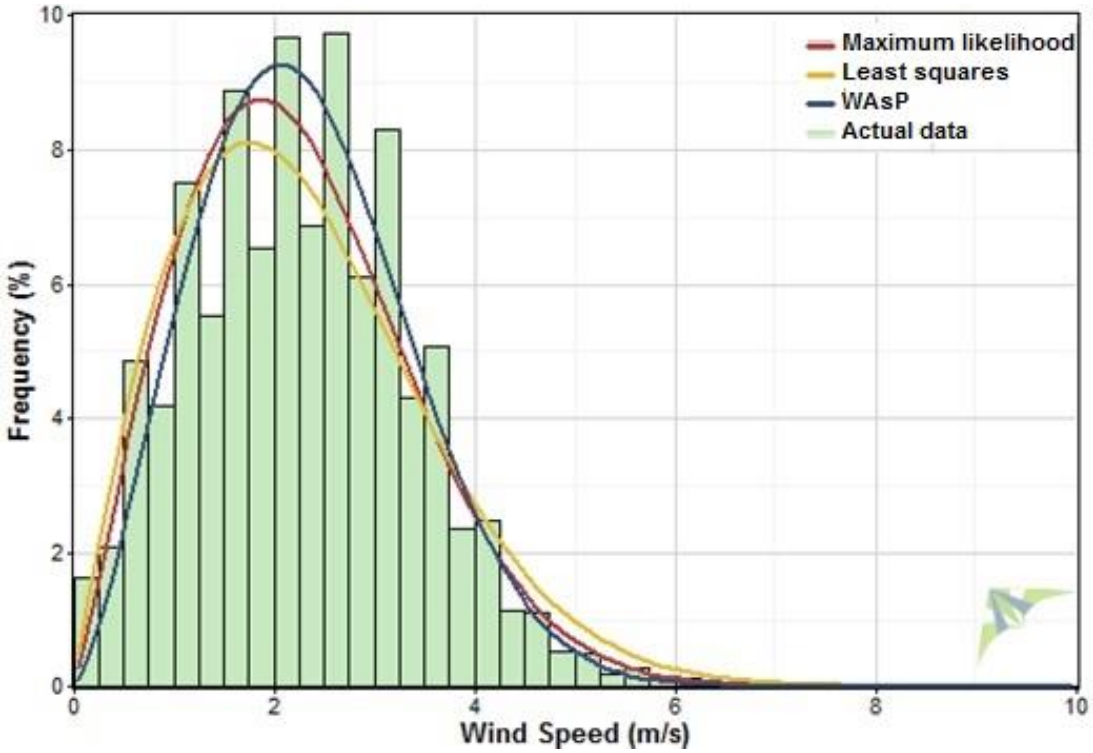


Figure 5.35 Weibull probability distributions (three methods) and actual data at Pearl Beach.

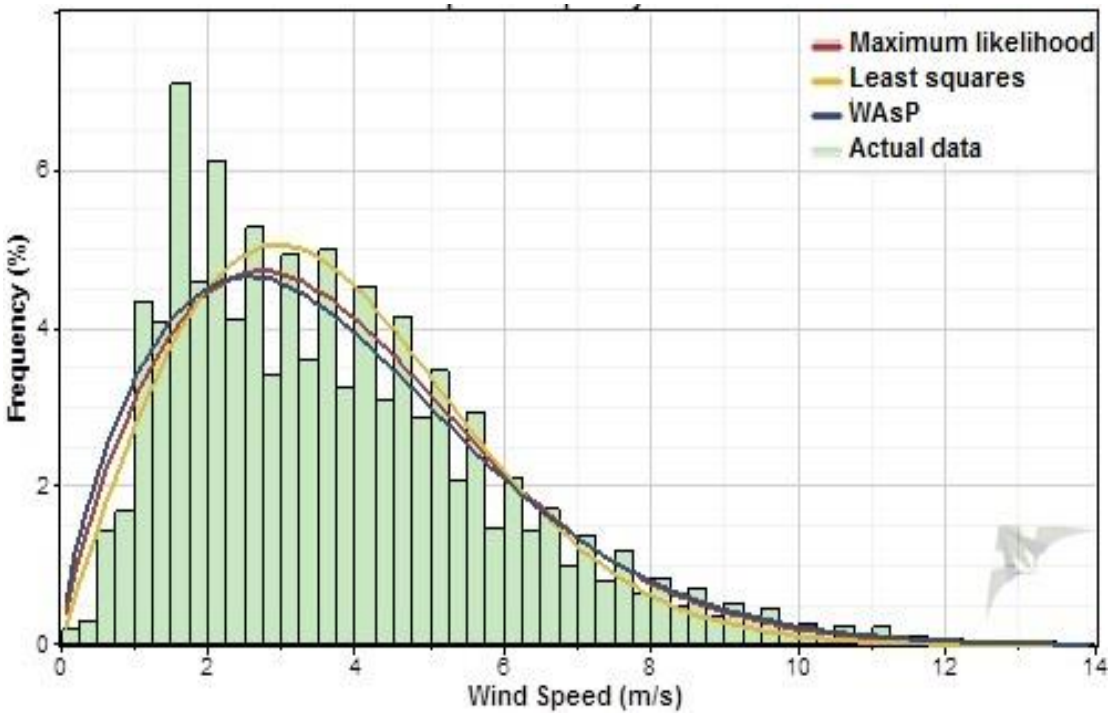


Figure 5.36 Weibull probability distributions (three methods) and actual data at Naval Base.



© University of Pretoria

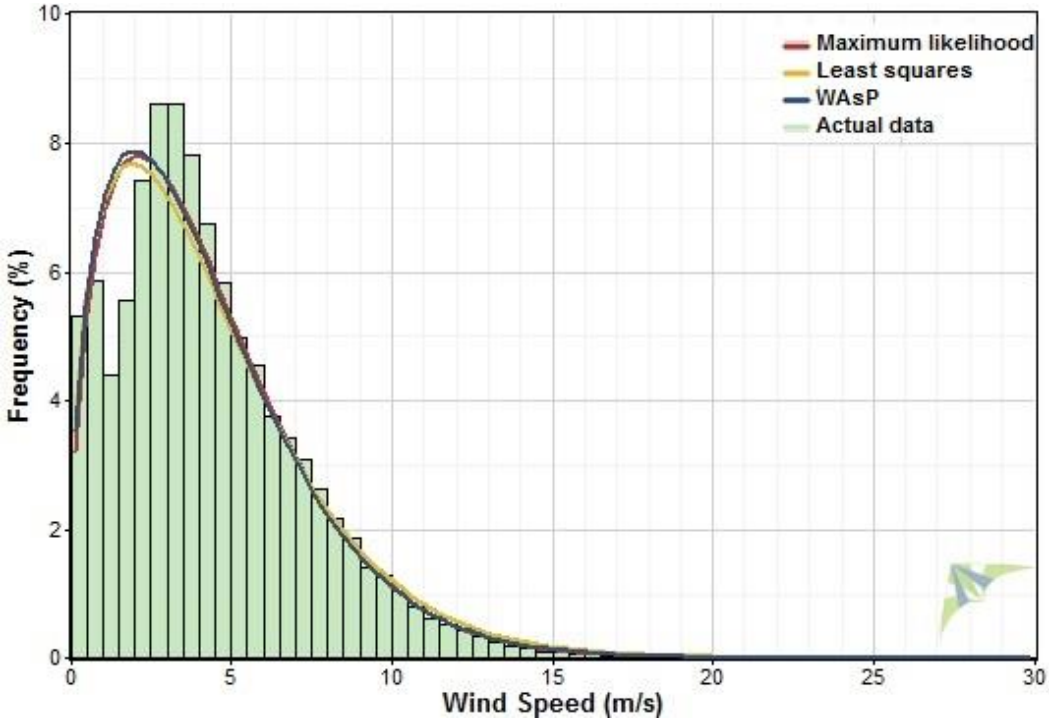


Figure 5.37 Weibull probability distributions (three methods) and actual data at Industrial Area 2 (South).

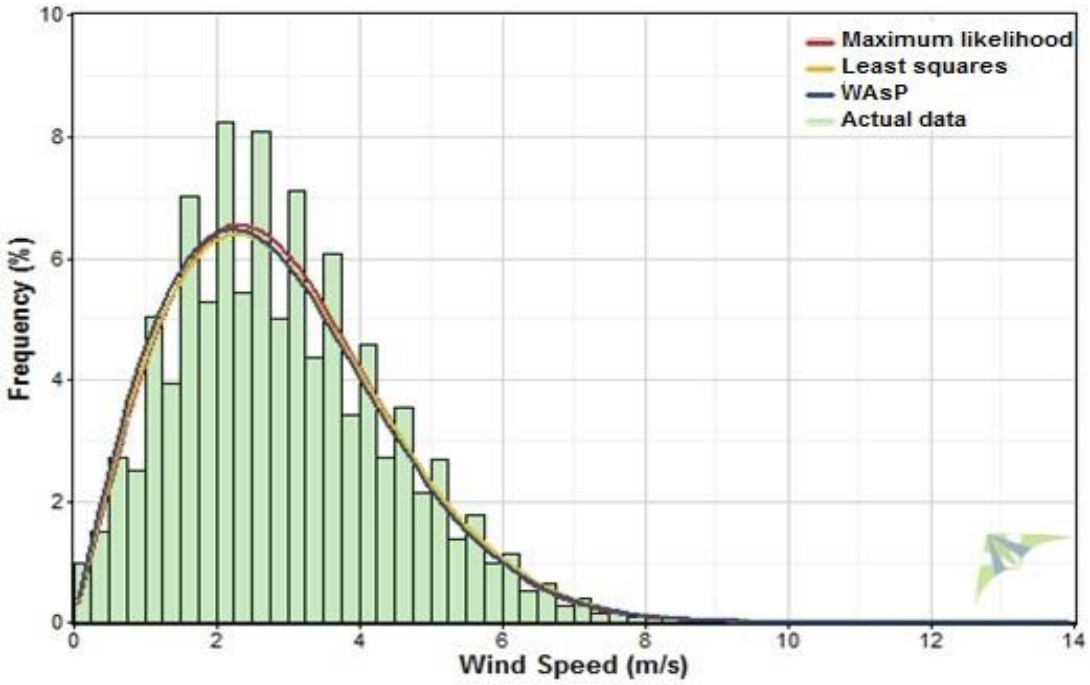


Figure 5.38 Weibull probability distributions (three methods) and actual data at Al-Reggah District.



© University of Pretoria

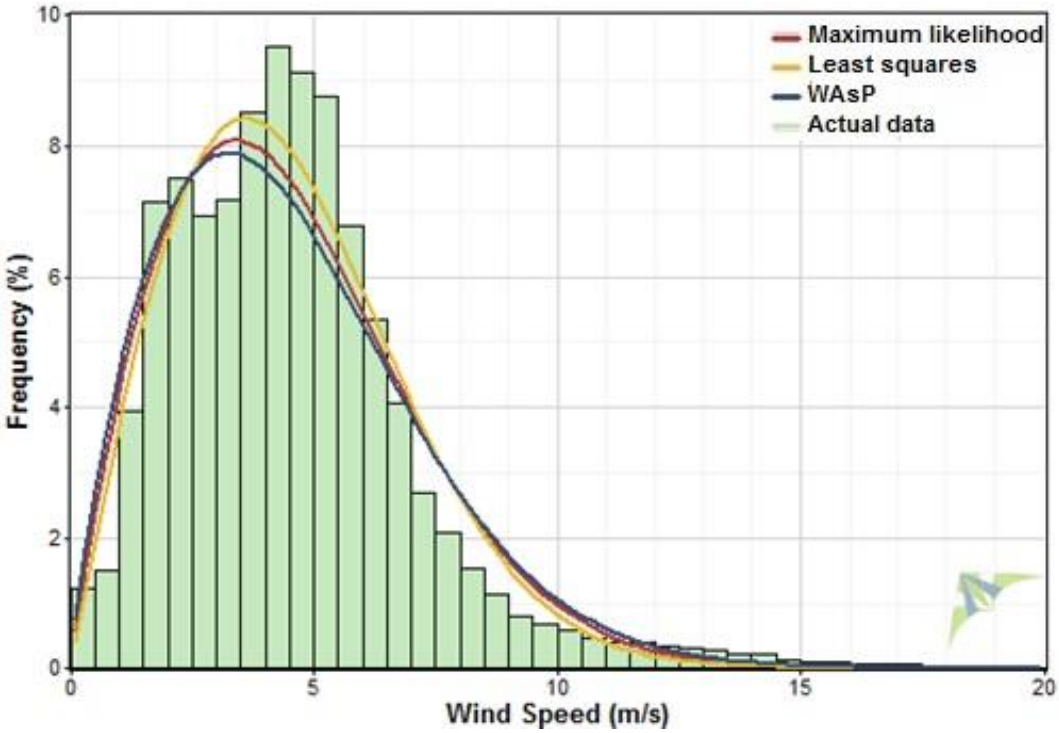


Figure 5.39 Weibull probability distributions (three methods) and actual data at Industrial Area (East).

### 5.1.2.2 Goodness-of-fit tests

To analyse the efficiency of the aforementioned Weibull parameter estimation methods, the following tests were conducted:

Coefficient of determination, $R^2$, is the square of correlation between the frequencies of Weibull to that of actual observations.

The coefficient of determination is computed according to the following equation [84, 59]:

$$R^2 = \frac{\sum_{i=1}^{N}(y_i - z_i)^2 - \sum_{i=1}^{N}(y_i - x_i)^2}{\sum_{i=1}^{N}(y_i - z_i)^2 -} \quad (5.18)$$

The root mean square error, *RMSE* is the measure of the residuals of frequency of Weibull and actual observations [seven towers20].

$$RMSE = \sqrt{\left[\frac{1}{N}\sum_{i=1}^{N}(y_i - x_i)^2\right]} \quad (5.19)$$



© University of Pretoria

The mean bias error (*MBE)*, and mean bias absolute error (*MAE)*, are a measure of how closely the frequency of Weibull match with that of the actual observations [59, 84].

$$MBE = \frac{1}{N}\sum_{i=1}^{N}(y_i - x_i) \quad (5.20)$$

$$MAE = \frac{1}{N}\sum_{i=1}^{N}|y_i - x_i| \quad (5.21)$$

Where:

$N$ is the number of observations, $y_i$ is the frequency of observation, $x_i$ is the frequency of Weibull and $z_i$ is the mean wind speed.

## 5.2 RESULTS AND DISCUSSION

The Weibull scale and shape parameters ($c$ and $k$), wind power density (WPD) and statistical results ($R^2$, RSME, MBE and MAE) for all sites estimated by Maximum likelihood method, least square regression method and WAsP method are shown in Tables 5.4 to 5.10. Considering overall data at all sites, the average error in calculating the WPD was found to be 0.25% for maximum likelihood method, 6.8% for LSRM and 5.7% for WAsP method. It can be clearly validated by goodness-of-fit test indicators, i.e., $R^2$, RSME, MBE and MAE at all sites that maximum likelihood method is the best method to represent the wind regime in Jubail, very closely followed by least square regression and WAsP method. The monthly and annual Weibull parameters obtained by the most accurate method, the maximum likelihood are tabulated in Table 5.11 and 5.12, respectively. The monthly and annual variation of Weibull parameters $k$ and $c$ is shown in Figures. 5.40, 5.41, 5.42 and 5.43. No regular seasonal trend of Weibull parameters could be observed at any of the seven sites. This irregularity is in agreement with findings in similar literature [26].



© University of Pretoria

Table 5.4 Weibull parameters, WPD and statistical results for Industrial Area (Central).

| **Parameter estimation method** | ***k*** | ***c* (m/s)** | **WPD ($W/m^2$)** | ***$R^2$*** | ***RMSE*** | ***MBE*** | ***MAE*** |
|---|---|---|---|---|---|---|---|
| Maximum likelihood method | 1.724 | 3.675 | 48.5 | 0.86 | 0.1750 | -0.0046 | 0.3132 |
| Least-Squares Regression Method | 1.845 | 3.640 | 43.1 | 0.85 | 0.1811 | -0.0047 | 0.3228 |
| WAsP method | 1.563 | 3.519 | 49.6 | 0.85 | 0.1849 | -0.0048 | 0.3547 |

Table 5.5 Weibull parameters, WPD and statistical results for Al-Bahar Desalination Plant.

| **Parameter estimation method** | **k** | **c (m/s)** | **WPD ($W/m^2$)** | **$R^2$** | **RMSE** | **MBE** | **MAE** |
|---|---|---|---|---|---|---|---|
| Maximum likelihood method | 1.800 | 4.218 | 69.2 | 0.96 | 0.0720 | -0.0042 | 0.1758 |
| Least-Squares Regression Method | 1.952 | 4.200 | 61.9 | 0.96 | 0.0725 | -0.0045 | 0.1784 |
| WAsP method | 1.548 | 4.012 | 74.8 | 0.91 | 0.1449 | -0.0030 | 0.2274 |

Table 5.6 Weibull parameters, WPD and statistical results for Pearl Beach.

| **Parameter estimation method** | **k** | **c (m/s)** | **WPD ($W/m^2$)** | **$R^2$** | **RMSE** | **MBE** | **MAE** |
|---|---|---|---|---|---|---|---|
| Maximum likelihood method | 2.104 | 2.539 | 12.7 | 0.91 | 0.0180 | -0.0047 | 0.1155 |
| Least-Squares Regression Method | 1.924 | 2.582 | 14.6 | 0.90 | 0.0230 | -0.0048 | 0.1433 |
| WAsP method | 2.367 | 2.611 | 12.5 | 0.90 | 0.0235 | -0.0050 | 0.1208 |

Table 5.7 Weibull parameters, WPD and statistical results for Naval Base.

| **Parameter estimation method** | **k** | **c (m/s)** | **WPD ($W/m^2$)** | **$R^2$** | **RMSE** | **MBE** | **MAE** |
|---|---|---|---|---|---|---|---|
| Maximum likelihood method | 1.799 | 4.263 | 71.4 | 0.86 | 0.1600 | -0.0050 | 0.3521 |
| Least-Squares Regression Method | 1.973 | 4.205 | 61.4 | 0.85 | 0.1717 | -0.0049 | 0.3619 |
| WAsP method | 1.718 | 4.218 | 73.7 | 0.84 | 0.1574 | -0.0050 | 0.3522 |

Table 5.8 Weibull parameters, WPD and statistical results for Industrial Area 2 (South).

| **Parameter estimation method** | **k** | **c (m/s)** | **WPD ($W/m^2$)** | **$R^2$** | **RMSE** | **MBE** | **MAE** |
|---|---|---|---|---|---|---|---|
| Maximum likelihood method | 1.450 | 4.740 | 139.2 | 0.92 | 0.0970 | -0.0034 | 0.1482 |
| Least-Squares Regression Method | 1.392 | 4.788 | 155.9 | 0.92 | 0.0958 | -0.0032 | 0.1624 |
| WAsP method | 1.421 | 4.678 | 139.4 | 0.92 | 0.0970 | -0.0030 | 0.1491 |



© University of Pretoria

Table 5.9 Weibull parameters, WPD and statistical results for Al-Reggah District

| **Parameter estimation method** | **k** | **c (m/s)** | **WPD ($W/m^2$)** | **$R^2$** | **RMSE** | **MBE** | **MAE** |
|---|---|---|---|---|---|---|---|
| Maximum likelihood method | 2.008 | 3.286 | 28.8 | 0.94 | 0.1770 | -0.0048 | 0.3504 |
| Least-Squares Regression Method | 1.957 | 3.304 | 30.1 | 0.93 | 0.1782 | -0.0048 | 0.3497 |
| WAsP method | 1.938 | 3.242 | 28.7 | 0.93 | 0.1780 | -0.0050 | 0.3485 |

Table 5.10 Weibull parameters, WPD and statistical results for Industrial Area (East)

| **Parameter estimation method** | **k** | **c (m/s)** | **WPD ($W/m^2$)** | **$R^2$** | **RMSE** | **MBE** | **MAE** |
|---|---|---|---|---|---|---|---|
| Maximum likelihood method | 1.876 | 5.098 | 116.0 | 0.94 | 0.0700 | -0.0048 | 0.2339 |
| Least-Squares Regression Method | 1.999 | 5.096 | 107.8 | 0.94 | 0.0705 | -0.0048 | 0.2139 |
| WAsP method | 1.799 | 5.100 | 122.3 | 0.93 | 0.0902 | -0.0050 | 0.2491 |



© University of Pretoria

Table 5.11 Monthly Weibull parameters at all sites (Maximum likelihood method)

| Site | Industrial Area (Central) | | Al-Bahar Desalination Plant | | Pearl Beach | | Naval Base | | Industrial Area 2 (South) | | Al-Reggah District | | Industrial Area (East) | |
|---|---|---|---|---|---|---|---|---|---|---|---|---|---|---|
| Month | *k* | *c* (m/s) | *k* | *c* (m/s) | *k* | *c* (m/s) | *k* | *c* (m/s) | *k* | *c* (m/s) | *k* | *c* (m/s) | *k* | *c* (m/s) |
| Jan | 1.892 | 3.691 | 1.572 | 4.869 | 2.016 | 2.539 | 2.013 | 4.202 | 1.666 | 4.443 | 1.845 | 3.467 | 2.415 | 4.591 |
| Feb | 1.680 | 3.962 | 1.697 | 5.254 | 2.126 | 2.913 | 1.880 | 4.913 | 1.556 | 5.247 | 1.893 | 3.760 | 1.942 | 5.579 |
| Mar | 1.700 | 4.003 | 1.835 | 4.556 | 2.108 | 2.698 | 1.730 | 5.053 | 1.566 | 5.058 | 1.942 | 3.483 | 1.910 | 5.817 |
| Apr | 1.649 | 3.504 | 1.871 | 3.938 | 2.118 | 2.509 | 1.896 | 4.203 | 1.528 | 5.117 | 2.045 | 3.246 | 1.938 | 5.363 |
| May | 1.662 | 4.106 | 1.759 | 4.247 | 2.253 | 2.644 | 1.825 | 4.409 | 1.382 | 5.662 | 2.178 | 3.314 | 1.909 | 5.644 |
| Jun | 1.673 | 4.476 | 1.731 | 4.442 | 2.047 | 2.785 | 1.704 | 4.876 | 1.351 | 5.800 | 2.063 | 3.484 | 1.721 | 6.133 |
| Jul | 1.675 | 4.133 | 1.885 | 4.159 | 2.307 | 2.651 | 1.692 | 4.279 | 1.266 | 4.378 | 2.259 | 3.313 | 1.940 | 5.706 |
| Aug | 1.608 | 3.392 | 2.035 | 3.724 | 2.267 | 2.406 | 1.787 | 3.556 | 1.356 | 3.686 | 2.229 | 2.966 | 1.938 | 5.060 |
| Sep | 1.762 | 3.533 | 2.033 | 3.802 | 2.256 | 2.343 | 1.888 | 3.543 | 1.643 | 4.753 | 2.165 | 2.950 | 1.473 | 4.244 |
| Oct | 1.759 | 3.189 | 2.044 | 3.941 | 2.118 | 2.229 | 1.821 | 3.755 | 1.697 | 4.237 | 2.127 | 2.883 | 2.410 | 4.095 |
| Nov | 2.056 | 3.639 | 2.169 | 4.180 | 2.258 | 2.436 | 2.101 | 4.237 | 1.625 | 4.436 | 2.024 | 3.290 | 2.699 | 4.516 |
| Dec | 2.020 | 3.492 | 2.231 | 3.643 | 1.989 | 2.355 | 2.009 | 4.191 | 1.461 | 4.101 | 1.912 | 3.282 | 2.535 | 4.380 |

Table 5.12 Annual Weibull parameters at all sites (Maximum likelihood method)

| Year | Industrial Area (Central) | | Al-Bahar Desalination Plant | | Pearl Beach | | Naval Base | | Industrial Area 2 (South) | | Al-Reggah District | | Industrial Area (East) | |
|---|---|---|---|---|---|---|---|---|---|---|---|---|---|---|
| | *k* | *c* (m/s) | *k* | *c* (m/s) | *k* | *c* (m/s) | *k* | *c* (m/s) | *k* | *c* (m/s) | *k* | *c* (m/s) | *k* | *c* (m/s) |
| 2008 | 1.714 | 3.971 | 1.603 | 4.777 | 2.128 | 2.667 | - | - | 1.989 | 5.480 | 1.941 | 3.363 | 2.434 | 4.757 |
| 2009 | 1.700 | 3.658 | 1.899 | 4.301 | 2.109 | 2.548 | - | - | 1.875 | 5.251 | 1.992 | 3.318 | 2.318 | 4.450 |
| 2010 | 1.701 | 3.611 | 1.913 | 4.163 | 2.111 | 2.443 | 1.811 | 4.151 | 1.660 | 4.338 | 1.996 | 3.141 | 2.457 | 4.671 |
| 2011 | 1.743 | 3.880 | 1.927 | 3.641 | 2.178 | 2.578 | 1.834 | 4.429 | 1.194 | 3.849 | 2.104 | 3.343 | 2.320 | 4.563 |
| 2012 | 1.724 | 3.675 | 1.987 | 4.229 | 2.057 | 2.467 | 1.763 | 4.212 | 1.096 | 4.685 | 2.025 | 3.261 | 1.876 | 5.098 |



© University of Pretoria

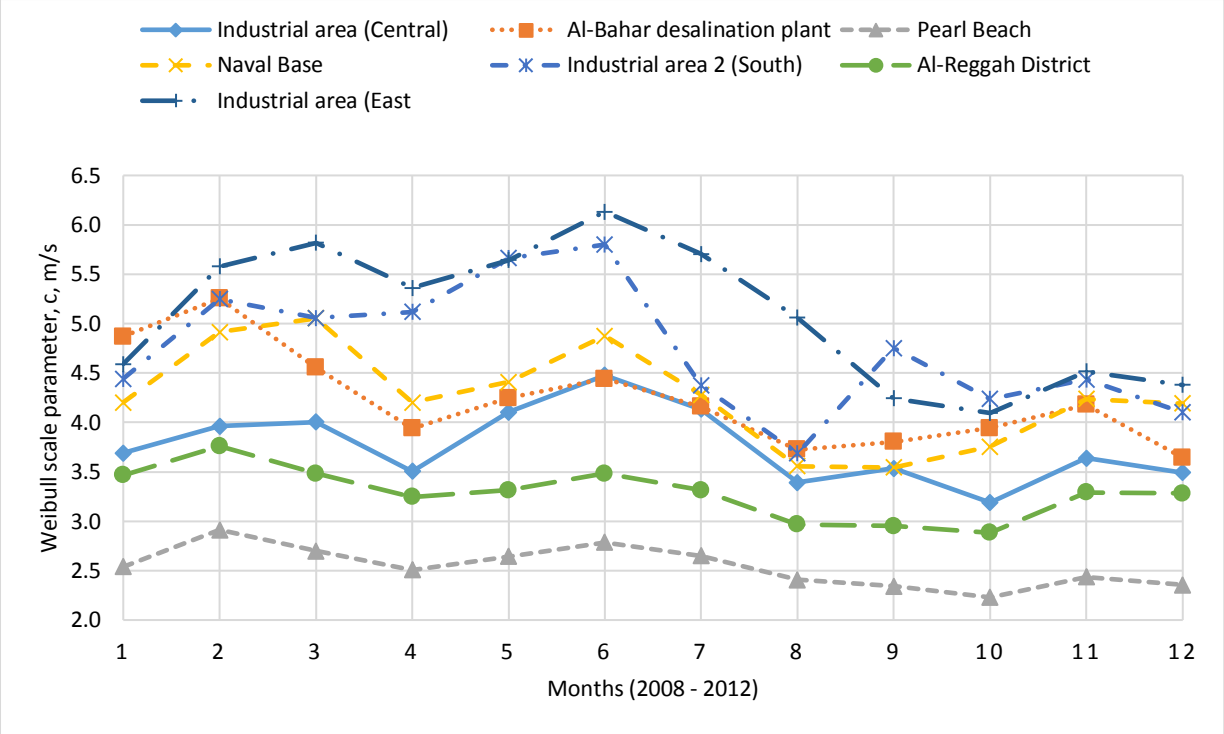


Figure 5.40 Monthly variation of Weibull scale parameter, c, m/s at all sites.

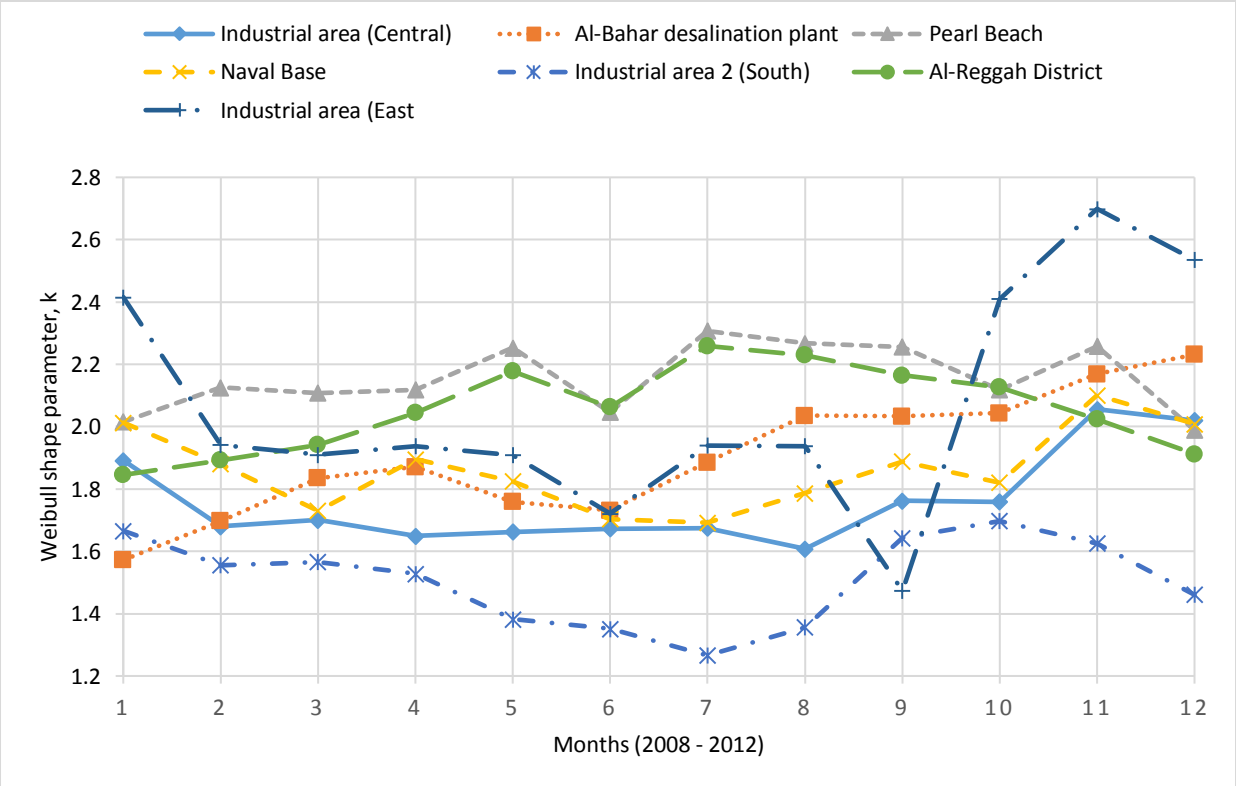


Figure 5.41 Monthly variation of Weibull shape parameter, *k* at all sites.



© University of Pretoria

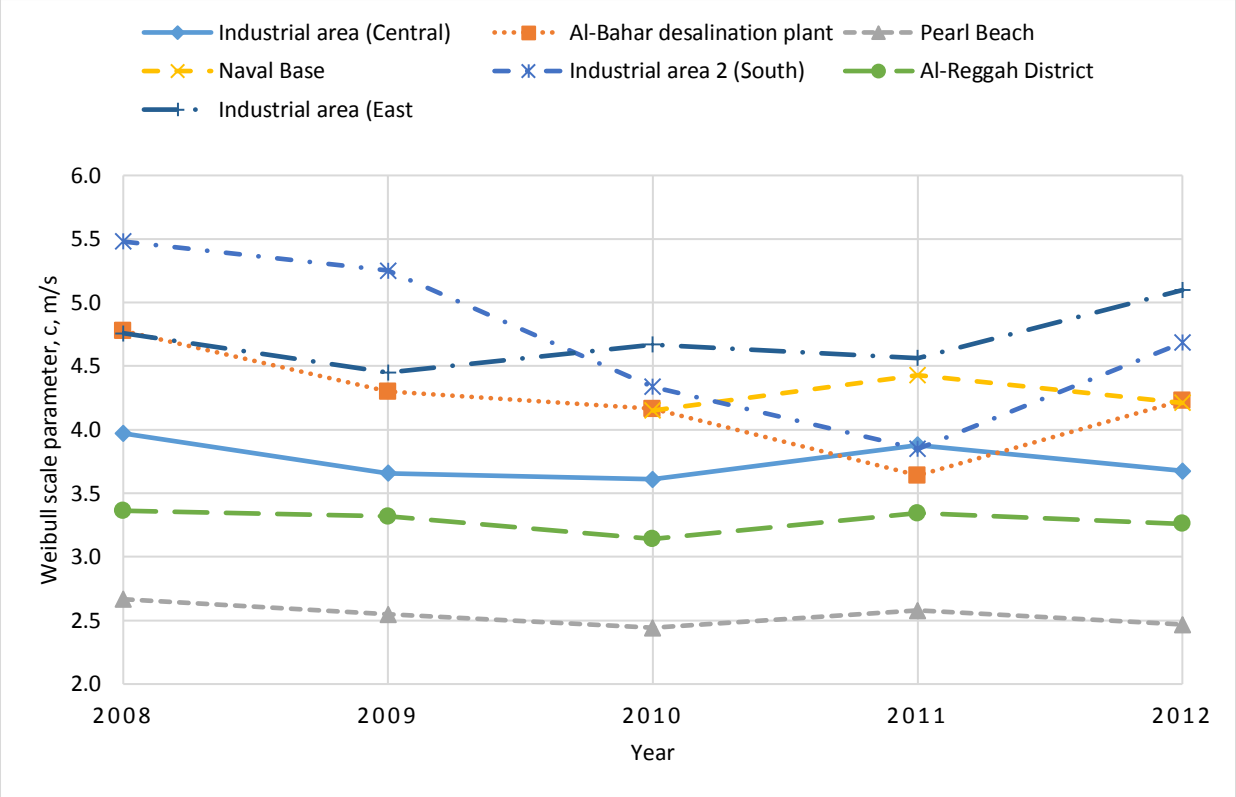


Figure 5.42 Annual variation of Weibull scale parameter, *c*, m/s at all sites.

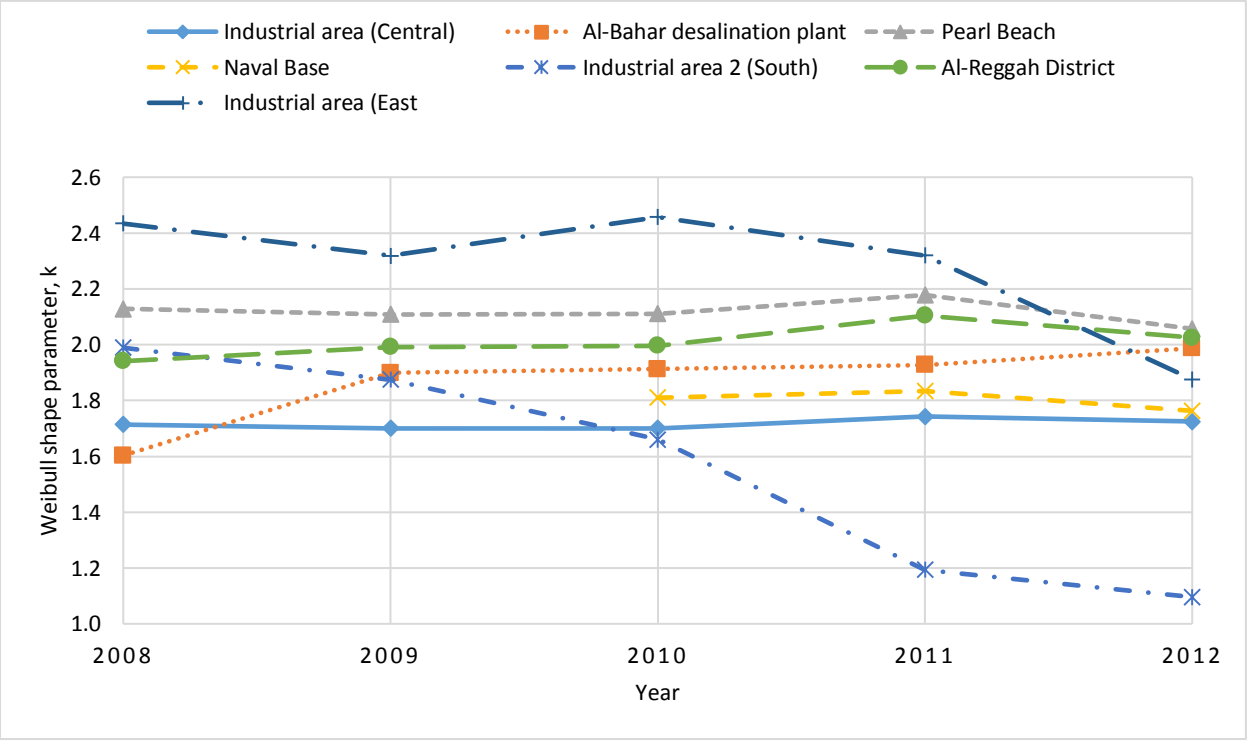


Figure 5.43 Annual variation of Weibull shape parameter, *k* at all sites.



© University of Pretoria

### 5.2.1 Most Probable Wind Speed

The most probable wind speed simply provides the most frequently occurring wind speed for a given wind probability distribution. In high wind potential sites, the most probable wind speed is close to the rated wind speed for a given wind machine. The most probable wind speed can be calculated using the Weibull shape and scale parameters via the following equation [85]:

$$V_{mp} = c\left(1 - \frac{1}{k}\right)^{\frac{1}{k}} \tag{5.22}$$

The most probable wind speed at all seven locations at 10 m AGL was found using all three estimation methods and is shown in Figure 5.44. All three estimation methods showed similar results. The highest most probable wind speeds determined by maximum likelihood method, least-square regression methods and WAsP are 3.39, 3.60 and 3.24 m/s, respectively and were observed at Industrial Area (East).

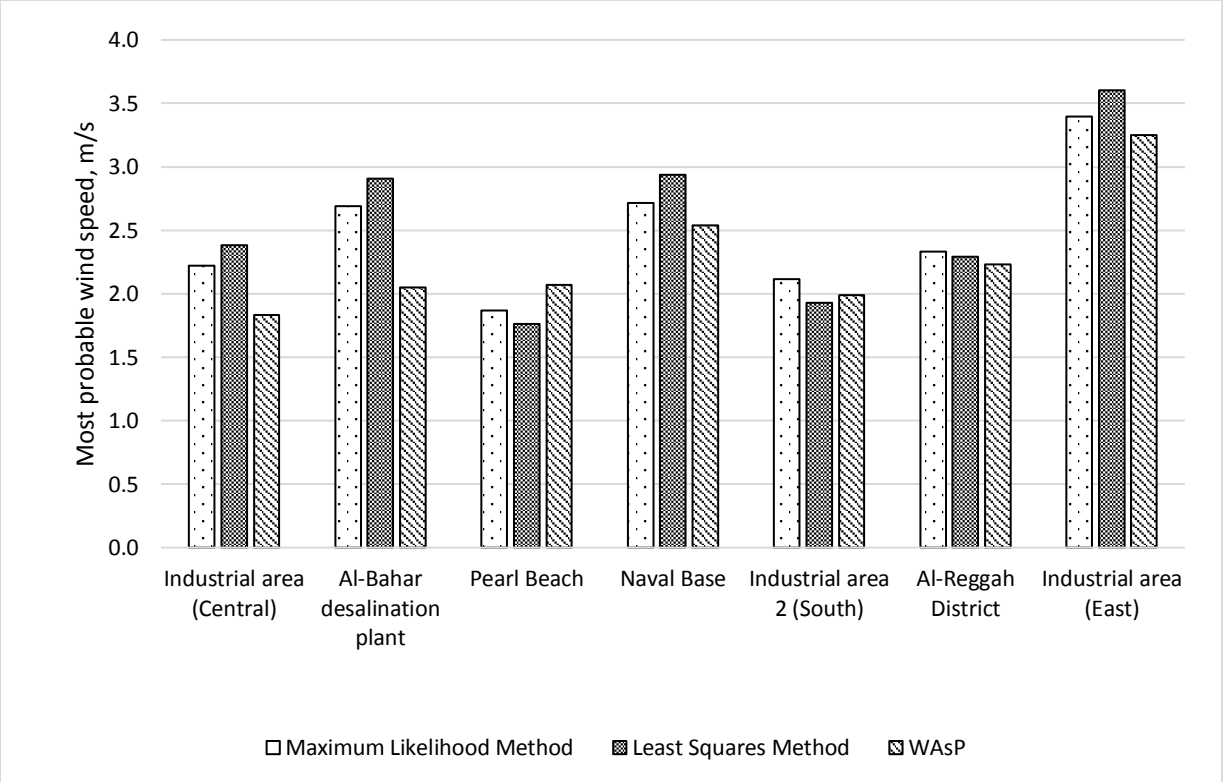


Figure 5.44 Most probable wind speed at all sites.



© University of Pretoria

### 5.2.2 Maximum energy carrying wind speed estimation

The maximum energy carrying wind speed is the speed which generates maximum energy. This can be estimated from the Weibull parameters through the following relationship [85]:

$$V_{max,E} = c\left(1 + \frac{2}{k}\right)^{\frac{1}{k}} \tag{5.23}$$

The maximum energy carrying wind speed at all seven locations at 10 m AGL was determined using all three estimation methods and is shown in Figure 5.45 below. All three estimation methods showed similar results. The highest maximum energy carrying wind speed values of 8.61, 9.0 and 8.68 m/s, determined by maximum likelihood method, least-square regression methods and WAsP, were observed at Industrial Area 2 (South), while at Industrial Area (East) the respective values were found to be 7.5, 7.2 and 7.7 m/s, respectively. These wind speeds are indicative of producing maximum energy at Industrial Area 2 (South) and Industrial Area (East).

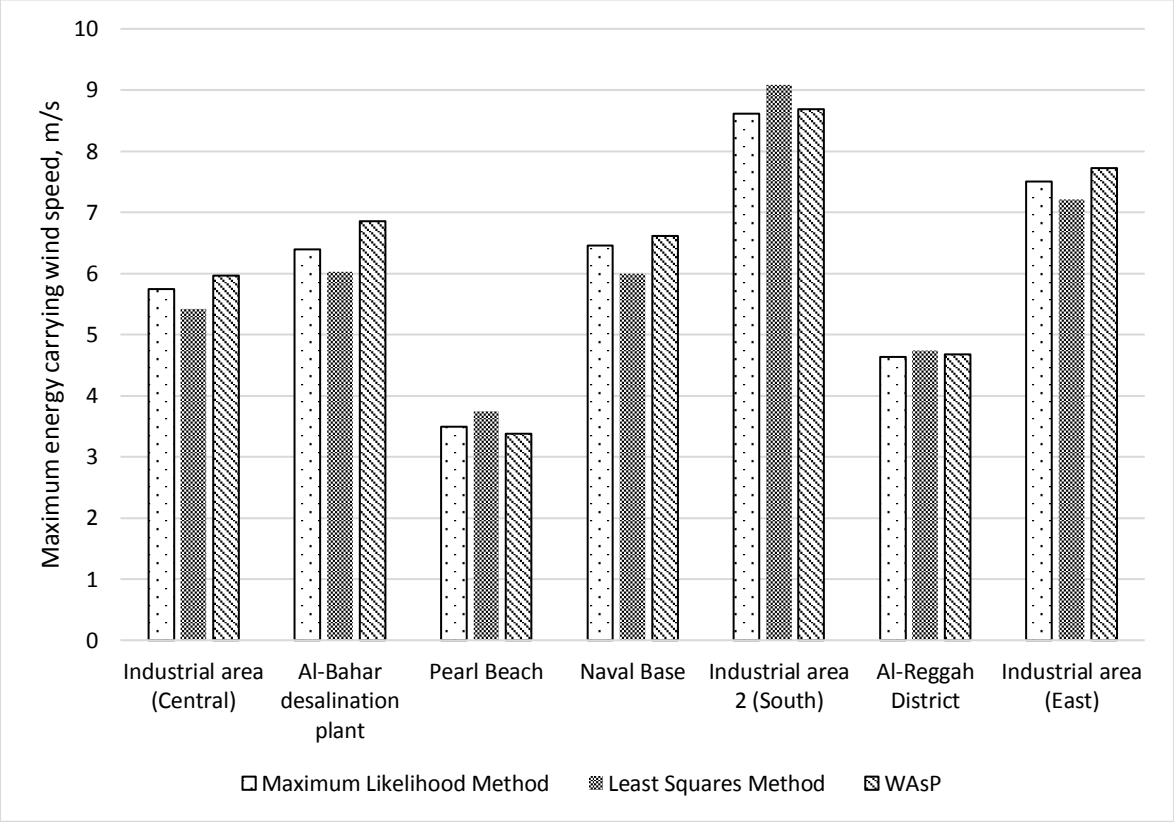


Figure 5.45 Maximum energy carrying wind speed at all sites.



© University of Pretoria

## SUMMARY

The following main observations can be drawn from this chapter:

- At 10, 50 and 90 m AGL, the annual mean wind speeds over the period 2008-2012 were 3.34, 4.79 and 5.35 m/s, respectively.
- There was not much variation in mean annual wind speed. The monthly variation showed that the wind speed was the highest in June and the lowest in October. The diurnal variation showed that the wind speed was high during daytime and low during night-time from 2008 – 2012.
- The most prevailing wind direction at all three heights was from the north-west.
- The percentage of calm winds (wind speed less than 0.5 m/s) decreased with increasing height, i.e. 1.82, 0.61 and 0.56% at 10, 50 and 90 m, respectively.
- The Weibull parameter, c, was the highest in the month of March and the lowest in the month of October at all the measurement heights.
- The wind speed was found to be above 3.5 m/s for 49.3, 75.7 and 77.7% of time at 10, 50 and 90 m in height, respectively. The air density was observed to be the lowest in the month of July and the highest in the month of January.
- The WSE obtained from power law fitting of the wind shear profile was 0.217. The diurnal variation showed low values of WSE during daytime, i.e. from 9:00 AM to 3:00 PM. The seasonal variation of WSE did not show any specific pattern.
- The annual energy production from a commercially available wind turbine WT1 of 3 MW rated power was estimated to be 6,285 MWh with a PCF of 25%.
- The wind characteristics of seven locations in Jubail, Saudi Arabia were analysed. At 10 m AGL, the annual mean wind speeds varied from 2.25 m/s (standard deviation 1.109 m/s) at Pearl Beach to 4.52 m/s (standard deviation 2.52 m/s) at Industrial Area (East).
- In general, at all sites, the highest monthly mean wind speed was observed in February/June and the lowest in September/October. The period of higher winds



© University of Pretoria

availability coincides with high power demand period of the area due to the air conditioning load.

- The most prevailing wind direction was from the north-west which means that the wind machines can spread facing the prevailing wind direction.

- The goodness-of-fit test indicators, i.e., $R^2$, *RSME*, *MBE* and *MAE* show that the maximum likelihood method is the most efficient method to estimate the Weibull parameter for Jubail region followed by least square regression method and WAsP.

- The highest value of most probable wind speed was found to be in the range 3.2 m/s to 3.6 m/s at Industrial Area (East) by three estimation methods.

- The highest value of maximum energy carrying wind speed was found to be in the range 8.6 m/s to 9.0 m/s at Industrial Area 2 (South) by three estimation methods.

- The wind energy output from five different commercially available wind machines with rated output ranging from 1.8 to 3.3 MW at all the sites shows that most feasible site for wind farm development in Jubail city is Industrial Area (East). At this site, the maximum energy output of 11,135 MWh/year with a PCF of 41.3% from a 3 MW rated power wind machine was obtained.

- The second best site for wind farm development is Industrial Area 2 (South). At this site, the maximum energy output of 10,180 MWh/year with a PCF of 37.8% from a 3 MW rated power wind machine was obtained.

- From percent PCF, it can be concluded that wind machine 5 (1.8 MW rated power) is the most efficient at all sites in Jubail as a low rated power wind machine is more efficient for mediocre wind potential areas.



© University of Pretoria

# CHAPTER 6

# WIND ENERGY YIELD ANALYSIS

In this chapter, for the first time, a comprehensive and accurate wind energy output analysis is performed for the largest Industrial city of Saudi Arabia based on some commercially available wind machines. The size of this industrial city is expanding and is expected to have more than doubled in the next decade. The Kingdom has taken initiatives to supplement its existing fossil fuel based energy through renewable sources particularly wind energy, in addition to solar PV and solar thermal options [9]. This study will provide useful information for wind power development program in this industrial city of Jubail.

## 6.1 WIND TURBINE SELECTION

The selection of the size of wind machine depends on the current global standard sizes, commercial availability, optimum energy output, high capacity factor, ease of transportation to the installation site, ease of maintenance etc. The choice of manufacturer will include the interest of the manufacturer for providing services in Saudi Arabia, competitive cost, technical support during installation phase, training of the operation and maintenance staff, terms and conditions for maintenance of the wind machines and the supply of spare parts during project life time and re-powering provision of the plant after the expiry of designed life [86].

The placement of the right turbine at the right place is very important and critical from an optimal energy production point of view. A detailed site suitability study is very important before building a wind farm. The other important aspects are its rated power, cut-in speed, working life span, capital cost, operating cost, corrosion resistivity and harsh weather resistance. Wind turbines are now available in multi-megawatt rated capacities and are being used successfully worldwide. The manufacturing technology is well developed and has a proven record. A wind machine consists of a nacelle unit, a tower and blades. The nacelle unit is the main unit of the whole assembly and houses the gearbox, the cooling system, the generator and other control systems. A schematic view of a typical nacelle unit is shown in Figure 6.1.



© University of Pretoria

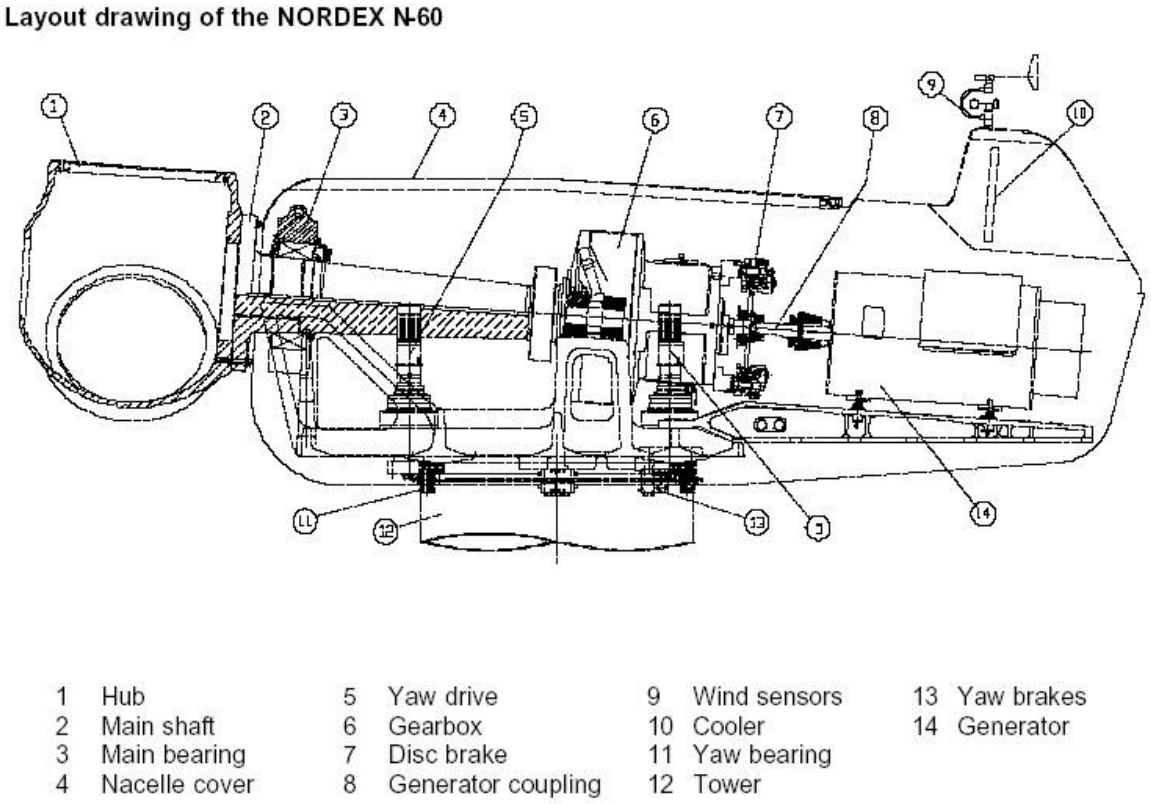


Figure 6.1. Layout drawing of nacelle unit of the Nordex N-60 wind turbine

The following guidelines should be considered when selecting wind turbines [86]:

- In order to optimise energy production, i.e., maximum energy output using minimum wind farm area, wind machines with high rated power should be chosen, especially when the land area is scarce, as in the case of Jubail.

- A wind turbine with a larger rotor diameter considerably increases the output in low wind regions. The knowledge of annual mean wind speed at the site is important for size selection.

- The choice of the tower is also important from a foundation and crane availability point of view. For example, a particular type of tower may not be suitable for a particular type of soil or cranes of required capacity may not be available. Therefore, before proceeding with the selection of wind turbine, soil conditions and information on the availability of crane and wide roads with spacious bands should be at hand.



© University of Pretoria

Jubail Industrial City is mostly desert area but not very loose sand as in south-eastern part of the country. Still soil consideration is very important.

- The maximum total height of the wind turbine may be restricted if the wind park site is in the proximity of airports or monuments.

- The maximum admissible noise emission values at the site may restrict the choice of a particular type of wind machine. Wind farms closer to settlements are affected by this criterion.

- In reference to Jubail, where the temperature reaches 50 °C and more, and relative humidity up to 90% is experienced during summer season, the wind turbine blades, nacelle unit and the tower should withstand these weather conditions. Moreover, the wind turbine material should be corrosion-resistant because Jubail is also a port city.

- The materials of the wind turbine blade and tower should be resistant towards erosion due to sand storms, which are common in Jubail.

- While selecting the wind turbine it should be agreed with the manufacturer that wind turbine towers must be manufactured locally. The technical knowledge will be transferred and the manpower will also be trained by the manufacturer.

## 6.2 ENERGY YIELD FROM A SINGLE WIND TURBINE

To find the wind energy output at Jubail, five different commercially available wind machines with rated power ranging from 1.8 to 3.3 MW, were selected then the frequency of occurrence of wind speed in different bins was determined. This wind speed at different hub heights was determined by vertical extrapolation of wind speed using the local WSE value of 0.217 for all the locations except Industrial Area (Central). These extrapolated wind speed values were used to determine the frequency distribution in different bins at the required hub-height. At this location the wind shear coefficient was obtained by using measured wind speed at 10, 50 and 90 m in heights AGL, for all the remaining six locations the data were available only at 10 m AGL.

At Industrial Area (Central), the wind shear coefficient, α, was calculated using Eq. 5.5.



© University of Pretoria

The air density used in energy output calculations was calculated using Eq. (5.3) where local pressure and temperature were deployed for the calculation.

An overall mean air density at this station was found to be 1.17 kg/m$^3$.

The technical specifications of wind turbines (WT1, WT2, WT3, WT4, and WT5) used in this study are summarised in Table 6.1. The power curves of all the selected wind turbines are shown in Figure 6.2.

Table 6.1 Technical data of wind machines [83]

| Wind machine | Cut-in speed (m/s) | Cut-out speed (m/s) | Rated output (kW) | Rated wind speed (m/s) | Hub height (m) | Rotor diameter (m) |
|---|---|---|---|---|---|---|
| WT 1 | 3 | 25 | 3,300 | 12 | 117 | 126 |
| WT 2 | 3 | 22.5 | 3,000 | 12 | 119 | 126 |
| WT 3 | 4 | 23 | 2,600 | 15 | 75 | 100 |
| WT 4 | 3 | 25 | 2,000 | 11.5 | 80 | 110 |
| WT 5 | 4 | 20 | 1,800 | 12 | 80 | 100 |

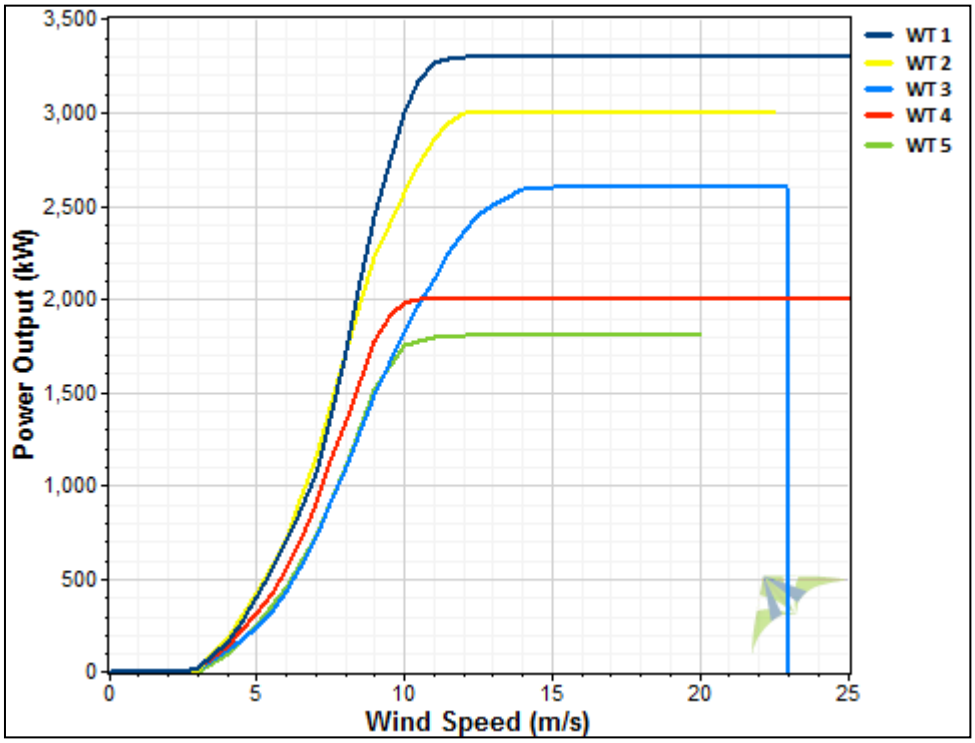


Figure 6.2. Power curves of the selected wind machines.



© University of Pretoria

The wind turbines with rated power in the range of 1.8 to 3.3. MW were selected based on:

(i) Commercial availability in the market,
(ii) Relatively low noise,
(iii) Compatibility with the prevailing wind speed at Jubail that can give optimum plant capacity factor.
(iv) Better utilisation of limited open space available in Industrial hub by using high rated power wind turbines,
(v) Saudi Aramco also installed 2.75 MW rated power wind turbine under the similar wind speed conditions in Turaif, the northern border of Saudi Arabia.

## 6.3 ANNUAL ENERGY OUTPUT AND PLANT CAPACITY FACTOR ANALYSIS

To find the annual energy output, the number of hours the wind speed remained in different wind speed bins per year at different selected turbine hub heights and at all seven sites were determined. The power curve data of all the selected wind turbines were procured [83] and the annual energy output was calculated based on wind speed frequency and turbine power curve data. The Plant Capacity Factor (PCF), is a measure of the actual energy production compared with the installed capacity or rated power of a wind energy conversion system (WECS). The larger the PCF, the better the wind energy conversion system is. The PCF generally varies from 25 to 45%. The PCF is calculated by dividing the actual energy production by the rated capacity of the WECS and number of hours in a year i.e. 8760.

Tables 6.2 to 6.8 show the wind speed frequency at turbine hub heights and power curves data of all selected wind turbines. Finally, the power output in kWh for each wind speed bin, total power output per year and the plant capacity factor (PCF) for each of the five selected wind machines for all seven sites is also presented in these tables. It can be observed from these data that the most feasible site for wind farm development in Jubail city is Industrial Area (East). At this site, the maximum energy output of 11,136 MWh/year was obtained at a PCF of 41.3% from a commercially available wind machine of 3 MW rated power.

By comparing the percent PCF of all five wind machines at all sites, it can be concluded that wind machine 5 (1.8 MW rated power) is most efficient at all sites in Jubail. A low rated power wind machine is more efficient for low or mediocre wind potential areas [28]. Even though the low rated power wind machine is more efficient, wind machine, WT2, with 3 MW rated power can be a better choice as it saves quite a bit of land area which is scarce in Jubail. Wind turbine WT1, with annual energy yield of 6,367 MWh and a PCF of 23.3%, was found to be the second best turbine for Industrial Area (Central). The third best turbine was WT4,



© University of Pretoria

with an annual energy yield of 3,486 MWh and a PCF of 22%. A PCF of 24% was reported in similar studies performed in Dhahran [21].

The worst location for wind farm development was found to be Pearl Beach area where the percent PCF could not cross the 8% mark for any of the mentioned wind turbines. Actually, it was observed that this station is located in Jubail residential area and surrounded by 3-4 storey buildings on all sides. This station is not suitable to record wind speed and direction due to interference from nearby buildings, but it is still suitable to record other weather parameters. The wind speed actually may be better at this location. Wind machines WT1, WT2, and WT4 of rated power 3.3, 3.0 and 2.0 MW, respectively were found to have similar efficiency. Wind machine WT3 (2.6 rated power) was found to be least efficient for all sites in Jubail. Figure 6.3 and 6.4 shows the annual energy output, MWh/year and percent PCF at all sites and for all selected wind machines.



© University of Pretoria

Table 6.2 Wind speed at different hub heights, the power curve data and power output from selected wind machines at Industrial Area (Central).

| | Number of hours/year | | | | Power curve data (kW) | | | | | Energy Calculations (kWh) | | | | |
|---|---|---|---|---|---|---|---|---|---|---|---|---|---|---|
| **Wind Speed (m/s)** | **75m** | **80m** | **117m** | **119m** | **WT 5 1.8MW** | **WT 4 2MW** | **WT 3 2.6MW** | **WT 2 3MW** | **WT 1 3.3MW** | **WT 5 1.8MW** | **WT 4 2MW** | **WT 3 2.6MW** | **WT 2 3MW** | **WT 1 3.3MW** |
| **0** | 143 | 143 | 126 | 126 | 0 | 0 | 0 | 0 | 0 | 0 | 0 | 0 | 0 | 0 |
| **1** | 818 | 804 | 725 | 720 | 0 | 0 | 0 | 0 | 0 | 0 | 0 | 0 | 0 | 0 |
| **2** | 1,132 | 1,094 | 923 | 919 | 0 | 0 | 0 | 0 | 0 | 0 | 0 | 0 | 0 | 0 |
| **3** | 1,217 | 1,189 | 1,031 | 1,023 | 0 | 23 | 11 | 14 | 20 | 0 | 27,358 | 13,392 | 14,316 | 20,611 |
| **4** | 1,269 | 1,245 | 1,063 | 1,063 | 89 | 140 | 116 | 179 | 162 | 110,844 | 174,361 | 147,253 | 190,191 | 172,128 |
| **5** | 1,272 | 1,247 | 1,132 | 1,112 | 228 | 314 | 239 | 416 | 395 | 284,415 | 391,694 | 304,107 | 462,797 | 447,331 |
| **6** | 1,049 | 1,072 | 1,048 | 1,052 | 424 | 549 | 432 | 712 | 694 | 454,322 | 588,261 | 452,960 | 748,685 | 726,979 |
| **7** | 717 | 748 | 872 | 874 | 688 | 900 | 717 | 1,148 | 1,060 | 514,388 | 672,892 | 513,855 | 1,002,893 | 923,899 |
| **8** | 527 | 562 | 693 | 691 | 1,034 | 1,347 | 1,093 | 1,713 | 1,714 | 580,843 | 756,669 | 575,745 | 1,183,139 | 1,187,253 |
| **9** | 305 | 327 | 512 | 527 | 1,440 | 1,775 | 1,479 | 2,219 | 2,432 | 470,668 | 580,164 | 450,883 | 1,168,872 | 1,244,620 |
| **10** | 130 | 142 | 279 | 288 | 1,716 | 1,972 | 1,817 | 2,566 | 2,999 | 243,566 | 279,902 | 236,096 | 738,677 | 836,345 |
| **11** | 76 | 76 | 165 | 165 | 1,794 | 1,999 | 2,102 | 2,858 | 3,260 | 136,284 | 151,857 | 159,682 | 471,354 | 537,654 |
| **12** | 55 | 59 | 78 | 85 | 1,800 | 2,000 | 2,362 | 3,000 | 3,300 | 106,150 | 117,945 | 129,857 | 254,890 | 257,281 |
| **13** | 31 | 32 | 60 | 61 | 1,800 | 2,000 | 2,504 | 3,000 | 3,300 | 57,569 | 63,966 | 77,584 | 182,909 | 197,904 |
| **14** | 13 | 15 | 32 | 31 | 1,800 | 2,000 | 2,584 | 3,000 | 3,300 | 26,995 | 29,994 | 33,569 | 92,952 | 105,543 |
| **15** | 5 | 5 | 13 | 15 | 1,800 | 2,000 | 2,600 | 3,000 | 3,300 | 9,004 | 10,004 | 13,005 | 44,991 | 42,871 |
| **16** | 1 | 1 | 6 | 6 | 1,800 | 2,000 | 2,600 | 3,000 | 3,300 | 1,798 | 1,997 | 2,596 | 18,002 | 19,802 |
| **17** | 0 | 0 | 4 | 4 | 1,800 | 2,000 | 2,600 | 3,000 | 3,300 | 0 | 0 | 0 | 11,984 | 13,182 |
| **18** | 0 | 0 | 1 | 1 | 1,800 | 2,000 | 2,600 | 3,000 | 3,300 | 0 | 0 | 0 | 2,996 | 3,296 |
| | | | | | | | **Power output per year ( kWh)** | | | **4,229,800** | **4,278,400** | **4,484,300** | **7,035,400** | **7,488,900** |
| | | | | | | | **Plant capacity factor %** | | | **26.8** | **24.4** | **19.7** | **26.1** | **25.9** |



© University of Pretoria

Table 6.3 Wind speed at different hub heights, the power curve data and power output from selected wind machines at Bahar desalination plant.

| Number of hours/year | | | | | Power curve data (kW) | | | | | Energy Calculations (kWh) | | | | |
|---|---|---|---|---|---|---|---|---|---|---|---|---|---|---|
| **Wind speed(m/s)** | **75m** | **80m** | **117m** | **119m** | **WT 5 1.8MW** | **WT 4 2MW** | **WT 3 2.6MW** | **WT 2 3MW** | **WT 1 3.3MW** | **WT 5 1.8MW** | **WT 4 2MW** | **WT 3 2.6MW** | **WT 2 3MW** | **WT 1 3.3MW** |
| 218 | 218 | 162 | 162 | 0 | 0 | 0 | 0 | 0 | 0 | 0 | 0 | 0 | 0 | 218 |
| 455 | 455 | 429 | 429 | 0 | 0 | 0 | 0 | 0 | 0 | 0 | 0 | 0 | 0 | 455 |
| 909 | 909 | 673 | 673 | 0 | 0 | 0 | 0 | 0 | 0 | 0 | 0 | 0 | 0 | 909 |
| 1,194 | 1,194 | 1,082 | 1,082 | 0 | 23 | 11 | 14 | 20 | 0 | 27,472 | 13,139 | 15,147 | 21,639 | 1,194 |
| 1,505 | 1,312 | 1,314 | 1,314 | 89 | 140 | 116 | 179 | 162 | 116,751 | 183,653 | 174,597 | 235,128 | 212,797 | 1,505 |
| 1,068 | 1,261 | 1,191 | 1,191 | 228 | 314 | 239 | 416 | 395 | 287,508 | 395,955 | 255,173 | 495,351 | 470,345 | 1,068 |
| 968 | 856 | 937 | 800 | 424 | 549 | 432 | 712 | 694 | 362,918 | 469,911 | 418,016 | 569,699 | 650,014 | 968 |
| 648 | 671 | 644 | 781 | 688 | 900 | 717 | 1,148 | 1,060 | 461,780 | 604,072 | 464,600 | 896,133 | 682,677 | 648 |
| 534 | 558 | 615 | 615 | 1,034 | 1,347 | 1,093 | 1,713 | 1,714 | 576,803 | 751,406 | 584,151 | 1,053,713 | 1,054,328 | 534 |
| 324 | 339 | 453 | 453 | 1,440 | 1,775 | 1,479 | 2,219 | 2,432 | 488,177 | 601,746 | 479,114 | 1,004,579 | 1,101,007 | 324 |
| 281 | 296 | 324 | 324 | 1,716 | 1,972 | 1,817 | 2,566 | 2,999 | 507,335 | 583,022 | 509,819 | 831,242 | 971,510 | 281 |
| 183 | 190 | 246 | 246 | 1,794 | 1,999 | 2,102 | 2,858 | 3,260 | 341,025 | 379,994 | 383,738 | 702,262 | 801,041 | 183 |
| 129 | 133 | 190 | 164 | 1,800 | 2,000 | 2,362 | 3,000 | 3,300 | 239,516 | 266,129 | 305,608 | 491,962 | 627,304 | 129 |
| 107 | 118 | 133 | 141 | 1,800 | 2,000 | 2,504 | 3,000 | 3,300 | 212,710 | 236,345 | 267,827 | 424,159 | 439,113 | 107 |
| 68 | 70 | 89 | 107 | 1,800 | 2,000 | 2,584 | 3,000 | 3,300 | 126,459 | 140,510 | 175,428 | 319,565 | 293,127 | 68 |
| 50 | 49 | 79 | 79 | 1,800 | 2,000 | 2,600 | 3,000 | 3,300 | 87,355 | 97,061 | 129,368 | 235,994 | 259,594 | 50 |
| 32 | 37 | 54 | 54 | 1,800 | 2,000 | 2,600 | 3,000 | 3,300 | 67,172 | 74,635 | 82,677 | 162,673 | 178,941 | 32 |
| 28 | 24 | 37 | 37 | 1,800 | 2,000 | 2,600 | 3,000 | 3,300 | 42,889 | 47,654 | 73,111 | 111,164 | 122,281 | 28 |
| 16 | 21 | 29 | 29 | 1,800 | 2,000 | 2,600 | 3,000 | 3,300 | 38,474 | 42,749 | 40,314 | 85,673 | 94,240 | 16 |
| 10 | 12 | 23 | 21 | 1,800 | 2,000 | 2,600 | 3,000 | 3,300 | 21,602 | 24,002 | 25,509 | 62,284 | 77,184 | 10 |
| 9 | 8 | 14 | 16 | 1,800 | 2,000 | 2,600 | 3,000 | 3,300 | 14,980 | 16,644 | 23,915 | 46,516 | 47,698 | 9 |
| 6 | 7 | 8 | 9 | 0 | 2,000 | 2,600 | 3,000 | 3,300 | 0 | 14,191 | 16,854 | 26,806 | 26,884 | 6 |
| 4 | 4 | 8 | 9 | 0 | 2,000 | 2,600 | 3,000 | 3,300 | 0 | 8,935 | 10,021 | 26,280 | 26,306 | 4 |
| 4 | 4 | 6 | 6 | 0 | 2,000 | 2,600 | 3,000 | 3,300 | 0 | 7,709 | 9,566 | 17,082 | 18,790 | 4 |
| 3 | 4 | 4 | 4 | 0 | 2,000 | 0 | 0 | 3,300 | 0 | 7,709 | 0 | 0 | 14,743 | 3 |
| 2 | 2 | 4 | 4 | 0 | 2,000 | 0 | 0 | 3,300 | 0 | 3,679 | 0 | 0 | 12,720 | 2 |
| 1 | 1 | 4 | 4 | 0 | 0 | 0 | 0 | 0 | 0 | 0 | 0 | 0 | 0 | 1 |
| 1 | 1 | 2 | 2 | 0 | 0 | 0 | 0 | 0 | 0 | 0 | 0 | 0 | 0 | 1 |
| 2 | 1 | 2 | 1 | 0 | 0 | 0 | 0 | 0 | 0 | 0 | 0 | 0 | 0 | 2 |
| 0 | 1 | 0 | 1 | 0 | 0 | 0 | 0 | 0 | 0 | 0 | 0 | 0 | 0 | 0 |
| 0 | 0 | 1 | 1 | 0 | 0 | 0 | 0 | 0 | 0 | 0 | 0 | 0 | 0 | 0 |
| | | | | | | | **Power output per year ( kWh)** | | | **4,697,800** | **4,734,200** | **5,029,000** | **6,766,800** | **8,362,000** |
| | | | | | | | **Plant capacity factor %** | | | **29.8** | **27.0** | **22.1** | **25.1** | **28.9** |



© University of Pretoria

Table 6.4 Wind speed at different hub heights, the power curve data and power output from selected wind machines at Pearl Beach.

| | Number of hours/year | | | | Power curve data (kW) | | | | | Energy Calculations (kWh) | | | | |
|---|---|---|---|---|---|---|---|---|---|---|---|---|---|---|
| **Wind Speed (m/s)** | **75m** | **80m** | **117m** | **119m** | **WT 5 1.8MW** | **WT 4 2MW** | **WT 3 2.6MW** | **WT 2 3MW** | **WT 1 3.3MW** | **WT 5 1.8MW** | **WT 4 2MW** | **WT 3 2.6MW** | **WT 2 3MW** | **WT 1 3.3MW** |
| **0** | 587 | 587 | 445 | 445 | 0 | 0 | 0 | 0 | 0 | 0 | 0 | 0 | 0 | 0 |
| **1** | 1,181 | 1,181 | 1,095 | 1,095 | 0 | 0 | 0 | 0 | 0 | 0 | 0 | 0 | 0 | 0 |
| **2** | 1,833 | 1,833 | 1,489 | 1,489 | 0 | 0 | 0 | 0 | 0 | 0 | 0 | 0 | 0 | 0 |
| **3** | 1,730 | 1,730 | 1,721 | 1,721 | 0 | 23 | 11 | 14 | 20 | 0 | 39,780 | 19,025 | 24,088 | 34,411 |
| **4** | 1,831 | 1,615 | 1,686 | 1,686 | 89 | 140 | 116 | 179 | 162 | 143,719 | 226,075 | 212,408 | 301,848 | 273,181 |
| **5** | 928 | 1,144 | 1,273 | 1,273 | 228 | 314 | 239 | 416 | 395 | 260,925 | 359,344 | 221,821 | 529,424 | 502,698 |
| **6** | 449 | 411 | 636 | 565 | 424 | 549 | 432 | 712 | 694 | 174,272 | 225,650 | 194,173 | 402,606 | 441,367 |
| **7** | 133 | 158 | 227 | 297 | 688 | 900 | 717 | 1,148 | 1,060 | 108,363 | 141,754 | 95,093 | 341,417 | 240,590 |
| **8** | 57 | 65 | 114 | 114 | 1,034 | 1,347 | 1,093 | 1,713 | 1,714 | 67,209 | 87,554 | 62,523 | 195,527 | 195,641 |
| **9** | 23 | 27 | 44 | 44 | 1,440 | 1,775 | 1,479 | 2,219 | 2,432 | 39,357 | 48,513 | 34,074 | 98,359 | 107,800 |
| **10** | 5 | 6 | 23 | 23 | 1,716 | 1,972 | 1,817 | 2,566 | 2,999 | 10,973 | 12,611 | 9,868 | 59,118 | 69,093 |
| **11** | 1 | 2 | 5 | 5 | 1,794 | 1,999 | 2,102 | 2,858 | 3,260 | 3,615 | 4,028 | 2,946 | 13,770 | 15,707 |
| **12** | 0 | 0 | 2 | 2 | 1,800 | 2,000 | 2,362 | 3,000 | 3,300 | 315 | 350 | 414 | 4,730 | 6,649 |
| **13** | 0 | 0 | 0 | 1 | 1,800 | 2,000 | 2,504 | 3,000 | 3,300 | 315 | 350 | 439 | 1,840 | 578 |
| **14** | 0 | 0 | 0 | 0 | 1,800 | 2,000 | 2,584 | 3,000 | 3,300 | 0 | 0 | 0 | 526 | 578 |
| | | | | | | | **Power output per year ( kWh)** | | | **1,233,500** | **1,146,500** | **1,180,400** | **2,057,000** | **2,215,100** |
| | | | | | | | **Plant capacity factor %** | | | **7.8** | **6.5** | **5.2** | **7.6** | **7.7** |



© University of Pretoria

Table 6.5 Wind speed at different hub heights, the power curve data and power output from selected wind machines at Naval Base.

| | Number of hours/year | | | | Power curve data (kW) | | | | | Energy Calculations (kWh) | | | | |
|---|---|---|---|---|---|---|---|---|---|---|---|---|---|---|
| **Wind Speed (m/s)** | **75m** | **80m** | **117m** | **119m** | **WT 5 1.8MW** | **WT 4 2MW** | **WT 3 2.6MW** | **WT 2 3MW** | **WT 1 3.3MW** | **WT 5 1.8MW** | **WT 4 2MW** | **WT 3 2.6MW** | **WT 2 3MW** | **WT 1 3.3MW** |
| **0** | 113 | 113 | 69 | 69 | 0 | 0 | 0 | 0 | 0 | 0 | 0 | 0 | 0 | 0 |
| **1** | 584 | 584 | 469 | 469 | 0 | 0 | 0 | 0 | 0 | 0 | 0 | 0 | 0 | 0 |
| **2** | 1,384 | 1,384 | 1,141 | 1,141 | 0 | 0 | 0 | 0 | 0 | 0 | 0 | 0 | 0 | 0 |
| **3** | 1,057 | 1,057 | 1,121 | 1,121 | 0 | 23 | 11 | 14 | 20 | 0 | 24,303 | 11,623 | 15,695 | 22,422 |
| **4** | 1,038 | 893 | 944 | 944 | 89 | 140 | 116 | 179 | 162 | 79,438 | 124,958 | 120,395 | 168,894 | 152,853 |
| **5** | 897 | 1,042 | 899 | 899 | 228 | 314 | 239 | 416 | 395 | 237,616 | 327,244 | 214,347 | 374,073 | 355,190 |
| **6** | 930 | 810 | 837 | 837 | 424 | 549 | 432 | 712 | 694 | 343,419 | 444,662 | 401,819 | 595,770 | 580,708 |
| **7** | 707 | 724 | 651 | 651 | 688 | 900 | 717 | 1,148 | 1,060 | 498,363 | 651,928 | 507,059 | 747,900 | 690,570 |
| **8** | 598 | 636 | 672 | 672 | 1,034 | 1,347 | 1,093 | 1,713 | 1,714 | 657,327 | 856,306 | 654,142 | 1,151,701 | 1,152,374 |
| **9** | 377 | 386 | 505 | 505 | 1,440 | 1,775 | 1,479 | 2,219 | 2,432 | 556,295 | 685,711 | 557,498 | 1,121,015 | 1,228,620 |
| **10** | 319 | 338 | 377 | 377 | 1,716 | 1,972 | 1,817 | 2,566 | 2,999 | 580,091 | 666,631 | 578,739 | 967,235 | 1,130,451 |
| **11** | 217 | 227 | 282 | 282 | 1,794 | 1,999 | 2,102 | 2,858 | 3,260 | 407,030 | 453,541 | 456,471 | 804,910 | 918,127 |
| **12** | 152 | 159 | 227 | 227 | 1,800 | 2,000 | 2,362 | 3,000 | 3,300 | 286,978 | 318,864 | 359,198 | 680,652 | 748,717 |
| **13** | 135 | 139 | 159 | 159 | 1,800 | 2,000 | 2,504 | 3,000 | 3,300 | 250,711 | 278,568 | 338,677 | 478,296 | 526,126 |
| **14** | 91 | 92 | 105 | 105 | 1,800 | 2,000 | 2,584 | 3,000 | 3,300 | 166,195 | 184,661 | 234,960 | 316,148 | 347,763 |
| **15** | 69 | 72 | 98 | 98 | 1,800 | 2,000 | 2,600 | 3,000 | 3,300 | 129,298 | 143,664 | 179,703 | 293,022 | 322,324 |
| **16** | 39 | 45 | 80 | 80 | 1,800 | 2,000 | 2,600 | 3,000 | 3,300 | 80,890 | 89,878 | 102,036 | 239,674 | 263,641 |
| **17** | 28 | 29 | 47 | 47 | 1,800 | 2,000 | 2,600 | 3,000 | 3,300 | 52,034 | 57,816 | 72,428 | 140,861 | 154,947 |
| **18** | 11 | 12 | 36 | 36 | 1,800 | 2,000 | 2,600 | 3,000 | 3,300 | 21,129 | 23,477 | 28,698 | 107,748 | 118,523 |
| **19** | 7 | 9 | 19 | 19 | 1,800 | 2,000 | 2,600 | 3,000 | 3,300 | 16,872 | 18,746 | 19,132 | 57,290 | 63,019 |
| **20** | 5 | 6 | 9 | 9 | 1,800 | 2,000 | 2,600 | 3,000 | 3,300 | 10,249 | 11,388 | 12,299 | 27,068 | 29,775 |
| **21** | 1 | 3 | 7 | 7 | 0 | 2,000 | 2,600 | 3,000 | 3,300 | 0 | 5,431 | 3,416 | 20,236 | 22,259 |
| **22** | 0 | 0 | 5 | 5 | 0 | 2,000 | 2,600 | 3,000 | 3,300 | 0 | 0 | 0 | 14,191 | 15,610 |
| **23** | 0 | 0 | 1 | 1 | 0 | 2,000 | 2,600 | 3,000 | 3,300 | 0 | 0 | 0 | 3,942 | 4,336 |
| | | | | | | | | **Power output per year ( kWh)** | | **5,042,400** | **5,118,600** | **5,423,200** | **8,385,000** | **8,934,600** |
| | | | | | | | | **Plant capacity factor %** | | **32.0** | **29.2** | **23.8** | **31.1** | **30.9** |



© University of Pretoria

Table 6.6 Wind speed at different hub heights, the power curve data and power output from selected wind machines at Industrial Area 2 (South)

| | Number of hours/year | | | | Power curve data (kW) | | | | | Energy Calculations (kWh) | | | | |
|---|---|---|---|---|---|---|---|---|---|---|---|---|---|---|
| **Wind Speed (m/s)** | **75m** | **80m** | **117m** | **119m** | **WT 5 1.8MW** | **WT 4 2MW** | **WT 3 2.6MW** | **WT 2 3MW** | **WT 1 3.3MW** | **WT 5 1.8MW** | **WT 4 2MW** | **WT 3 2.6MW** | **WT 2 3MW** | **WT 1 3.3MW** |
| **0** | 726 | 726 | 651 | 651 | 0 | 0 | 0 | 0 | 0 | 0 | 0 | 0 | 0 | 0 |
| **1** | 473 | 473 | 475 | 475 | 0 | 0 | 0 | 0 | 0 | 0 | 0 | 0 | 0 | 0 |
| **2** | 647 | 647 | 497 | 497 | 0 | 0 | 0 | 0 | 0 | 0 | 0 | 0 | 0 | 0 |
| **3** | 799 | 799 | 735 | 735 | 0 | 23 | 11 | 14 | 20 | 0 | 18,371 | 8,786 | 10,294 | 14,706 |
| **4** | 1,058 | 906 | 892 | 892 | 89 | 140 | 116 | 179 | 162 | 80,630 | 126,834 | 122,722 | 159,721 | 144,552 |
| **5** | 850 | 1,002 | 892 | 892 | 228 | 314 | 239 | 416 | 395 | 228,449 | 314,618 | 203,146 | 371,012 | 352,283 |
| **6** | 835 | 722 | 781 | 664 | 424 | 549 | 432 | 712 | 694 | 306,313 | 396,618 | 360,835 | 472,462 | 541,921 |
| **7** | 584 | 606 | 573 | 691 | 688 | 900 | 717 | 1,148 | 1,060 | 416,698 | 545,100 | 418,686 | 792,953 | 607,743 |
| **8** | 579 | 587 | 559 | 559 | 1,034 | 1,347 | 1,093 | 1,713 | 1,714 | 607,419 | 791,289 | 632,312 | 956,925 | 957,484 |
| **9** | 398 | 417 | 497 | 497 | 1,440 | 1,775 | 1,479 | 2,219 | 2,432 | 599,815 | 739,355 | 588,204 | 1,101,965 | 1,207,742 |
| **10** | 408 | 419 | 398 | 398 | 1,716 | 1,972 | 1,817 | 2,566 | 2,999 | 719,439 | 826,768 | 741,092 | 1,020,508 | 1,192,714 |
| **11** | 299 | 309 | 356 | 356 | 1,794 | 1,999 | 2,102 | 2,858 | 3,260 | 554,598 | 617,972 | 628,453 | 1,017,466 | 1,160,581 |
| **12** | 249 | 254 | 309 | 257 | 1,800 | 2,000 | 2,362 | 3,000 | 3,300 | 456,484 | 507,204 | 587,835 | 772,106 | 1,020,163 |
| **13** | 219 | 230 | 254 | 268 | 1,800 | 2,000 | 2,504 | 3,000 | 3,300 | 414,698 | 460,776 | 548,815 | 802,591 | 836,887 |
| **14** | 145 | 149 | 170 | 208 | 1,800 | 2,000 | 2,584 | 3,000 | 3,300 | 267,583 | 297,314 | 375,076 | 622,573 | 559,659 |
| **15** | 138 | 126 | 162 | 162 | 1,800 | 2,000 | 2,600 | 3,000 | 3,300 | 226,113 | 251,237 | 360,089 | 484,603 | 533,064 |
| **16** | 85 | 107 | 135 | 135 | 1,800 | 2,000 | 2,600 | 3,000 | 3,300 | 192,527 | 213,919 | 222,066 | 406,289 | 446,918 |
| **17** | 72 | 66 | 105 | 105 | 1,800 | 2,000 | 2,600 | 3,000 | 3,300 | 119,048 | 132,276 | 188,130 | 315,886 | 347,474 |
| **18** | 47 | 52 | 76 | 76 | 1,800 | 2,000 | 2,600 | 3,000 | 3,300 | 94,450 | 104,945 | 122,307 | 227,059 | 249,765 |
| **19** | 45 | 49 | 57 | 50 | 1,800 | 2,000 | 2,600 | 3,000 | 3,300 | 87,670 | 97,411 | 116,385 | 149,796 | 186,746 |
| **20** | 23 | 27 | 48 | 47 | 1,800 | 2,000 | 2,600 | 3,000 | 3,300 | 48,565 | 53,962 | 60,356 | 141,124 | 158,127 |
| **21** | 21 | 23 | 37 | 40 | 0 | 2,000 | 2,600 | 3,000 | 3,300 | 0 | 46,778 | 55,573 | 120,625 | 123,148 |
| **22** | 10 | 12 | 21 | 25 | 0 | 2,000 | 2,600 | 3,000 | 3,300 | 0 | 24,002 | 26,420 | 75,949 | 68,512 |
| **23** | 10 | 10 | 19 | 19 | 0 | 2,000 | 2,600 | 3,000 | 3,300 | 0 | 19,973 | 25,281 | 57,816 | 63,598 |
| **24** | 8 | 9 | 12 | 12 | 0 | 2,000 | 0 | 0 | 3,300 | 0 | 18,221 | 0 | 0 | 39,604 |
| **25** | 4 | 5 | 10 | 9 | 0 | 2,000 | 0 | 0 | 3,300 | 0 | 9,986 | 0 | 0 | 32,955 |
| **26** | 5 | 4 | 7 | 7 | 0 | 0 | 0 | 0 | 0 | 0 | 0 | 0 | 0 | 0 |
| **27** | 3 | 4 | 6 | 7 | 0 | 0 | 0 | 0 | 0 | 0 | 0 | 0 | 0 | 0 |
| **28** | 3 | 3 | 5 | 4 | 0 | 0 | 0 | 0 | 0 | 0 | 0 | 0 | 0 | 0 |
| **29** | 2 | 3 | 3 | 4 | 0 | 0 | 0 | 0 | 0 | 0 | 0 | 0 | 0 | 0 |
| **30** | 2 | 2 | 3 | 3 | 0 | 0 | 0 | 0 | 0 | 0 | 0 | 0 | 0 | 0 |
| **31** | 2 | 3 | 3 | 2 | 0 | 0 | 0 | 0 | 0 | 0 | 0 | 0 | 0 | 0 |
| | | | | | **Power output per year ( kWh)** | | | | | **5,989,700** | **6,214,600** | **6,925,600** | **10,180,300** | **10,129,600** |
| | | | | | **Plant capacity factor %** | | | | | **38.0** | **35.5** | **30.4** | **37.8** | **35.0** |



© University of Pretoria

Table 6.7 Wind speed at different hub heights, the power curve data and power output from selected wind machines at Al-Reggah district.

| | Number of hours/year | | | | Power curve data (kW) | | | | | Energy Calculations (kWh) | | | | |
|---|---|---|---|---|---|---|---|---|---|---|---|---|---|---|
| **Wind Speed (m/s)** | **75m** | **80m** | **117m** | **119m** | **WT 5 1.8MW** | **WT 4 2MW** | **WT 3 2.6MW** | **WT 2 3MW** | **WT 1 3.3MW** | **WT 5 1.8MW** | **WT 4 2MW** | **WT 3 2.6MW** | **WT 2 3MW** | **WT 1 3.3MW** |
| **0** | 365 | 365 | 289 | 289 | 0 | 0 | 0 | 0 | 0 | 0 | 0 | 0 | 0 | 0 |
| **1** | 747 | 747 | 660 | 660 | 0 | 0 | 0 | 0 | 0 | 0 | 0 | 0 | 0 | 0 |
| **2** | 1,421 | 1,421 | 1,122 | 1,122 | 0 | 0 | 0 | 0 | 0 | 0 | 0 | 0 | 0 | 0 |
| **3** | 1,433 | 1,433 | 1,421 | 1,421 | 0 | 23 | 11 | 14 | 20 | 0 | 32,952 | 15,760 | 19,892 | 28,417 |
| **4** | 1,535 | 1,328 | 1,385 | 1,385 | 89 | 140 | 116 | 179 | 162 | 118,225 | 185,971 | 178,031 | 247,876 | 224,334 |
| **5** | 1,072 | 1,278 | 1,185 | 1,185 | 228 | 314 | 239 | 416 | 395 | 291,363 | 401,263 | 256,094 | 492,982 | 468,096 |
| **6** | 887 | 781 | 928 | 797 | 424 | 549 | 432 | 712 | 694 | 330,939 | 428,503 | 383,011 | 567,453 | 643,813 |
| **7** | 548 | 569 | 572 | 703 | 688 | 900 | 717 | 1,148 | 1,060 | 391,446 | 512,066 | 392,558 | 806,932 | 606,443 |
| **8** | 396 | 438 | 523 | 523 | 1,034 | 1,347 | 1,093 | 1,713 | 1,714 | 452,892 | 589,986 | 432,488 | 896,001 | 896,524 |
| **9** | 185 | 208 | 317 | 317 | 1,440 | 1,775 | 1,479 | 2,219 | 2,432 | 298,835 | 368,356 | 273,761 | 703,088 | 770,577 |
| **10** | 103 | 112 | 185 | 185 | 1,716 | 1,972 | 1,817 | 2,566 | 2,999 | 193,013 | 221,807 | 186,865 | 474,964 | 555,111 |
| **11** | 41 | 46 | 93 | 93 | 1,794 | 1,999 | 2,102 | 2,858 | 3,260 | 82,820 | 92,284 | 85,991 | 264,882 | 302,139 |
| **12** | 16 | 19 | 46 | 42 | 1,800 | 2,000 | 2,362 | 3,000 | 3,300 | 33,901 | 37,668 | 38,899 | 125,618 | 152,345 |
| **13** | 9 | 9 | 19 | 22 | 1,800 | 2,000 | 2,504 | 3,000 | 3,300 | 17,029 | 18,922 | 22,154 | 66,226 | 62,152 |
| **14** | 2 | 4 | 6 | 7 | 1,800 | 2,000 | 2,584 | 3,000 | 3,300 | 7,569 | 8,410 | 6,112 | 21,550 | 20,525 |
| **15** | 1 | 1 | 7 | 7 | 1,800 | 2,000 | 2,600 | 3,000 | 3,300 | 1,734 | 1,927 | 3,189 | 21,024 | 23,126 |
| **16** | 0 | 1 | 1 | 1 | 1,800 | 2,000 | 2,600 | 3,000 | 3,300 | 1,104 | 1,226 | 456 | 3,679 | 4,047 |
| **17** | 0 | 0 | 1 | 1 | 1,800 | 2,000 | 2,600 | 3,000 | 3,300 | 0 | 0 | 1,139 | 2,365 | 2,602 |
| **18** | 0 | 0 | 0 | 0 | 1,800 | 2,000 | 2,600 | 3,000 | 3,300 | 788 | 876 | 0 | 0 | 0 |
| **19** | 0 | 0 | 0 | 0 | 1,800 | 2,000 | 2,600 | 3,000 | 3,300 | 0 | 0 | 0 | 1,314 | 1,445 |
| **20** | 0 | 0 | 0 | 0 | 1,800 | 2,000 | 2,600 | 3,000 | 3,300 | 0 | 0 | 0 | 0 | 0 |
| **21** | 0 | 0 | 0 | 0 | 0 | 2,000 | 2,600 | 3,000 | 3,300 | 0 | 350 | 456 | 0 | 0 |
| **22** | 0 | 0 | 0 | 0 | 0 | 2,000 | 2,600 | 3,000 | 3,300 | 0 | 0 | 0 | 0 | 0 |
| **23** | 0 | 0 | 0 | 0 | 0 | 2,000 | 2,600 | 3,000 | 3,300 | 0 | 0 | 0 | 526 | 578 |
| | | | | | | | | **Power output per year ( kWh)** | | **2,856,600** | **2,759,600** | **2,776,100** | **4,686,500** | **5,006,400** |
| | | | | | | | | **Plant capacity factor %** | | **18.1** | **15.8** | **12.2** | **17.4** | **17.3** |



© University of Pretoria

Table 6.8 Wind speed at different hub heights, the power curve data and power output from selected wind machines at Industrial Area (East)

| | Number of hours/year | | | | Power curve data (kW) | | | | | Energy Calculations (kWh) | | | | |
|---|---|---|---|---|---|---|---|---|---|---|---|---|---|---|
| **Wind Speed (m/s)** | **75m** | **80m** | **117m** | **119m** | **WT 5 1.8MW** | **WT 4 2MW** | **WT 3 2.6MW** | **WT 2 3MW** | **WT 1 3.3MW** | **WT 5 1.8MW** | **WT 4 2MW** | **WT 3 2.6MW** | **WT 2 3MW** | **WT 1 3.3MW** |
| **0** | 147 | 147 | 124 | 124 | 0 | 0 | 0 | 0 | 0 | 0 | 0 | 0 | 0 | 0 |
| **1** | 258 | 258 | 216 | 216 | 0 | 0 | 0 | 0 | 0 | 0 | 0 | 0 | 0 | 0 |
| **2** | 802 | 802 | 592 | 592 | 0 | 0 | 0 | 0 | 0 | 0 | 0 | 0 | 0 | 0 |
| **3** | 785 | 785 | 808 | 808 | 0 | 23 | 11 | 14 | 20 | 0 | 18,045 | 8,630 | 11,312 | 16,160 |
| **4** | 837 | 719 | 732 | 732 | 89 | 140 | 116 | 179 | 162 | 64,024 | 100,712 | 97,094 | 130,978 | 118,539 |
| **5** | 849 | 967 | 768 | 768 | 228 | 314 | 239 | 416 | 395 | 220,440 | 303,588 | 202,957 | 319,520 | 303,390 |
| **6** | 1,171 | 999 | 930 | 760 | 424 | 549 | 432 | 712 | 694 | 423,535 | 548,398 | 505,812 | 540,945 | 645,333 |
| **7** | 934 | 957 | 834 | 1,004 | 688 | 900 | 717 | 1,148 | 1,060 | 658,497 | 861,406 | 669,923 | 1,152,774 | 884,082 |
| **8** | 937 | 974 | 938 | 938 | 1,034 | 1,347 | 1,093 | 1,713 | 1,714 | 1,007,594 | 1,312,601 | 1,023,629 | 1,606,379 | 1,607,317 |
| **9** | 582 | 615 | 778 | 778 | 1,440 | 1,775 | 1,479 | 2,219 | 2,432 | 885,405 | 1,091,384 | 860,151 | 1,725,745 | 1,891,398 |
| **10** | 467 | 489 | 582 | 582 | 1,716 | 1,972 | 1,817 | 2,566 | 2,999 | 839,696 | 964,966 | 848,849 | 1,492,325 | 1,744,148 |
| **11** | 242 | 261 | 411 | 411 | 1,794 | 1,999 | 2,102 | 2,858 | 3,260 | 467,691 | 521,135 | 508,581 | 1,175,945 | 1,341,350 |
| **12** | 173 | 183 | 261 | 217 | 1,800 | 2,000 | 2,362 | 3,000 | 3,300 | 330,182 | 366,869 | 408,029 | 650,167 | 860,302 |
| **13** | 140 | 151 | 183 | 201 | 1,800 | 2,000 | 2,504 | 3,000 | 3,300 | 272,471 | 302,746 | 350,741 | 602,338 | 605,334 |
| **14** | 82 | 84 | 114 | 141 | 1,800 | 2,000 | 2,584 | 3,000 | 3,300 | 150,427 | 167,141 | 211,192 | 422,582 | 376,960 |
| **15** | 72 | 65 | 95 | 95 | 1,800 | 2,000 | 2,600 | 3,000 | 3,300 | 116,210 | 129,122 | 187,219 | 286,452 | 315,097 |
| **16** | 48 | 62 | 70 | 70 | 1,800 | 2,000 | 2,600 | 3,000 | 3,300 | 111,164 | 123,516 | 125,951 | 209,977 | 230,975 |
| **17** | 49 | 42 | 59 | 59 | 1,800 | 2,000 | 2,600 | 3,000 | 3,300 | 74,898 | 83,220 | 127,546 | 176,864 | 194,551 |
| **18** | 37 | 42 | 44 | 44 | 1,800 | 2,000 | 2,600 | 3,000 | 3,300 | 75,213 | 83,570 | 97,026 | 130,874 | 143,962 |
| **19** | 38 | 39 | 43 | 35 | 1,800 | 2,000 | 2,600 | 3,000 | 3,300 | 69,695 | 77,438 | 98,165 | 105,908 | 141,071 |
| **20** | 29 | 29 | 35 | 37 | 1,800 | 2,000 | 2,600 | 3,000 | 3,300 | 51,877 | 57,641 | 74,478 | 111,953 | 114,476 |
| **21** | 26 | 27 | 33 | 32 | 0 | 2,000 | 2,600 | 3,000 | 3,300 | 0 | 54,487 | 66,734 | 95,134 | 108,405 |
| **22** | 16 | 19 | 23 | 29 | 0 | 2,000 | 2,600 | 3,000 | 3,300 | 0 | 37,142 | 40,314 | 87,775 | 76,606 |
| **23** | 11 | 12 | 24 | 24 | 0 | 2,000 | 2,600 | 3,000 | 3,300 | 0 | 24,178 | 28,242 | 70,956 | 78,052 |
| **24** | 10 | 11 | 19 | 19 | 0 | 2,000 | 0 | 0 | 3,300 | 0 | 21,725 | 0 | 0 | 61,285 |
| **25** | 6 | 7 | 12 | 11 | 0 | 2,000 | 0 | 0 | 3,300 | 0 | 13,315 | 0 | 0 | 39,893 |
| **26** | 8 | 6 | 10 | 10 | 0 | 0 | 0 | 0 | 0 | 0 | 0 | 0 | 0 | 0 |
| **27** | 3 | 5 | 6 | 7 | 0 | 0 | 0 | 0 | 0 | 0 | 0 | 0 | 0 | 0 |
| **28** | 2 | 3 | 6 | 6 | 0 | 0 | 0 | 0 | 0 | 0 | 0 | 0 | 0 | 0 |
| **29** | 1 | 1 | 6 | 6 | 0 | 0 | 0 | 0 | 0 | 0 | 0 | 0 | 0 | 0 |
| **30** | 0 | 0 | 3 | 3 | 0 | 0 | 0 | 0 | 0 | 0 | 0 | 0 | 0 | 0 |
| **31** | 0 | 0 | 2 | 2 | 0 | 0 | 0 | 0 | 0 | 0 | 0 | 0 | 0 | 0 |
| | | | | | | | | **Power output per year ( kWh)** | | **6,588,900** | **6,708,500** | **7,216,600** | **11,136,200** | **10,863,200** |
| | | | | | | | | **Plant capacity factor %** | | **41.8** | **38.3** | **31.7** | **41.3** | **37.6** |



© University of Pretoria

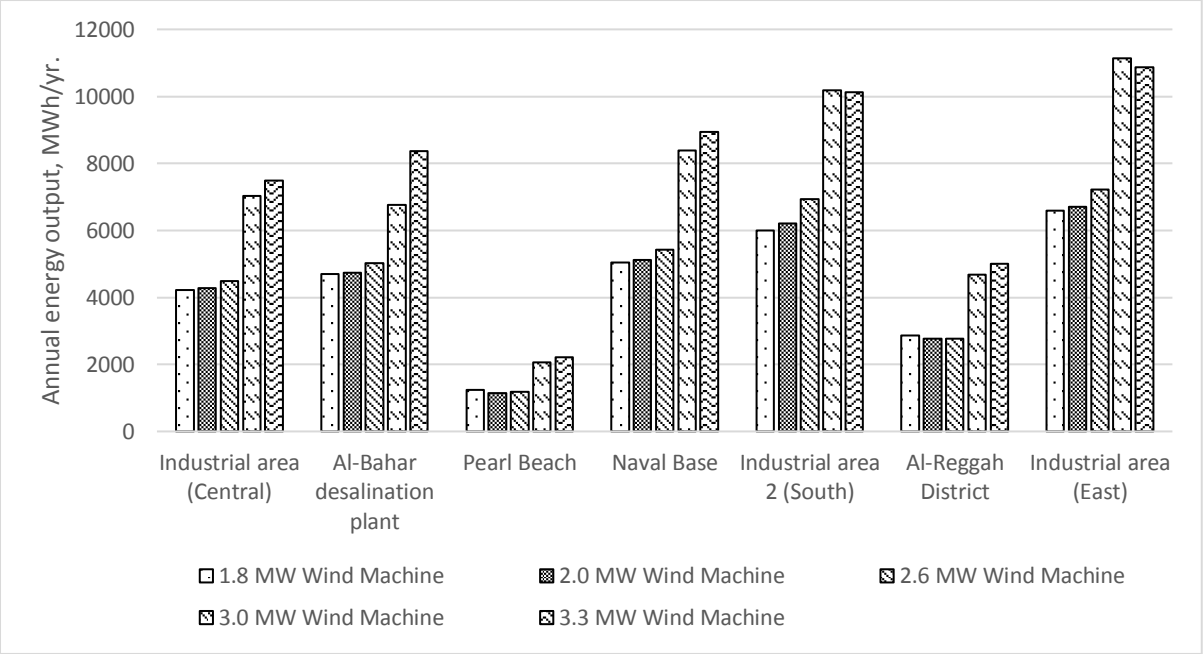


Figure 6.3. Annual energy output of different wind machines at all sites.

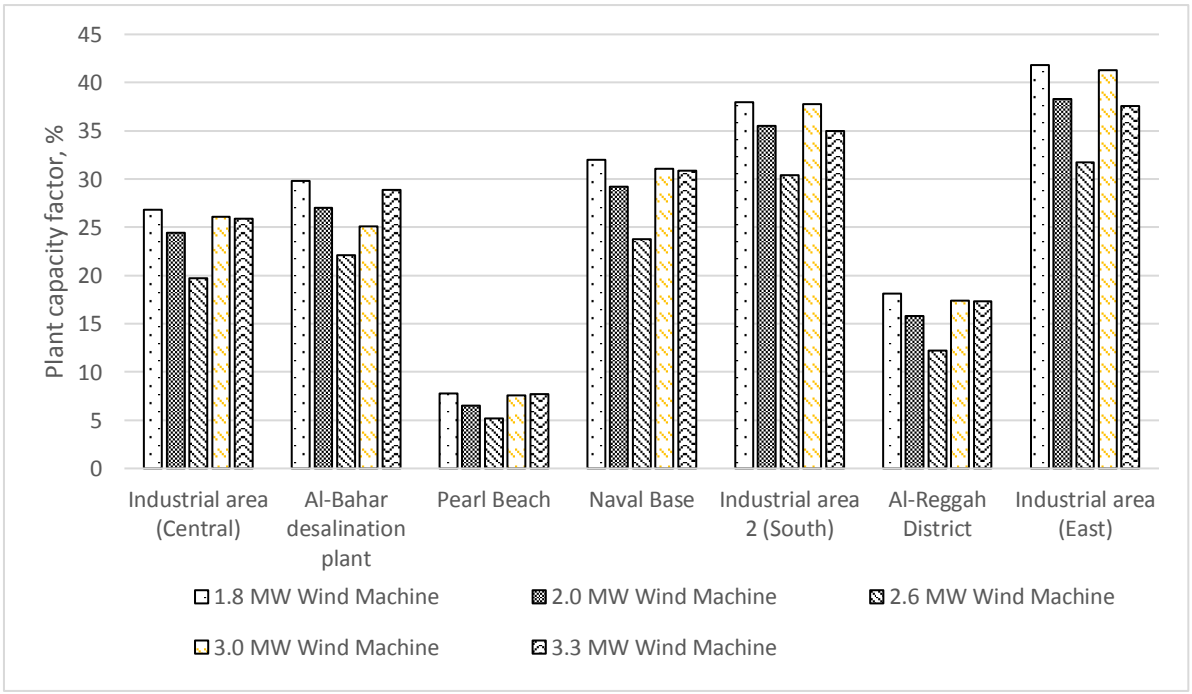


Figure 6.4. Plant capacity factor of different wind machines at all sites.



© University of Pretoria

The ranking of selected wind machines at all seven locations in Jubail based on percent PCF is shown in Table 6.9. At all sites, WT5 (Rated power 1.8 MW) was observed to be ranked as the best option and WT3 (Rated power 2.6 MW) as the worst option. The second best wind turbine was WT2 (rated power 3 MW) at all locations except Al-Bahar Desalination Plant and Pearl Beach. At these locations WT1 (Rated power 3.3 MW) was the second best option.

Table 6.9 Ranking of selected wind turbines at all the locations.

| **Site** | **Wind turbine (WT)** | | | | |
|---|---|---|---|---|---|
| | **Best** | **Good** | **Fair** | **Bad** | **Worst** |
| Industrial Area (Central) | 5 | 2 | 1 | 4 | 3 |
| Al-Bahar Desalination Plant | 5 | 1 | 4 | 2 | 3 |
| Pearl Beach | 5 | 1 | 2 | 4 | 3 |
| Naval Base | 5 | 2 | 4 | 1 | 3 |
| Industrial Area 2 (South) | 5 | 2 | 4 | 1 | 3 |
| Al-Reggah District | 5 | 2 | 1 | 4 | 3 |
| Industrial Area (East) | 5 | 2 | 4 | 1 | 3 |

The comparison of diurnal and seasonal energy output from the selected wind machines at Industrial Area (Central) is shown in Figures 6.5 and 6.6, respectively. The diurnal power output indicates two peaks, one at 3 AM and another at 5 PM for all wind machines. The seasonal power output indicates that the minimum monthly mean wind power availability in the months of April and October while the maximum in March. In general, an increasing trend was observed in monthly power output from all turbines from January until March and then a decreasing trend towards the end of the year except for dips in April and October. Similar diurnal and season trends were observed at all the other locations in Jubail.



© University of Pretoria

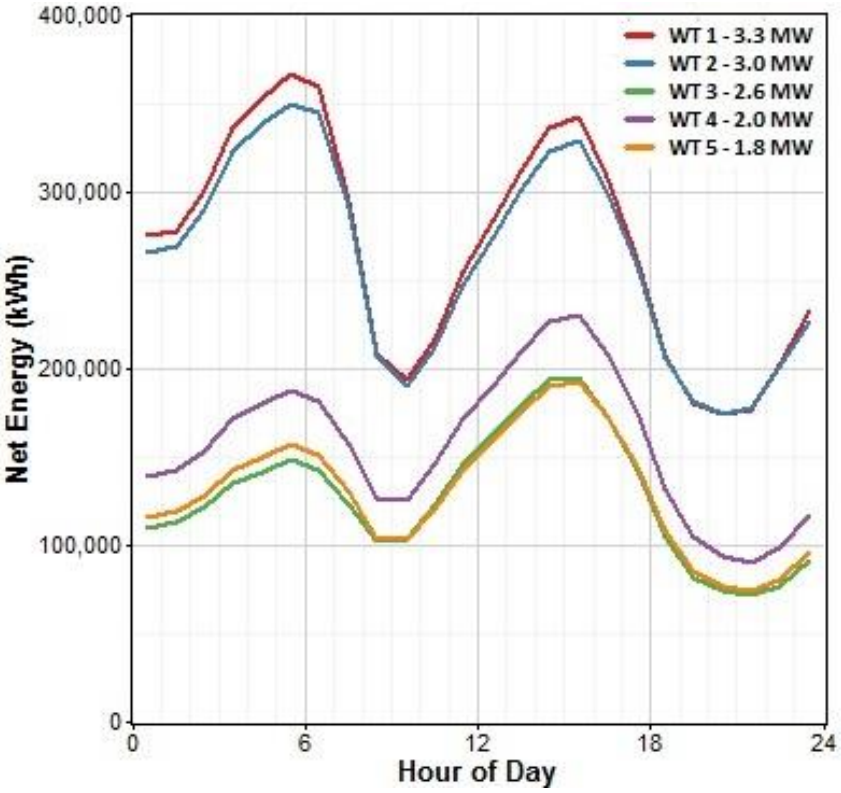


Figure 6.5. Comparison of the diurnal energy output from the selected wind machines at Industrial Area (Central).

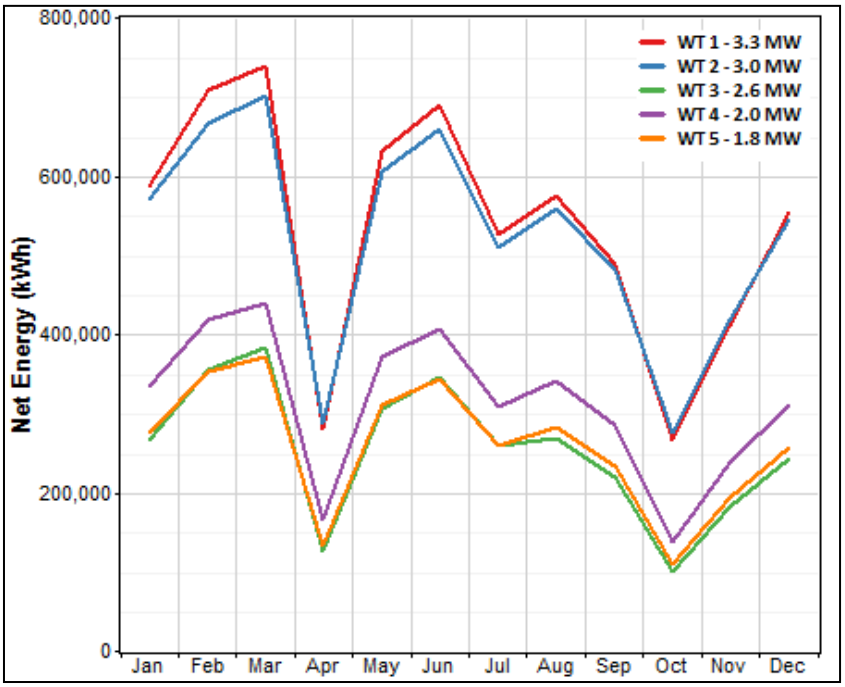


Figure 6.6. Comparison of the seasonal energy output from the selected wind machines at Industrial Area (Central).

## 6.4 RATED AND ZERO POWER OUTPUT

A wind turbine has zero power output when the wind speed is less than the cut-in speed of that particular wind turbine or when the wind speed is above the cut-out speed. A wind turbine can produce maximum power when the wind speed is exactly or above the rated wind speed but below the cut-out speed for that wind turbine. The percentage duration during which the wind turbine remained idle or with zero energy yield and the percentage duration during which the wind turbine produced the rated output was determined for all five wind turbines at all seven locations, as shown in Figures 6.7 to 6.13.

The maximum duration of rated power output between 8 to 16.6% was obtained at Industrial Area 2 (South). The minimum duration of rated power output, less than 0.3% for all wind turbines was obtained at Pearl Beach. The maximum duration of zero power output between 35 to 60% was also obtained at Pearl Beach. The minimum duration of zero power output between 12 to 23% was obtained at Industrial Area (East).

Overall, the percentage of rated power duration for wind turbines, WT1 and WT2 was observed to be better than the remaining three wind turbines and the percentage of zero power duration was also less for the same two turbines, WT1 and WT2. It can be concluded that, for wind characteristics of Jubail Industrial City, wind turbines, WT1 and WT2 of rated power 3.3 and 3 MW are most suitable. The most suitable location for developing a wind farm is Industrial Area 2 (South) and Industrial Area (East).

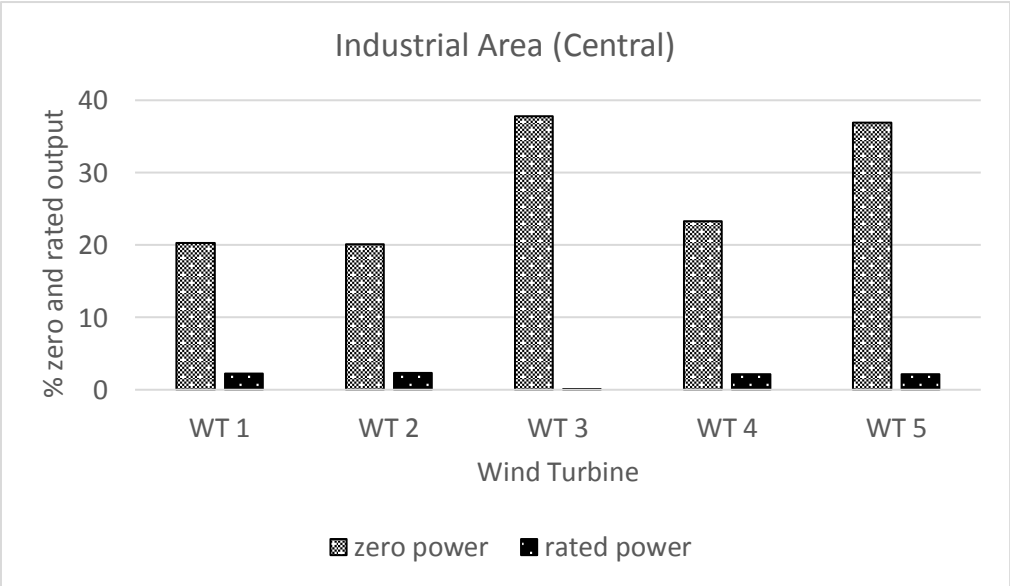


Figure 6.7. Percentages of rated and zero output at Industrial Area (Central)

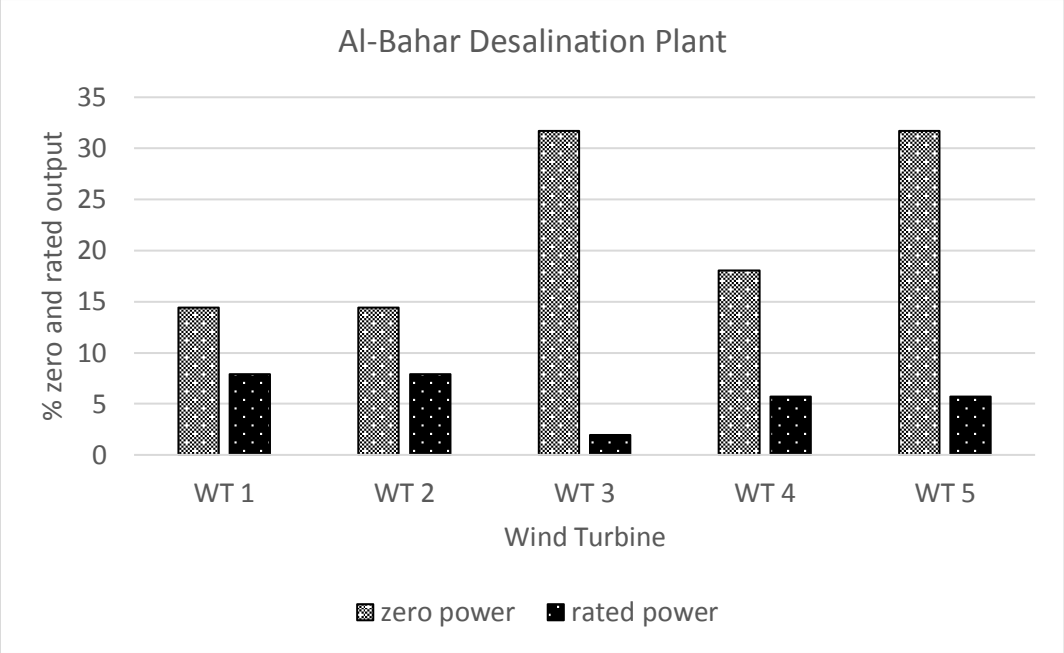


Figure 6.8. Percentages of rated and zero output at Al-Bahar Desalination Plant

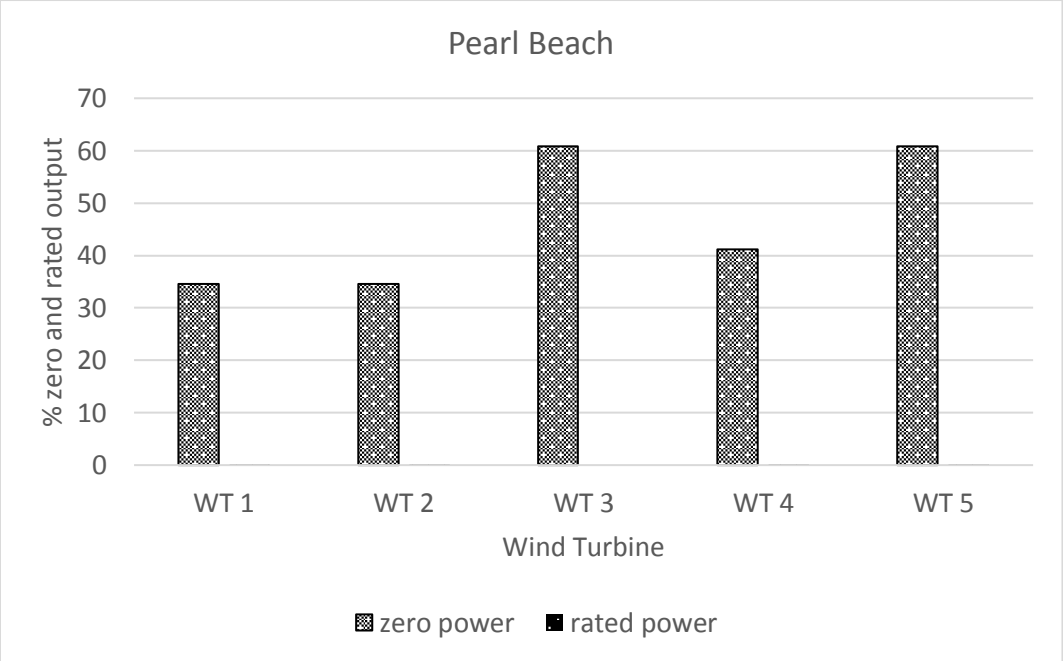


Figure 6.9. percentages of rated and zero output at Pearl Beach

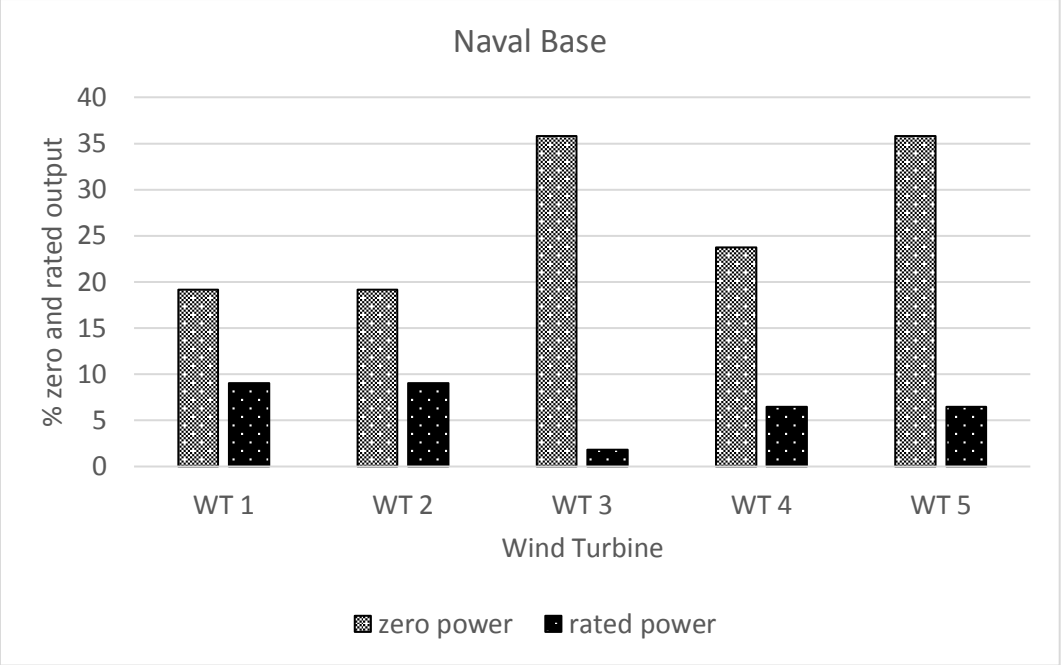


Figure 6.10. Percentages of rated and zero output at Naval Base

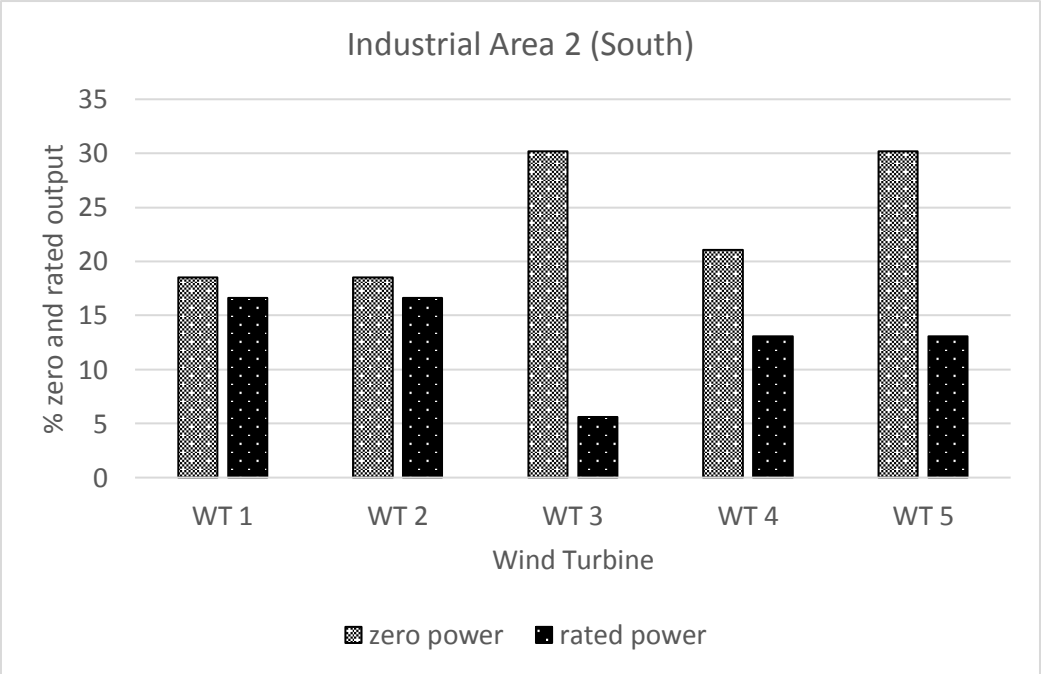


Figure 6.11. Percentages of rated and zero output at Industrial Area 2 (South)

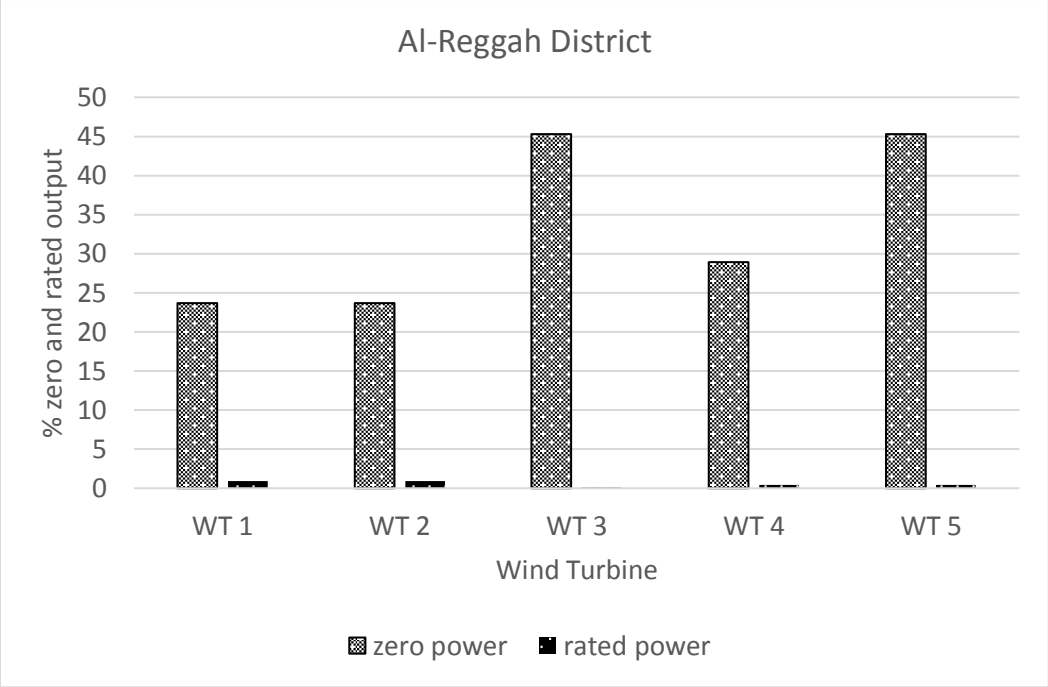


Figure 6.12. Percentages of rated and zero output at Al-Reggah District

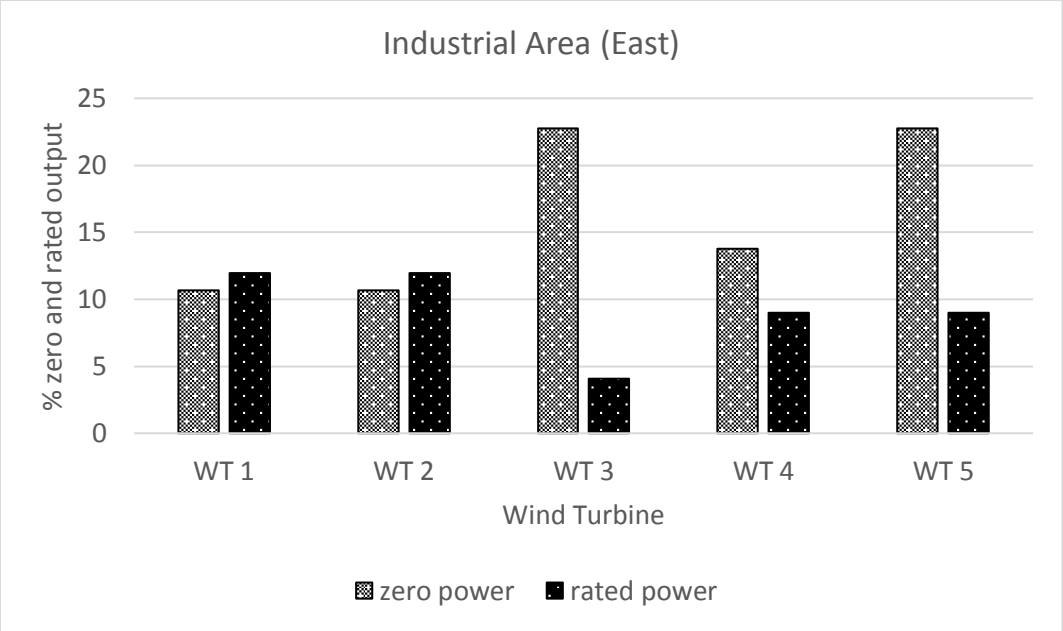


Figure 6.13. Percentages of rated and zero output at Industrial Area (East)



© University of Pretoria

## 6.5 COST ANALYSIS:

The cost of wind energy is averaged under 0.025 $/kWh at sites with a good wind resource which is at an all-time low [87, 88]. A sharp decline in the cost of wind energy is witnessed from the 1980s to the early 2000s. In the United States, capital costs achieved their lowest level from roughly 2001 to 2004, approximately 65% below costs from the early 1980s [88]. The cost of wind energy is a function of the cost to erect and operate the facility and the amount of energy produced by it during its lifetime.

A simplified approach to calculate the cost of electricity per kilowatt-hour includes investment costs, operation and maintenance costs, and capital costs. In order to calculate the present value of costs, PVC of electricity produced, following expression, given by Lysen [89] and referred by [90, 91, 92, 93, 94] is used in the present study:

$$PVC = I + C_{omr}\left(\frac{1+i}{r-i}\right)X\left[1-\left(\frac{1+i}{1+r}\right)^{n}\right]-S\left(\frac{1+i}{1+r}\right)^{n} \qquad (6.1)$$

Where,

(i) $I$ is the investment costs of the wind machine;

(ii) $C_{omr}$ is the operation and maintenance costs;

(iii) $i$ is the inflation rate;

(iv) $r$ is the discount rate;

(v) n is the life of machine; and

(vi) $S$ is the scrap value.

The investment costs, $I$ include the wind turbines cost, construction costs like foundation and grid connection, as well as planning and licensing costs. The operation and maintenance costs, $C_{omr}$, includes the repair, insurance, monitoring and management costs assumed to be 25% of the annual cost of the turbine (machine price/lifetime). The inflation rate, $i$, and discount rate, $r$, is assumed to be 6% and 8% respectively. The scrap value, $S$ is assumed to be 10% of the capital cost excluding the civil construction and cable costs. The wind machine life, n is assumed to be 20 years.

In order to calculate the cost of wind power generation per kilowatt-hour at seven locations in Jubail, five wind machines of different rated powers have been chosen. The technical data of the chosen wind machines are given in Table 6.1.



© University of Pretoria

The civil construction cost was calculated by designing the sizes of the foundations for these five types of wind machines. The design of foundation is based on the static weight of the nacelle, weight of the rotor, weight of the tower, and the dynamic wind load for a survival speed of 65 m/s. The civil construction also included the cost of a control room for housing computer, control devices, regularly required inventory items, and space for human occupancy. The cost of concreting, including reinforcement and labour, is taken as 148 US$/m$^3$.

Table 6.10 Cost related data of wind machines used in the study.

| | **Wind Machines** | | | | |
|---|---|---|---|---|---|
| **Cost (US$)** | WT 5<br>1.8 MW | WT 4<br>2 MW | WT 3 2.6<br>MW | WT 2<br>3 MW | WT 1<br>3.3 MW |
| Investment | 2,561,257 | 2,847,297 | 3,706,757 | 4,280,598 | 4,729,638 |
| Tower foundation | 30,869 | 36,908 | 56,369 | 70,210 | 99,250 |
| Control room | 10,388 | 10,388 | 10,388 | 10,388 | 10,388 |
| Total civil work | 41,257 | 47,297 | 66,757 | 80,598 | 109,638 |
| Operation and maintenance | 48,500 | 48,500 | 48,500 | 48,500 | 48,500 |
| Control room | 10,388 | 10,388 | 10,388 | 10,388 | 10,388 |
| **PVC** | **3,403,921** | **3,696,000** | **4,574,922** | **5,162,603** | **5,640,684** |

The sizes of the foundation so calculated are 40 ft×23 ft×8 ft. (12.2 m×7.0 m×2.4 m) for 1800 kW machine, 44 ft×25 ft×8 ft. (13.4 m×7.6 m×2.4 m) for 2000 kW machine, 48 ft×28 ft×10 ft. (14.6 m×8.5 m×3.0 m) for 2600 kW machine, 54 ft×31 ft×10 ft. (16.5 m×9.4 m×3.0 m) for 3000 kW machine and 58 ft×34 ft×12 ft. (17.7 m×10.4 m×3.7 m) for 3300 kW machine. The control room size is taken as 25 ft×15 ft. or (7.5 m×4.5 m). The operation and maintenance cost is taken as 48,500 US$ per annum. The local civil works cost, operation and maintenance costs and facility investment cost were estimated from Global construction cost book [95], Plant cost indicators [96], Location factors for Saudi Arabia [97], Technical reports and books published by governmental renewable energy organisations [98, 99], similar studies done previously for Saudi Arabia [92, 100]

The present value costs, PVC for 20 years estimated working life of wind turbine is obtained using Eq. 6.1 are given in Table 6.10 in the last row. The cost of electricity, COE per kWh at each location is obtained by dividing the PVC of each wind machine by the annual power output, kWh given in Tables 6.2 – 6.8. The summary of COE at 7 locations in Jubail is given in Table 6.11. The minimum cost of 0.023 US$ per kWh is obtained for Industrial Area (East) for the wind machine of 2,000 kW.

Table 6.11 Summary of cost (US$/kWh) of wind power generation at 7 locations using five types of wind machines.

| Location | | COE/kWh (US$) | | | | |
|---|---|---|---|---|---|---|
| | | Wind machine | | | | |
| | | WT 5 1.8 MW | WT 4 2 MW | WT 3 2.6 MW | WT 2 3 MW | WT 1 3.3 MW |
| Jubail | Industrial Area (Central) | 0.040 | 0.043 | 0.051 | 0.037 | 0.038 |
| | Al-Bahar Desalination Plant | 0.036 | 0.039 | 0.045 | 0.038 | 0.034 |
| | Pearl Beach | 0.138 | 0.161 | 0.194 | 0.125 | 0.127 |
| | Naval Base | 0.034 | 0.036 | 0.042 | 0.031 | 0.032 |
| | Industrial Area 2 (South) | 0.028 | 0.030 | 0.033 | 0.025 | 0.028 |
| | Al-Reggah District | 0.060 | 0.067 | 0.082 | 0.055 | 0.056 |
| | Industrial Area (East) | 0.026 | 0.023 | 0.032 | 0.028 | 0.026 |

## SUMMARY

Five different commercially available wind machines with rated capacities ranging from 1.8 to 3.3 MW were chosen based on selection criteria. The most feasible site for wind farm development in Jubail city is Industrial Area (East). At this site, the maximum energy output of 11,135 MWh/year with a PCF of 41.3% from a 3 MW rated power wind machine was obtained. This site is located slightly away from industries and is surrounded mainly by plain sandy terrain with very few warehouses of 8 - 10 m in height about 150 m away in north-west direction.

The second best site for wind farm development is Industrial Area 2 (South) is located far away from the industries and surrounded by plain sandy terrain with very few warehouses of 8 - 10 m in height and about 1,000 m away in north-west direction. At this site, the maximum energy output of 10,180 MWh/year with a PCF of 37.8% from a 3 MW rated power wind machine was obtained. From percent PCF, it can be concluded that wind machine 5 (1.8 MW rated power) is most efficient at all sites in Jubail as a low rated power wind machine is more efficient for mediocre wind potential areas. In locations of scarce land, a high rated power wind turbine can be a better option. The maximum duration of rated power output between 8 to 16.6% was obtained at Industrial Area 2 (South). The minimum duration of rated power output, less than 0.3% for all wind turbines was obtained at Pearl Beach. The maximum duration of zero power output between 35 to 60% was also obtained at Pearl Beach. This site is located in the middle of Jubail residential area close to beach and surrounded by 3-4 storey buildings (about 9 to 12 m height). Therefore, minimum turbine output was recorded at this

station. The minimum duration of zero power output between 12 to 23% was obtained at Industrial Area (East). The cost of electricity, COE per kWh was estimated at each of the seven locations in Jubail, based on present value cost, PVC method of five selected wind machines and annual power output at these locations. The minimum cost of 0.023 US$ per kWh is obtained for Industrial Area (East) for the wind machine of size 2,000 kW.

# CHAPTER 7

## A GIS-BASED APPROACH FOR OPTIMAL WIND FARM SITE SELECTION

## CASE STUDY: SAUDI ARABIA

The availability of renewable energy resources is a geographical based criterion, and the first step in the siting process is always an assessment of the availability of a resource at a given location. For wind energy, this consists of assessing and measuring wind characteristics, such as speed, power, density, prevailing direction, daily and seasonal variation, long-term consistency (climate cycles), turbulence and wake, temperature, and uncertainty of the wind at various heights above the Earth's surface.

The first challenge for the wind planner in designing and developing a wind farm is to identify suitable sites for wind farm installation. The potential sites should not only cater the wind energy requirements but also satisfy several environmental and socio-economic factors. The exactitude of this wind farm planning is largely dependent on the availability and accuracy of the wind and geographic data. GIS is a popular decision support system involving the assimilation of spatially referenced data in a problem solving environment. On the other hand, multi-criteria decision analysis provides a thorough collection of techniques and procedures for structuring, designing, evaluating and prioritising alternative decisions.

In this study, firstly, a general GIS-based model for wind farm site selection is developed which can be applied anywhere globally and then this model is applied to the entire Kingdom of Saudi Arabia. This wind farm site suitability study is the first of its kind in the Gulf Cooperation Council, GCC region to the best of authors' knowledge.

Saudi Arabia is the largest country in the Middle East, with its high growth in population and fast industrialisation. The demand for energy is also increasing rapidly. According to government estimates, the projected demand for electricity in Saudi Arabia is expected to exceed 120 GW by 2032 [9]. The overall demand for fossil fuels for industry, transportation and desalination is estimated to grow from 3.4 million barrels of oil equivalent per day in 2010 to 8.3 million barrels of oil equivalent per day in 2028 [9]. Therefore, Saudi Arabia is exploring alternative energy sources for generating power and reducing consumption of the nation's diminishing fossil fuel reserves.



© University of Pretoria

## 7.1 DESCRIPTION OF STUDY AREA.

Saudi Arabia lies between latitudes 16° and 33° N, and longitudes 34° and 56° E and is spread over 2,150,000 square kilometres, occupying almost 80% of the Arabian Peninsula. The country is located in the southwest corner of Asia. It is surrounded by the Red Sea on the west, by Yemen and Oman on the south, the Arabian Gulf and the United Arab Emirates and Qatar on the east, and Jordan, Iraq and Kuwait on the north [101].

Desert covers more than half the total area of Saudi Arabia. A narrow coastal plain runs through the Kingdom's western coast while a range of mountains run parallel to the coastal plain along the Red Sea. Along the Arabian Gulf in the east is a low-lying region called Al-Hasa. There are mountains in the west of the Kingdom. Almost the entire Kingdom is arid, although there is rainfall in the north and along the mountain range to the west, especially in the far southwest, which receives the monsoon rains in summer. Temperatures can vary considerably from a mid-summer maximum of 51°C in the shade to winter lows close to -8°C in the mountainous areas and, sometimes, at night in the heart of the desert [101, 102].

### 7.1.1 Wind energy potential

The average interpolated wind speed is the main and highest weighted criterion in siting a wind farm in almost all similar studies [73, 75, 76, 77, 78, 103]. The mean wind speed and data collection duration for all the stations at 10 m AGL are given in Chapter 4, Table 4.1. The location of all the weather stations and mean wind speed values are shown on Saudi Arabian map in Chapter 4, Figure 4.1. It is very clear from this map that wind speed is better at north-east and south-west coastal areas and north-west country borders. The north-east coastal area is surrounded by Gulf-Arabian Sea where, the wind speed is found to be good in general. The south-west coastal area is surrounded by the Red Sea. This area is known as Hijaz. The wind speed is found to be higher towards the western coast and as we move along the coast towards south the wind resource seems to deteriorate. As we move to the centre of the country like towards the capital, Riyadh, the wind speed seems to be very low. There are no weather stations and population in the eastern corner of the country which is also known as Empty Quarter due to scarce population, lack of connectivity and dense desert.

The monthly wind speed statistics at all 29 stations in Saudi Arabia are shown in Figures 7.1 to 7.29. The mean, maximum and minimum monthly wind speeds are shown in these statistics. The statistics of overall data are also shown in the same figures. It can be seen from

these statistics that in general, at all stations, the mean wind speed is higher in the months of June and July. The trend is similar to seasonal variation at locations in Jubail shown in Figure 5.12. As stated earlier in Chapter 5, in summer, the wind particles are more agile due to rapid convection process. This is summer season in Saudi Arabia and fortunately matches with the peak energy demand due to the air conditioning. The mean daily wind speed was high in north-eastern coastal regions of Dammam and Dhahran, south-western coastal region of Yanbu and near north-western country's border, Al-Jawf.

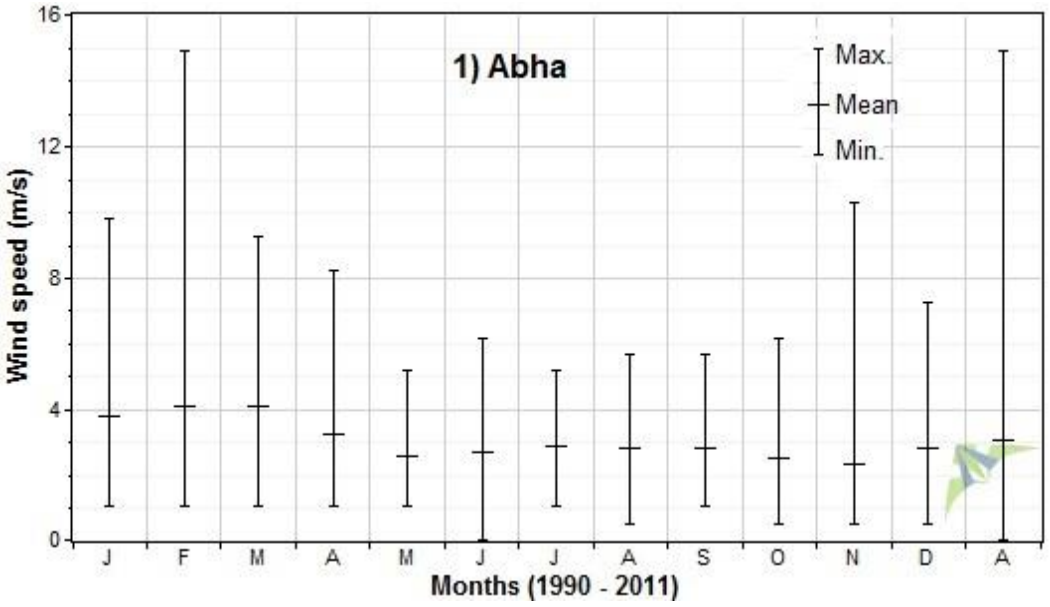


Figure 7.1 Monthly maximum, mean and minimum wind speed at Abha

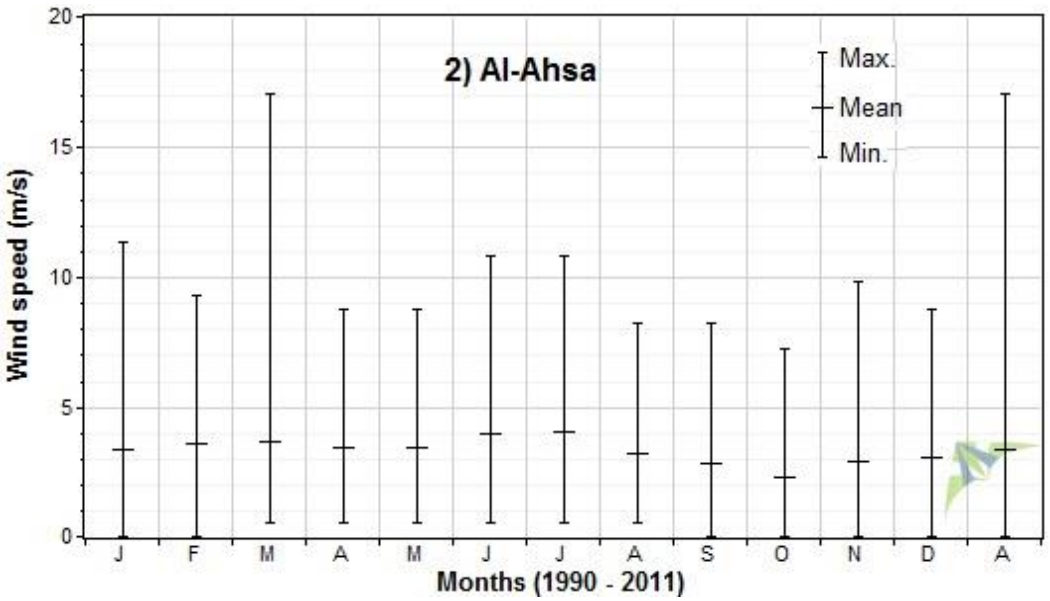


Figure 7.2 Monthly maximum, mean and minimum wind speed at Al-Ahsa



© University of Pretoria

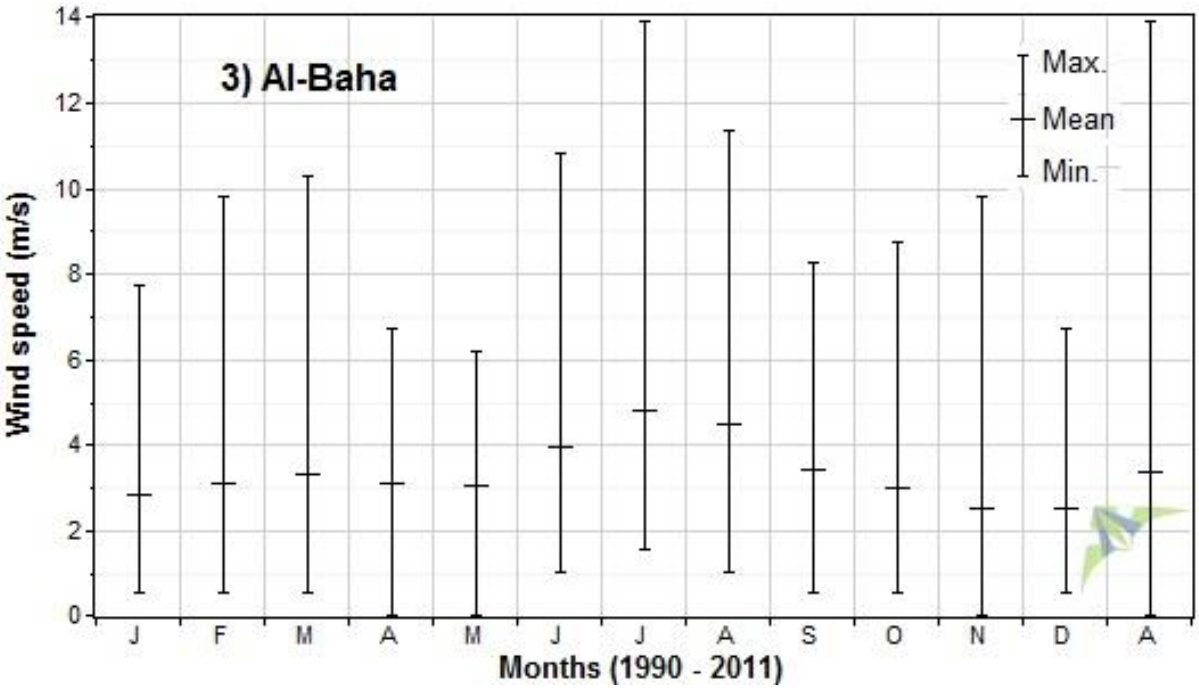


Figure 7.3 Monthly maximum, mean and minimum wind speed at Al-Baha

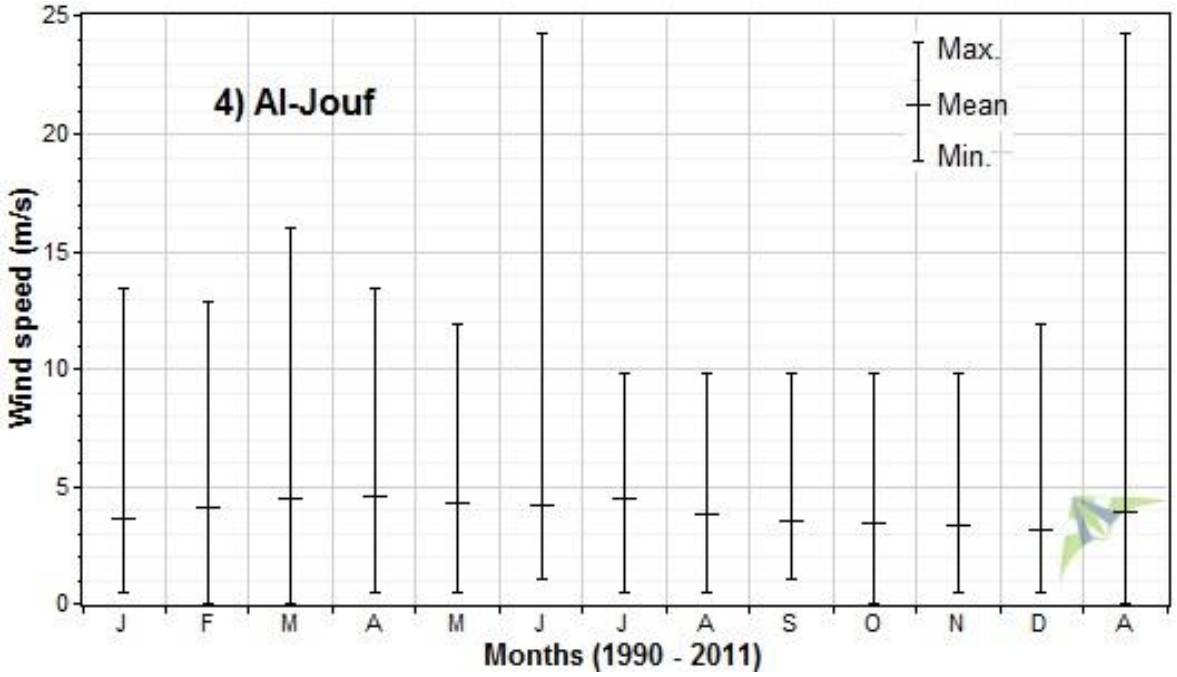


Figure 7.4 Monthly maximum, mean and minimum wind speed at Al-Jouf

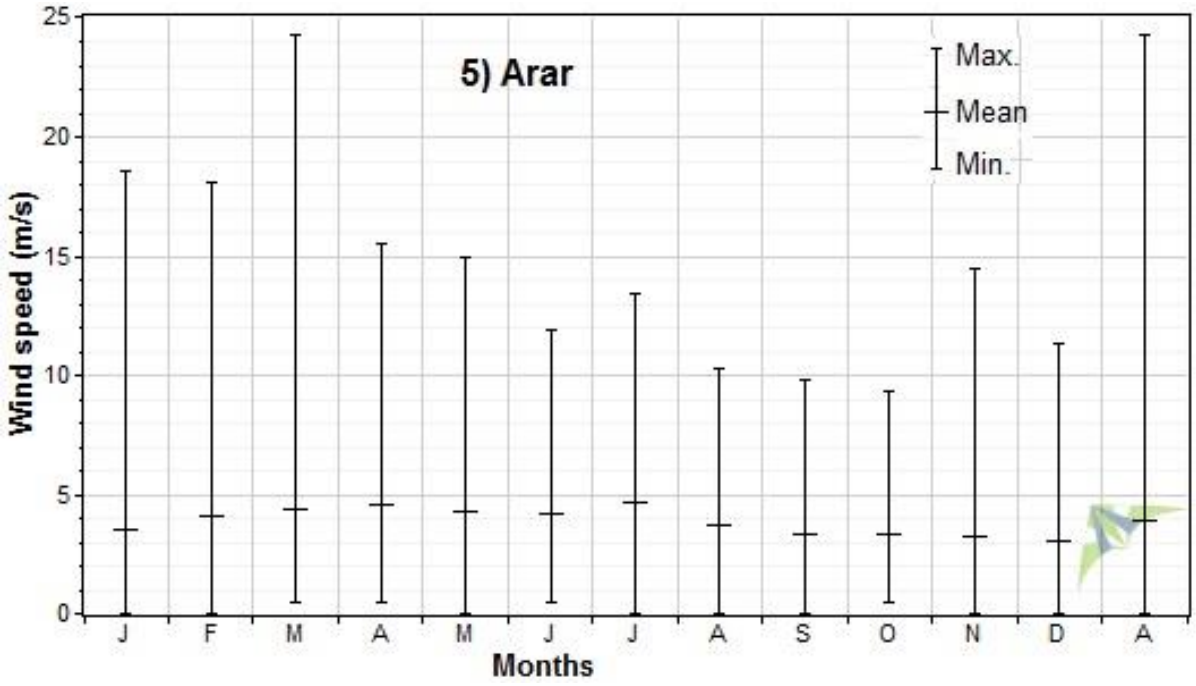


Figure 7.5 Monthly maximum, mean and minimum wind speed at Arar

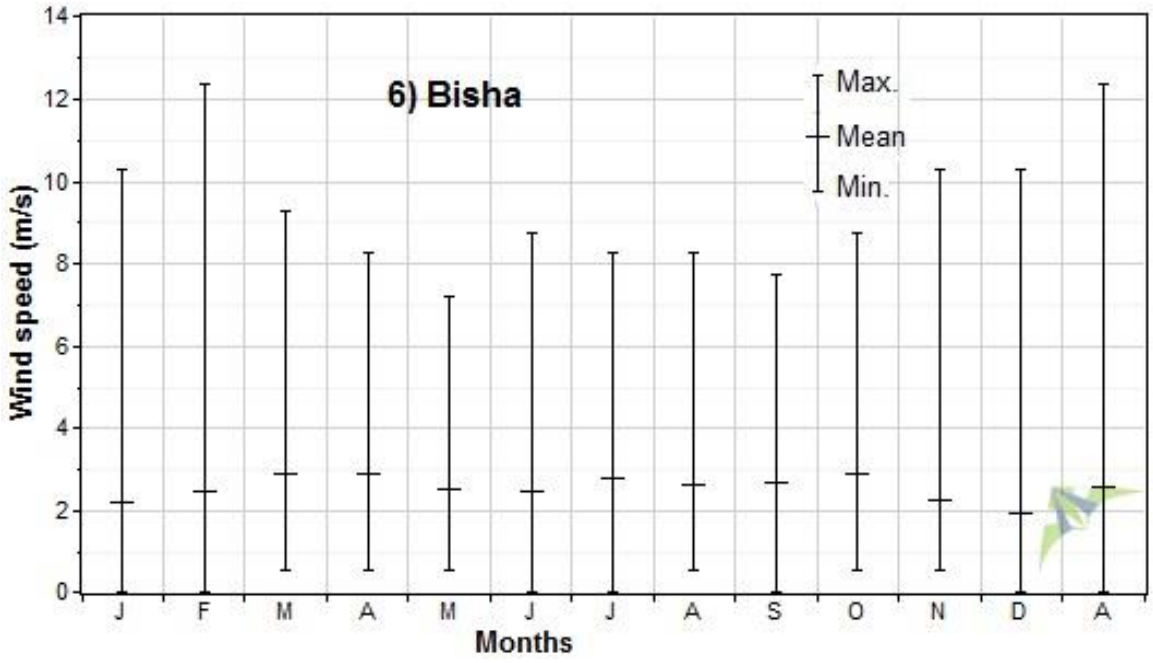


Figure 7.6 Monthly maximum, mean and minimum wind speed at Bisha

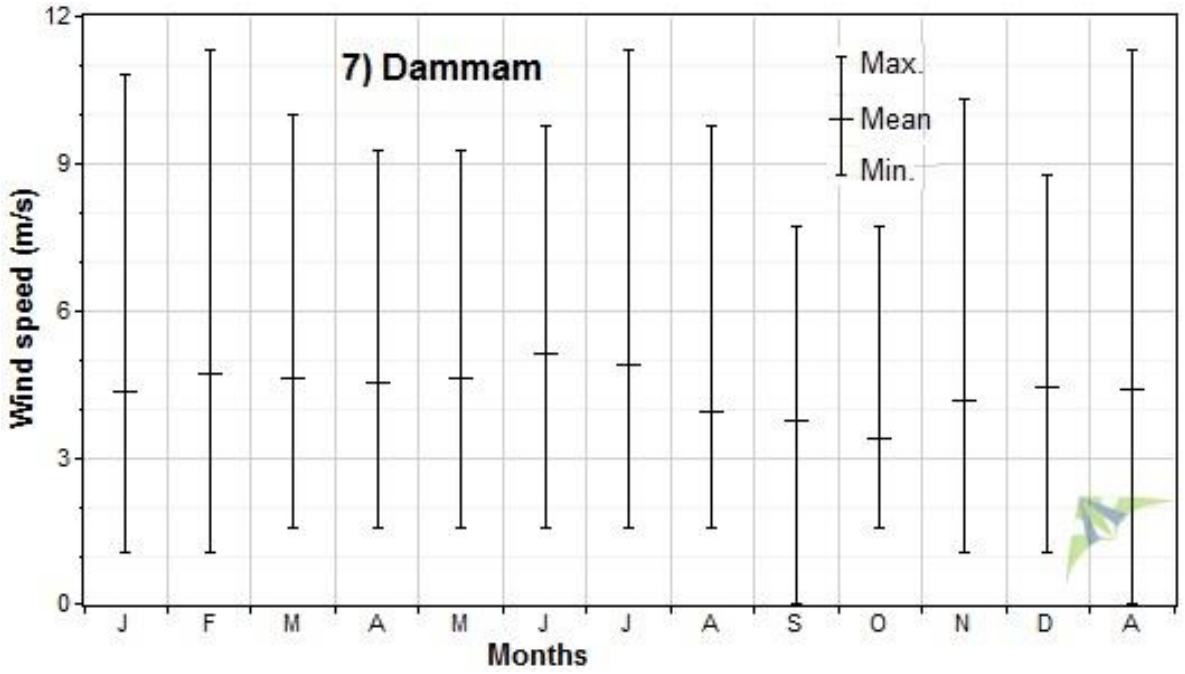


Figure 7.7 Monthly maximum, mean and minimum wind speed at Dammam

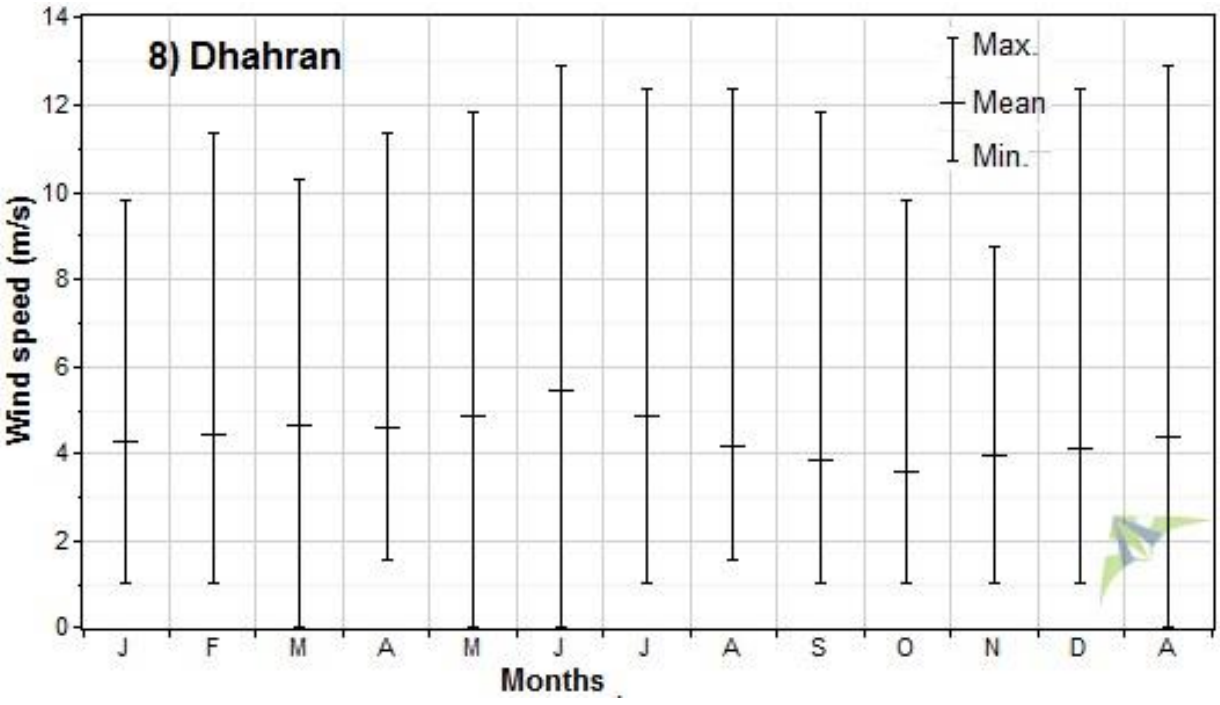


Figure 7.8 Monthly maximum, mean and minimum wind speed at Dhahran

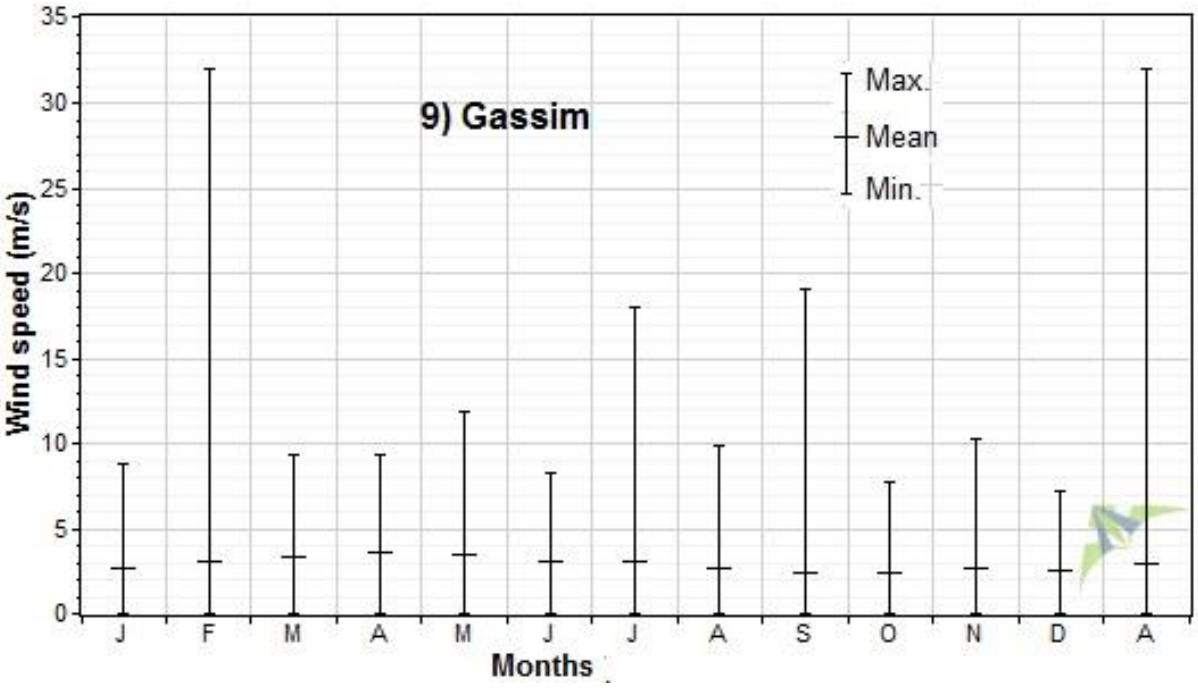


Figure 7.9 Monthly maximum, mean and minimum wind speed at Gassim

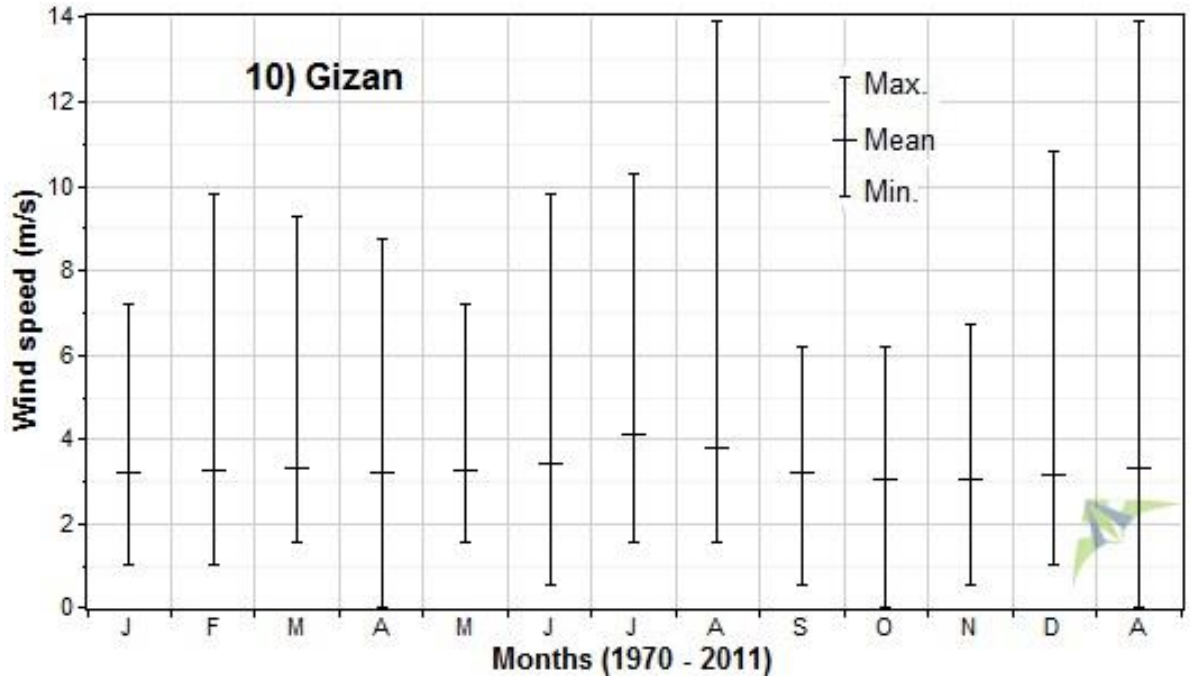


Figure 7.10 Monthly maximum, mean and minimum wind speed at Gizan

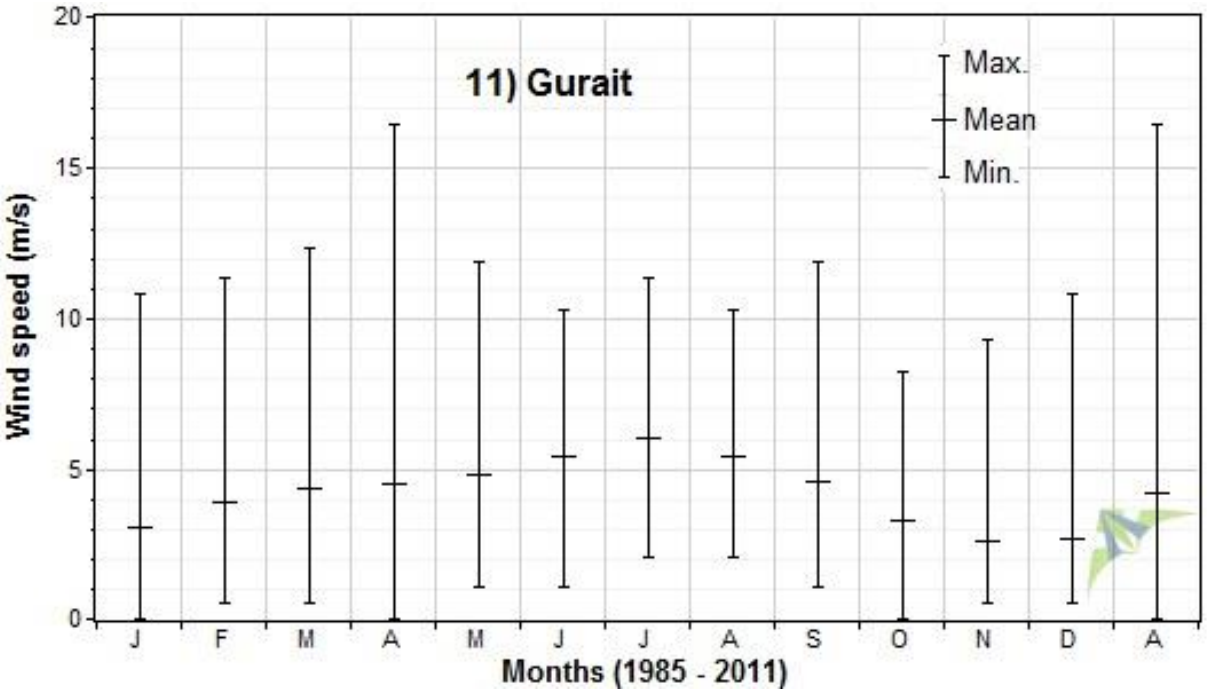


Figure 7.11 Monthly maximum, mean and minimum wind speed at Gurait

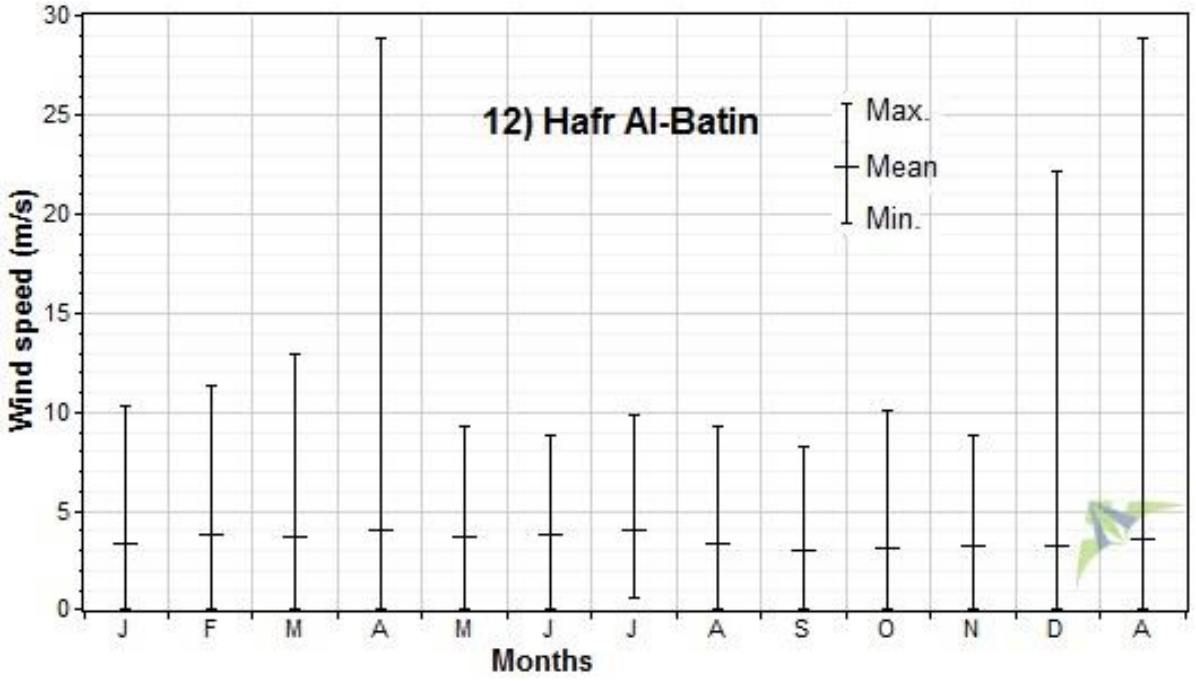


Figure 7.12 Monthly maximum, mean and minimum wind speed at Hafr Al-Batin



© University of Pretoria

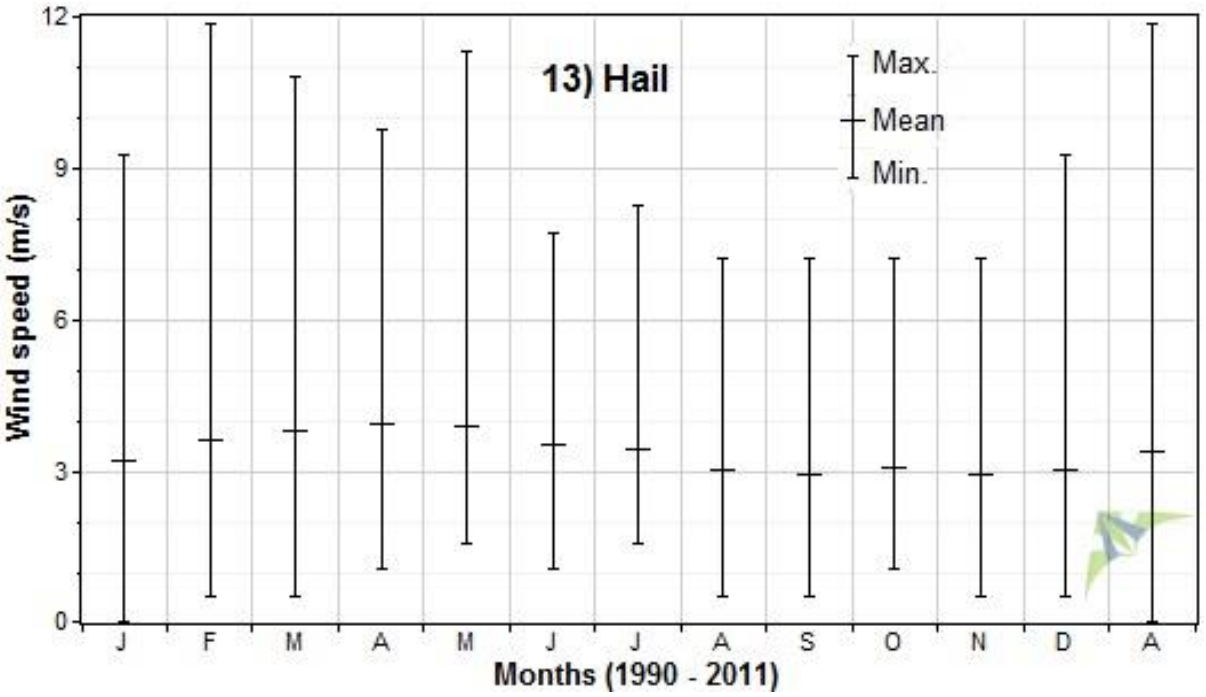


Figure 7.13 Monthly maximum, mean and minimum wind speed at Hail

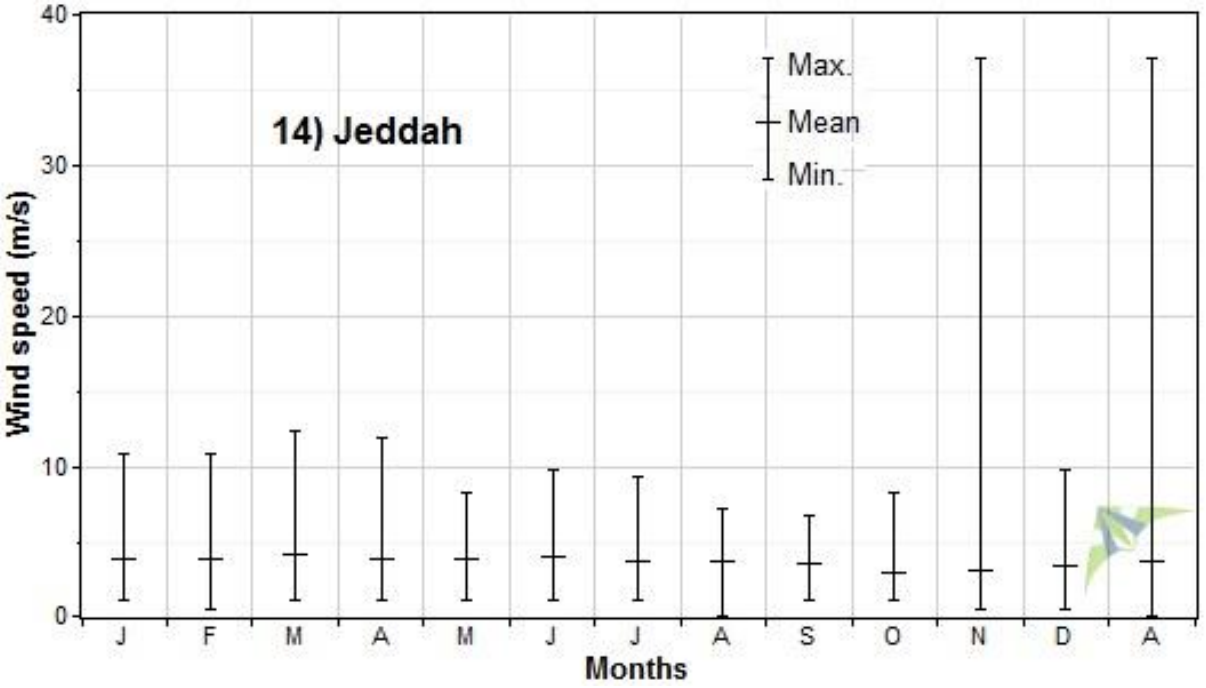


Figure 7.14 Monthly maximum, mean and minimum wind speed at Jeddah

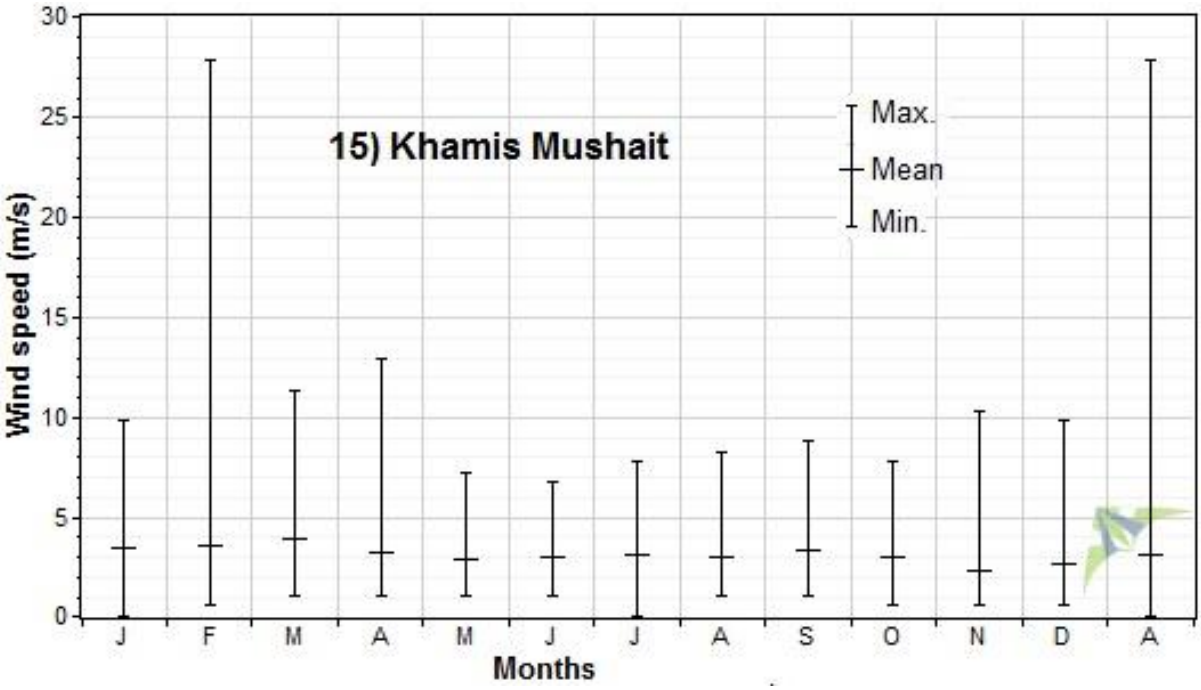


Figure 7.15 Monthly maximum, mean and minimum wind speed at Khamis Mushait

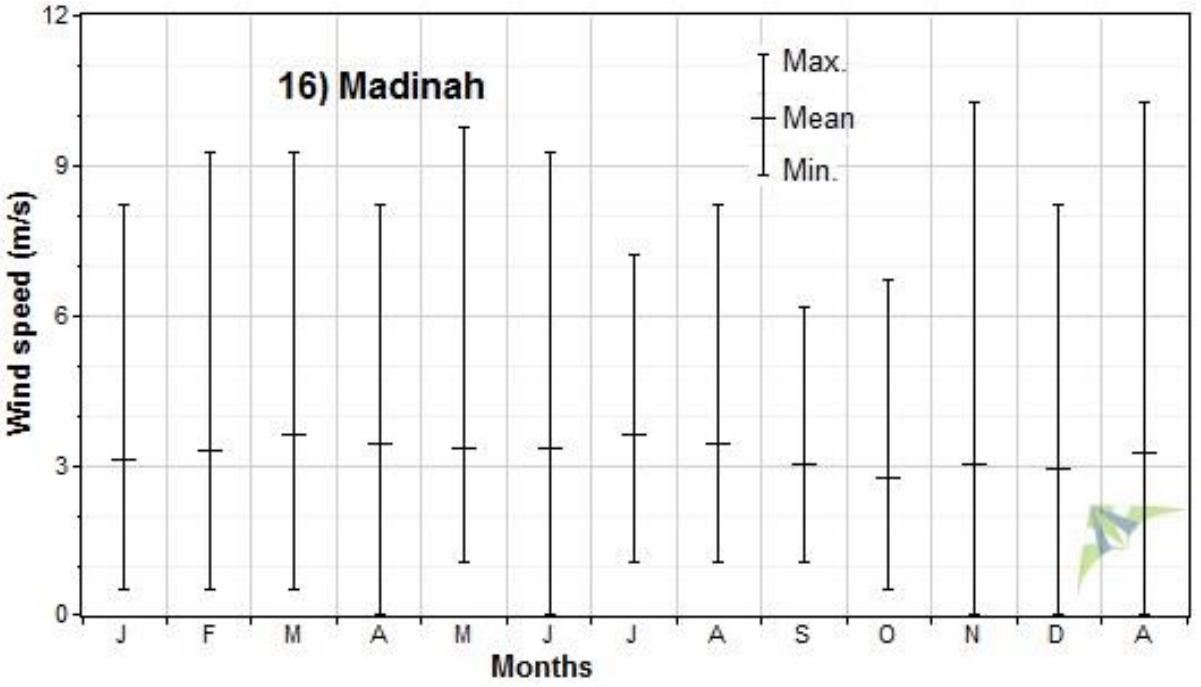


Figure 7.16 Monthly maximum, mean and minimum wind speed at Madinah

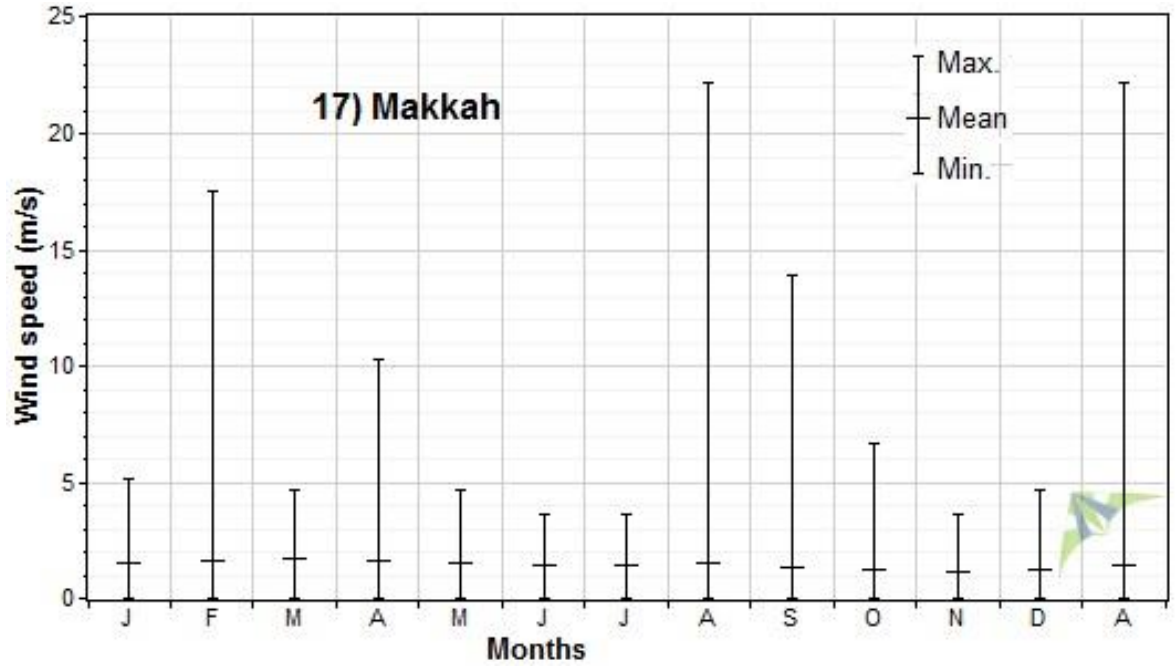


Figure 7.17 Monthly maximum, mean and minimum wind speed at Makkah

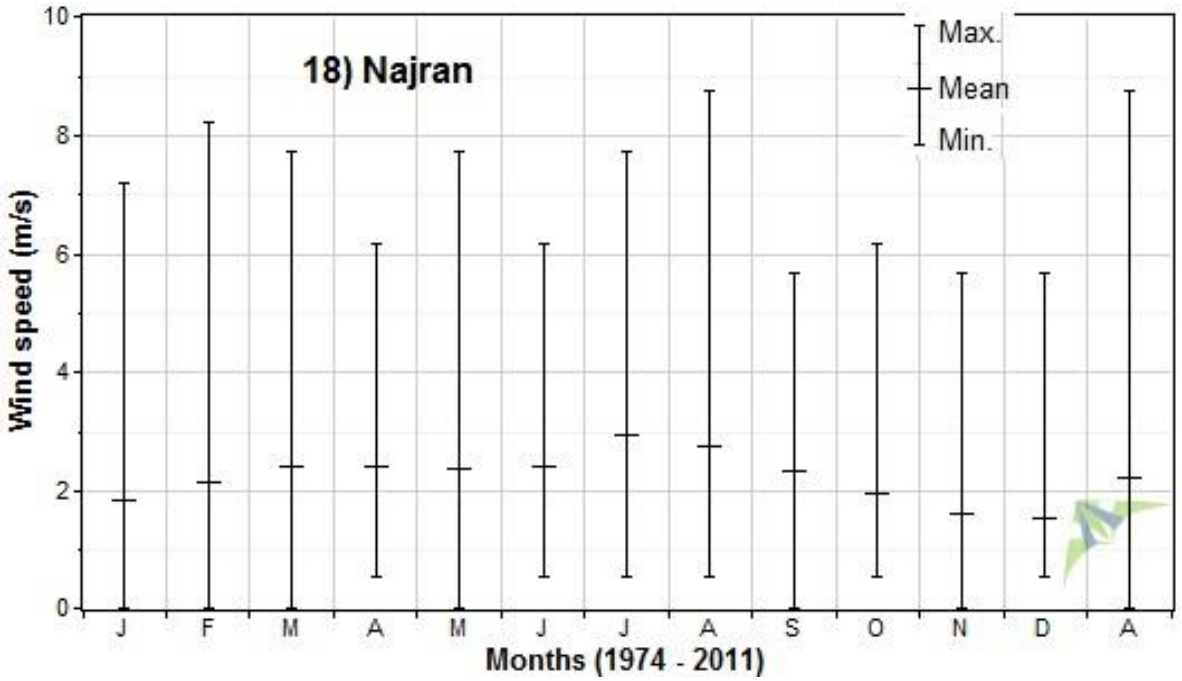


Figure 7.18 Monthly maximum, mean and minimum wind speed at Najran

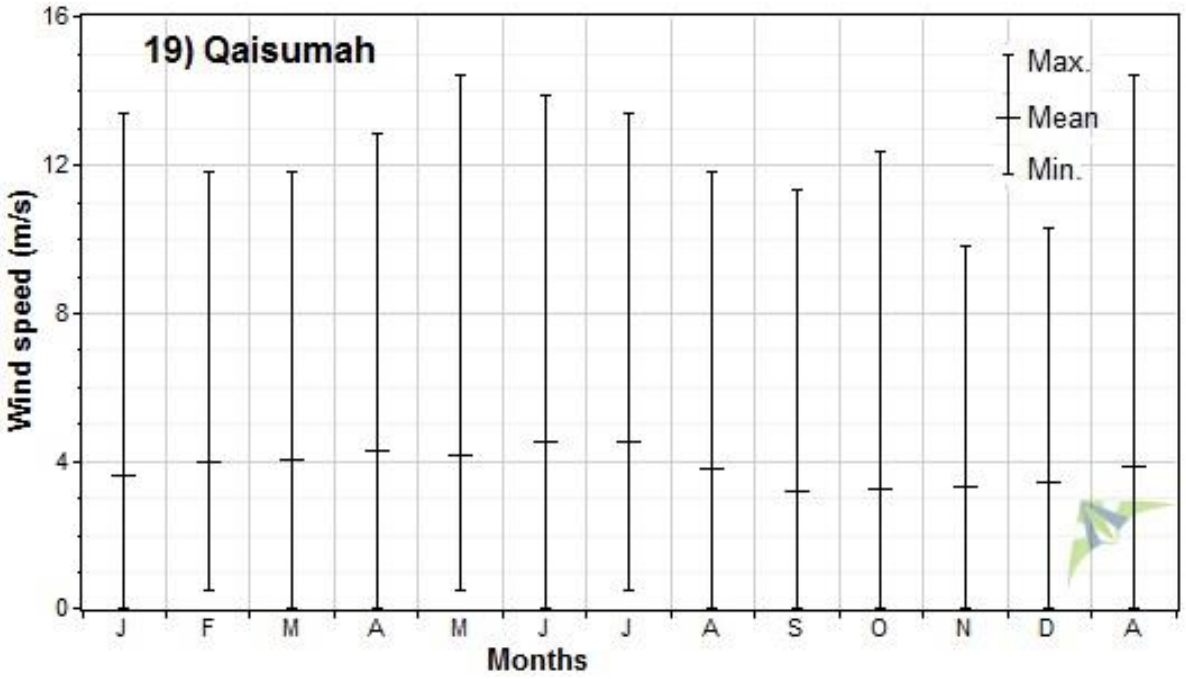


Figure 7.19 Monthly maximum, mean and minimum wind speed at Qaisumah

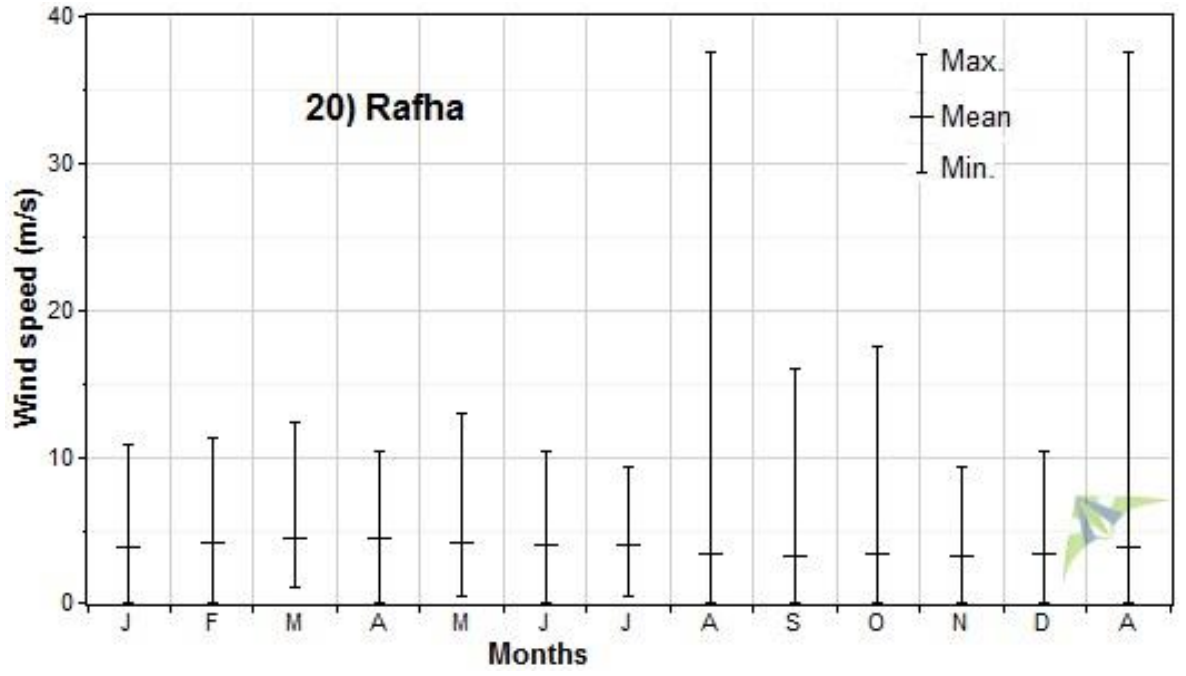


Figure 7.20 Monthly maximum, mean and minimum wind speed at Rafha

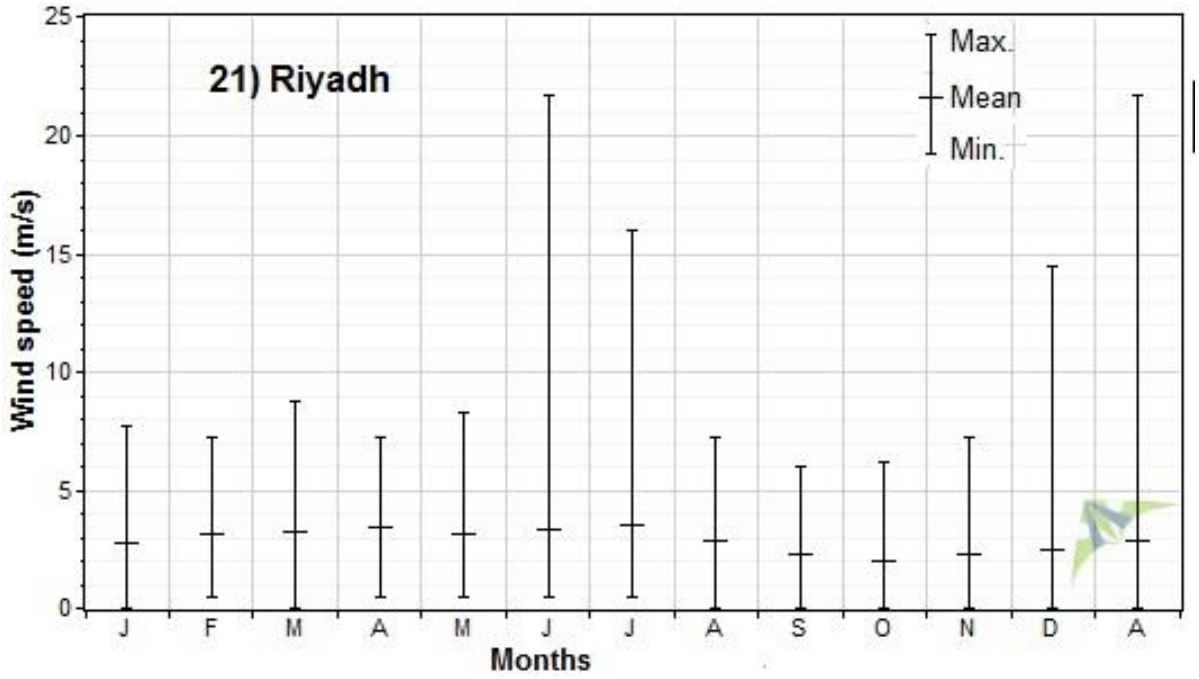


Figure 7.21 Monthly maximum, mean and minimum wind speed at Riyadh

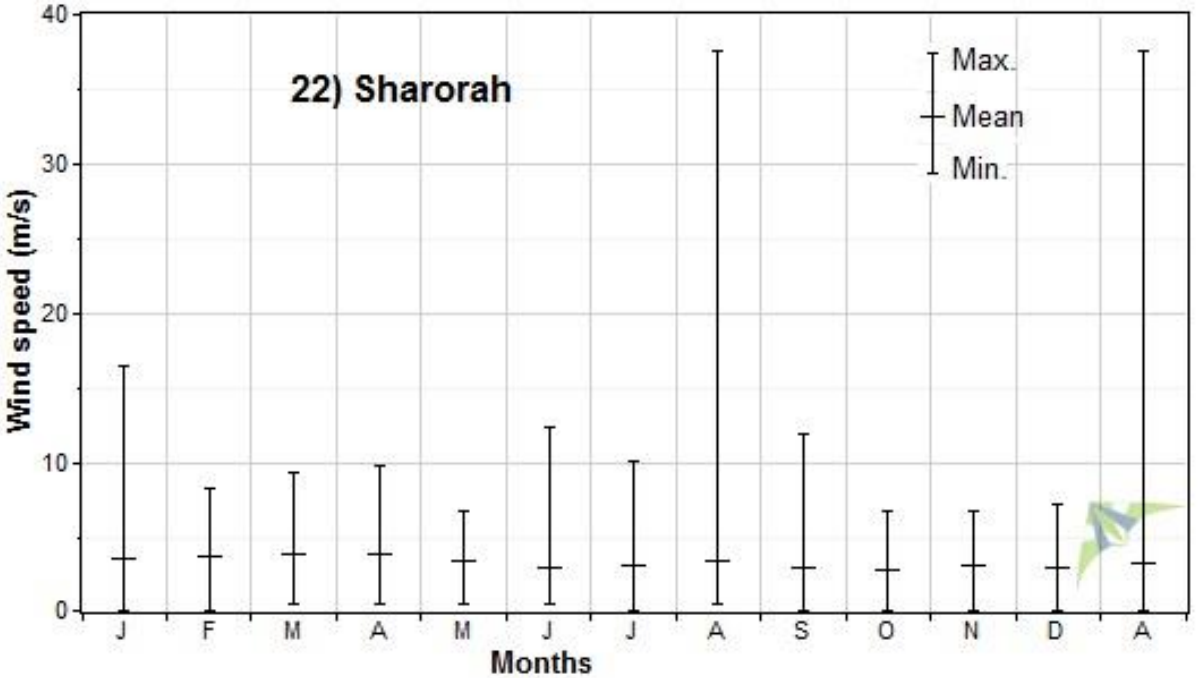


Figure 7.22 Monthly maximum, mean and minimum wind speed at Sharorah

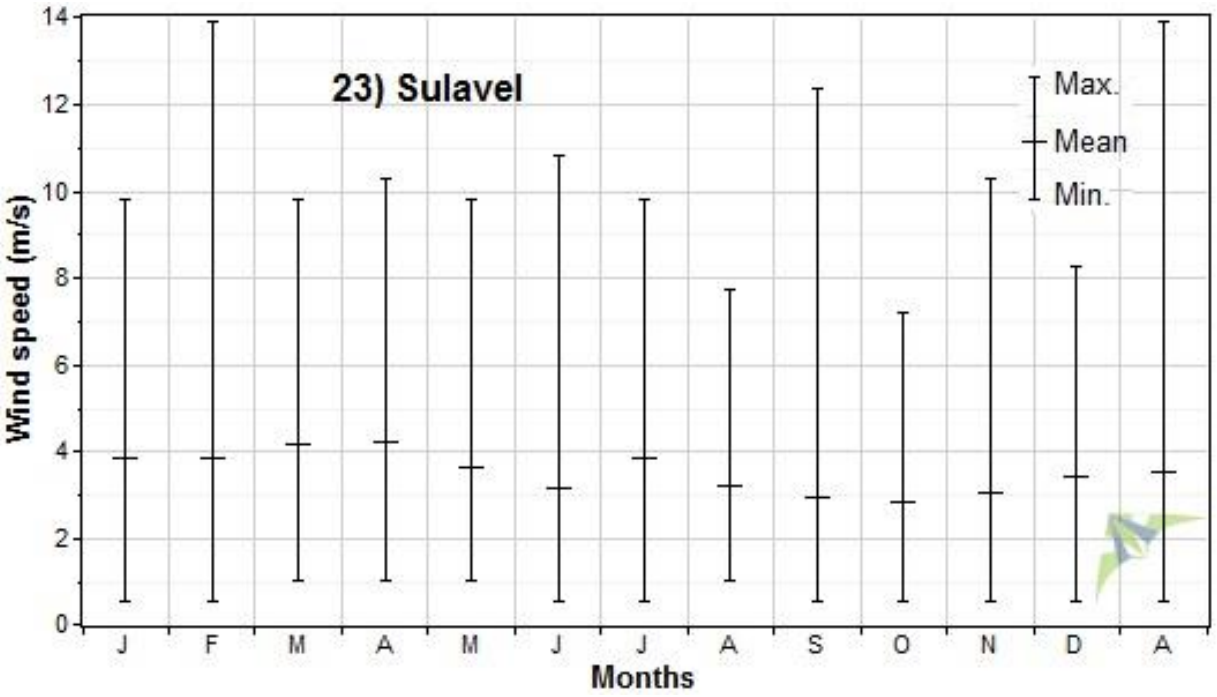


Figure 7.23 Monthly maximum, mean and minimum wind speed at Sulavel

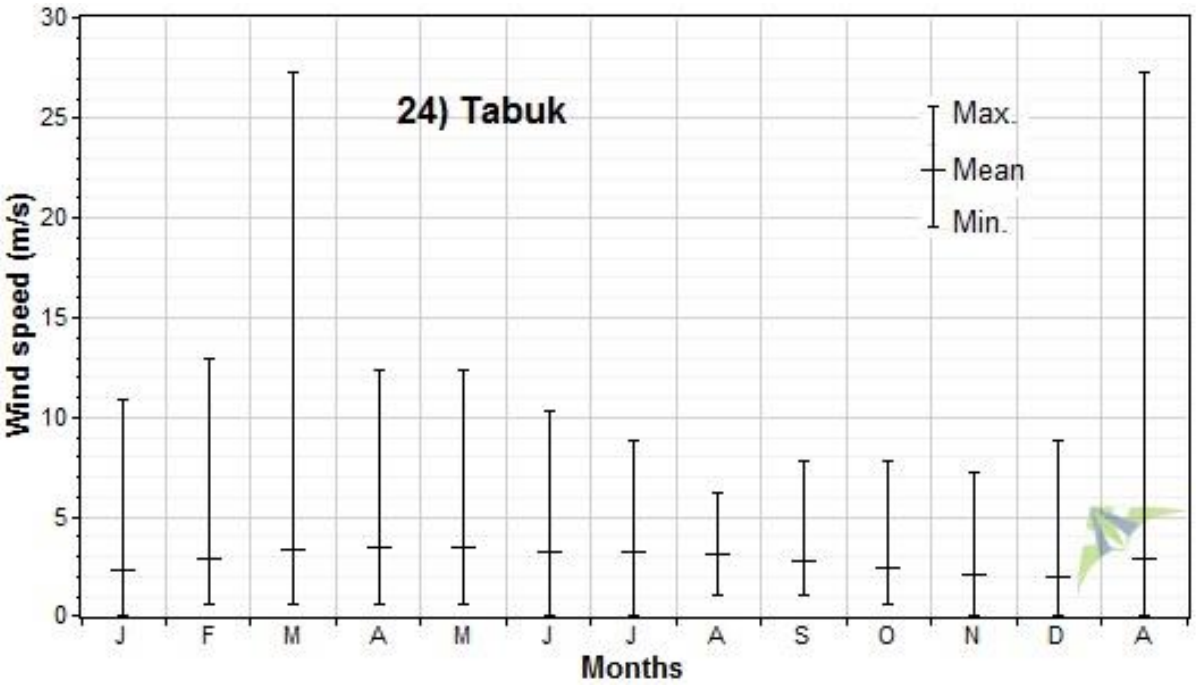


Figure 7.24 Monthly maximum, mean and minimum wind speed at Tabuk

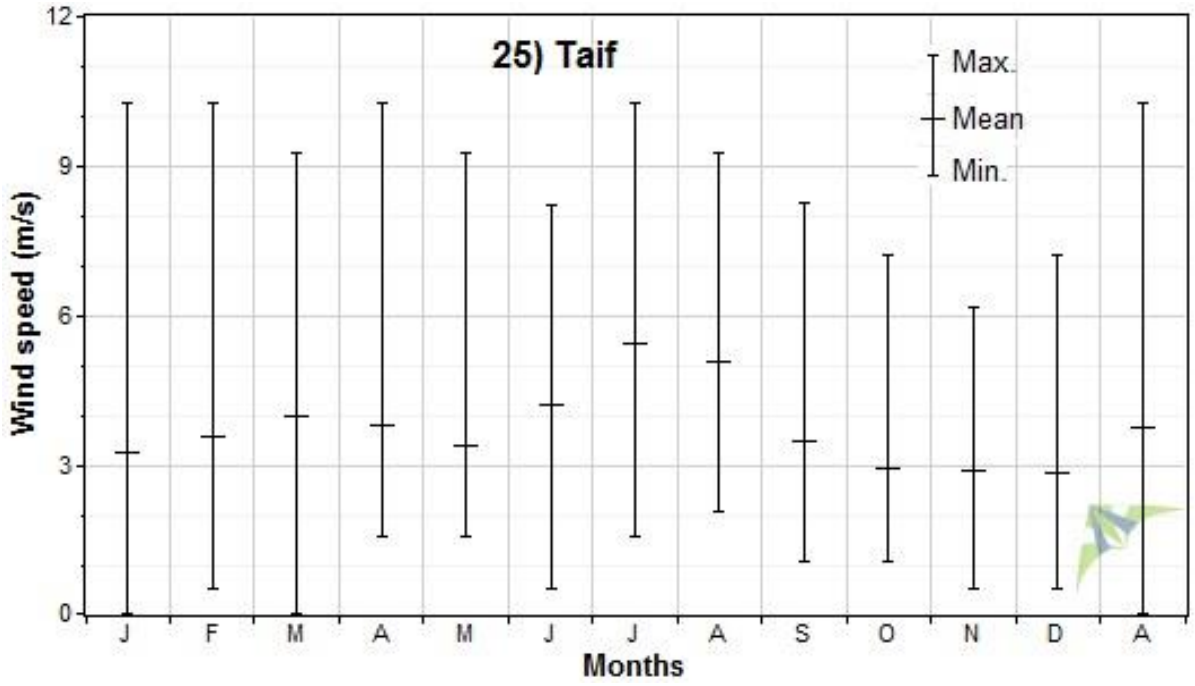


Figure 7.25 Monthly maximum, mean and minimum wind speed at Taif

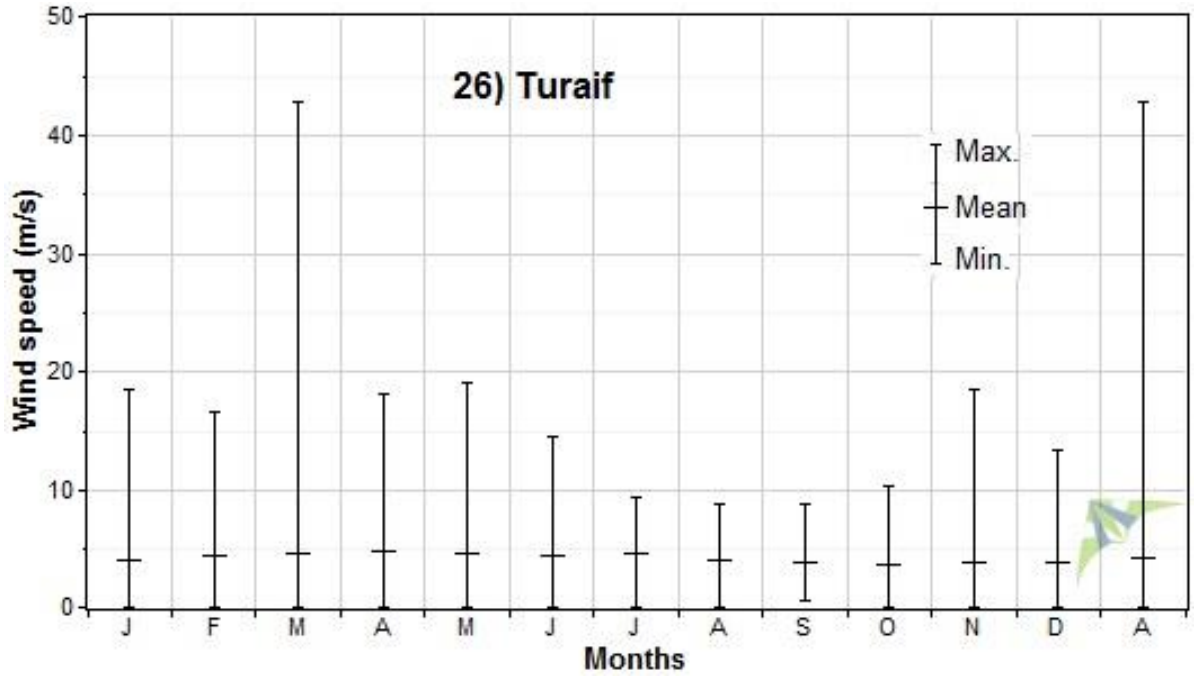


Figure 7.26 Monthly maximum, mean and minimum wind speed at Turaif

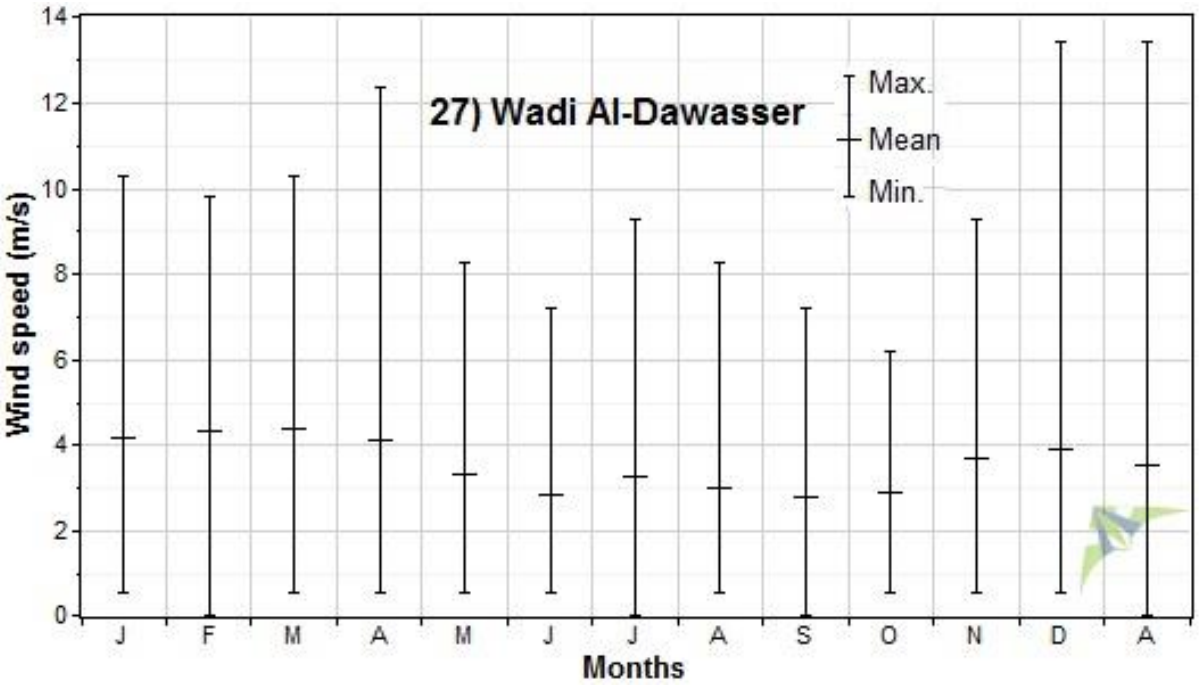


Figure 7.27 Monthly maximum, mean and minimum wind speed at Wadi Al-Dawasser

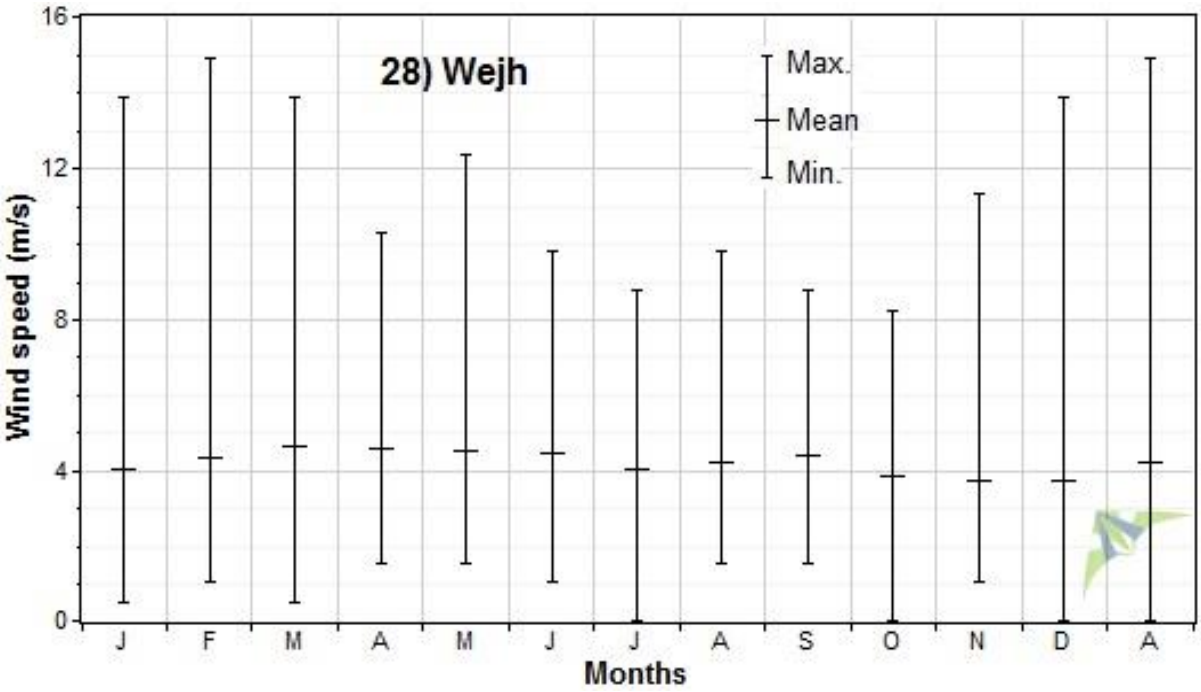


Figure 7.28 Monthly maximum, mean and minimum wind speed at Wejh

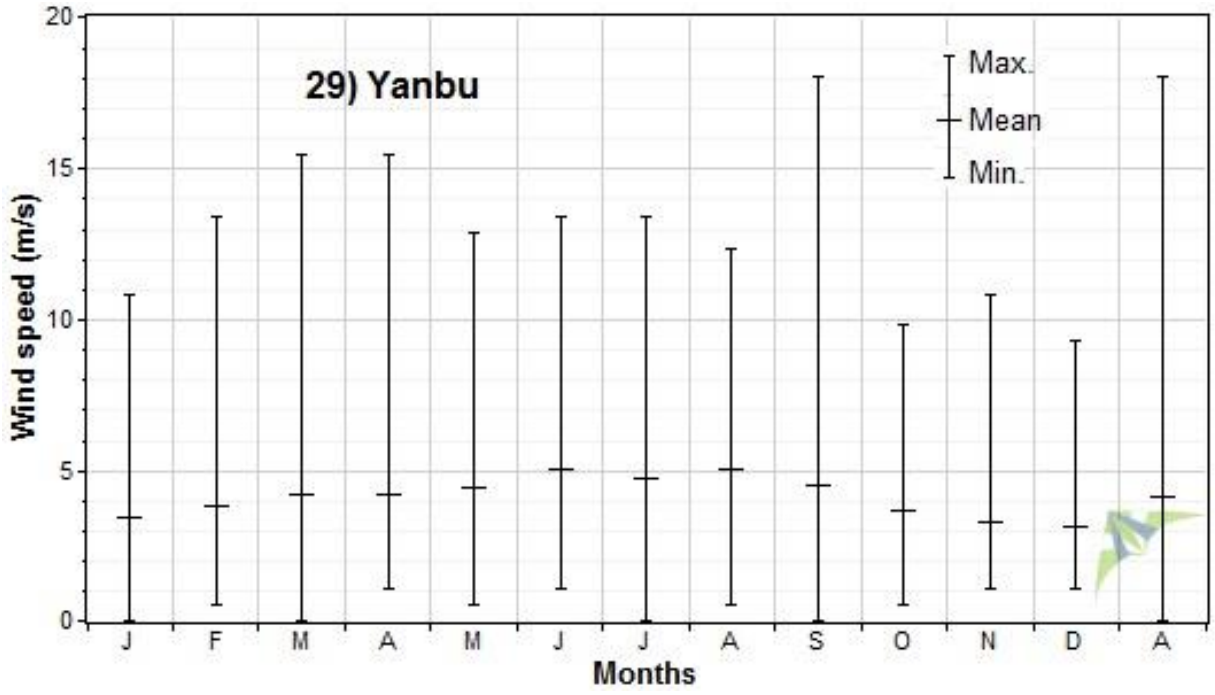


Figure 7.29 Monthly maximum, mean and minimum wind speed at Yanbu

The wind speed used in the criterion is interpolated to 100 m from 10 m AGL by using traditional one-seventh power law [104, 105].

$$V_2 = V_1 \left(\frac{Z_2}{Z_1}\right)^n \qquad (7.1)$$

Where $V_1$ and $V_2$ are the wind speeds at heights $Z_1$ and $Z_2$, respectively and the value of wind shear coefficient, n is taken as 1/7.

All 29 weather stations are distributed quite evenly in the entire Kingdom. A spatial interpolation technique is used to predict the wind speed in locations where data are not available. In this analysis, the method used to convert the point data into raster format is the inverse distance weighted, IDW. It determines cell values using a linearly weighted combination of a set of sample points. The weight is a function of inverse distance. The surface being interpolated should be a variable dependent on location. Ali et al. [106] tested five wind speed interpolation methods (i.e. IDW, global polynomial interpolation, local polynomial interpolation, spline with 3 sub-types, and kriging with 4 sub-types) in Iraq. Based on the root mean square error values, the predicted values are compared with actual values for period between 1971 and 2010. The results demonstrated that the IDW yielded the best results, while the ordinary Kriging method occupied second rank [106].



© University of Pretoria

### 7.1.2 Distance from electricity grid

Long transmission lines between wind farms and electricity grid are associated with costs related to cabling and electricity losses. Wind farms should be sited in the close vicinity of the electricity grid. Many studies have neglected this criterion in their analysis [70, 71, 72, 75, 77].

For the current analysis, maps of the national electrical grid and power station were obtained from the electrical data book of the Saudi Electrical Company (SEC) [16]. The SEC is a national electric utility company responsible for generation, transmission and distribution of electric power.

### 7.1.3 Distance from settlements

The buffer (preventive) distances of wind farm from residential areas for avoiding noise, nuisance and natural surroundings must be defined. This is a very important criterion in wind farm siting. In all similar studies, these distances are well defined. These buffer zones are flexible [70, 71, 72, 73, 74, 75, 76, 77, 78] and their application has to be justified case-by-case by the respective planning authority (e.g. the municipal administration). On the other hand, it is important that wind farm locations should be within a reasonable close distance from settlements to minimise transmission losses. Many studies present a range of distances from the settlements where wind farm siting analysis is done, distances on either side of this range are completely infeasible [70, 72].

The national demographics data of Saudi Arabia was obtained from the Central Department of Statistics and Information [6]. The Central Department of Statistics and Information falls under the authority of the Ministry of Economy and Planning and is the principal agency in the Kingdom for the collation, analysis and distribution of statistical information.

### 7.1.4 Distance from roads/highways

To minimise the construction and maintenance costs of wind farms, it is necessary that the distance between the proposed wind farm location and road network should be as less as possible. However, many studies recommend a buffer distance as well [71, 75, 76, 77, 78]. This buffer or preventive distance is decided by regional planning authorities. The access roads to wind farm must also have a minimum width of 4 m with a pavement [73]. In most

wind farm siting assessments, the areas further away from roads are considered less suitable than those closer to roads [71, 73, 74, 103, 107, 108, 109]. However, there is no generally valid definition of a maximum distance from the wind turbines to the road network. Out of seven studies which considered distance from road criterion, two used a maximum distance of 5000 m [71, 73], one used 10000 m [74] and three others used buffer distance of 100 and 200 m only [75, 76].

The GIS shape files of national highways and roads were downloaded from GIS data websites [110] and were compared with maps provided by ministry of transport, Saudi Arabia [111].

### 7.1.5 Safe distance from airports

Wind turbines can interfere with aviation radar signal and would require a significant buffer around areas, such as airports. Most of the similar studies present a buffer distance around airports [70, 71, 72, 73, 74, 78]. These buffer distances can vary for domestic, military and international airports. There are 36 airports (international, domestic and military) in Saudi Arabia. All these airports were considered and a buffer distance was given around them in the current case study.

### 7.1.6 Slope of terrain

The accessibility for installation and maintenance of wind turbines is hindered by steep slope of a terrain indirectly having a negative economic impact. In literature, allowed maximum slope threshold ranges from 10% [74] to 30% [109]. Rodman and Meentemeyer [112] even prefer ridge crests and set the threshold for slope to 40°, which corresponds to approximately 84%. In few studies, [70, 72, 103, 107] the slope is not at all considered as a criterion.

### 7.1.7 Impact on birds

Wind energy is the energy source that has least impact on animals and human beings in the world [113]. However, there are some minor impacts on migrating birds reported by few researchers [70, 73], mainly due to their collision with turbine rotor. Studies also show that climate changes have much more significant threat to wildlife than wind farms [114]. The Arabian Peninsula, which comprises of Kuwait, Bahrain, Qatar, United Arab Emirates, Oman, Yemen and Saudi Arabia is a transit point for birds migrating between Asia, Africa



© University of Pretoria

and Europe, particularly during the fall from August to October and returning between March and May heading toward the north, covering 70,000 km every year [115].

Although, there are fifteen important bird areas, IBA in the Arabian Peninsula [116] including bottleneck areas for soaring birds, sites for feeding and moulting and seabird breeding islands as shown in Figure 7.30, only five IBA's are located near the Saudi Arabian national boundary and none completely inside Saudi Arabia as birds fly over mountain ranges, waterbodies and natural habitats for survival.

The important bird areas, IBA i.e. breeding grounds, non-breeding areas, including intermediate resting and feeding places should fall at least 300 m away from a prospective wind farm [70 , 73]. In few similar studies, [74, 77, 117, 118] the acceptance criteria in terms of bird habitat is not considered as a criterion maybe due to non-interference with IBAs.

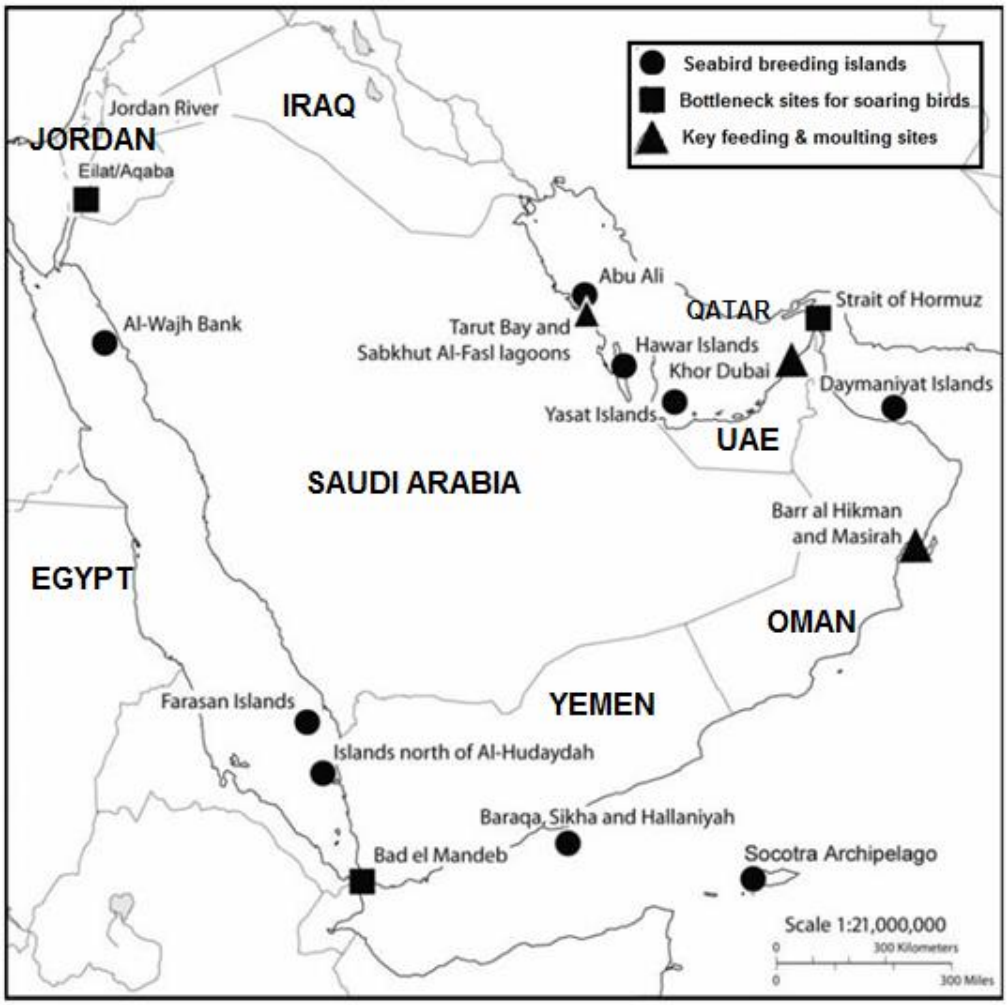


Figure 7.30 Important bird areas, IBA in Arabian Peninsula [116]

In this site suitability analysis, seven criteria are selected, as shown in Table 7.1. The criteria selected are based on more than 25 similar studies. The common criteria of water bodies and terrain slope as reported in other studies are not considered in this study as there are no perennial lakes and rivers in Saudi Arabia and even though few mountains exist in the north-western region, the slope is not that steep to be included as criteria. The birds 'migration criteria is not considered in this study as Saudi Arabia mostly comprises of arid desert with very limited mountain ranges and water bodies due to which there is factually no IBA causing hindrance in the wind farm site selection within the country. The restriction on the selected criteria, i.e., areas where wind farm installation is not feasible includes sites where wind speed is less than 5 m/s at 100 m AGL, sites which are more than 10,000 m away from roads and highways, sites where electricity grid is more than 10,000 m away, sites which are within a distance of 500 m from settlements, sites which are within a distance of 2,500 m from airports. Moreover, in order to give different rating scheme to criteria, as shown in Table 7.2, the data layers were reclassified into suitability scores of 1–6, with 6 having excellent and 1 lowest suitability. To define the range of the rating scheme, similar studies were reviewed [118]. The rating breakdown with paired suitability score is presented in Table 7.2.

Table 7.1 Constraints criteria for location of wind farm.

| **Criteria** | **Constraint factor** | **Considerations** |
|---|---|---|
| High mean wind speed (>5 m/s) | Wind resource | Climatic |
| Proximity to roads (<10 000 m) | Access | Economic |
| Proximity to highways (<10 000 m) | Access | Economic |
| Proximity to national grid (<10 000 m) | Access | Economic |
| Buffer distance away from airports (>2 500 m) | Safe/aesthetic | Planning |
| Buffer distance from settlements (> 500 m) | Noise | Planning |
| Proximity to population (rating scheme) | Optimum utilisation | Economic |



© University of Pretoria

Table 7.2 Rating scheme for criteria.

| Criteria | Suitability score | | | | | |
|---|---|---|---|---|---|---|
| | **Excellent-6** | **Very Good-5** | **Good-4** | **Mediocre-3** | **Low-2** | **Lowest-1** |
| High mean wind speed, m/s | > 6 | 6 – 5.8 | 5.8 – 5.6 | 5.6 – 5.4 | 5.4 – 5.2 | 5.2 - 5 |
| Proximity to roads/highways, m | < 2,000 | 2,000 – 4,000 | 4,000 – 5,500 | 5,500 – 7,000 | 7,000 – 8,500 | 8,500 – 10,000 |
| Proximity to national grid, m | < 2,000 | 2,000 – 4,000 | 4,000 – 5,500 | 5,500 – 7,000 | 7,000 – 8,500 | 8,500 – 10,000 |
| Proximity to population, m | 2,000 – 4,000 | 4,000 – 5,500 | 5,500 – 7,000 | 7,000 – 8,500 | 8,500 – 10,000 | < 2,000 |

## 7.2 METHODOLOGY AND GIS-BASED MODELLING

All of the selected criteria were first converted into the raster data structure and then reclassified into suitability scores, as shown in Table 7.2. In this study, ArcGIS 10 [119], was used for the development of a GIS-based model. In the reclassification of feasible areas according to wind potential, wind speeds above 6 m/s were considered to have excellent suitability. The suitability score decreased uniformly until it reached a lowest suitability score for areas where wind speed range is 5.2 – 5 m/s. Suitability scores increased with proximity to the electrical grid, major roads and highways. Same rating scheme was selected for all three criteria, i.e., electrical grid, major roads and highways. Distance less than 2000 m was considered to have excellent suitability, the suitability score decreased gradually until it reached a lowest suitability score of 1 for distance range of 8,500 – 10,000 m [112]. A distance between 2000 – 4000 m from population was considered to have excellent suitability. Suitability scores decreased gradually until a score of 1 was reached for distance range of 8,500 – 10,000 m. Since a prospective site should not be too close to settlements, due to noise, nuisance and disturbance to natural surroundings, lowest suitability score of 1 was given to a distance less than 2000 m.

Baban and Parry [74] used two different approaches. The first considered all the layers as being equally important and gave them equal weight. The second grouped the layers and graded them according to perceived importance. The first grade factors, roads and urban centres were assigned a combined weight of around 55%. The second grade factors, rivers,

water bodies, ecological sites, and railways were assigned a combined weight of around 25%. The third grade factors, historical sites and national trust properties were assigned a combined weight of around 12%. Finally, the fourth grade factors, paths, were assigned a weight of around 8%. Miller and Li [118] assigned a maximum weight of 25% to wind energy potential, 16.6% each to slope, land use, distance to transmission lines, distance to roads, and 8.5% to population density.

The weights assigned in these studies were also dependent on the land cover, terrain and national wind energy policies. Saudi Arabia is new to utilising renewable energy and specially wind energy. Therefore, currently, no such national wind energy policies are available to the best of the authors' knowledge. The weights assigned to each criterion in this study is shown in Table 7.3. The modelling is based on two methods, in Method 1, all the layers were given equal weightage of 20%. In Method 2, different weightage was given to different layers (criteria). The maximum weightage of 40% was given to wind resource. A weightage of 15% each was given to other four criteria. The weightage in Method 2, is based on similar studies elsewhere [74, 118] and wind energy policies worldwide [120, 121, 122].

Table 7.3 Weightage allocated to criteria.

| **Criteria** | **Weightage %** | |
|---|---|---|
| | **Method 1** | **Method 2** |
| Mean interpolated wind speed | 20 | 40 |
| Proximity to roads and highways | 20 | 15 |
| Proximity to national electrical grid. | 20 | 15 |
| Proximity and buffer from settlements. | 20 | 15 |
| Buffer from airports. | 20 | 15 |



© University of Pretoria

## 7.3 DATA LAYERS (SHAPE FILES) USED FOR THE ANALYSIS

The different layers used in this suitability analysis are shown schematically from Figures 7.31 to 7.35. The study was performed on ArcMap 10.3.1 [119], the main component of ESRI's ArcGIS suite of geospatial processing programs.

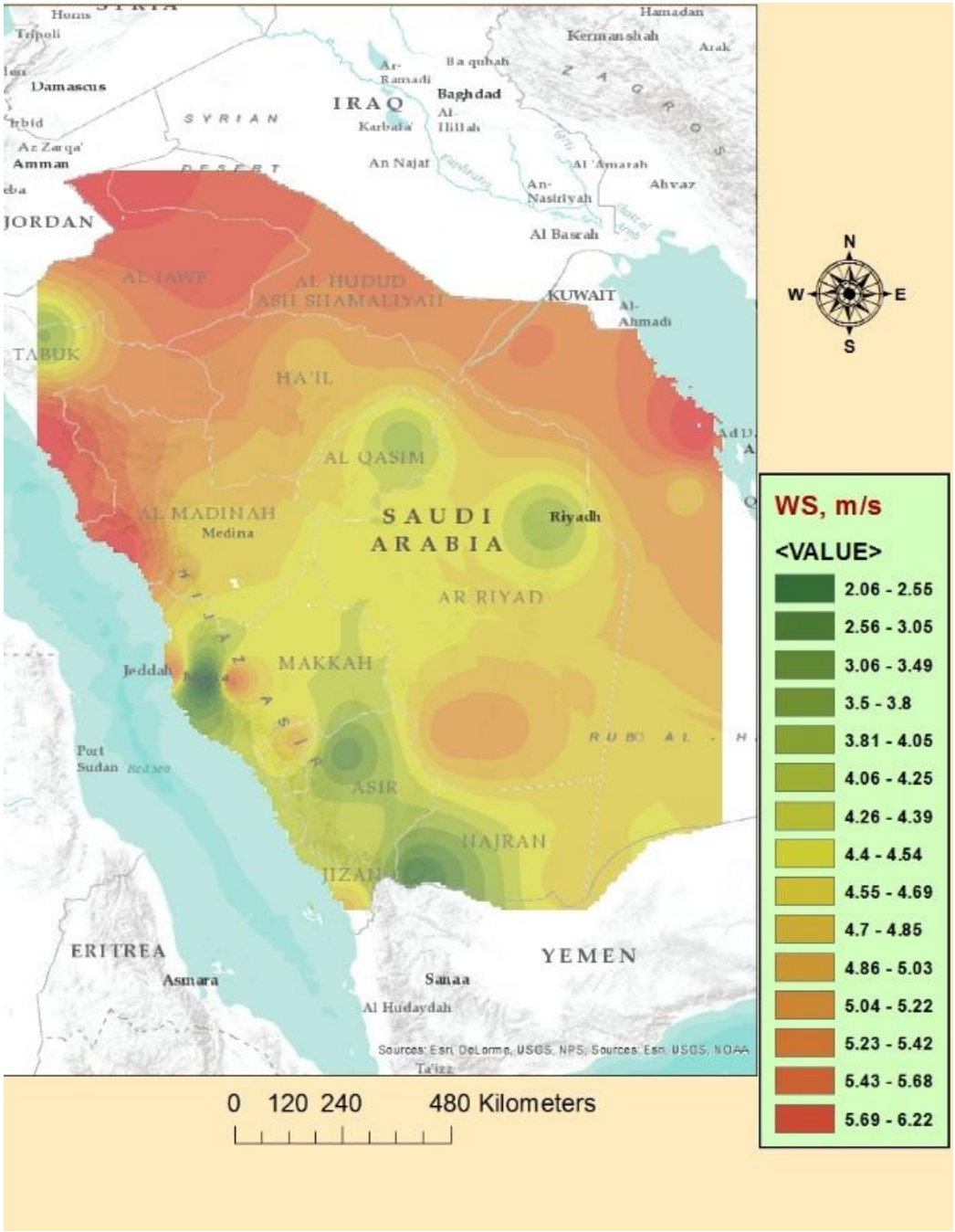


Figure 7.31 Interpolated wind speed at 100 m AGL.


Figure 7.32 Highways of Saudi Arabia.


Figure 7.33 Roads of Saudi Arabia.


Figure 7.34 International, domestic and military airports of Saudi Arabia.

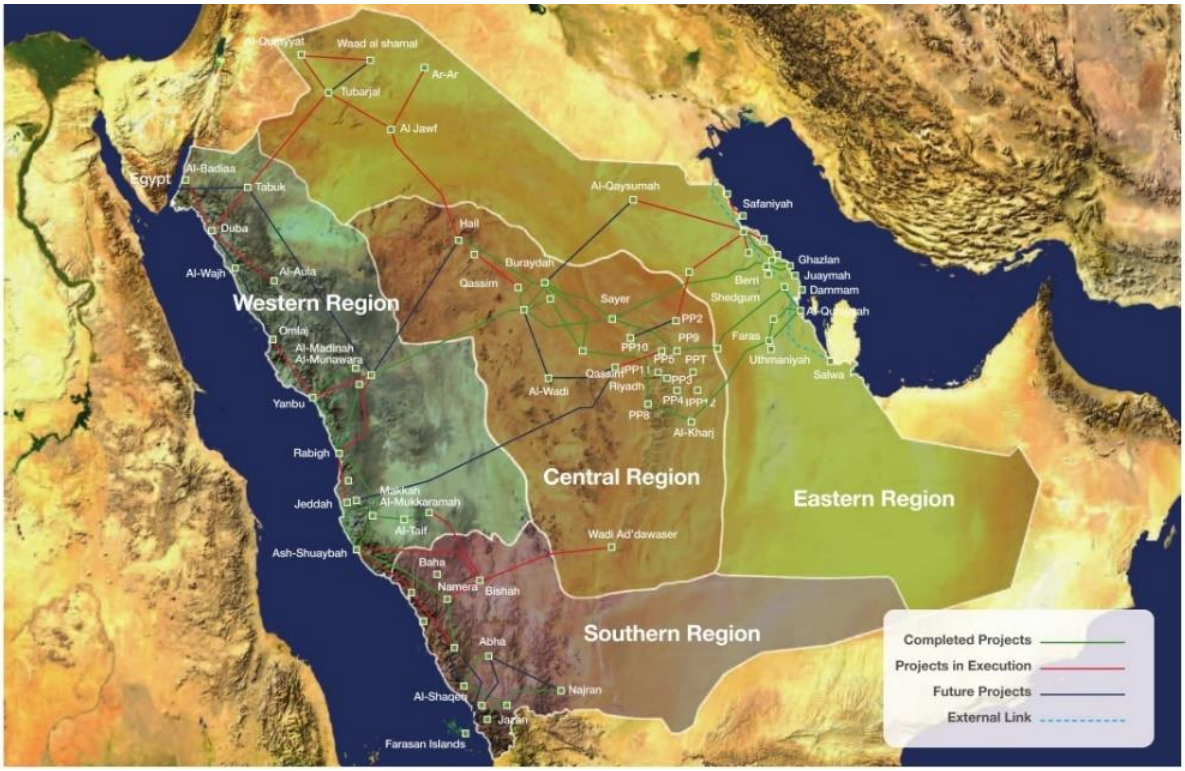


Figure 7.35 National electricity grid of Saudi Arabia [16].

The shapefiles of roads and highways of Saudi Arabia were combined using the merge function in ArcMap 10.3.1 [119] as the constraints, rating scheme and weightage applied to both were the same.

The site suitability model with the criteria restrictions and its reclassification is shown in Figure.7.36. All data layers were combined using the weighted overlay method as shown by the flowchart model in Figure 7.36. The final suitability indices for the entire country were determined by reclassifying the scores derived from the weighted overlay into six classes. This is a generalised model and can be applied for any region worldwide where wind data and all related shape files are available. The wind farm site suitability analysis was done by two different methods, as shown in Table 7.3. In both methods, all five layers i.e., interpolated wind speed, national electrical grid, roads and highways, settlements and airports were used, but the weightage given to these layers was different.



© University of Pretoria

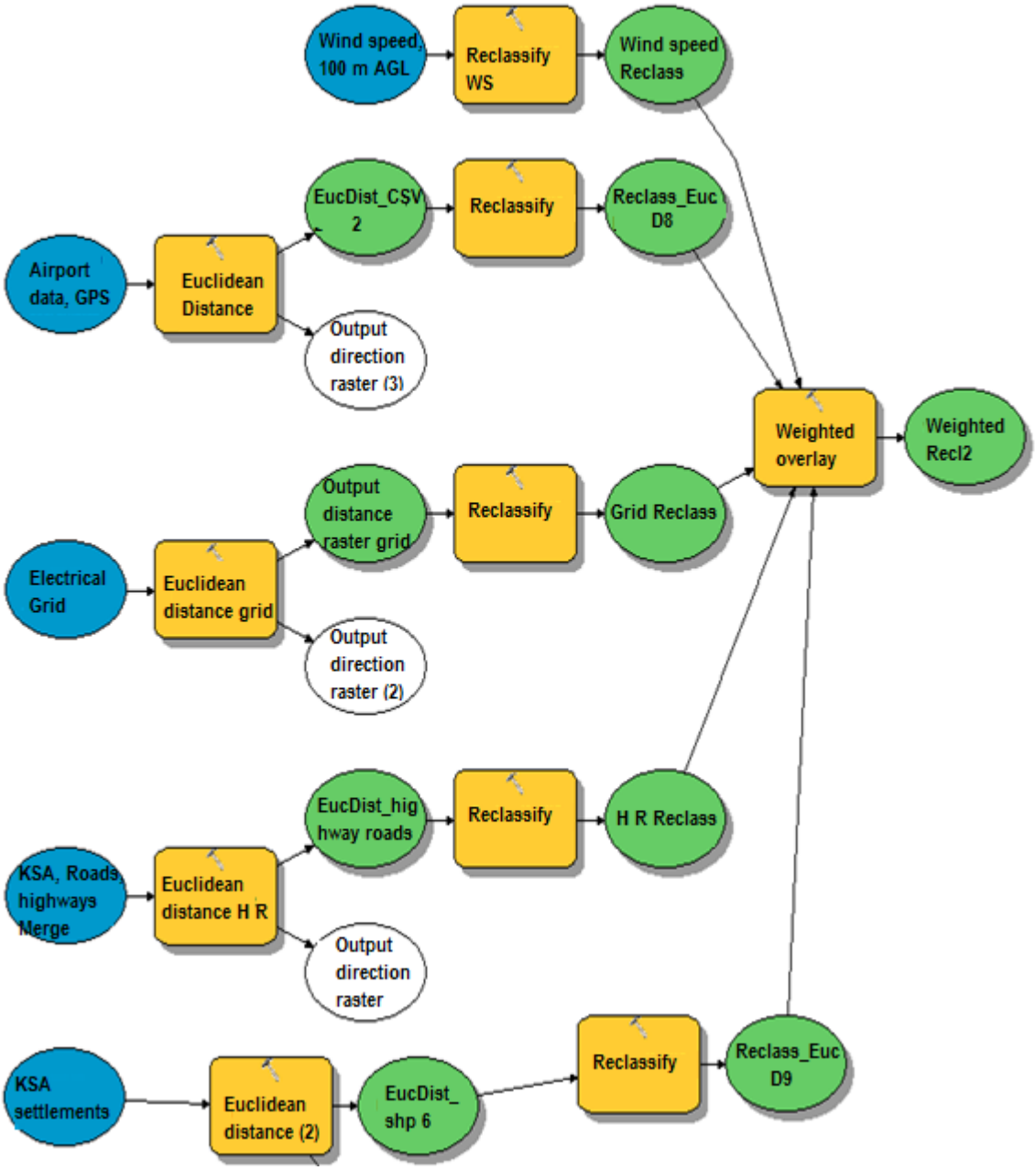


Figure 7.36 Wind farm site suitability model for both methods.

## 7.4 WIND FARM SUITABILITY MAPS

The wind farm suitability maps based on Method 1 and 2 are shown in Figures 7.37 and 7.38, respectively. These maps are distributed into six classes, where class 6 is the most suitable area for wind farm development and class 1 is the least suitable area. The index of suitability decreases with increasing distance from roads and electrical grid until a critical distance is reached after which the area is completely unsuitable, as shown in Tables 7.2 and 7.3 . Therefore, these maps also contain some left out areas which cannot be considered at all for

wind farm development as they are not windy and far away from large settlements, roads and the electrical grid. Also, none of the suitable locations fall within a vicinity of less than 300 m from important bird sites, therefore, inclusion of this criteria will not alter the suitability of identified regions.

In the suitability map based on Method 1, 1.03% of the total classed area falls under the most suitable wind farm area, whereas in Method 2, the percentage is 1.86%. The percentage area of the next best area is 29.13% and 14.65% in the maps based on Method 1 and 2, respectively. It can be deduced that in the map based on Method 2, there is slight increase in the geographical extent of the most suitable area, whereas the extent of second best area is more in the map based on Method 1.

In both maps, three most suitable locations for development of wind farms are identified as follows:

(i) In the eastern Province, near Ras Tanura and Safwa close to Dammam city along the coast

(ii) In the northern- region, near Turaif, Kaf and Al-Isawiyah close to Al-Jawf

(iii) In the north western borders region, near Al-Wajh and Yanbu

Some central areas and the entire south-eastern area were found to be completely unsuitable for wind farm development mainly due to low mean wind speeds, scarce population and less connectivity by roads and the national electrical grid. Since this study was done for the entire country of Saudi Arabia, in which three regions were identified as most suitable, a lot of alternatives in these regions still remain. Detailed and pertinent siting of wind farm locations for these regions individually can be considering as significant and interesting future work. Also, as many studies on wind farm siting and wind energy polies were reviewed and a first of its kind study performed in Saudi Arabia, this thesis can provide insight in the national wind energy policy making.

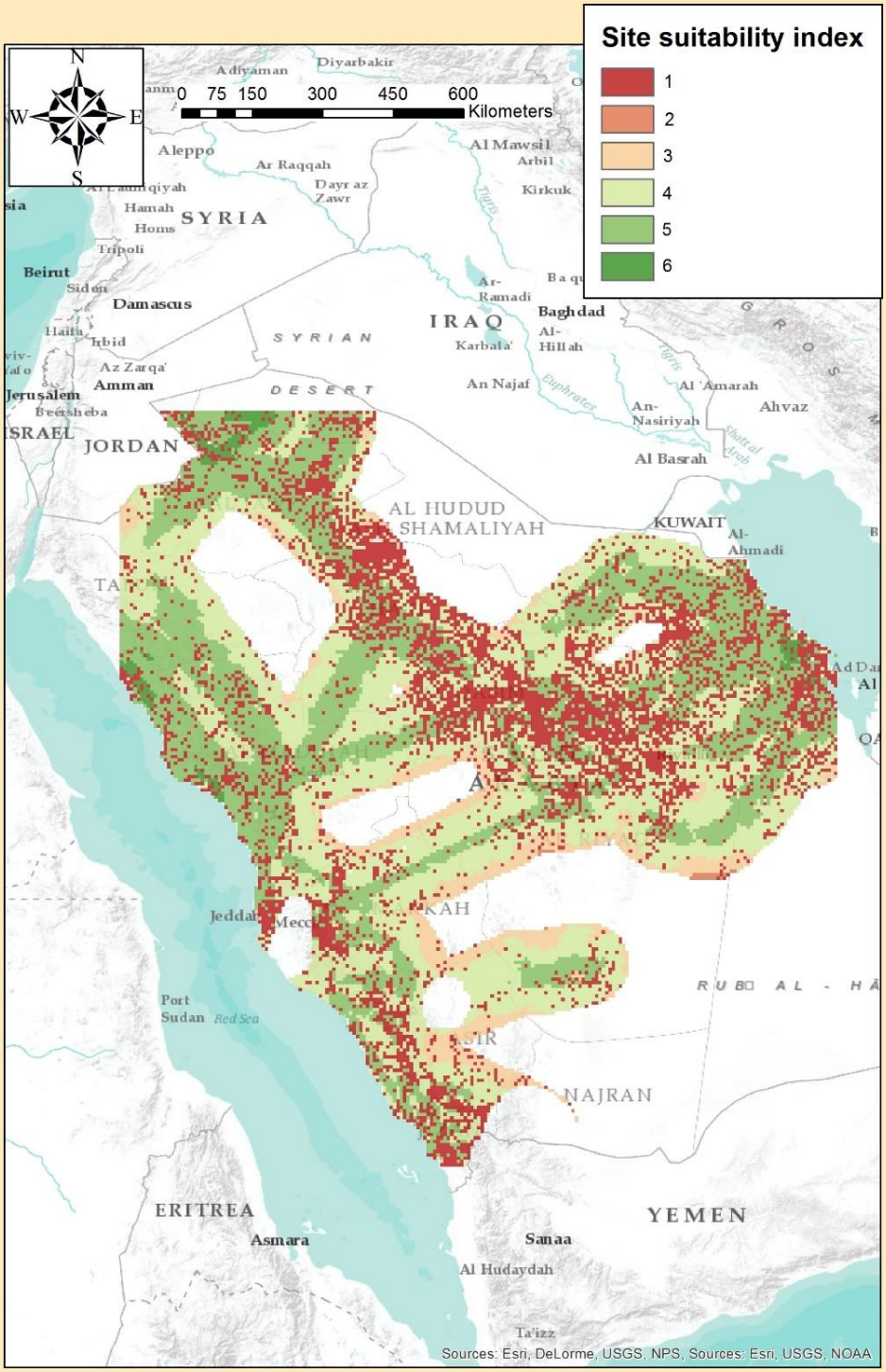


Figure 7.37 Wind farm site suitability map based on Method 1.

1=least suitable 6=most suitable




© University of Pretoria

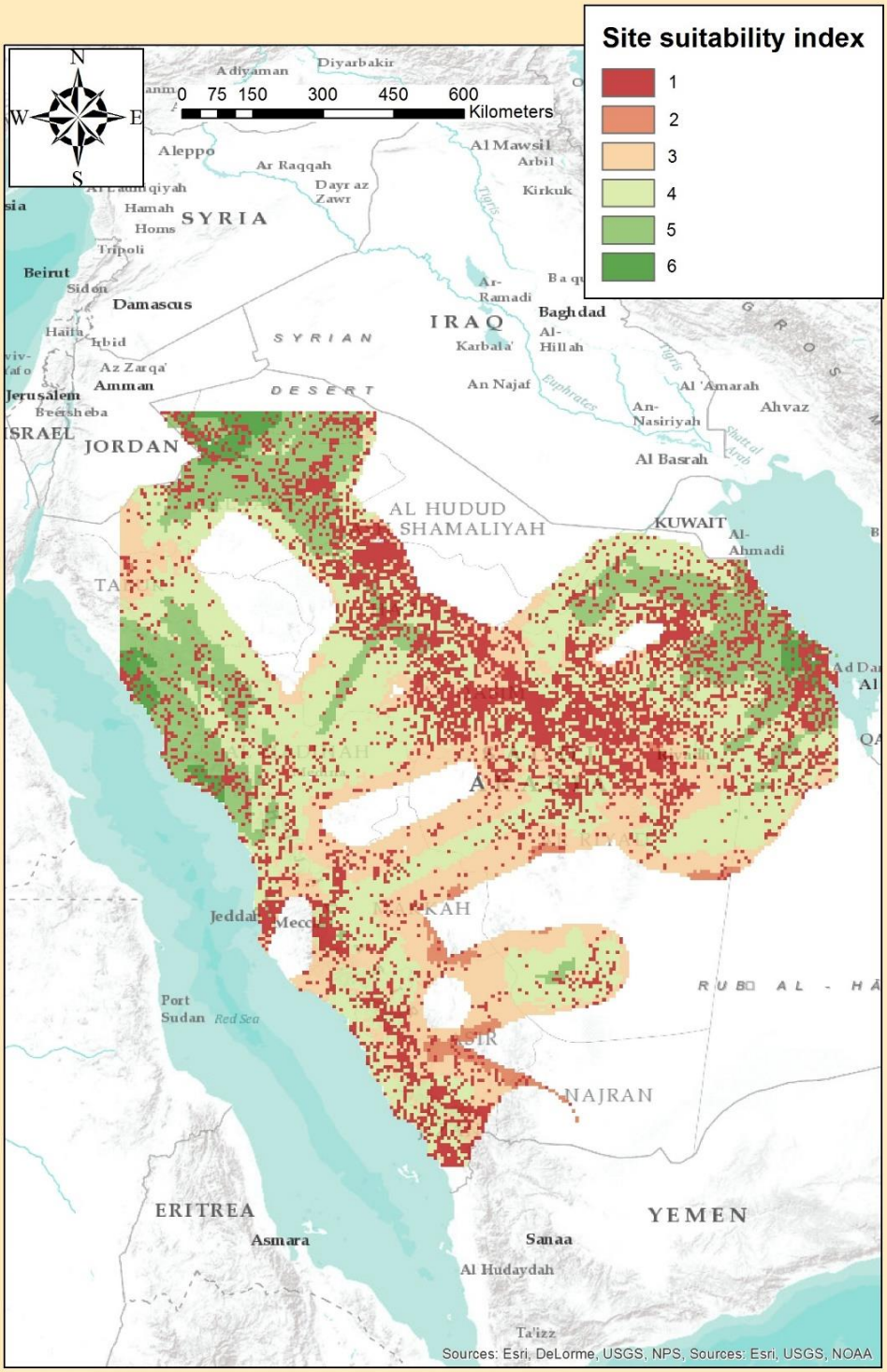


Figure 7.38 Wind farm site suitability map based on Method 2.

1=least suitable 6=most suitable




© University of Pretoria

## SUMMARY

- A generalised GIS-based multi-criteria model has been developed for wind farm siting considering important parameters, such as wind resource, proximity to national electricity grid, roads/highways network accessibility, etc.
- A GIS-based multi-criteria wind farm site suitability analysis for the entire Kingdom of Saudi Arabia was conducted.
- The climatic, economic, aesthetic and environmental criteria constraints used in this analysis were: wind resource, accessibility by roads/highways, proximity to national electrical grid, and optimum/safe distance from settlements and airports.
- A comprehensive literature review was conducted to identify criteria and apply constraints, and rating and weightage to each.
- Two different approaches were used in this analysis, one in which equal weightage was given to all the criteria and the other in which different weightage was given to different criteria for site selection.
- The most suitable sites for wind farm development based on both methods were found to be (i) near Ras Tanura and Safwa along the coast in the eastern Province, (ii) Turaif, Kaf and Al-Isawiyah in Al-Jawf region along northern borders, and (iii) Al-Wajh and Yanbu along the coast in the western region.
- Some central areas and the entire south-eastern area were found to be completely unsuitable for wind farm development mainly due to low mean wind speeds, scarce population and lack of connectivity by roads and national electrical grid.
- A detailed suitable siting study of wind farm locations for these three selected regions can be considered for future work.
- This study can provide insight in developing appropriate national wind energy policy. At present there is no such policy exist in Saudi Arabia.

# CHAPTER 8

# CONCLUSIONS AND RECOMMENDATIONS

The growing world population, rapid industrialisation, materialistic higher living standards, usage of energy intensive appliances and so on are causing phenomenal rising demands of electricity. Consequently, the global annual energy demand increased from 1,600 to 20,000 TWh from 2001 to 2010, a 25% increase in a short period of 10 years only. It is not feasible to depend on fossil-fuel based resources alone to cater to this increasing power needs, as this resource is not only diminishing but also releasing harmful greenhouse gases into the atmosphere.

The utilisation of renewable sources of energy can overcome the negative repercussions of usage of conventional fossil-fuel based energy. One of the rapidly growing renewable sources of energy is wind energy. To make effective utilisation of wind energy, a comprehensive literature review has been performed based on a large number of research papers published in international journals and official reports and articles published by organisations from the energy sector. Thorough analyses have been carried out about the wind resource assessment, state of the art global wind energy planning procedures, global wind power scenario, power output from wind turbines. A GIS-based site selection model has been developed and comprehensive site suitability analysis has been performed for the entire region of Saudi Arabia. In conclusion, the outcome of the present study and possibility of the future work is summarised in the following sub-sections.

## 8.1 SUMMARY OF FINDINGS

- The world population reached 7 billion in 2012 and the new projections indicate that the 8 billion marker will be reached by year 2025. The global cumulative installed wind power capacity increased from 3,760 to 63,467 MW, a 25-fold increase, in the last 15 years.

- The total population of Saudi Arabia increased from 5772000 in 1970 to 30770375 in 2014, a 5-fold increase in the last four and a half decades. The total energy consumption in Saudi Arabia from 2000 to 2014 increased from 126,191 to 311,807 GWh, a 2.5-fold increase in the last one and a half decades.



© University of Pretoria

The following conclusions can be drawn from the wind resource assessment conducted at Industrial Area (Central):

- The annual mean wind speeds over the period from 2008 to 2012 were 3.34, 4.79 and 5.35 m/s at 10, 50 and 90 m AGL, respectively. The wind speed was found to be above 3.5 m/s for 49.3, 75.7 and 77.7% of the time at 10, 50 and 90 m in height, respectively. Subsequently, a wind machine with rated wind speed of 3.5 m/s and hub height more than 50 m AGL can continuously produce power at least 75% of the time.

- There was not much variation in mean annual wind speed. A distinct seasonal wind speed pattern was observed, it was the highest in June and the lowest in October. The diurnal variation shows the wind speed to be high during the daytime and low during the night-time.

- The most prevailing wind direction at three heights was from the north-west. The percentage of calm winds (wind speed less than 0.5 m/s) decreased with increasing height, i.e. 1.82, 0.61 and 0.56% at 10, 50 and 90 m, respectively.

- The Weibull parameter, *c*, was the highest in March and the lowest in October at all wind speed measurement heights. The Weibull parameter, *k*, did not show any specific seasonal pattern.

- The air density was observed to be the lowest in July and the highest in January. The WSE obtained from power law fitting of the wind shear profile was 0.217. The diurnal variation showed low values of WSE during the daytime, i.e. from 9:00 AM to 3:00 PM. The seasonal variation of the WSE did not show any specific pattern.

- The annual energy production from a commercially available wind turbine WT1 of 3 MW rated power was estimated to be 6,285 MWh with a PCF of 25%.

The following conclusions can be drawn from the wind resource assessment conducted at seven locations in Jubail:

- At 10 m AGL, the annual mean wind speeds varied from 2.25 m/s (standard deviation 1.109 m/s) at the Pearl Beach to 4.52 m/s (standard deviation 2.52 m/s) at industrial Area (East). In general, at all sites, the highest monthly mean wind speed was observed in February/June and the lowest in September/October. The period of higher

winds availability coincides with high power demand period of the area due to the air conditioning load.

- The most prevailing wind direction at all seven sites of Jubail was from the north-west, which means that the wind machines can spread facing the prevailing wind direction.

- The goodness-of-fit test indicators, i.e., $R^2$, RSME, MBE and MAE show that the maximum likelihood method is the most accurate method for Weibull parameter estimation to represent the wind regime in Jubail followed by WAsP algorithm and least square regression method. Considering overall data at all sites, the average error in calculating the WPD was found to be 0.25% for maximum likelihood method, 6.8% for LSRM and 5.7% for WAsP method.

- The highest most probable wind speeds of 3.39, 3.60, 3.24 m/s at Industrial Area (East) and the lowest values of 1.86, 1.76, 2.07 m/s at the Pearl Beach were determined by maximum likelihood method, least-square regression methods and WAsP, respectively.

- The highest maximum energy carrying wind speed values of 8.61, 9.0, 8.68 m/s at Industrial Area (South) and the lowest values of 3.48, 3.73, 3.38 m/s at the Pearl Beach were determined by maximum likelihood method, least-square regression methods and WAsP, respectively.

- The wind energy output from five different commercially available wind machines with rated output ranging from 1.8 to 3.3 MW at all the sites shows that most feasible site for wind farm development in Jubail city is Industrial Area (East). At this site, the maximum energy output of 11,135 MWh/year with a PCF of 41.3% from a 3 MW rated power wind machine was obtained. The second best site for wind farm development is Industrial Area 2 (South). At this site, the maximum energy output of 10,180 MWh/year with a PCF of 37.8% from a 3 MW rated power wind machine was obtained.

- From percent PCF, it can be concluded that wind machine 5 (1.8 MW rated power) is most efficient at all sites in Jubail, as a low rated power wind machine is more efficient for mediocre wind potential areas. Even though the 1.8 MW wind machine is



© University of Pretoria

found to be most efficient, installation of higher rated power wind machine like 3 MW is a smart option as it would occupy lesser of the scarce land in the Industrial city

A GIS-based model was developed for suitable wind farm site selection considering various climatic, economic, aesthetic and environmental parameters. Furthermore, a GIS-based multi-criteria wind farm site suitability analysis for the entire Kingdom of Saudi Arabia was performed. The following main conclusions can be drawn from the analysis:

- From the investigation of long-term, historical wind speed data (40 years for most of the locations) of 29 meteorological stations spread countrywide, the highest annual average wind speed of 4.38 m/s was observed at Dhahran at 10 m AGL with a standard deviation of 1.66 m/s. Encouraging mean wind speed of more than 4 m/s were observed at Dammam, Guriat, Turaif, Wejh and Yanbo with a standard deviation ranging from 1.4 to 2 m/s. The lowest wind speed of 1.59 m/s was observed at Makkah.

- In general, the monthly statistics variations of all 29 stations show two peaks, one in the month of February/March and another in June/July. The mean wind speed was high in north-eastern coastal regions of Dammam and Dhahran, south-western coastal region of Yanbu and near north-western country's border, Al-Jawf.

- The climatic, economic, aesthetic and environmental criteria constraints used in this analysis were wind resource, accessibility by roads/highways, proximity to national electrical grid, and optimum/safe distance from settlements and airports.

- The wind data of 29 stations were obtained from Presidency of Metrology and Environment control, a governmental organisation. The wind speed used in the criterion is interpolated to 100 m from 10 m AGL by using traditional one-seventh power law.

- A spatial interpolation technique was used to predict the wind speed in locations where data are not available. In this analysis, the method used to convert the point data into raster format is the inverse distance weighted, IDW. It determines cell values using a linear weighted combination of a set of sample points. The weight is a



© University of Pretoria

function of inverse distance. The surface being interpolated should be a variable dependent on location.

- The data and GIS shape files of other criteria mentioned above were also obtained from governmental organisations. The GIS shape files for roads and highways were merged as identical constraints were applied to both the criteria. Subsequently, the data of all the criteria are reclassified into suitability scores.

- As there are no perennial lakes and rivers in Saudi Arabia, no weightage was given to the criteria of water bodies when the model was applied to the case study of Saudi Arabia. Suitable buffer distance was applied around the 36 international, domestic and military airports of the country.

- Two different approaches were used in this analysis, one in which equal weightage was given to all the criteria components and another in which different weightage was given to different criteria components for site selection.

- The suitable sites for wind farm development based on both methods were found to be (i) near Ras Tanura and Safwa along the coast in the eastern Province, (ii) Turaif, Kaf and Al-Isawiyah in Al-Jawf region along northern borders, and (iii) Al-Wajh and Yanbu along the coast in the western region.

- Some central areas and the entire south-eastern area were found to be completely unsuitable for wind farm development mainly due to low mean wind speeds, scarce population and lack of connectivity by roads and national electrical grid.

In conclusion, this study will help in identifying the feasible wind farm sites throughout Saudi Arabia and also includes WRA of a significant industrial base within the Kingdom. The energy consumption in Saudi Arabia is projected to increase threefold by 2030. At present, there is a lack of proper renewable energy sector. “Saudi Arabia vision 2030” [18] sets an initial target of producing 9.5 GW of renewable energy by 2023. This study will help in achieving this target explicitly from the point of view of the optimum harnessing of wind energy. Also, since the local wind energy policies are not well defined, this study is based on worldwide similar policies, few of which are modified to suit the regional criteria. Therefore, this study can provide insight in developing appropriate national wind energy policy.

## 8.2 LIMITATIONS AND FUTURE DIRECTION

Wind resource assessment for seven locations in Jubail:

- Non-availability of recent meteorological data, from 2013 to 2015, for latest representation of the region of Jubail.
- The meteorological tower near the pearl beach, Jubail is not suitable to monitor wind speed as it is closely surrounded by two to three floor building. An alternative location can be suggested to the Meteorological Department.
- GIS-based site suitability analysis can be conducted separately for Jubail and nearby region.
- The design and analysis of wind-pv-diesel hybrid system for Jubail may provide an optimum mix energy solution.

GIS-based multi-criteria wind farm site suitability analysis for Saudi Arabia:

- Since wind energy policies are not well defined for Saudi Arabian location, this study is based on global wind energy policies. Once Saudi Arabia defines comprehensive wind energy policies, the GIS-based site selection work has to be revised.
- At the three identified suitable locations, the wind data is mostly available from airports. Wind masts should be installed to get comprehensive data for the specific region and more accurate siting of the wind farm.
- Pertinent wind farm site suitability analysis can be conducted discretely for three identified regions, namely, (i) Ras Tanura and Safwa, (ii) Turaif, Kaf and Al-Isawiyah, and (iii) Al-Wajh and Yanbu. Additional explicit analysis for these three sites may include (i) applying buffer distances around single dwellings for noise emission control and to avoid visual and scenic intrusion of the wind turbines, (ii) placing restrictions on certain areas due to negative effects of flora and fauna, (iii) applying buffer distances around certain regions restricted by planning authority like

the municipal administration, (iv) checking soil conditions for suitability of mounting wind turbine towers and so on.

- One of the suitable sites is very close to the biggest thermal desalination plant in the world, operated by Saline Water Conversion Corporation (SWCC). Thermal desalination process is an energy intensive process and supply of this energy can be provided by wind energy.

- The developed wind speed extrapolated maps, the frequency distributions, wind shear exponents and identification and annexation of local criteria in GIS site suitability model for the entire country will be of great help in defining the further line of action and policy-building towards wind power development and utilisation in the Kingdom. (To the author's knowledge, no such national policies are published to date.)

## REFERENCES

1. M. Carlowicz. (2010) "World of change: Global temperatures: Feature articles," NASA Earth Observatory [Online]. Available at: http://earthobservatory.nasa.gov/Features/WorldofChange/decadaltemp.php. Accessed: 30 June 2016.
2. O. Edenhofer. (2012) Special report on renewable energy sources and climate change mitigation: summary for policymakers and technical summary. Geneva: Intergovernmental Panel on Climate change.
3. United States Census Bureau (2016) Available at: http://www.census.gov/en.html Accessed: 30 June 2016.
4. Energy Information Administration. (2016) International Energy Outlook 2016 - [Online]. Available: http://www.eia.gov/forecasts/ieo/index.cfm. Accessed: 30 June 2016.
5. The Organization for Economic Cooperation and Development OECD. (2015) International Energy Agency. Available at: http://www.worldenergyoutlook.org/ Accessed: 30 June 2016.
6. Central Department of Statistics and Information of Saudi Arabia. (2014) Government Annual Report on Demographic Survey. Available at: http://www.cdsi.gov.sa/english/index.php Accessed: 30 June 2016
7. Saudi Industrial Development Fund. (2014) Government annual report on Industrial growth of Saudi Arabia by, 2014. Available at: <http://www.sidf.gov.sa/En/Pages/default.aspx> Accessed: 30 June 2016
8. Global Wind Energy Council Statistics. Available at: <http://www.gwec.net/global-figures/graphs> Accessed: 30 June 2016
9. The Vision, King Abdullah City of Atomic and Renewable energy (KACARE). Available at: <https://www.kacare.gov.sa/en/FutureEnergy/Pages/vision.aspx> Accessed: 30 June 2016
10. P. Chefurka (2007) World energy and population [Online]. Available: http://www.paulchefurka.ca/WEAP/WEAP.html. Accessed: 30 June 2016
11. "Saudi Arabia | Data". *Data.worldbank.org*. N.p., 2017. Web. 7 Jan. 2017. http://data.worldbank.org/country/saudi-arabia

12. Department of Economic and Social Affairs. Available at: http://www.un.org/en/development/desa/population/publications/development/population-development-database-2014.shtml Accessed: 30 June 2016.
13. E. Ortiz-Ospina and M. Roser. (2016) World Population Growth. Published online at OurWorldInData.org. Available at: https://ourworldindata.org/world-population-growth Accessed: 30 June 2016.
14. H. Karoui. (2006) Global trends in gulf and Middle East population evolution. [Online]. Available at: http://papers.ssrn.com/sol3/papers.cfm?abstract_id=942744. Accessed: 30 Jun 30 2016.
15. International Herald Tribune (2007) Middle East: Population growth poses huge challenge for Middle East and North Africa. Available at: http://www.nytimes.com/2007/01/18/news/18iht-oxan.0118.4250941.html?_r=0 Accessed: 30 June 2016.
16. Saudi Electricity Company (2014) Available at: https://www.se.com.sa/en-us/Pages/ShareHoldersReports.aspx. Accessed: 1 June 2016.
17. KSA power consumption 3 times world average (2014) Available at: http://www.arabnews.com/news/598481 (Accessed: 1 June 2016).
18. Saudi Vision 2030 (2016) Available at: http://vision2030.gov.sa/en. Accessed: 18 January 2017.
19. Global Wind Energy Council. (2015) "Global wind report 2015," [Online]. Available at: http://www.gwec.net/publications/global-wind-report-2/global-wind-report-2015-annual-market-update/. Accessed: Jun. 30, 2016.
20. Ministry of New and Renewable Energy. (2015) Physical progress (achievements) (2015) Available at: http://www.mnre.gov.in/mission-and-vision-2/achievements Accessed: 16 June 2016.
21. S. Rehman and N.M. Al-Abbadi. (2007) Wind shear coefficients and energy yield for Dhahran, Saudi Arabia. Renewable Energy. 32(5): 738–749. doi:10.1016/j.renene.2006.03.014
22. N. Masseran, A.M. Razali, K. Ibrahim, A. Zaharim and K. Sopian. (2013) Research Journal of Applied Sciences, Engineering and Technology 6(10): 1774-1779.
23. S. Rehman , T.O. Halawani, T. Husain. (1994) Weibull parameters for wind speed distribution in Saudi Arabia. Solar Energy. 53(6): 473–479.
24. S. Rehman and T.O. Halawani. (1994) Statistical characteristics of wind in Saudi Arabia. Renewable Energy. 4(8): 949-956.

25. M.R. Islam, R. Saidur and N.A. Rahim (2011) Assessment of wind energy potentiality at Kudat and Labuan, Malaysia using Weibull distribution function. Energy. 36(2): 985–92.
26. S. Rehman, A. M. Mahbub Alam, J. P. Meyer and L. M. Al-Hadhrami. (2012) Wind speed characteristics and resource assessment using Weibull Parameters. International Journal of Green Energy. 9: 800–814.
27. J. Ansari, I.K. Madni, H Bakhsh. (1986) Saudi Arabian wind energy atlas. Riyadh, Saudi Arabia: KACST: 1–27.
28. S.H. Alawaji, N.N. Eugenio and U.A. Elani. (1996) Wind energy resource assessment in Saudi Arabia. Part II: Data Collection and Analysis. Renewable energy. 9 (4): 818–821.
29. S.M. Shaahid, L.M. Al-Hadhrami and M.K. Rahman. (2014) Potential of Establishment of Wind Farms in western Province of Saudi Arabia. Energy Procedia. 52: 497–505.
30. R.D. Prasad, R.C. Bansal and M. Sauturaga. (2009) Some of the design and methodology considerations in wind resource assessment. IET Renewable Power Generation. 3(1): 53-64.
31. F. Fazelpour, N. Soltani, S. Soltani and M.A. Rosen. (2015) Assessment of wind energy potential and economics in the north-western Iranian cities of Tabriz and Ardabil. Renewable and Sustainable Energy Reviews. 45: 87-99.
32. S.H. Pishgar-Komleh, A. Keyhani, and P. Sefeedpari. (2015) Wind speed and power density analysis based on Weibull and Rayleigh distributions (a case study: Firouzkooh county of Iran). Renewable and Sustainable Energy Reviews. 42: 313-322.
33. S.S. Chandel, P. Ramasamy and K.S.R. Murthy. (2015) Wind power potential assessment of 12 locations in western Himalayan region of India. Renewable and Sustainable Energy Reviews. 39: 530-545.
34. F. Kose, M.H. Aksoy and M. Ozgoren. (2014) An Assessment of Wind Energy Potential to Meet Electricity Demand and Economic Feasibility in Konya, Turkey. International Journal of Green Energy. 11(6): 559-576.
35. A. Ucar and F. Balo. (2009) Evaluation of wind energy potential and electricity generation at six locations in Turkey. Applied Energy. 86: 1864–1872.
36. ALF Jowder. (2009) Wind power analysis and site matching of wind turbine generators in Kingdom of Bahrain, Applied Energy. 86: 538-545.

37. Fyrippis, J.P Axaopoulos and G. Panayiotou. (2010) Wind energy potential assessment in Naxos Island Greece. Applied Energy. 87: 577–586.
38. X. Gao, H. Yang and L. Lu. (2014) Study on offshore wind power potential and wind farm optimisation in Hong Kong. Applied Energy. 88(5): 1848-1856.
39. F. Onea and E. Rusu. (2014) An evaluation of the wind energy in the north-west of the black sea. International Journal of Green Energy. 11(5): 465-487.
40. M.E. Lee, G. Kim, S.T. Jeong, D.H. Ko and K.S. Kang. (2013) Assessment of offshore wind energy at Younggwang in Korea. Renewable and Sustainable Energy Reviews. 21: 131–141.
41. J. Wu, J. Wang and D. Chi. (2013) Wind energy potential assessment for the site of Inner Mongolia in China. Renewable and Sustainable Energy Reviews. 21: 215–228.
42. M. Irwanto, N. Gomesh, M.R. Mamat and Y.M. Yusoff. (2014) Assessment of wind power generation potential in Perlis, Malaysia. Renewable and Sustainable Energy Reviews. 38: 296–308.
43. Türk Togrul and M. Imas Kizi. (2008) Determination of wind energy potential and wind speed data in Bishkek, Kyrgyzstan. International Journal of Green Energy. 5: 157–173.
44. S.F. Khahro, K. Tabbassum, A. Mahmood Soomro, X. Liao, M.B. Alvi, L. Dong and M.F. Manzoor. (2014) Techno-economical evaluation of wind energy potential and analysis of power generation from wind at Gharo, Sindh Pakistan. Renewable and Sustainable Energy Reviews. 35: 460–474.
45. S.AL-Yahyai, Y. Charabi, A. Gastli and S. Al-Alawi. (2010) Assessment of wind energy potential locations in Oman using data from existing weather stations. Renewable and Sustainable Energy Reviews. 14: 1428–1436.
46. C. Ikilic. (2012) Wind energy and assessment of wind energy potential in Turkey. Renewable and Sustainable Energy Reviews. 16: 1165–1173.
47. Y. Himri, S. Rehman, B. Draoui and S. Himri. (2008) Wind power potential assessment for three locations in Algeria. Renewable and Sustainable Energy Reviews. 12: 2495–2504.
48. P. Alamdari, O. Nematollahi, M. Mirhosseini. (2012) Assessment of wind energy in Iran: A review. Renewable and Sustainable Energy Reviews. 16: 836– 860.
49. A.S. Ahmed. (2012) Potential wind power generation in south Egypt. Renewable and Sustainable Energy Reviews. 16: 1528– 1536.

50. O.S. Ohunakin. (2011) Assessment of wind energy resources for electricity generation using WECS in north-Central region, Nigeria. Renewable and Sustainable Energy Reviews. 15: 1968–1976.
51. K. Philippopoulos, D. Deligiorgi and G. Karvounis. (2012) Wind speed distribution modelling in the greater area of Chania, Greece. International Journal of Green Energy. 9: 174–193.
52. Q. Hernández-Escobedo, R. Saldaña-Flores, E.R. Rodríguez-García and F. Manzano-Agugliaro. (2014) Wind energy resource in northern Mexico. Renewable and Sustainable Energy Reviews. 32: 890–914.
53. B.W. Raichle and W.R. Carson. (2009) Wind resource assessment of the southern Appalachian Ridges in the south-eastern United States. Renewable and Sustainable Energy Reviews. 13: 1104–1110.
54. F. González-Longatt, J. Serrano González, M. Burgos Payán and J.M. Riqueme Santos. (2014) Wind-resource atlas of Venezuela based on on-site anemometry observation. Renewable and Sustainable Energy Reviews. 39: 898–911.
55. T. Wentink. (1976) Study of Alaskan wind power potential and its possible applications. Final Report (Rep. No. NSF/RANN/SE/AER 74-00239/FR-76/ 1), Geophysical Institute, University of Alaska.
56. M.J.M. Stevens and P.T. Smulders. (1979) The estimation of the parameters of the Weibull wind speed distribution for wind energy utilisation purposes. Wind Engineering. 3(2): 132-45.
57. J.V. Seguro and T.W. Lambert. (2000) Modern estimation of the parameters of the Weibull wind speed distribution for wind energy analysis. Journal of Wind Engineering and Industrial Aerodynamics 85: 75-84.
58. H.S. Bagiorgas, M. Giouli, S Rehman and L.M. Al-Hadhrami. (2011) Weibull parameters estimation using four different methods and most energy-carrying wind speed analysis. International Journal of Green Energy 8 (5): 529-554.
59. P.A. Costa Rocha, R.C. de Sousa, C.F. de Andrade and M.E.V. da Silva. (2012) Comparison of seven numerical methods for determining Weibull parameters for wind energy generation in the northeast region of Brazil. Applied Energy 89: 395–400.
60. S.A. Akdag and A. Dinler. (2009) A new method to estimate Weibull parameters for wind energy applications. Energy Conversion and Management 50: 1761–1766.

61. J. Malczewski J (2006) GIS-based multicriteria decision analysis: a survey of the literature. International Journal of Geographical Information Science. 20(7): 703-726.
62. O.A. Omitaomu, B.R. Blevins, W.C. Jochem, G.T. Mays, R. Belles, S.W. Hadley, T.J. Harrison, B.L. Bhaduri, B.S. Neish and A.N. Rose. (2012) Adapting a GIS-based multicriteria decision analysis approach for evaluating new power generating sites. Applied Energy. 96: 292–301
63. J.S. Rodrígueza and J.N. Pinob. (2014) Evaluation of on-shore wind techno-economical potential in regions and islands. Applied Energy. 124-129.
64. H. Viana, W.B. Cohen, D. Lopes and J. Aranha. (2010) Assessment of forest biomass for use as energy. GIS-based analysis of geographical availability and locations of wood-fired power plants in Portugal. Applied Energy. 87(8): 2551-2560.
65. J. Höhn, E. Lehtonen, S Rasi, J. Rintala. (2014) A Geographical Information System (GIS) based methodology for determination of potential biomasses and sites for biogas plants in southern Finland. Applied Energy. 113: 1-10.
66. A. Comber, J. Dickie, C. Jarvis, M. Phillips and K. Tansey. (2015) Locating bioenergy facilities using a modified GIS-based location–allocation-algorithm: Considering the spatial distribution of resource supply. Applied Energy. 154: 309-316.
67. B.C. Kusre, D.C. Baruah, P.K. Bordoloi and S.C. Patra. (2010) Assessment of hydropower potential using GIS and hydrological modelling technique in Kopili River basin in Assam (India). Applied Energy. 87(1): 298-309.
68. J. Xu, X. Song, Y. Wu and Z. Zeng. (2015) GIS-modelling based coal-fired power plant site identification and selection. Applied Energy. 159: 520-539.
69. S. Kucuksari, A.M. Khaleghi, M. Hamidi, Y. Zhang, F. Szidarovszky, G. Bayraksan and Y.J. Son. (2014) An Integrated GIS, optimisation and simulation framework for optimal PV size and location in campus area environments. Applied Energy. 113: 1601-1613.
70. N.Y. Aydin, E. Kentel and S. Duzgun. (2001) GIS-based environmental assessment of wind energy systems for spatial planning: A case study from western Turkey. Renewable and Sustainable Energy Reviews. 14(1): 364-373.
71. D. Latinopoulos and K. Kechagia. (2015) A GIS-based multi-criteria evaluation for wind farm site selection. A regional scale application in Greece. Renewable Energy. 78: 550-560.

72. H.S. Hansen. (2005) GIS-based multi-criteria analysis of wind farm development. Scan GIS Proceedings: 75–87.
73. R. Haaren and V. Fthenakis. (2011) GIS-based wind farm site selection using spatial multi-criteria analysis (SMCA): Evaluating the case for New York State. Renewable and Sustainable Energy Reviews. 15 (7): 3332– 3340.
74. S.M.J. Baban and T. Parry. (2001) Developing and applying a GIS-assisted approach to locating wind farms in the UK. Renewable Energy. 24 (1): 59-71.
75. W. Krewitt and J. Nitsch. (2003) The potential for electricity generation from on-shore wind energy under the constraints of nature conservation: a case study for two regions in Germany. Renewable Energy. 28:1645
76. B. Sliz-Szkliniarz and J. Vogt. (2011) GIS-based approach for the evaluation of wind energy potential: a case study for the Kujawsko–Pomorskie Voivodeship. Renew Sustain Energy Rev. 15: 1696–707.
77. K.Q. Nguyen. (2007) Wind energy in Vietnam: resource assessment, development status and future implications. Energy Policy. 35: 1405–13.
78. S.S. Hussain, U. Mörtberg, D. Mentis, M. Welsch, I. Babelon, and M. Howells. (2015) Wind Energy Assessment considering Geographic and Environmental Restrictions in Sweden: A GIS-based Approach. Energy. 83: 447-61.
79. F. Alkolibi. (2002) Possible effects of global warming on agriculture and water resources in Saudi Arabia: impacts and responses. Climatic Change. 54: 225–245.
80. The presidency of Metrology and Environment. <http://www.pme.gov.sa/> [Accessed 26 December 2016]
81. F.C. Odo, S.U. Offiah and P.E. Ugwuoke. (2012) Weibull distribution-based model for prediction of wind potential in Enugu, Nigeria. Advances in Applied Science Research. 3(2): 1202-1208.
82. C.G. Justus, W.R. Hargraves, A. Mikhail and D. Graber. (1978) Methods for estimating wind speed frequency distributions. Journal of Applied Meteorology 17: 350–353.
83. Windographer 3.2.3. (2014) Wind Resource Assessment Tool. http://www.mitsaya.com.
84. A.De Miguel and J. Bilbao. (2005) Test reference year generation from meteorological and simulated solar radiation data. Solar Energy. 78 (6): 695-822.

85. E.K. Akpinar and S. Akpinar. (2005) An assessment on seasonal analysis of wind energy characteristics and wind turbine characteristics. Energy Conversion and Management 46(11–12): 1848–1867.
86. S. Rehman. "Wind Power Resource Assessment, Design Of Grid Connected Wind Farm And Hybrid Power System". PhD. University of Pretoria, 2012.
87. "Study Finds That The Price Of Wind Energy In The United States Is At An All-Time Low, Averaging Under 2.5¢/Kwh | Berkeley Lab". News Center. N.p., 2017. Web. 13 Jan. 2017.
88. M.R. Islam, S. Mekhilef, and R. Saidur. (2013) Progress and Recent Trends of Wind Energy Technology. Renewable and Sustainable Energy Reviews. 21: 456-468.
89. E.H. Lysen. (1983). Introduction to wind energy. The Netherlands: CWD, 261-279.
90. W.E. Alnaser. (1993). Assessment of the possibility of using three types of wind turbine in Bahrain. Renewable Energy. 3(2–3): 179–84.
91. S.M. Habali, M.A.S. Hamdan, B.A. Jubran, A.I.O. Zaid. (1987) Wind speed and wind energy potential of Jordan. Solar Energy. 38(1): 59–70.
92. S. Rehman, T.O Halawani, and M Mohandes. (2003) Wind Power Cost Assessment At Twenty Locations In The Kingdom Of Saudi Arabia. Renewable Energy. 28.4: 573-583.
93. M. Sarkar and M. Hussain. (1991) The Potential Of Wind Electricity Generation In Bangladesh. Renewable Energy. 1.5-6: 855-857.
94. A.S. Ahmed Shata, and R. Hanitsch. (2006) Evaluation Of Wind Energy Potential And Electricity Generation On The Coast Of Mediterranean Sea In Egypt. Renewable Energy. 31.8: 1183-1202.
95. Yearbook, 2017. " Global Construction Costs Yearbook - Compass International". Compass International. N.p.,. Web. 14 Jan. 2017.
96. "Chemical Engineering Plant Cost Index - Chemical Engineering". Chemengonline.com. N.p., 2016. Web. 14 Jan. 2017.
97. Plant Location Factors. Intratech Solutions, LLC, 2016. Print.
98. Moné, Christopher et al. (2014) Cost Of Wind Energy Review. 1st ed. National Renewable Energy Laboratory, 2017. Print.
99. Bolinger, Mark and Ryan Wiser. Understanding Trends In Wind Turbine Prices Over The Past Decade. Berkeley National Laboratory, 2012. Print. Environmental Energy Technologies Division.



© University of Pretoria

100. Eltamaly, Ali M. and Hassan M. Farh. (2012) Wind Energy Assessment For Five Locations In Saudi Arabia. Journal of Renewable and Sustainable Energy. 4.2 022702.
101. The Ministry of Foreign Affairs, Kingdom of Saudi Arabia. <http://www.mofa.gov.sa/sites/mofaen/EServ/VisitingSaudiArabia/aboutKingDom/Pages/KingdomGeography46466.aspx> [Accessed 12.4.2016]
102. F. Rahman, S. Rehman and M.A. Abdulmajeed. (2012) Overview of energy storage systems for storing electricity from renewable energy sources in Saudi Arabia. Renewable and Sustainable Energy Reviews. 16: 274-283.
103. J.R. Janke. (2010).Multicriteria GIS modelling of wind and solar farms in Colorado. Renewable Energy. 35(10): 2228–2234.
104. S. Rehman, M. Shoaib, I. Siddiqui, F. Ahmed, M.R. Tanveer and S. Jilani. (2015) Effect of Wind Shear Coefficient for the Vertical Extrapolation of Wind Speed Data and its Impact on the Viability of Wind Energy Project. Journal of Basic & Applied Sciences. 11: 90-100.
105. B. Peros, I. Boko and V. Divic. (2009) Wind shear characteristics of local winds. The Seventh Asia-Pacific Conference on Wind Engineering, Taipei, Taiwan.
106. S.M. Ali, A.S. Mahdi and A.H. Shaban. (2012) Wind Speed Estimation for Iraq using several Spatial Interpolation Methods. British Journal of Science. 7(2): 48-55.
107. P.V. Gorsevski, S.C. Cathcart, G. Mirzaei, M.M. Jamali, X. Ye and E. Gomezdelcampo. (2013) A group-based spatial decision support system for wind farm site selection in northwest Ohio. Energy Policy, 55: 374–385.
108. I.J. Ramírez-Rosado, E. García-Garrido, L.A. Fernández-Jiménez, P.J. Zorzano-Santamaría, C. Monteiro and V. Miranda. (2008) Promotion of new wind farms based on a decision support system. Renewable Energy, 33(4): 558–566.
109. L.I. Tegou, H. Polatidis and D.A. Haralambopoulos. (2010) Environmental management framework for wind farm siting: Methodology and case study. Journal of Environmental Management, 91(11): 2134–2147.
110. DIVA-GIS. Mapping and geographical data. <http://www.diva-gis.org> [Accessed 26.12.2015]
111. Ministry of Transport, Saudi Arabia. <http://www.mot.gov.sa/> [Accessed 26.12.2015]
112. L.C. Rodman and R.K. Meentemeyer. (2006) A geographic analysis of wind turbine placement in northern California. Energy Policy. 34(15): 2137–2149.

113. R. Saidur, N. Rahim, M. Islam, and K. Solangi. (2011). Environmental impact of wind energy. Renewable and Sustainable Energy Reviews. 15(5): 2423-2430.
114. G. Pavokovic, E. Mandusik. Risk for wildlife by wind turbines. Opatiga, Croatia; 2006.
115. Arab News. (2017). Arabian Peninsula a transit hub of migrating birds. [online] Available at: http://www.arabnews.com/news/arabian-peninsula-transit-hub-migrating-birds [Accessed 3 Jan. 2017].
116. M. Shobrak. (2011). Bird flyways and stopover conservation sites in the Arabian Peninsula. Zoology in the Middle East. 54(3): 27-30.
117. J. Hossain, V. Sinha, and V. Kishore. (2011). A GIS based assessment of potential for windfarms in India. Renewable Energy. 36(12): 3257-3267.
118. A. Miller and R. Li. (2014) A Geospatial Approach for Prioritising Wind Farm Development in northeast Nebraska, USA. ISPRS International Journal of Geo-Information. 3(3): 968-979.
119. ESRI. ArcMap 10.3.1. 2015.
120. S.K. Kar and A. Sharma. (2015) Wind power developments in India. Renewable and Sustainable Energy Reviews. 48, 264-275.
121. Y. Kumar, J. Ringenberg, S.S Depuru, V.K. Devabhaktuni, J.W. Lee, E. Nikolaidis and A. Afjeh. (2016) Wind energy: Trends and enabling technologies. Renewable and Sustainable Energy Reviews. 53: 209-224.
122. Z. Liao. (2016). The evolution of wind energy policies in China (1995–2014): An analysis based on policy instruments. Renewable and Sustainable Energy Reviews. 56: 464-472.